Isolation, Synthesis and Structure–Activity Relationship Study of Anticancer and Antimalarial Agents from Natural Products

Yumin Dai

Dissertation submitted to the faculty of Virginia Polytechnic Institute and State University in partial fulfillment of the requirements for the degree of

Doctor of Philosophy in Chemistry

David G. I. Kingston, chair

Harry W. Gibson

Richard D. Gandour

Webster L. Santos

Oct. 29th, 2013

Blacksburg, Virginia

Keywords: Natural Products, Anticancer, Antimalarial, Acetogenins, Sesquiterpenoid, Flavonoid, Bufadienolide, Triterpene saponin, Anthraquinone.

Isolation, Synthesis and Structure–Activity Relationship Study of Anticancer and Antimalarial Agents from Natural Products

Yumin Dai

Abstract

The Kingston group's engagement in an International Cooperative Biodiversity Group (ICBG) program and a collaborative research project established between Virginia Tech and the Institute for Hepatitis and Virus Research (IHVR) has focused on the search for bioactive natural products from tropical forests in both Madagascar and South Africa. As a part of this research, a total of four antiproliferative extracts were studied, leading to the isolation of fourteen novel compounds with antiproliferative activity against the A2780 human ovarian cancer line. One extract with antimalarial activity was studied, which led to the isolation of two new natural products with antiplasmodial activity against a drug-resistant Dd2 strain of *Plasmodium falciparum*.

The plants and their secondary metabolites are discussed in the following order: two new antiproliferative acetogenins from a *Uvaria sp.* (Annonaceae); two new antiproliferative calamenene-type sesquiterpenoids from *Sterculia tavia* (Malvaceae); two new antiproliferative triterpene saponins from *Nematostylis anthophylla* (Rubiaceae); six new antiproliferative homoisoflavonoids and two new bufatrienolides from *Urginea depressa* (Asparagaceae); and two new antiplasmodial anthraquinones from *Kniphofia ensifolia* (Asphodelaceae).

The structures of all these compounds were determined by analysis of their mass spectrometric, 1D and 2D NMR, UV and IR spectroscopic and optical rotation data. Other than

structural elucidation, this work also involved bioactivity evaluations of all the isolates, as well as total synthesis of the two antiproliferative sesquiterpenoids, and a structure–activity relationship (SAR) studies on the antiplasmodial anthroquinones.

Dedication

I would like to dedicate this dissertation to my parents Mingliang Dai and Huiling Fan, and my brother Wei Zhang for their love and support.

Acknowledgement

I think the most chronologically accurate place to begin my dissertation acknowledgements is with my parents, who long, long ago introduced me to the periodic table that hung on the wall, describing it as a "building" and telling me there were different residents living in each "house". I still remember my mom explained who they were, while my father created a doggerel in our dialect, which included all those residents. I think that is my earliest touch of chemistry. Thanks Mom and Dad for your love, and for allowing a little boy's fascination with the world to lead him into science and never stopping believing in him.

While my family may have set the stage, the ones who opened the curtain were my high school chemistry teachers, Miss Juan Zheng and Mr. Yunzhong Mao. Under their guidance, I came to know how to design and conduct a chemistry experiment independently. And I still remember how happy I was when my first research paper was published in a local magazine. Later on, Professor Min Chen from China Agricultural University accepted me as an undergraduate student in her laboratory. I owe Prof. Chen a lot for teaching, encouraging, and being forgiving with all the mistakes I made during that time.

I was not totally involved in chemistry until I finished my M.Sc studies in the Department of Food Science and Technology at Virginia Tech. Instead of moving to the Ohio State University, today I still think I have made a correct decision to join chemistry department at VT, where I met with my advisor Dr. David Kingston, who has had the most influence on my career; thus the most important acknowledgement must go to him. Elegance and professionalism are the two words that come to mind when someone mentions Dr. Kingston. He continually taught me the

knowledge of chemistry from all aspects, and forced me to learn how to learn and discover on my own, which is truly the goal of a Ph.D. Rather than an advisor, I respect Dr. Kingston more as a grandfather. Besides the science, he kept encouraging me to get rid of flaws, refresh myself and be confident. Thanks Dr. Kingston for your tolerance, forgiveness and support.

My committee, Dr. Webster Santos, Dr. Harry Gibson and Dr. Richard Gandour provided invaluable resources during my study in the past three years. I learned and will always remember the word "punctiliousness" from Dr. Gandour, and I think it is the right attitude a real scientist should possess. Meanwhile, I really appreciate that Dr. Gandour gave me the good suggestions on speaking good English. Dr. Gibson did not talk much, but his words always led me to think in depth. I still remember his word "ask yourself what your aim is when make a presentation" once I spent only 31 minutes to finish a seminar with 60 slides. For Dr. Santos, almost all my knowledge of organic synthesis is directly from him. Thanks Dr. Gandour, Dr. Gibson and Dr. Santos for your selflessness.

The next acknowledgement should be delivered to Dr. Liva Harinantenaina, who directly taught me the basic knowledge and techniques in the field of natural products. I enjoyed the past three years working with him, getting trained by him, and also learning from him. Without his help, my exposure to natural products may have experienced more obstacles along the way. Much closer to a friend, he always acted as a big brother to me, including sharing life experiences, the tricks during the social time, etc. Thanks Liva for your help.

The same thanks should go to all my collaborators, including Dr. Yongchun Shen from Eisai Inc. for anticancer bioassays, Dr. Michael Goetz from the Natural Products Discovery Institute

for the extract supply, Dr. Maria Caserra from the Department of Biochemistry for the antimalarial assay, and Dr. Giulio Paciotti from CytImmune for coordinating the AZ project, etc. I would also like to thank the Chemistry staff for all of their help over the past three years, especially Dr. Hugo Azumendi, Mr. Bill Bebout and Mr. Geno Iannaccone for NMR and MS service.

I would like to thank all of my lovely labmates who have befriended me. Dr. Shugeng Cao, Dr. Yanpeng Hou, Dr. Jun Qi, Dr. Jielu Zhao, Dr. Ende Pan, Dr. Qiaohong Chen and Mr. Zhibing Xu left me a lot of treasure and valuable suggestions before they left the group. The current group members, including Karen Iannaccone, Peggy Brodie, Yixi Liu, Alex Eaton, Amrapali Dengada, Chris Presley, Qingxi Su and Long Xia always gave me a hand when I needed it. Peggy Brodie took care of all the cell culture bioassays involved in my research, and she helped me proofread all my papers. I would especially like to thank Yixi Liu for all of the discussions, laughter, lunches, tailgates, and social hours. Every time, when my mood was extremely down, she pulled me out from the valley in time. Special acknowledgement should also be delivered to Long Xia for the happiness, and optimism he brought me both in and out of work. Thanks Yixi, thanks Long, thanks all my group members. I always knew that someone would be there for me to talk to and I hope that our paths cross again someday.

Lastly, I would like to thank all the friends I met at Virginia Tech, including Lei Pan, Liyun Ye, Jie Zhu, Wenrui Zhang, Bohan Bao, Xueyan Zheng, Xiangtao Meng, Yufeng Ma, Ran Liu, Xinyi Tan, Haoyu Liu, Tinghui Li, Ming Wang, Yongle Du, Xiaoyan Jia and Shi Yu. My life became wonderful with you guys in the past five years staying in Blacksburg. And also please forgive me for any names not mentioned here.

Table of Contents

List of Abbreviations

BuOH	Butanol
COSY	Correlation Spectroscopy
DAD	Diode Array Detector
DCM	Dichloromethane
DDQ	2,3-Dichloro-5,6-Dicyano-1,4-Benzoquinone
DMSO	Dimethyl Sulfoxide
ECD	Electronic Circular Dichroism
EI–MS	Electron Ionization Mass Spectroscopy
HR–ESI–MS	High Resolution Electrospray Ionization Mass Spectroscopy
EtOAc	Ethyl Acetate
EDCI	1-Ethyl-3-(3-dimethylaminopropyl)carbodiimide
ICBG	International Cooperative Biodiversity Groups
IHVR	Institute of Heptitise and Virus Research
HMBC	Heteronuclear Multiple Bond Correlation
HM(S)QC	Heteronuclear Multiple (Single) Quantum Coherence
HPLC	High Performance Liquid Chromatography
MeOH	Methanol
MPA	Methoxyphenylacetiac Acid
NIH	National Institute of Health
NMR	Nuclear Magnetic Rosanance
NOE	Nuclear Overhauser Effect
NMO	*N*-Methyl-Morpholine-*N*-Oxide
NP	Nanoparticles
SPE	Solid Phase Extraction
THF	Tetrahydrofuran
WET	Water Suppression Enhanced through T1 Effects

List of Tables

List of Schemes

List of Figures

Chapter 1: Introduction

1.1 Cancer and Anticancer Agents from Natural Products

Cancer is the general name for a group of more than 100 diseases, in which cells in a part of the body begin to grow out of control. It is a severe life-threatening disease, with annual health care costs in the billions of dollars.[1] According to statistics from the American Cancer Society in 2007, cancer is the second leading cause of death in the USA with 562,875 deaths from different types of cancer, accounting for 23.2% of all deaths in the United States.[2] In 2013, a total of 1,660,290 new cancer cases and 580,350 deaths from cancer were projected to occur.[3] The increasing death rate from cancer is always a big concern not only in United States, but all over the world.

The current drugs used to treat cancer are mainly derived from two sources: natural products and synthetic compounds through combinatorial chemistry. In particular, after combinatorial chemistry, which initially focused on establishing small peptide libraries, was introduced into the pharmaceutical industry, this fast and efficient method was expected to promote cancer drug discovery. However, as small peptides do not enter cells, they are in general not suitable drug candidates.[4] Later, even the improved combinatorial chemistry was applied on modifying the structures of drugs that originated from natural products; the basic skeleton of these new drugs are seldom novel; thus it is of less help to identify the drugs with new anticancer mechanism.[5] As Newman and Craig indicated, only one *de novo* combinatorial compound was approved as a drug in the last 30 years.[6] Therefore, the developments of synthetic compounds to be anticancer drugs still relies on the identification of new natural compounds to some extent.

Natural products have served as an important resource for anticancer drugs since the early

1940s. According to the data from the National Cancer Institute (NCI), more than two thirds of the anticancer drugs approved between 1946 and 2006 are either natural products or natural product derivatives through chemical modification.[7]

Among all the biological sources, plants have a long history of use in the treatment of cancer. People in modern China and Central Africa still prefer to use herbal remedies to prevent or even treat cancer, and to date, Chinese medicine remains widely used. In spite of intensive investigation of botanical resources, it is estimated that only 5–15% of the approximately 250,000 species of higher plants have been systematically investigated, both chemically and pharmacologically.[8] Moreover, several plant-derived anticancer agents are in clinical use. The vinca alkaloids, vinblastine (**1.1**) and vincristine (**1.2**), isolated from *Catharanthus roseus*, the Madagascar

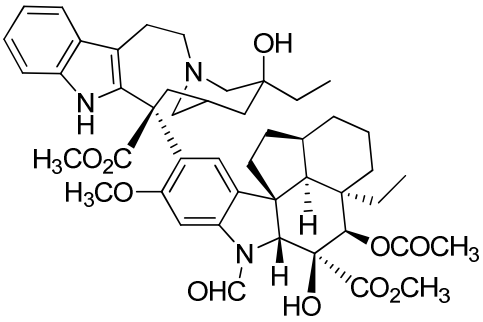

1.1

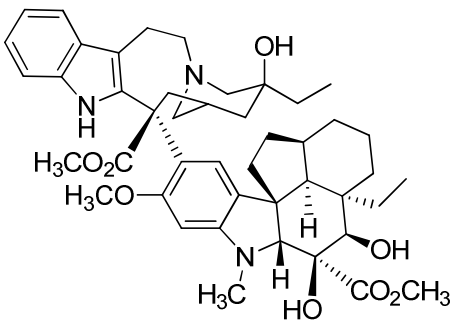

1.2

periwinkle, are the earliest plant-derived anticancer drugs in clinical use.[9] They are antimicrotubule agents that have been widely used to treat different kinds of cancer, including lung cancer, breast cancer, testicular cancer, etc. Later, paclitaxel (**1.3**), also known as Taxol^{TM}, which is also a mitotic inhibitor, was isolated from the bark of *Taxus brevifolia*, and has been proven to be effective in the treatment of breast cancer, lung cancer, and Kaposi's sarcoma (a tumor caused by human herpesvirus).[10] Current research on paclitaxel is focusing on the treatment of later phase

advanced cancer.[11]

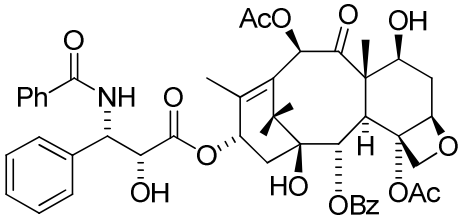

1.3

Other plant-derived natural products, such as camptothecin (**1.4**), isolated from *Camptotheca acuminata*,[12] and podophyllotoxin (**1.7**)[13], isolated from rhizomes of *Podophyllum peltatum* have provided the precursors to the clinical drugs topotecan (**1.5**), irinotecan (**1.6**),[14] etoposide (**1.8**) and teniposide (**1.9**).[15]

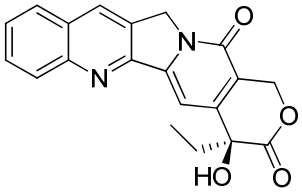

1.4

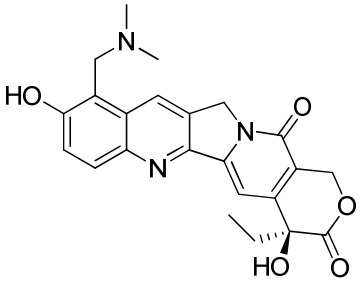

1.5

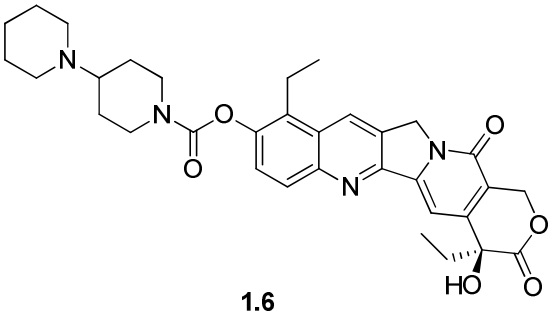

1.6

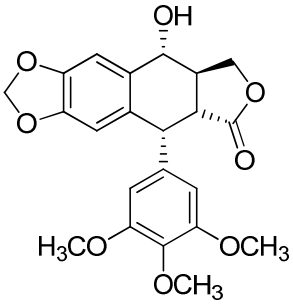

1.7

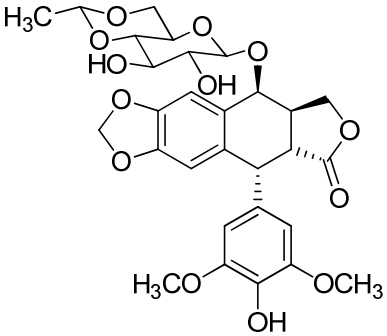

1.8

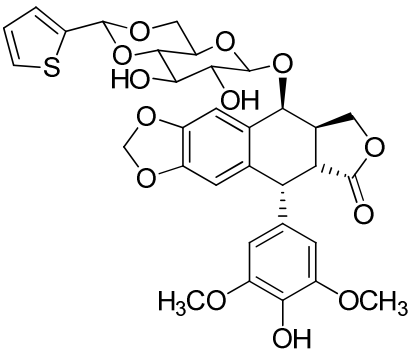

1.9

Besides plants, the marine environment is a rich source of bioactive compounds, many of which belong to totally novel families not discovered in terrestrial sources.[16] Although very few

compounds isolated from a marine source have yet been developed as clinical drugs, many of them have been tested as potential anticancer agents through various phases of clinical trials. Ecteinascidin-743 (**1.10**), known as trabectedin, was isolated originally from the tunicate *Ecteinascidia turbinate*. Due to its encouraging antitumor activity indicated in clinical tests, it was approved by the European Union as an anticancer drug to treat advanced or metastatic non-gastrointestinal stromal tumor soft tissue sarcoma (STS) in 2007.[17] Halichondrin B (**1.11**) is a naturally-occurring compound originally isolated from the marine sponge *Halichondria okadai* by Hirata and Uemura in 1986.[18] Its synthetic analogue Eribulin (**1.12**) was approved by the U.S. Food and Drug Administration on November 15, 2010, to treat patients with metastatic breast cancer who have received at least two prior chemotherapy regimens for late-stage disease.[19]

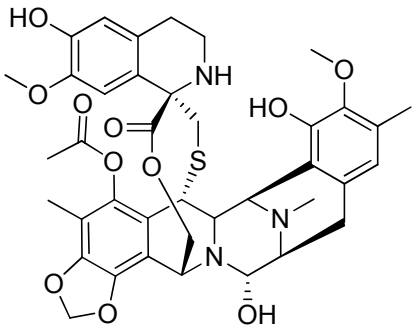

1.10

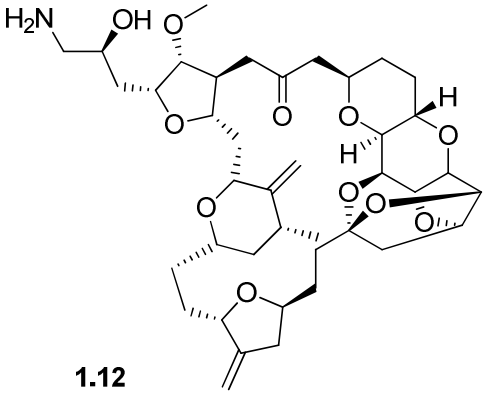

1.12

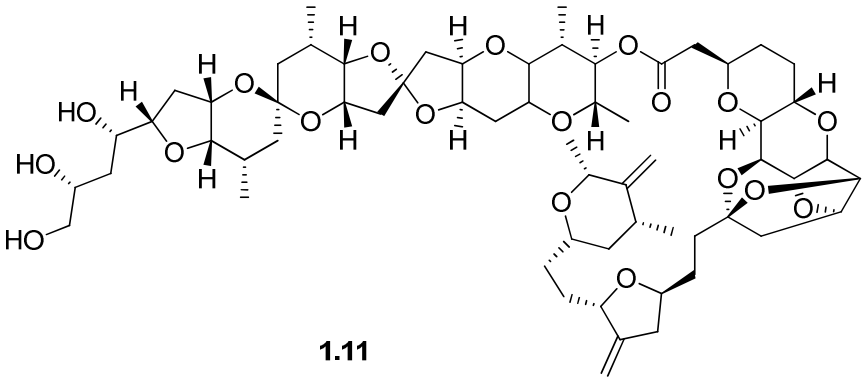

1.11

It is conceded that natural-derived compounds have made great contributions to the pharmaceutical industry and clinical use. Like almost all anticancer drugs, they have great side effects that cannot be ignored. For instance, vincristine has salient neurotoxicity due to its interaction with mitotic spindles.[20] Loss of appetite, nausea and vomiting always accompany the treatment with paclitaxel.[21] More importantly, lack of selectivity, being harmful to the immune system and multi-drug resistance effects are three urgent problems confronting most of the current anticancer drugs. There is, thus, a continuing need to search for the new anticancer compounds that have selectivity and have little or no toxicity to the normal tissues or cells in the human body.

1.2 Malaria and Antimalarial Agents from Natural Products

Malaria is a mosquito-borne infectious disease of humans and other animals caused by parasitic protozoans of the genus *Plasmodium*. The disease is widespread in tropical and subtropical regions in a broad band around the equator, including much of Sub-Saharan Africa, Asia, and the America.[22]

Malaria remains one of the major infectious diseases that threaten human lives. According to the latest estimates from the World Health Organization (WHO), there were about 219 million cases of malaria and an estimated 660,000 deaths from malaria in 2010, with about 90% of all of these deaths occurring in Africa.[23]

People started looking for anti-malarial agents from natural products in the 17th century, and quinine (**1.13**), isolated from the bark of the Cinchona tree, was the first effective treatment for malaria caused by *Plasmodium falciparum*.[24] It remained the main antimalarial drug of choice

until the 1940s, when chloroquine (**1.14**) was discovered. Compared to quinine, chloroquine is more effective in curing all forms of malaria with fewer side effects.[25] However, most strains of *falciparum* malaria are now resistant to chloroquine. Other antimalarial agents such as mepacrine (**1.15**) and mefloquinone (**1.16**) were discovered afterwards, and the structures of all these drugs share similar heterocyclic rings.

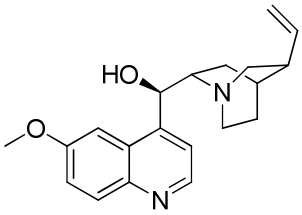

1.13

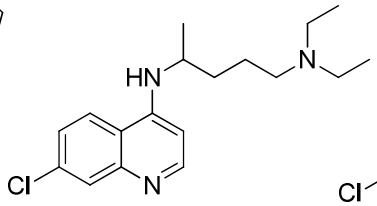

1.14

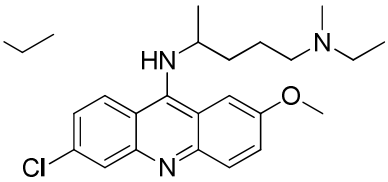

1.15

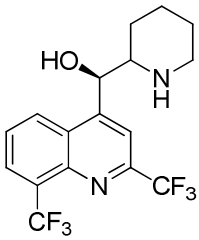

1.16

In 1972, a new type of antimalarial agent artemisinin (**1.17**) from the hexanes extract of the traditional Chinese medicinal plants, *Artemesia annua* (Asteraceae) was discovered, *A. annua* has been used for the treatment of fever and malaria since ancient times. Artemisinin is a sesquiterpene lactone peroxide. Unlike most other conventional antimalarial agents, there is no aromatic heterocyclic ring system in its structure. It was found to be a superior plasmocidal and blood schizontocidal agent without obvious side effects when used to treat patients.[26] Due to its low solubility in both oil and water, poor bioavailability and rapid biotransformation, which limited its effectiveness,[27] some semi-synthetic derivatives of artemisinin were developed. Semi-synthetic artemisinins are obtained from dihydroartemisinin (**1.18**), the main active metabolite of artemisinin. The first generation of semi-synthetic artemisinins includes artesunate (**1.19**), a hydrophilic artemisinin, while artemether (**1.20**) and arteether (**1.21**) are the oil soluble derivatives. Artemisone (**1.22**), a second-generation artemisinin, has been reported to

have improved pharmacokinetic properties, including longer half-life and lower toxicity.[28] So far, artesunate is the derivative that is commonly used in antimalarial combination therapy (ACT).[29]

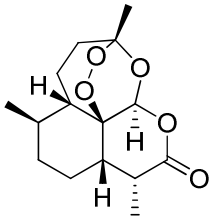

1.17

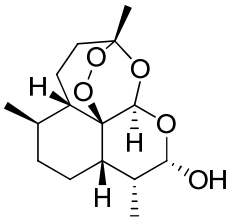

1.18

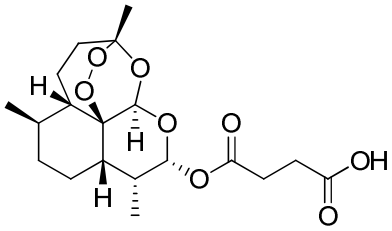

1.19

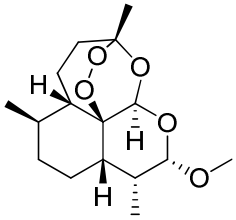

1.20

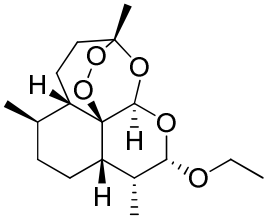

1.21

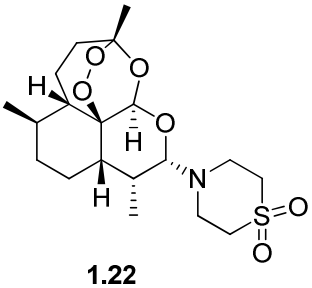

1.22

Although current anti-malarial drugs such as mefloquinone analogues[30] and artemisinins have achieved significant success in controlling the spread of the disease, malaria still remains a burden to humanity due to increasing drug resistance and the lack of multistage therapies to target the complex life cycle of the parasites.[31] The recent emergence of resistance to artemisinin in the Cambodia–Thailand border area is particularly troubling.[32] Therefore, there is a continuing interest in looking for new anti-malarial drugs with lower resistance to the parasite, while maintaining a higher potency.

1.3 Dereplication and Its Application in Natural Product Research

1.3.1 *Dereplication and Hyphenated Techniques*

Since the middle of the 20th century, chromatography has played an important role in natural

products research, especially in the field of isolation of new compounds. Later, the development of multiple spectroscopies further enriched the methods of identification of these compounds. Combining both techniques, the field of drug discovery encountered a big revolution, and thousands of new bioactive compounds were identified from various plants, marine organisms, and microorganism, etc. during the past 50 years. However, conventional natural products research, including manual liquid–liquid partition, open column chromatography, HPLC, and MS and NMR spectroscopy is a time-consuming process. In addition, there is less chance to identify a totally new compound, since the compounds discovered often differ from known ones only in minor ways in many cases. Facing this challenging situation, there is a growing interest in the development of hyphenated techniques, which combine separation technologies with NMR spectroscopy and MS. Dereplication is an important method to prevent unnecessary use of resources on the isolation of known or undesirable compounds from extracts identified by the screening process, [33] and it emphasizes these hyphenated techniques due to their convenience, power, time-saving, effectiveness and so on. The time saved from this approach can be used to search for novel bioactive compounds instead of repeating the laborious work merely to discover known ones.

In the past 15 years, several hyphenated techniques have been developed for dereplication in natural products research. LC–MS, which is the most common one, has become a widely used tool.[34] With the development of diode array detectors, it is possible to get a compound's UV spectrum directly from HPLC chromatography. Meanwhile, mass spectrometry, which is highly sensitive (1–100 ng is sufficient), can provide information about the molecular weight (Electrospray ionization) and fragmentation (Electron ionization) of the compounds. Since the

nominal molecular weight can be used as a search query in nearly all major databases, and fragmentation patterns can give information on the family of the compound, LC–MS serves as a rapid and significant method in dereplication. However, information from MS can only provide a preliminary structure and rarely results in a definitive identification. In order to obtain more information, considerable attention has been directed to the coupling of HPLC and NMR, regardless of the fact that NMR has much lower sensitivity compared to MS. In the few last decades, several changes have been made to NMR to facilitate LC–NMR work, such as the use of higher field magnets and digital signal processing to increase sensitivity, and the design of new probes, which allow the use of gradient pulse sequences to provide efficient and specific suppression of the NMR signals due to the HPLC solvents, etc.[35] After these improvements, LC–NMR is now a powerful technique for structure elucidation of unknown compounds in natural product research. Some typical hyphenated techniques that have been used in dereplication are discussed in detail below.

1.3.1.1 *LC–NMR*

There is a big difference in the principles of work between traditional NMR and NMR coupled with HPLC. In traditional NMR spectroscopy, the sample is prepared in a deuterated solvent, such as D_2O, $CDCl_3$, CD_3OD, etc., and is transferred into a long cylindrical NMR tube at a volume of about 0.5 mL. The tube is placed into the NMR probe within the magnet for determination of the spectrum. However, for NMR coupled with HPLC, normally, the sample submitted for LC–NMR test is first injected into the HPLC, and is separated by a normal phase or reverse phase column; after passing through UV–DAD/PDA detector, the effluent flows into a

polytetrafluoroethylene tube which is directly or indirectly connected to the NMR probe. The probe must thus be modified to allow continuous flow of the solution under test, while some other factors need to be considered, such as the pressure, solvent, and volume of the cell within the NMR coil, which may influence the sensitivity of the method. The status of the fraction during the NMR measurement divides the LC–NMR into two different modes in real applications: continuous-flow LC–NMR and stopped-flow LC–NMR (shown in **Fig. 1.1**).[36]

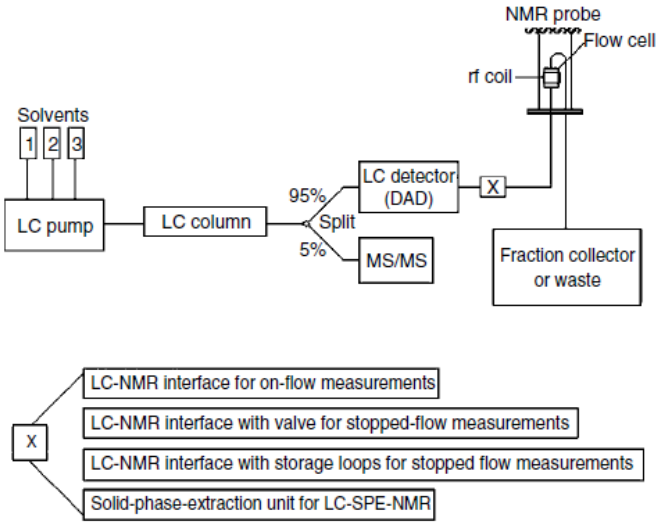

Figure 1.1 Different Hyphenated Techniques Used in Dereplication[36]

(Reprinted with permission, Copyright © 2005, John Wiley & Sons, Ltd.)

1.3.1.1.1 *Continuous-flow LC–NMR*

In continuous-flow mode, the HPLC components are measured by NMR continuously without stopping the HPLC pump. This mode, compared to the traditional approach, which needs to collect the fraction from HPLC, dry it, add deuterated solvent, then test in NMR, is a much more effective way to separate the compounds while getting NMR information at the same time. Thus, it is a useful method to do a rapid screening with a mixture that contains major compounds. As a

result of one injection, the data displayed would be the one similar to LC–MS, since we can obtain a two-dimensional time–frequency plot consisting of a set of one-dimensional spectra at specific retention times. Normally, when applying traditional NMR, a proton NMR spectrum may need 2.5 minutes for 64 scans while 1 hour or more is needed for carbon NMR. In this case, a poor S/N ratio of proton NMR spectra is obtained due to the limited time for the sample stay in the *rf* coil, and carbon NMR is not applicable in this mode. The only way to improve this method is to slow down the flow rate of the HPLC separation and allow the fraction to stay in the probe for a longer time. However, the slow flow rate of HPLC may affect the separation in the column. Another important issue is when the solvent system of HPLC is gradient instead of isocratic, the spectra may change as time goes, since the change of solvent leads to varied chemical shifts of solvent protons, further altering the whole chemical shift of the analytes. Thus, in continuous-flow mode of LC–NMR, an isocratic mobile phase is preferred rather than a gradient solvent system.

1.3.1.1.2 *Stopped-flow LC–NMR*

In stopped-flow mode, a fraction is separated by HPLC and detected by NMR, while the solvent flow is stopped while the sample is in the NMR flow cell. There are two major methods to reach this goal. The first one is to use a valve within the *rf* coil to control the flow of analytes, the other one is to use a bunch of different sample loops to store the individual fractions obtained from the HPLC column. In this way, fractions are given more time to stay in the *rf* coil for detection. Since the time for stopping the pump can be controlled manually, there are more opportunities to obtain good spectra as longer time as possible. In addition, carbon NMR or even 2D NMR, such as H–H COSY may also be feasible in this case. The only thing that is essential for this mode is to

calculate the delay time, corresponding to the time required for transport of the fraction from the UV detector of the HPLC to the optimal position within the flow-cell, as well as the time for the analytes transported from the loops to the flow-cell when loops are used. However, for the valve regulated stopped-flow modes, frequent stopping of the pump may also influence the efficiency of the separation, and thus samples with few major constituents are preferred in this mode. For the stopped-flow mode involving loops, NMR detection always takes longer time than separation work by HPLC. Although it is still time-consuming, good spectra can be obtained, and the automatic system can prevent a great inconvenience compared to traditional NMR.

1.3.1.2 *LC–NMR–MS/MS*

Since mass spectrometry has a higher sensitivity and only needs a very small amount of sample for testing, it is entirely possible to couple a MS detector parallel to the NMR instrument after obtaining the separated fraction from the HPLC system. The balance between the detectors can be controlled by a splitter, and is usually 95% for NMR detection and 5% for MS. Both continuous-flow mode and stopped-flow mode LC–NMR can be used, although in the stopped mode, the MS is idle for most of time when the NMR spectrometer is collecting data. In sum, LC–NMR–MS/MS is a powerful technique, which can provide the both NMR and MS information about a compound with only one injection.

1.3.1.3 *LC–SPE–NMR*

In order to further increase the sensitivity of small amounts of sample, the solid phase extraction technique was introduced into the LC–NMR system. The SPE (solid phase extraction) cartridge, which is placed between the UV detector and the NMR spectrometer, can absorb the

diluted sample and filter out the solvent that was used for separation. In this manner, it is possible to use the normal protonated solvent for separation, regardless of its effect on NMR sensitivity, since deuterated solvent would be used to elute the sample from the SPE cartridge for NMR detection. The biggest advantage of LC–SPE–NMR is that solvent selection for HPLC is not so restricted while diluted fractions can be concentrated to increase their detectability by NMR. Other modes of LC–NMR require the use of solvent suppression methods.

1.3.1.4 *A Comparison among Different Hyphenated Techniques*

A summary of the pros and cons of different modes is shown in **Table 1.1** below.

Table 1.1 A Comparison among Different LC–NMR Modes

LC–NMR	Advantages	Disadvantages	Preferred sample for test
Continuous flow mode	**(1)** Effective and fast; **(2)** Especially useful for sample screening.	**(1)** Low sensitivity, and poor S/N ratio due to time limitations; **(2)** Gradient solvent system for HPLC may affect NMR; **(3)** Carbon NMR is not applicable	a mixture that contains major compounds
Valve stopped mode	**(1)** Allows more time to test the sample in NMR, thus giving better spectra; **(2)** 2D NMR is feasible	**(1)** Frequent stopping of the pump may affect the efficiency of separation; **(2)** Need to calculate the delay time.	a sample with few major constituents
Loops stopped mode	**(1)** Allows more time to test the sample in NMR, thus give good spectra; **(2)** 2D NMR is feasible; **(3)** Pump is not stopped, separation work is not greatly affected.	**(1)** Needs a relatively longer time to finish the whole task; **(2)** Need to calculate two types of delay time; **(3)** Wash loops as routine work	No preference for sample, just need time to finish.
Coupling with MS	Provides NMR and MS information about the compounds simultaneously	MS may stay idle for a long time when the valve stopped mode is used	No preference of sample
Coupling with SPE	**(1)** Less restrictions on the solvent system used in HPLC; **(2)** increased sensitivity by concentrating samples	Relatively expensive to buy the cartridges which may be disposable.	Especially good for dilute samples

1.3.2 *Applications of Hyphenated Techniques*

In order to identify the bioactive acetogenin compounds from natural products by the dereplication approach, LC–APCI–MS was applied by Gu and coworkers, and four new compounds were discovered from *Rollinia mucosa*, along with 36 known ones.[37] Although LC–NMR and related techniques have not been applied to acetogenin compounds, a great many other bioactive compounds have been discovered by these powerful methods, as discussed below.

1.3.2.1 *LC– (valve stopped) NMR–MS/MS*

Bobzin and coworkers applied LC–NMR–MS/MS to identify bioactive compounds from a marine sponge *Aaptos* sp. whose crude extract show a high activity for inhibiting a specific enzyme activity.[35] A Varian Unity INOVA 500 MHz spectrometer equipped with ^{1}H (^{13}C) pulsed field gradient LC–NMR flow probe with a 60 μL flow cell was used in these experiments. ^{1}H NMR spectra were obtained in valve stopped flow mode, since HPLC chromatography indicated well resolved peaks. WET solvent suppression techniques were used to suppress signals from the HPLC solvent acetonitrile, its ^{13}C satellites, and the residual water. In the chromatography conditions, D_2O was used as the other aqueous component of the solvent system, and the eluent from the HPLC column was split into two, 5% flowed into the mass spectrometer, while 95% was directed through a UV detector and then through the LC–NMR flow probe.

At 10.3 min, the LC–MS spectrum indicated the molecular weight of the fraction was 228.25. After comparison with a database, candidate compounds were suggested to be aaptosine, aaptamine or paragracine. However, the spectrum obtained from the LC–NMR (**Fig. 1.2**) revealed four coupled signals and one singlet in the aromatic region, and two large singlets at 3.83 and 3.97

ppm, suggesting that paragracine, which has only two singlet protons, could be eliminated. On further analysis, the compound was assigned as aaptamine, instead of aaptosine, based on the chemical shift of the aromatic proton. All three rings in aaptosine are aromatic, while only one ring in aaptamine is; thus, the proton of aaptamine in the aromatic region would be relatively less deshielded than the proton of aaptosine, as confirmed by the NMR spectrum.

This is a good example to show the advantage of coupling the LC–NMR with MS. Since MS can only provide information about the molecular weight and suggest candidates that are consistent with it, NMR data provide additional information on the structure, thus further eliminating incorrect ones while keeping the correct one. In this example, all of the compounds were known compounds, and combining the use of LC–MS and LC–NMR accelerated the whole speed of separation and structural elucidation, and prevented the unnecessary process of the conventional approach.

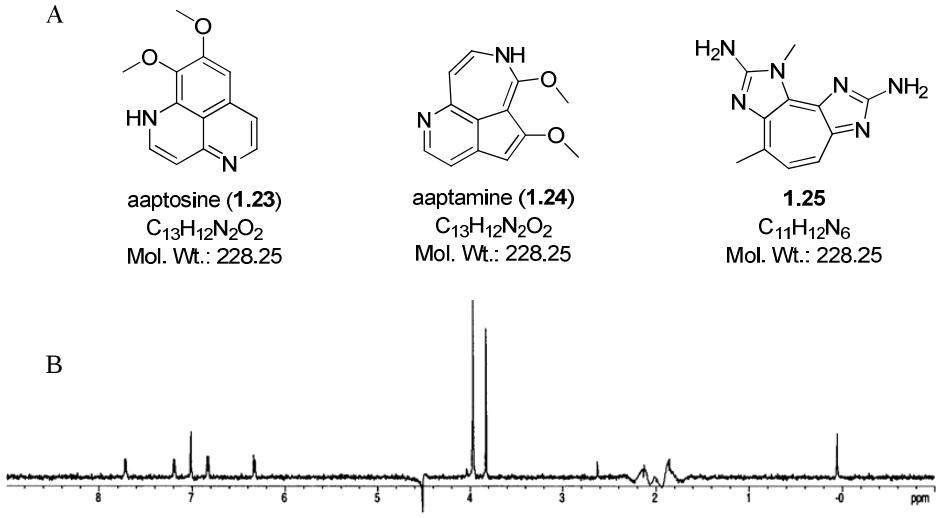

Figure 1.2 The Application of LC–NMR-MS/MS to Obtain Aaptosine[35]

A. Three compounds shared the same molecular weight of 228.25 suggested by LC–MS
B. The ^{1}H NMR spectrum of aapatamine.

1.3.2.2 *LC–SPE–NMR and LC–DAD–ESI–MS*

Gao and coworkers applied LC–SPE–NMR and LC–DAD–ESI–MS to identify the cytotoxic compounds from toad venom in *Bufo melanosticus*.[38] Toad venom has been widely used to treat heart failure, sores, and pains in China and recently for different types of cancer. From the venom, sterols, bufogenins and bufotoxins have been isolated. However, due to its broad activity, the types of compounds that are responsible for the cancer treatment were still unknown. In Gao's study, LC–MS analyses were performed on an UltiMate 3000 RSLC system, with a DAD detector coupled to the ESI Iontrap mass spectrometer. LC–SPE–NMR was performed on a Bruker BioSpin LC–SPE–NMR (600 Hz). According to the HPLC chromatogram (**Fig. 1.3**), the major peaks had been identified as known compounds, such as hellebrigenin, a 14*β*-hydroxy steroid, whose molecular weight is 416.51, confirmed by LC–MS. However, there was no correlated structural information about the small peaks (1–6), which showed high cytotoxicity, revealed by the MTT test. Due to the small amounts of peaks 1–6 presented, SPE was employed to trap and concentrate the samples, in preparation for NMR analysis. After the trapped peaks were dried with nitrogen gas, 30 μL of acetonitrile-d_3 was used to elute the SPE cartridge and the eluent directly flowed to the NMR probe for testing. SPE–LC–NMR system is similar to the loop stopped mode, and the HPLC pump thus did not need to be stopped, and the fractions collected from HPLC were placed in a queue for ^{1}H and ^{13}C NMR analysis.

LC–ESI–MS was applied to get the molecular weights, which were 499, 497, 483, 483, 483, and 475 Da respectively for compounds **1.26–1.31,** corresponding to the peaks 1–6 in the chromatogram. A loss of 80 Da in the fragmentation patterns, indicated an SO_3 groups, was present

in compounds **1.26**–**1.30**, suggesting they may be bufadienolide sulfates with different functional groups attached. From LC–^{1}H NMR, the resonances at δ_H 7.29 (d, J = 2.6 Hz, 1H), 7.86 (dd, J = 9.8, 2.6 Hz, 1H), and 6.18 (d, J = 9.8 Hz, 1H) showed the characteristic features of an α-pyrone ring, confirming the bufadienolide structure. Further analysis of LC–^{13}C NMR and LC–MS spectrum indicated the presence of additional functional groups.

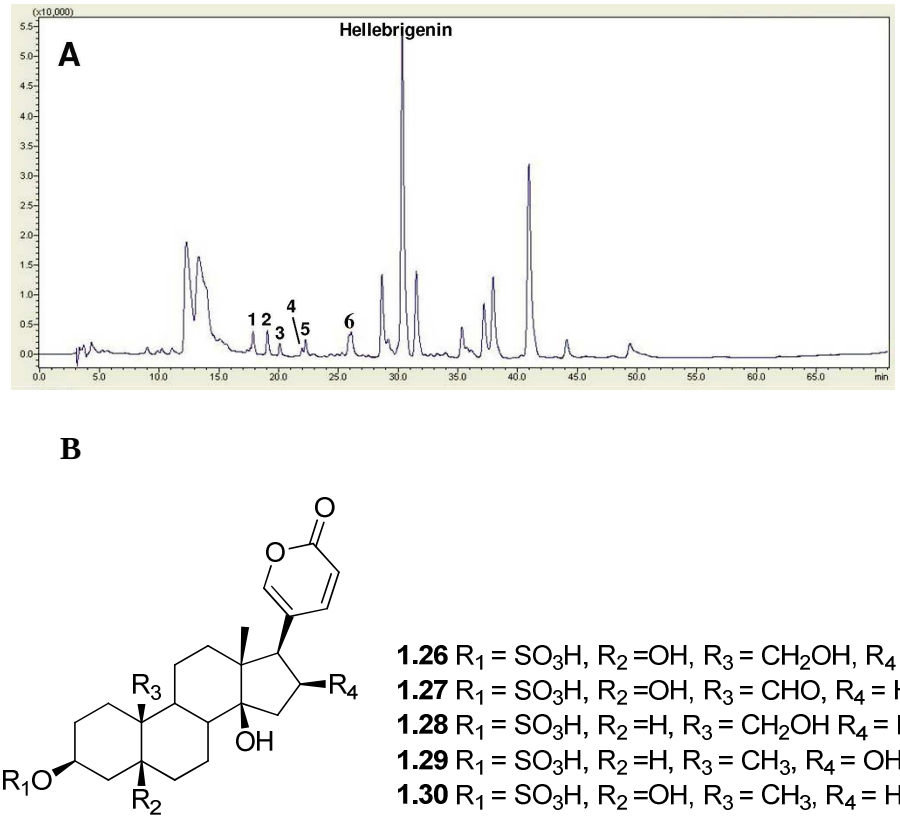

Figure 1.3 The Application of LC–SPE–NMR and LC–DAD–ESI–MS[38]
A HPLC chromatogram of MeOH extract from toad venom
B Bufadienolide sulfate compounds discovered in toad venom
(Reprinted with permission, Copyright © 2010, American Chemical Society)

In this example, the SPE cartridge was used to concentrate the small amount of sample in order to get high resolution NMR spectra and also to allow enough time for NMR analysis. In

contrast to the continuous-flow mode, ^{13}C NMR and 2D NMR are applicable in this situation. Meanwhile, by introduction of SPE, the problem of HPLC solvent interference with NMR was solved, since the HPLC solvent was replaced with a deuterated one for NMR analysis. Through the LC–MS and LC–NMR method, hellebrigenin, which is a known compound, was quickly detected, while 5 unknown bufadienolide sulfates compounds were identified at the same time. In this study, LC–MS and LC–NMR were separated; combining both techniques to make LC–DAD–ESI–MS–SPE–NMR would give an even higher efficiency.

1.4 The ICBG Program and IHVR Project

1.4.1 *The ICBG Program*

As stated, plants provide a major source of bioactive natural products. The tropical rain and dry forests of the world contain a vast variety of plants, some of which have not yet been identified, and therefore, hold the potential for the drug discovery. However, as the economies of developing countries change, these forests are disappearing at a rapid speed, to make way for agriculture and to provide timber for construction.

Based on this background, the International Cooperative Biodiversity Group program (ICBG) was started in 1992 to promote drug discovery and biodiversity conservation via economic development in developing countries. The objectives of this program are to discover new drugs and to share any benefits with host countries if a drug as discovered from their biological resources. It is currently jointly funded by the National Institutes of Health (NIH), the National Science Foundation (NSF), Department of Agriculture (USDA), Department of Energy (DOE) and the

National Oceanic and Atmospheric Administration (NOAA) of USA.[39]

As a part of the ICBG program since 1993, the Kingston Group from Virginia Tech has been collaborating with the Centre National de Recherche Oceanographique (CNRO), Centre National de Recherche pour l'Environmente (CNRE) and Centre National d'Application des Recherches Pharmaceutiques (CNARP) from Madagascar, as well as the Missouri Botanical Garden and Eisai Inc. The group focused on isolation and structural elucidation of anti-cancer and antimalarial compounds from the tropical plants of Madagascar, the fourth biggest island in the world.

1.4.2 *The IHVR Project*

The detail of this project will be discussed in chapter 5.

1.5 Objectives

This dissertation will emphasize the discovery novel antiproliferative and antiplasmodial agents from the tropical forests of Madagascar (ICBG plants) and South Africa (IHVR plants).

The research involves the isolation and structural elucidation of bioactive compounds from the various plant extracts. Bioassay guided separation and modern analytical techniques, including 1D and 2D NMR, LC–MS, UV, IR, optical rotation and circular dichroism (CD), etc. were the major methods applied in the whole procedure. The A2780 human ovarian cancer cell line was the antiproliferative assay used most frequently, and the A2058 melanoma and the H522 lung cancer cell lines were used as secondary assays. The Dd2 drug-resistant strain of *Plasmodium falciparum* was the only parasite that was used in the antimalarial assay.

After isolating the bioactive compounds, some of the structures may still be ambiguous, thus the chemical modification methods, including Mosher's ester, acid/base hydrolysis, and total synthesis, were used in facilitating the structural elucidation as a complement to spectroscopy.

Novelty and bioactivity are the two important characteristics of the compounds that were emphasized. Thus, when a novel compound was isolated with low bioactivity, the structure–activity relationship study was applied to look for the most potent compound with a similar skeleton.

The detailed research work is discussed in the following chapters.

1.6 References and Notes

1. Smigal, C.; Jemal, A.; Ward, E.; Cokkinides, V.; Smith, R.; Howe, H. L.; Thun, M. Trends in breast cancer by race and ethnicity: update 2006. *CA Cancer. J. Clin.* **2006,** *56*, 168–183.

2. http://www.cancer.org. Cancer Facts & Figures 2012-2013. (Accessed Sep. 16, 2013)

3. Jemal, A.; Siegel, R.; Xu, J.; Ward, E. Cancer statistics, 2010. *CA Cancer J. Clin.* **2010,** *60*, 277–300.

4. Sausville, E. A.; Johnson, J. I.; Cragg, G. M.; Decker, S. Cancer drug discovery and development: New paradigms for a new millennium. In *Anticancer Agents*, American Chemical Society: **2001**; First Edition; Vol. 796, pp 1–15.

5. Mann, J. Natural products in cancer chemotherapy: past, present and future. *Nat. Rev. Cancer* **2002,** *2*, 143–148.

6. Newman, D. J.; Cragg, G. M. Natural products as sources of new drugs over the Last 25 Years. *J. Nat. Prod.* **2007,** *70*, 461–477.

7. Efferth, T. Cancer therapy with natural products and medicinal plants. *Planta Med.* **2010,** *76*, 1035–1036.

8. Balandrin Manuel, F.; Kinghorn, A. D.; Farnsworth Norman, R. Plant-derived natural Products in drug discovery and development. In *Human Medicinal Agents from Plants*, American Chemical Society: **1993**; First Edition; Vol. 534, pp 2–12.

9. Tafur, S.; Jones, W. E.; Dorman, D. E.; Logsdon, E. E.; Svoboda, G. H. Alkaloids of *Vinca rosea* L. (*Catharanthus roseus* G. Don) XXXVI: Isolation and characterization of new dimeric

alkaloids. *J. Pharm. Sci.* **1975,** *64*, 1953–1957.

10. Cragg, G. M. Paclitaxel (Taxol): a success story with valuable lessons for natural product drug discovery and development. *Med. Res. Rev.* **1998,** *18*, 315–331.

11. Gogas, H.; Pectasides, D.; Kostopoulos, I.; Lianos, E.; Skarlos, D.; Papaxoinis, G.; Bobos, M.; Kalofonos, H. P.; Petraki, K.; Pavlakis, K.; Bafaloukos, D.; Fountzilas, G. Paclitaxel and carboplatin as neoadjuvant chemotherapy in patients with locally advanced breast cancer: A phase II trial of the hellenic cooperative oncology group. *Clin. Breast Cancer* **2010,** *10*, 230–237.

12. Oberlies, N. H.; Kroll, D. J. Camptothecin and taxol: historic achievements in natural products research. *J. Nat. Prod.* **2004,** *67*, 129–135.

13. Eyberger, A. L.; Dondapati, R.; Porter, J. R. Endophyte fungal isolates from *Podophyllum peltatum* produce podophyllotoxin. *J. Nat. Prod.* **2006,** *69*, 1121–1124.

14. Kushner, B. H.; Kramer, K.; Modak, S.; Cheung, N. K. Camptothecin analogs (irinotecan or topotecan) plus high-dose cyclophosphamide as preparative regimens for antibody-based immunotherapy in resistant neuroblastoma. *Clin. Cancer Res.* **2004,** *10*, 84–87.

15. Rappa, G.; Lorico, A.; Sartorelli, A. C. Potentiation by novobiocin of the cytotoxic activity of etoposide (VP-16) and teniposide (VM-26). *Int. J. Cancer* **1992,** *51*, 780–787.

16. Blunt, J. W.; Copp, B. R.; Munro, M. H.; Northcote, P. T.; Prinsep, M. R. Marine natural products. *Nat. Prod. Rep.* **2010,** *27*, 165–237.

17. Schoffski, P.; Dumez, H.; Wolter, P.; Stefan, C.; Wozniak, A.; Jimeno, J.; Van Oosterom, A. T. Clinical impact of trabectedin (ecteinascidin-743) in advanced/metastatic soft tissue sarcoma. *Expert. Opin. Pharmacother.* **2008,** *9*, 1609–1618.

18. Hirata, Y.; Uemura, D. Halichondrins – antitumor polyether macrolides from a marine sponge. *Pure Appl. Chem.* **1986,** *58*, 701–710.

19. Mani, S.; Swami, U. Eribulin mesylate, a halichondrin B analogue, in the treatment of breast cancer. *Drugs Today (Barc)* **2010,** *46*, 641–653.

20. Gomber, S.; Dewan, P.; Chhonker, D. Vincristine induced neurotoxicity in cancer patients. *Indian J. Pediatr.* **2010,** *77*, 97–100.

21. Gracias, N. G.; Cummins, T. R.; Kelley, M. R.; Basile, D. P.; Iqbal, T.; Vasko, M. R. Vasodilatation in the rat dorsal hindpaw induced by activation of sensory neurons is reduced by paclitaxel. *Neurotoxicology* **2010**, *32*, 140–149.

22. http://en.wikipedia.org/wiki/Malaria. (Accessed, Aug. 23, 2013)

23. WHO. *World Malaria Report 2012*. World Health Organization: Geneva, Switzerland, **2012**.

24. Schlitzer, M. Malaria chemotherapeutics part I: History of antimalarial drug development, currently used therapeutics, and drugs in clinical development. *ChemMedChem.* **2007,** *2*, 944–986.

25. Watt, G.; Long, G. W.; Padre, L. P.; Alban, P.; Sangalang, R.; Ranoa, C. P. Chloroquine and quinine: a randomized, double-blind comparison of efficacy and side effects in the treatment of *Plasmodium falciparum* malaria in the Philippines. *Trans. R. Soc. Trop. Med. Hyg.* **1988,** *82*, 205–208.

26. Chaturvedi, D.; Goswami, A.; Pratim Saikia, P.; Barua, N. C.; Rao, P. G. Artemisinin and its derivatives: a novel class of anti-malarial and anti-cancer agents. *Chem. Soc. Rev.* **2010,** *39*, 435–454.

27. Gordi, T.; Huong, D. X.; Hai, T. N.; Nieu, N. T.; Ashton, M. Artemisinin pharmacokinetics and

efficacy in uncomplicated-malaria patients treated with two different dosage regimens. *Antimicrob. Agents Chemother.* **2002,** *46*, 1026–1031.

28. Haynes, R. K. From artemisinin to new artemisinin antimalarials: biosynthesis, extraction, old and new derivatives, stereochemistry and medicinal chemistry requirements. *Curr. Top Med. Chem.* **2006,** *6*, 509–537.

29. Crespo-Ortiz, M. P.; Wei, M. Q. Antitumor activity of artemisinin and its derivatives: from a well-known antimalarial agent to a potential anticancer drug. *J. Biomed. Biotechnol.* **2012,** *2012*, 247–597.

30. Boudreau, E. F.; Pang, L. W.; Chaikummao, S.; Witayarut, C. Comparison of mefloquine, chloroquine plus pyrimethamine-sulfadoxine (Fansidar), and chloroquine as malarial prophylaxis in eastern Thailand. *Southeast Asian J. Trop. Med. Public Health* **1991,** *22*, 183–189.

31. Pérez, B. C.; Teixeira, C.; Albuquerque, I. S.; Gut, J.; Rosenthal, P. J.; Gomes, J. R. B.; Prudêncio, M.; Gomes, P. *N*-Cinnamoylated chloroquine analogues as dual-stage antimalarial leads. *J. Med. Chem.* **2012,** *56*, 556–567.

32. Dondorp, A. M.; Fairhurst, R. M.; Slutsker, L.; MacArthur, J. R.; Breman, J. G.; Guerin, P. J.; Wellems, T. E.; Ringwald, P.; Newman, R. D.; Plowe, C. V. The threat of artemisinin-resistant malaria. *N. Engl. J. Med.* **2011,** *365*, 1073–1075.

33. Cordell, G. A.; Beecher, C. W. W.; Kinghorn, A. D.; Pezzuto, J. M.; Constant, H. L.; Chai, H. B.; Fang, L.; Seo, E. K.; Long, L.; Cui, B.; Slowing-Barillas, K. The dereplication of plant-derived natural products. In *Studies in Natural Products Chemistry*, Atta ur, R., Ed. Elsevier: 1996; Vol. Volume 19, pp 749–791.

34. Rudi, A.; Kashman, Y. Aaptosine–a new cytotoxic 5,8-diazabenz[cd]azulene alkaloid from the Red Sea sponge. *Tetrahedron Lett.* **1993,** *34*, 4683–4684.

35. Bobzin, S. C.; Yang, S.; Kasten, T. P. LC–NMR: a new tool to expedite the dereplication and identification of natural products. *J Ind. Microbiol. Biotechnol.* **2000,** *25*, 342–345.

36. Exarchou, V.; Krucker, M.; van Beek, T. A.; Vervoort, J.; Gerothanassis, I. P.; Albert, K. LC–NMR coupling technology: recent advancements and applications in natural products analysis. *Magn. Reson. Chem.* **2005,** *43*, 681–687.

37. Gu, Z.M.; Zhou, D.; Wu, J.; Shi, G.; Zeng, L.; McLaughlin, J. L. Screening for Annonaceous acetogenins in bioactive plant extracts by liquid chromatography/mass spectrometry. *J. Nat. Prod.* **1997,** *60*, 242–248.

38. Gao, H.; Zehl, M.; Kaehlig, H.; Schneider, P.; Stuppner, H.; Moreno, Y. B. L.; Kiss, R.; Kopp, B. Rapid structural identification of cytotoxic bufadienolide sulfates in toad venom from *Bufo melanosticus* by LC–DAD–MS and LC–SPE–NMR. *J. Nat. Prod.* **2010,** *73*, 603–608.

39. http://www.icbg.org/. (Accessed, Aug. 23, 2013)

Chapter 2: Antiproliferative Acetogenins from a *Uvaria sp.* from the Madagascar Dry Forest

This chapter is a slightly expanded version of a published article. (Dai, Y.; Harinantenaina, L.; Brodie, P. J.; Callmander, M. W.; Randrianaivo, R.; Rakotonandrasana, S.; Rakotobe, E.; Rasamison, V. E.; Shen, Y.; TenDyke, K.; Suh, E. M.; Kingston, D. G. I. Antiproliferative acetogenins from a *Uvaria sp.* from the Madagascar dry forest. *J. Nat. Prod.* **2011,** *75*, 479–483.) Attributions of co-authors of the articles are described as follows in the order of the names listed. The author of this dissertation (Mr. Yumin Dai) conducted the isolation and structural elucidation part of the titled compounds, and drafted the manuscript. Dr. Liva Harinantenaina was a mentor for this work, and in particular, he provided invaluable advice and hints for the structural elucidation of the compounds, and he also proofread the manuscript before submission. Ms. Peggy Brodie performed the A2780 bioassay on the isolated fractions and compounds. Dr. Martin W. Callmander and Dr. Richard Randrianaivo from Missouri Botanical Garden did the plant collections and identification. Dr. Stephan Rakotonandrasana, Dr. Etienne Rakotobe and Dr. Vincent E. Rasamison from Madagascar carried out the initial plant extraction. Dr. Yongchun Shen, Dr. Karen TenDyke, and Dr. Edward M. Suh from Eisai Inc. performed the A2058 and H522 bioassays on the compounds isolated. Dr. David G. I. Kingston was a mentor for this work and the corresponding author for the published article. He provided critical suggestions for this work and edited the final manuscript.[1]

2.1 Introduction

As part of the Kingston group's engagement in an International Cooperative Biodiversity Group (ICBG) program, it has focused on searching for antiproliferative natural products from both tropical dry forests and rain forests in Madagascar. As a part of this research, an EtOH extract from the aerial parts of a *Uvaria sp.* (Annonaceae) from the dry forest of northern Madagascar exhibited modest antiproliferative activity against the A2780 human ovarian cancer cell line, with an IC_{50} value of 20 μg/mL Compounds of the Annonaceae family are well-known for their broad range of bioactivity, including immunosuppressive, antimalarial, insecticidal, antifeedant, and antitumor activities.[2-5] The genus *Uvaria* has been investigated extensively, with over 300 references in the chemical and biological literature, and the chemical constituents of *Uvaria* species have been summarized in two reviews.[6, 7] The genus *Uvaria* is also one of only seven of the 120 genera of the Annonaceae family known to produce acetogenins,[8] and uvaricin (**2.1**), the first example of these compounds, was isolated from the roots of *Uvaria accuminata* Oliv. by Jolad *et al*. in 1982.[9]

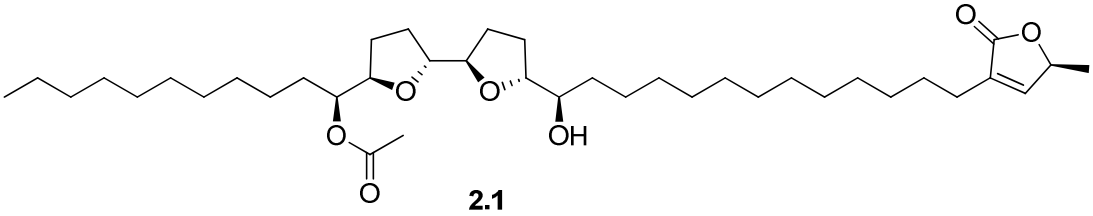

2.1

Although the genus *Uvaria* has been well investigated, no work has been done on this new species. A total of seventeen *Uvaria* species are currently known in Madagascar, and eleven remain to be described.[10] This extract was thus selected for bioassay guided fractionation to isolate its active components.

2.2 Results and Discussion

2.2.1 *Isolation of Active Compounds*

Bioassay guided separation, including liquid–liquid partition, LH-20 size exclusion, silica gel normal-phase and C_{18} reverse-phase chromatography was used to obtain the two new acetogenins uvaricin A (**2.1**) and uvaricin B (**2.2**) with modest antiproliferative activity against A2780 ovarian cancer cells (**Scheme 2.1**). Herein, we report the structural elucidation and antiproliferative properties of the two isolates.

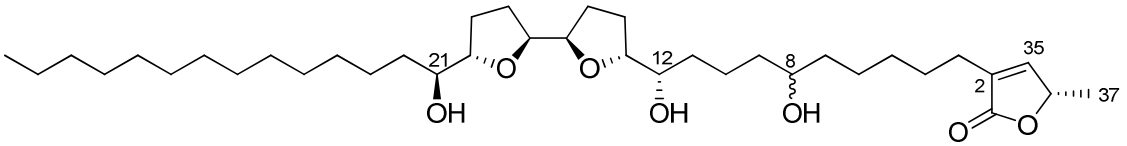

Uvaricin A (**2.2**)

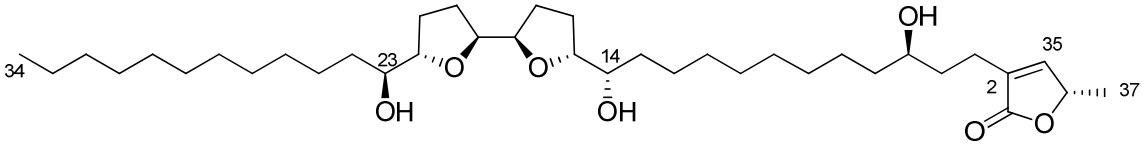

Uvaricin B (**2.3**)

Figure 2.1 Chemical Structure of Compounds **2.2** and **2.3**

2.2.2 *Structure Elucidation of Compound **2.2***

Uvaricin A, $[\alpha]^{21}_{D}$ +23 (*c* 0.12, MeOH), was isolated as a white wax-like solid. The positive ion HR–ESI–MS of uvaricin A revealed a quasi-molecular ion peak at *m/z* 623.4908 $[M+H]^+$ and adduct ions at *m/z* 640.5147 $[M+NH_4]^+$ and 645.4726 $[M+Na]^+$, corresponding to a molecular formula of $C_{37}H_{66}O_7$. The presence of a carbonyl absorption at 1747 cm^{-1} in its IR spectrum, a UV absorption at 210 nm (MeOH), ^{1}H NMR signals at δ_H 6.98 (H-35), 4.98 (H-36) and 0.88 (H-34),

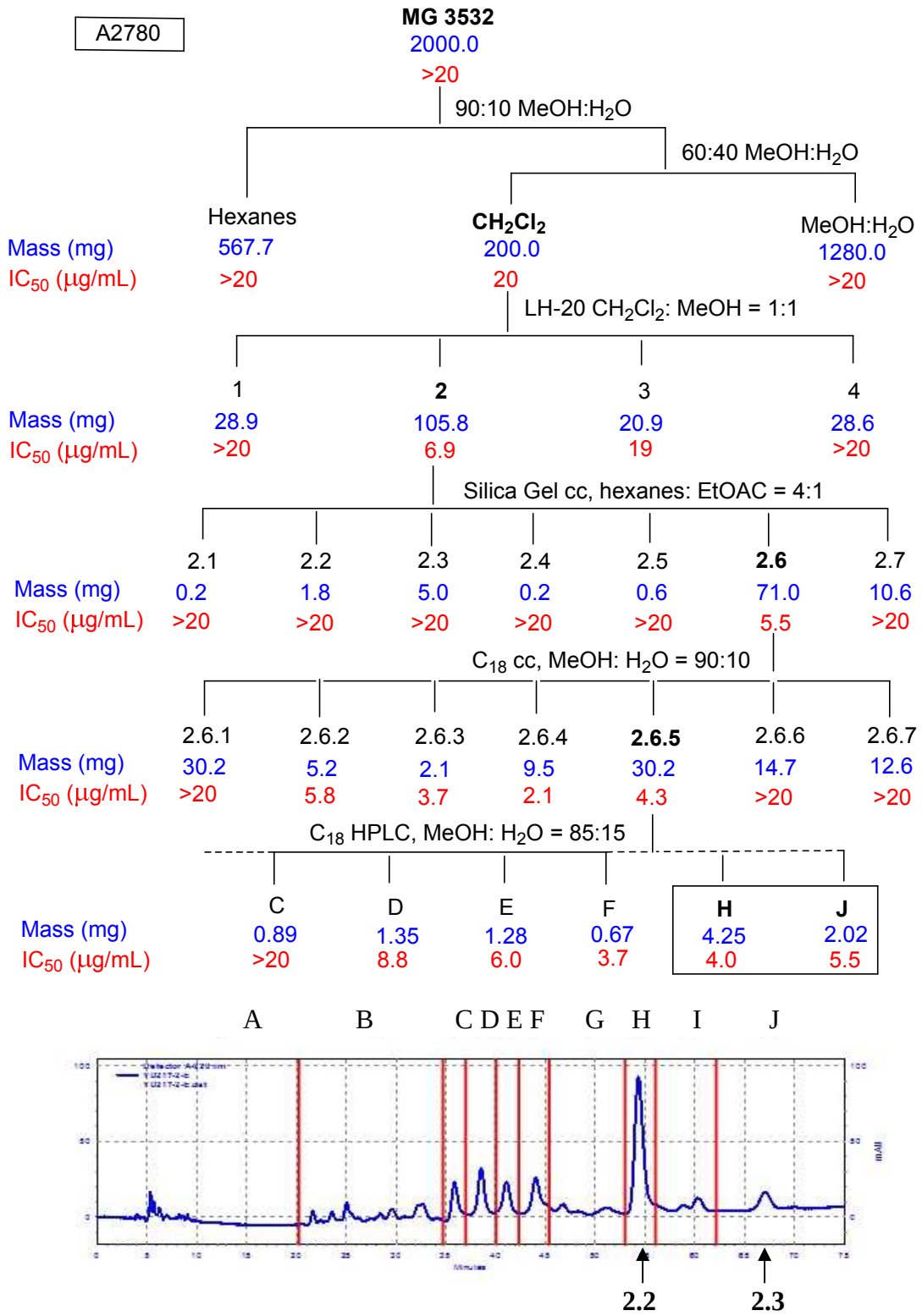

Scheme 2.1 Bioassay Guided Separation of the Extract of a *Uvaria sp.* and HPLC Chromatogram of fraction 2.6.5.

and ^{13}C NMR resonances at δ_C 174.2 (C-1), 149.1 (C-35), 134.6 (C-2), 77.6 (C-36), and 19.4 (C-37) are all characteristic spectroscopic features for a methylated α, β-unsaturated γ-lactone ring (**Table 2.1**).[11, 12] This structure was confirmed by three bond HMBC correlations observed between H-35 and C-1 and between H-35 and C-37, as well as two bond HMBC correlations between H-35 and C-2 and between H-36 and C-37, as shown in **Fig. 2.2**. In addition, the presence of three hydroxy functionalities in **2.2** was evident from the IR absorption at 3376 cm^{-1}, and the ^{13}C NMR resonances at δ_C 74.3 (C-21), 72.1 (C-8) and 71.6 (C-12). The presence of a *bis*-THF ring system with two flanking OH groups was suggested by the four ^{13}C NMR resonances at δ_C 83.5, 83.0, 82.8, and 82.5, which were correlated to the proton signals at δ_H 3.79–3.93 (5H) in the HMQC spectrum in the same way as described for similar structures.[13] The presence of the THF ring was confirmed by the HMBC correlations between C-13 and H-16. The one-bond ^{1}H–^{13}C correlations detected in the HMQC spectrum, along with the observed multiple-bond ^{1}H–^{13}C correlations in the HMBC spectrum, permitted the assignment of the carbon signals at δ_C 74.4 and 71.6 to the carbons adjacent to the THF rings at C-12 and C-21, respectively, with the proton signals at δ_H 3.39 and δ_H 3.87. The presence of a third hydroxy group in the hydrocarbon chain was suggested by the resonances at δ_H 3.60 and δ_C 72.1.

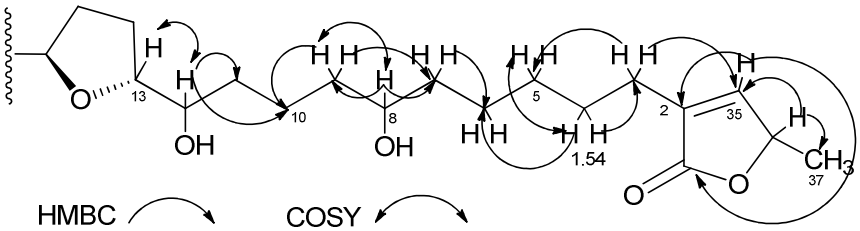

Figure 2.2 HMBC and COSY Correlations of Compound **2.2**

Table 2.1 NMR Spectroscopic Data for **2.2** and **2.3** in $CDCl_3$ (500 MHz)

	2.2		**2.3**	
position	δ_H (J in Hz)	δ_C, type	δ_H (J in Hz)	δ_C, type
1	-	174.2, C	-	174.0, C
2	-	134.6, C	-	133.9, C
3a	2.26 tdd (7.2, 1.6, 1.6)	25.1, CH_2	2.37 dtd (15.2, 7.6,1.6)	21.6, CH_2
3b	2.26 tdd (7.2, 1.6, 1.6)		2.51 dtd (15.2, 7.6,1.6)	
4	1.54 m	27.6, CH_2	1.65 m	35.4, CH_2
5	1.25 m	29.6–29.9, CH_2	3.60 m	70.9, CH
6	1.25 m	25.4, CH_2	1.39 m	37.6, CH_2
7	1.39–1.42 m	37.7, CH_2	1.48 m	26.1, CH_2
8	3.60 m	72.1, CH	1.26 m	29.6–29.8, CH_2
9	1.39–1.42 m	37.4, CH_2	1.26 m	29.6–29.8, CH_2
10	1.25 m	22.2, CH_2	1.26 m	29.6–29.8, CH_2
11	1.39–1.42 m	32.7, CH_2	1.26 m	29.6–29.8, CH_2
12	3.87 m	71.6, CH	1.48 m	25.6, CH_2
13	3.83 m	83.0, CH	1.41 m	32.5, CH_2
14a	1.62 m	28.6, CH_2	3.86 m	71.4, CH
14b	1.87 m			
15a	1.62 m	29.1, CH_2	3.83 m	82.9, CH
15b	1.87 m			
16a	3.93 m	82.5, CH	1.67 m	28.4, CH_2
16b			1.82 m	
17a	3.91 m	82.8, CH	1.67 m	29.0, CH_2
17b			1.82 m	
18a	1.60 m	29.1, CH_2	3.93 m	82.4, CH
18b	1.97 m			
19a	1.60 m	28.6, CH_2	3.91 m	82.6, CH
19b	1.97 m			
20a	3.84 m	83.5, CH	1.61 m	29.1, CH_2
20b			1.95 m	
21a	3.39 m	74.4, CH	1.61 m	29.4, CH_2
21b			1.95 m	
22	1.39–1.42 m	33.5, CH_2	3.84 m	83.3, CH
23	1.25 m	25.9, CH_2	3.37 m	74.2, CH
24	1.25 m	29.6–29.9, CH_2	1.41 m	33.5, CH_2
25	1.25 m	29.6–29.9, CH_2	1.48 m	25.7, CH_2
26–31	1.25 m	29.6–29.9, CH_2	1.26 m	29.6–29.8, CH_2
32	1.25 m	32.1, CH_2	1.26 m	32.00, CH_2
33	1.25 m	22.8, CH_2	1.26 m	22.8, CH_2
34	0.88 t (6.8)	14.3, CH_3	0.86 t (6.8)	14.2, CH_3
35	6.98 td (1.6, 1.6)	149.1, CH	7.05 td (1.6, 1.6)	149.3, CH
36	4.98 qdd (6.8, 1.6, 1.6)	77.6, CH	5.01 qd (6.8, 1.6)	77.7, CH
37	1.41, d (6.8)	19.4, CH_3	1.40 d (6.8)	19.3, CH_3

The locations of the THF rings and the third hydroxy group on the hydrocarbon chain were determined by analysis of 1D NMR, HMBC, HMQC, and COSY spectroscopic data, and further confirmed by analysis of EI–MS fragmentation. As illustrated in **Fig. 2.2**, in the vicinity of the THF moiety, the chemical shift at 22.2 ppm in the ^{13}C NMR spectrum was assigned to C-10 by the observation of an HMBC long-range correlation between H-12 (δ_H 3.87) and C-10 (δ_C 22.2). The third hydroxy group was then assigned to C-8 by the presence of HMBC correlations between H-9 and C-10, and H-8 and C-9, as well as the COSY coupling of H-9 and H-8. Meanwhile, at the end containing the lactone ring, the presence of an oxygen-bearing methine at C-8 could be confirmed by the HMBC correlations between H-9 and C-7, H-8 and C-7, H-7 and C-6, H-4 and C-6, H-4 and C-3, H-3 and C-5, and H-3 and C-35, as well as a COSY cross-peak between H-4 and H-5. The number of carbons between the THF rings and the lactone ring was therefore restricted to ten.

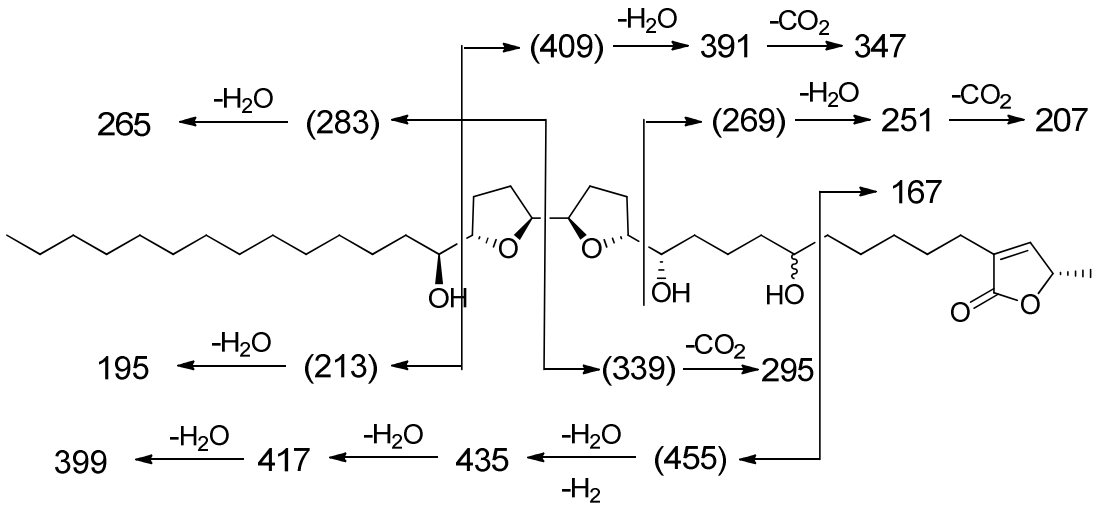

Figure 2.3 EI–MS Fragmentation of Compound **2.2**

The planar structure was further supported by the analysis of EIMS fragmentation. Intense fragment ions were observed at *m/z* 399, 347, 295, and 207. As shown in **Fig. 2.3**, the ion at *m/z* 295

is most probably formed by α-cleavage between the two THF rings, followed by loss of CO_2 from the lactone. A less intense ion at *m/z* 265 can be explained by a similar α-cleavage followed by loss of H_2O. The ion at *m/z* 399 is most probably due to α-cleavage adjacent to the C-8 hydroxy group, followed by loss of H_2O and H_2 to give a weak ion at *m/z* 435, and then successive losses of H_2O to give ions at *m/z* 417 and 399. The ion at *m/z* 207 must be formed by α-cleavage between C-12 and C-13 followed by loss of H_2O to give an ion at *m/z* 251, which then loses CO_2. Finally, the ion at *m/z* 347 is most probably formed by α-cleavage between C-20 and C-21, followed by loss of H_2O to give an ion at *m/z* 391, followed by loss of CO_2. Although these fragmentations have not been proved unambiguously, they are consistent with fragmentations observed for similar acetogenins, and they fully support the assigned structure.[14] In particular, the unusual loss of H_2O accompanied by H_2 has been observed before.[15]

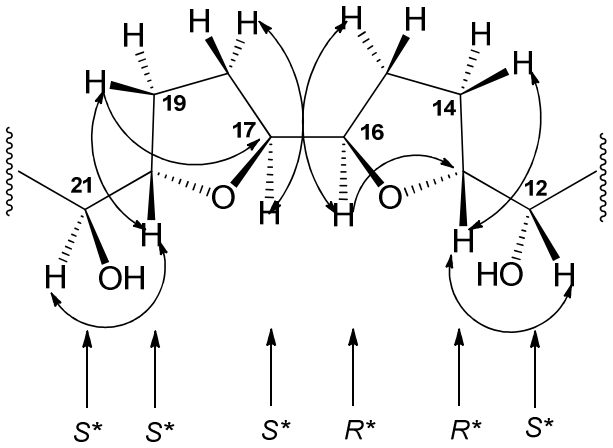

Figure 2.4 HMBC and COSY Correlation of *bis*-THF Rings of Compound **2.2**

The relative configurations around the *bis*-THF rings were determined by analysis of the data from the ^{1}H NMR spectrum and comparison with literature data. In **Fig. 2.4**, the chemical shifts at δ_H 3.39 (H-21) and 3.84 (H-20) indicated the *S** and *S** relative configurations of C-20 and C-21,

while the *S** and *R** relative configurations were deduced for C-12 and C-13 and for C-16 and C-17, due to the similarity of the chemical shift of H-12 (δ_H 3.87) and H-13 (δ_H 3.83), and H-16 (δ_H 3.93) and H-17 (δ_H 3.91).[16, 17] The methylene protons H-18 and H-19 were assigned to signals at δ_H 1.60 and 1.97, based on COSY correlations between H-20 and H-21, H-19 and H-20, and H-18 and H-17, combined with HMBC coupling between H-19 and C-17. The difference between these chemical shifts indicated a *trans* stereochemistry for the C-17/C-20 THF ring.[18] In the same manner, a *trans* configuration was assigned to the C-13/C-16 THF ring based on the divergent chemical shifts at δ_H 1.62 and 1.87 for H-14 and H-15.[18] From the above evidence, the relative configuration around the *bis*-THF rings was concluded to be *S**–*R**–*R**–*S**–*S**–*S** for C-12, C-13, C-16, C-17, C-20 and C-21 (*threo–trans–erythro–trans–erythro* configuration). The absolute configuration of C-36 was determined by electronic circular dichroism spectroscopic analysis. The negative n–π^* Cotton effect ($\Delta\varepsilon$= –1.13) at 238 nm and a positive π–π^* Cotton effect ($\Delta\varepsilon$ = 8.79) at 208 nm, clearly indicated an *S* configuration at this stereogenic center (C-36) in the lactone ring. The absolute configurations of the two hydroxy groups adjacent to the THF rings were determined by Mosher ester methodology[19] using the (*R*)–MPA and (*S*)–MPA derivatives[20] and the "in NMR tube" method.[21] As shown in **Fig. 2.5**, the $\Delta\delta_H$ (= $\delta_S - \delta_R$) was negative on both chain sides and positive along the THF rings, indicating *S* configurations at both C-12 and C-21.[22] The configuration of C-8 could not be determined due to the negative $\Delta\delta_H$ values displayed by both H-7 and H-9 on the hydrocarbon chain.

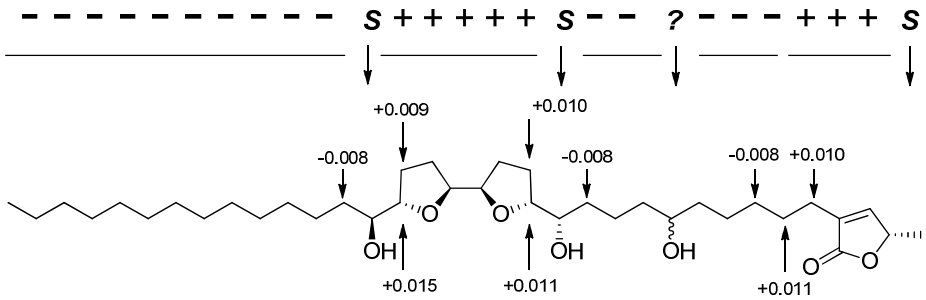

Figure 2.5 δ_H (= $\delta_S - \delta_R$) Data of (*R*) and (*S*)–MPA Derivatives of Compound **2.2**

Overall, the structure of compound **2.2** was concluded to be (5*S*)-3-((10*S*)-6,10-dihydroxy-10-((2*R*,2'*S*,5*R*,5'*S*)-5'-((*S*)-1-hydroxytetradecyl)octahydro-[2,2'-bifuran]-5-yl)decyl)-5-methylfuran-2(5*H*)-one. (The numbering is shown below)

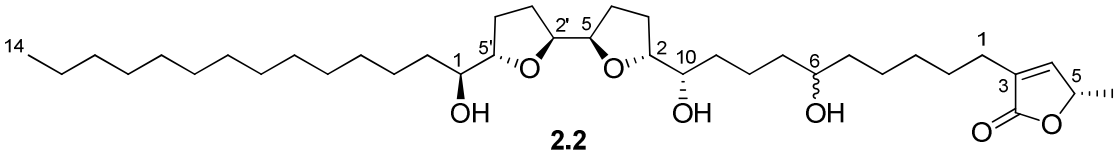

2.2.3 *Structure Elucidation of Compound **2.3***

Uvaricin B, $[\alpha]^{21}_{D}$ +18 (*c* 0.12, MeOH), was also isolated as a white wax-like solid. The positive ion HR–ESI–MS of uvaricin B revealed a quasi-molecular ion peak at *m/z* 623.4908 $[M+H]^+$ and adduct ions at *m/z* 640.5147 $[M+NH_4]^+$ and 645.4713 $[M+Na]^+$, corresponding to a molecular formula of $C_{37}H_{66}O_7$. The NMR spectroscopic, IR and UV data of compound **2.3** were very similar to those of compound **2.2**. As with compound **2.2**, the typical absorptions of a methylated *α*,*β*-unsaturated *γ*-lactone ring in its IR and UV spectra and of a *bis*-THF ring system with two flanking OH groups in the ^{1}H and ^{13}C NMR spectra were observed (**Table 2.1**). These structures were also confirmed by the long-range HMBC correlations as shown in **Fig. 2.6**. A third hydroxy group was also present in the hydrocarbon chain, as indicated by NMR signals at δ_H 3.60

and δ_C 70.9.

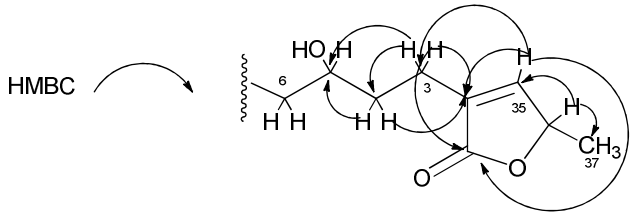

Figure 2.6. HMBC Correlations of Compound **2.2**

The locations of the THF rings and of the third hydroxy group on the hydrocarbon chain were determined by analysis of the 1D NMR, HMBC, HMQC, and COSY spectra, and further confirmed by analysis of EI–MS fragmentations. As illustrated in **Fig. 2.6**, two diastereotopic protons (δ_H 2.37/2.51) were assigned to H_2-3 based on HMBC correlations between H-3 and C-1, H-3 and C-2, and H-35 and C-3. The presence of an HMBC long-range coupling between a methylene carbon at δ_C 21.5 ppm and H-3, as well as its connected proton (δ_H 1.65) and C-2, confirmed the assignment of this methylene carbon at C-4. The adjacent oxygen bearing carbon was located at C-5 by the presence of HMBC correlations between H-4 and C-5, and H-3 and C-5. Hydroxylation at C-5 was confirmed by comparing the chemical shift of H-35 with those of other acetogenins of the same molecular formula with hydroxy groups at C-4, C-5, C-6, C-12 or C-15. As previously reported, the chemical shift of H-35 in C-5 hydroxylated acetogenins such as narumicin I (**2.4**) and calamistrin F (**2.5**)[23, 24] is always more shielded (δ_H 7.05) than with C-4 hydroxylated acetogenins, such as bullatacin (**2.6**, $\delta_{H\text{-}35}$ 7.16) and squamotacin (**2.7**, $\delta_{H\text{-}35}$ 7.17).[23] Its chemical shift is however deshielded compared with the corresponding protons of acetogenins without a hydroxy group near the lactone ring, such as the C-12 hydroxylated acetogenin, folianin B (**2.8**, $\delta_{H\text{-}35}$ 6.98)[24] and the C-15 hydroxylated acetogenin, guanaconetin-1 (**2.9**, $\delta_{H\text{-}35}$ 6.98).[25]

Acetogenins with a hydroxy group at C-5 could be distinguished from C-6 hydroxylated acetogenins by their divergent chemical shift at H-3, albeit sharing similar $\delta_{\text{H-35}}$ values.[26]

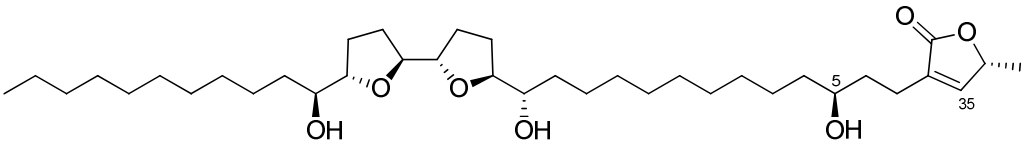

2.4

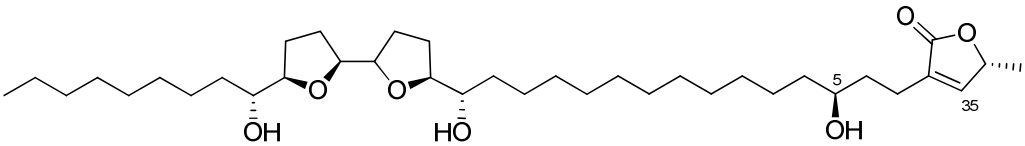

2.5

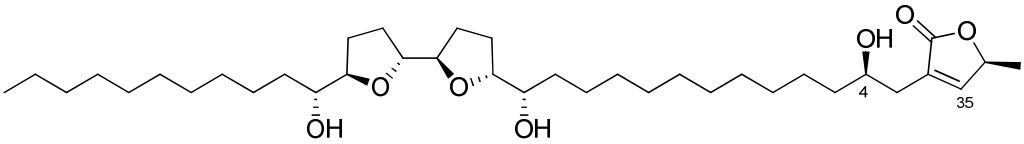

2.6

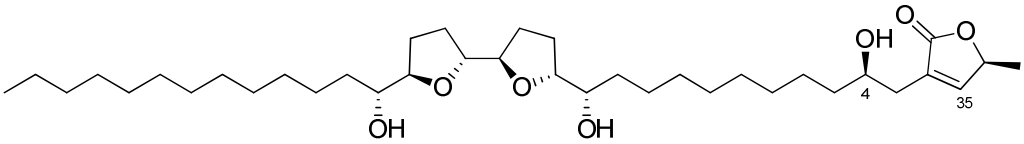

2.7

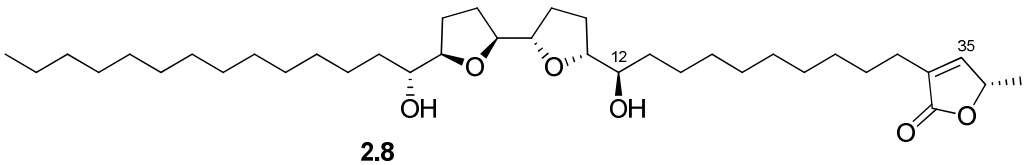

2.8

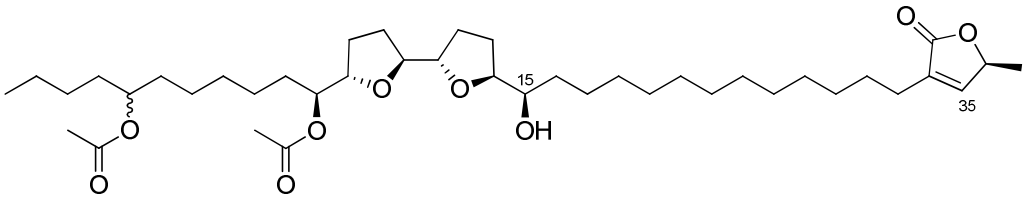

2.9

Analysis of the EI–MS fragmentation supported the above structure. The fragment ions at *m/z* 155 and 135 are consistent with the conclusion that the third hydroxy group is connected to C-5,

while the fragment ions at *m/z* 437, 367, 355, and 267 and their subsequent daughter ions indicated that the *bis*-THF rings and the two flanking hydroxy groups are located between C-14 and C-23 (**Fig. 2.7**).

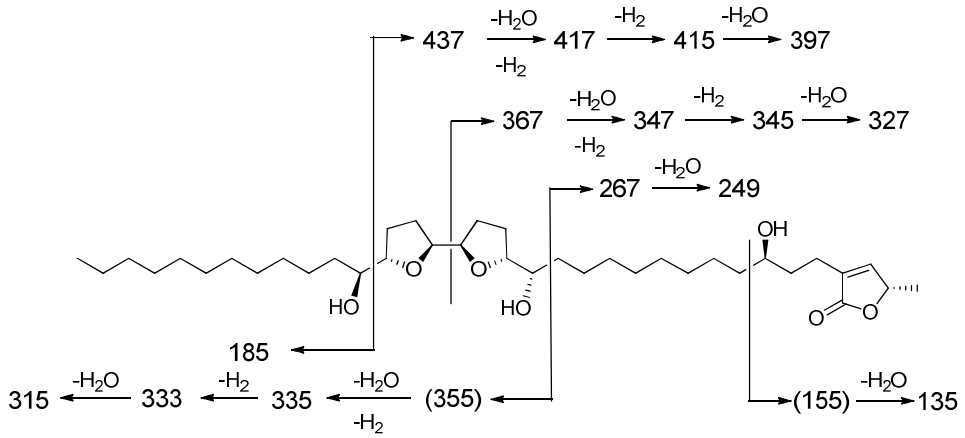

Figure 2.7 EI-MS Fragmentation of Compound **2.3**.

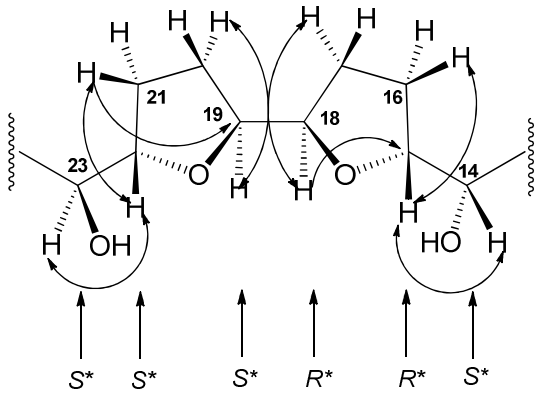

Figure 2.8 HMBC and COSY Correlation of *bis*-THF Rings of Compound **2.3**

The relative configurations around the *bis*-THF rings were determined by examination of the data from proton NMR spectra and comparison to those in the literature. As shown in **Fig. 2.8**, the ^{1}H NMR chemical shifts around the *bis*-THF rings for compound **2.3** were similar to those of compound **2.2**, and the relative configurations were therefore assigned as *S**–*R**–*R**–*S**–*S**–*S**

for C-14, C-15, C-17, C-18, C-22 and C-23 (*threo–trans–erythro–trans–erythro* configuration). The CD spectrum of **2.3** revealed a negative n–π^* Cotton effect ($\Delta\varepsilon = -1.15$) at 238 nm and a positive π–π^* Cotton effect ($\Delta\varepsilon = 9.64$) at 208 nm, indicating an *S* configuration at the stereogenic center (C-36) in the lactone ring.[15] The absolute configurations of the three secondary alcohols were determined by Mosher ester methodology in the same way as for **2.2**. As depicted in **Fig. 2.9**, the $\Delta\delta_H$ (= $\delta_S - \delta_R$) is negative on the chain side and positive towards the THF rings, indicating the *S* configuration of both C-14 and C-23.[22] The positive values for H-3 and H-4 and negative values for H-6 to H-8 indicated an *S* configuration for C-5.

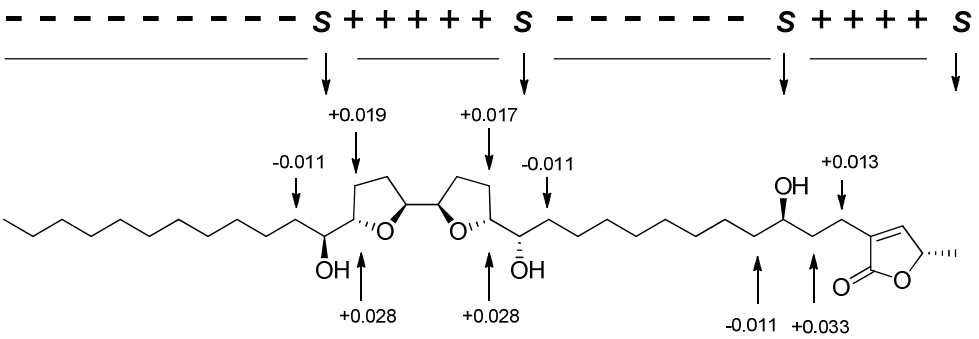

Figure 2.9 δ_H (= $\delta_S - \delta_R$) Data of (*R*) and (*S*)–MPA Derivatives of Compound **2.3**.

Overall, the structure of compound **2.3** was concluded to be (5*S*)-3-((3*R*,12*S*)-3,12-dihydroxy-12-((2*R*,2'*S*,5*R*,5'*S*)-5'-((*S*)-1-hydroxydodecyl)octahydro-[2,2'-bifuran]-5-yl)dodecyl)-5-methylfuran-2(5*H*)-one. (The numbering is shown below)

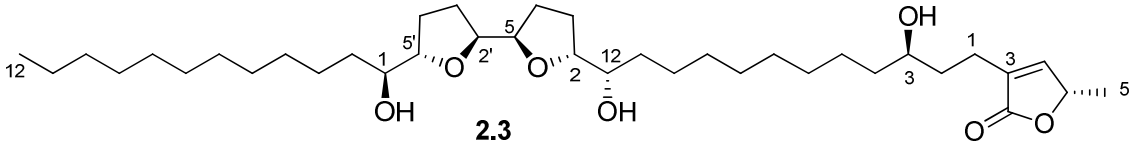

2.3

2.2.4 *Antiproliferative Activities of the Isolated Compounds.*

Uvaricin A (**2.2**) and B (**2.3**) were tested for antiproliferative activity against the A2780 ovarian cancer, the A2058 melanoma, and the H522 lung cancer cell lines (**Table 2.2**).

Both compounds showed modest inhibition of all three cell lines, with IC_{50} values in the low micromolar range. Several hundred acetogenins have been identified from these plants, but not all of them have antiproliferative activity. According to previous studies of the structure–activity relationships of acetogenins, the relative stereochemistry of the THF rings and the positions of the hydroxy groups on the hydrocarbon chains have significant influence on their activities. The *threo–cis–threo–cis–erythro* configuration was described as the most potent subgroup of acetogenins with *bis*-THF rings;[27] as an example, rolliniastatin-1 has an IC_{50} value of 0.7×10^{-7} μM against SW480 human colon cancer cells.[28] In addition, the presence of two hydroxy groups adjacent to the THF rings is necessary for potent inhibitory effects. The moderate cytotoxicity of uvaricins A and B can thus be explained by the stereochemistry of the *bis*-THF rings flanked by the two hydroxy groups, whose configuration is different from that of rolliniastatin-1. The modest antiproliferative activity of may also be due to the number and the location of the hydroxy groups.[29, 30]

Table 2.2 Antiproliferative Activities of Compounds **2.2** and **2.3**

	IC_{50} (μM)		
Compound	A2780	A2058	H522
2.2	6.4 ± 0.8	6.6	>3.3, <10
2.3	8.8 ± 1.4	7.2	>3.3, <10
Paclitaxel	0.02 ± 0.003	ND	ND

2.3 Experimental Section

2.3.1 *General Experimental Procedures.*

Optical rotations were recorded on a JASCO P-2000 polarimeter. UV and IR spectroscopic data were measured on a Shimadzu UV-1201 spectrophotometer and a MIDAC M-series FTIR spectrophotometer, respectively. CD spectra were obtained on a JASCO J-815 Circular Dichroism spectrometer. NMR spectra were recorded in CD_3OD or $CDCl_3$ on either JEOL Eclipse 500 or Bruker Avance 600 spectrometers. The chemical shifts are given in δ (ppm), and coupling constants (*J*) are reported in Hz. Mass spectra were obtained on an Agilent 6220 LC–TOF–MS in the positive ion mode. HPLC was performed on a Shimadzu LC-10AT instrument with a semi-preparative C_{18} Varian Dynamax column (5 μm, 250 × 10 mm).

2.3.2 *Antiproliferative Bioassay*

The A2780 ovarian cancer cell line assay was performed by Ms. Peggy Brodie at Virginia Polytechnic Institute and State University. In brief, as previously reported, "Human ovarian cancer cells (A2780) grown to 95% confluency were harvested and resuspended in growth medium (RPMI1640 supplemented with 10% fetal bovine serum and 2 mM L-glutamine). Cells were counted using a hemacytometer and a solution containing 2.5 $x10^5$ cells per mL was prepared in growth media. Eleven columns of a 96 well microtitre plate were seeded with 199 μL of cell suspension per well, and the remaining column contained media only (one hundred percent inhibition control). The plate was incubated for 3 hours at 37 ºC/5% CO_2 to allow the cells to adhere to the wells. Following this incubation, potential cytotoxic agents, prepared in DMSO, were

added to the wells in an appropriate series of concentrations, 1 μL per well. One column of wells was left with no inhibitor (zero percent inhibition control), and 4 dilutions of a known compound (paclitaxel or actinomycin) was included as a positive control. The plate was incubated for 2 days at 37 ºC/5% CO_2, then the media gently shaken from the wells and replaced with reaction media (supplemented growth medium containing 1% Alamar Blue), and incubated for another 3 hours. The level of alamarBlue converted to a fluorescent compound by living cells was then analyzed using a Cytofluor Series 4000 plate reader (Perseptive Biosystems) with an excitation wavelength of 530 nm, an emission wavelength of 590 nm, and gain of 45. The percent inhibition of cell growth was calculated using the zero percent and one hundred percent controls present on the plate, and an IC_{50} value (concentration of cytotoxic agent which produces 50% inhibition) was calculated using a linear extrapolation of the data which lie either side of the 50% inhibition level. Samples were analyzed in triplicate on at least two separate occasions to produce a reliable IC_{50} value.[31] The A2780 cell line is a drug sensitive ovarian cancer cell line.[32]

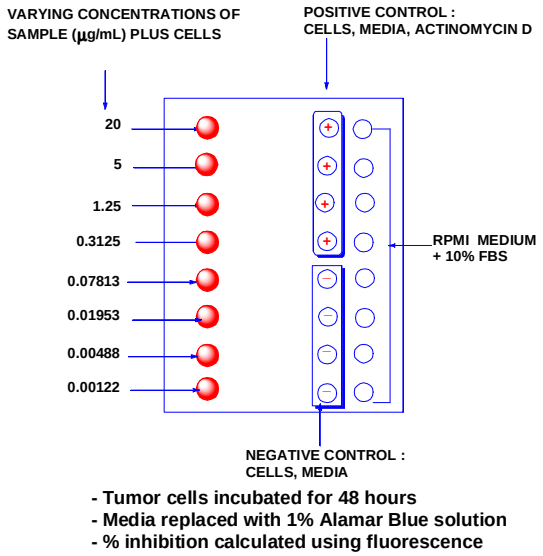

Scheme 2.2 A2780 assay: 96–well Plate Template

2.3.3 *Plant Material*

A sample of the above-ground parts of *Uvaria sp.* was collected in July 2005. The collected plant was a liana with immature yellowish green fruit, and probably represents a new species still to be described.[33] The collection was made in dry degraded evergreen broadleaf forest near Betsimiranjana, in the Ambilobe region of Madagascar, at coordinates 13°02'35"S 049°09'15"E. Voucher specimens have been deposited at the Parc Botanique and Zoologique de Tsimbazaza (TAN), at the Centre National d'Application des Recherches Pharmaceutiques in Antananarivo, Madagascar (CNARP), the Missouri Botanical Garden in St. Louis, Missouri (MO), and the Muséum National d'Histoire Naturelle in Paris, France (P), voucher Stéphan Rakotonandrasana et al. 923.

2.3.4 *Extraction and Isolation*

Dried aerial parts of *Uvaria sp.* (250 g) were ground in a hammer mill, then extracted with EtOH by percolation for 24 h at room temperature to give the crude extract MG 3352 (24.9 g), of which 6.9 g was shipped to Virginia Tech for bioassay guided isolation. A 1.0 g sample of MG 3352 (IC_{50} 20.0 μg/mL) was suspended in aqueous MeOH (MeOH/H_2O, 9:1, 100 mL), and extracted with hexanes (3 × 100 mL portions). The aqueous layer was then diluted to 60% MeOH (v/v) with H_2O and extracted with CH_2Cl_2 (3 × 150 mL portions). The hexanes fraction was evaporated in vacuo to leave 567 mg of material with IC_{50} > 20 μg/mL. The residue from the CH_2Cl_2 fraction (200 mg) had an IC_{50} of 20 μg/mL, and the remaining aqueous MeOH fraction had an IC_{50} > 20 μg/mL. LH-20 size exclusion open column chromatography of the CH_2Cl_2 fraction

was used to obtain four fractions, of which the most active fraction (106 mg) had an IC_{50} of 6.9 μg/mL. This fraction was then applied to a silica gel column with elution by a gradient of hexanes/EtOAc, 9:1, 4:1, and 0:1 to give four fractions, of which the 100% EtOAc fraction (71.0 mg) was the most active (IC_{50} 5.5 μg/mL). A C_{18} open column was employed for further separation, eluted by 90% MeOH to give 8 fractions, and the most active one (IC_{50} 4.3 μg/mL) was separated by C_{18} HPLC on a column that had previously seen an ammonia modifier with the solvent system MeOH/H_2O, 85:15 and a flow rate of 2 mL/min. This yielded two active compounds, with IC_{50} values of 4.0 and 5.5 μg/mL, and with elution times of 28.3 and 35.0 min, respectively.

2.3.5 *Preparation of the (R)– and (S)–MPA Ester Derivatives of* ***2.2*** *and* ***2.3***.

In a 25-mL round-bottom flask, 5.00 mg *R*–(–)-*α*-methoxyphenylacetic acid ((*R*)–MPA) were dissolved in 5 mL CH_2Cl_2 and 15 mg oxalyl chloride. Several drops of dimethylformamide were added to the reaction system as a catalyst. The reactants were mixed with a magnetic stir bar in an ice bath for 1 h to obtain 4.98 mg (*R*)–MPA chloride (91% yield). The in-NMR tube reaction was carried out to prepare the MPA ester derivatives.[21] The selected acetogenin (0.2 mg) dissolved in $CDCl_3$ was transferred to a clean NMR tube and the solvent was completely evaporated. (*R*)–MPA chloride (0.5 mg) was dissolved in $CDCl_3$ (0.5 mL) and added to the NMR tube immediately under an N_2 gas flow, and the NMR tube was shaken carefully to mix the acetogenin and (*R*)–MPA chloride. The reaction NMR tube was kept at room temperature under N_2 for 6 hours to form the (*R*)–MPA ester and was then analyzed by ^{1}H NMR spectroscopy. The (*S*)–MPA ester of the acetogenin was prepared from (*S*)–MPA by the same method.

2.3.6. *(5S)-3-((10S)-6,10-dihydroxy-10-((2R,2'S,5R,5'S)-5'-((S)-1-hydroxytetradecyl)octahydro-[2,2'-bifuran]-5-yl)decyl)-5-methylfuran-2(5H)-one (Uvaricin A, **2.2**).*

White wax-like solid; $[\alpha]_D^{21}$ +23 (*c* 0.12, MeOH); UV (MeOH) λ_{max} (ε) 210 (2.60); IR ν_{max} cm^{-1}: 3376, 2920, 1748, 1466, 1027 cm^{-1}. ^1H NMR (500 MHz, $CDCl_3$), and ^{13}C NMR (125 MHz, $CDCl_3$), see **Table 2.1**; HR–ESI–MS *m/z* 645.4726 $[M+Na]^+$ (calc. for $C_{37}H_{66}NaO_7^+$, 645.4701).

2.3.7 *(5S)-3-((3R,12S)-3,12-dihydroxy-12-((2R,2'S,5R,5'S)-5'-((S)-1-hydroxydodecyl)octahydro-[2,2'-bifuran]-5-yl)dodecyl)-5-methylfuran-2(5H)-one (Uvaricin B, **2.3**).*

White wax-like solid; $[\alpha]_D^{21}$ +18 (*c* 0.12, MeOH); UV (MeOH) λ_{max} (ε) 210 (2.20); IR ν_{max} cm^{-1}: 3449, 2923, 1753, 1460, 1024 cm^{-1}. ^1H NMR (500 MHz, $CDCl_3$), and ^{13}C NMR (125 MHz, $CDCl_3$), see **Table 2.1**; HR–ESI–MS *m/z* 645.4713 $[M+Na]^+$ (calc. for $C_{37}H_{66}NaO_7^+$, 645.4701).

2.4 References and Notes

1. Dai, Y.; Harinantenaina, L.; Brodie, P. J.; Callmander, M. W.; Randrianaivo, R.; Rakotonandrasana, S.; Rakotobe, E.; Rasamison, V. E.; Shen, Y.; TenDyke, K.; Suh, E. M.; Kingston, D. G. I. Antiproliferative acetogenins from a *Uvaria sp.* from the Madagascar dry forest. *J. Nat. Prod.* **2011,** *75*, 479–483.

2. Alali, F. Q.; Kaakeh, W.; Bennett, G. W.; McLaughlin, J. L. Annonaceous acetogenins as natural pesticides: potent toxicity against insecticide-susceptible and -resistant German cockroaches (Dictyoptera: Blattellidae). *J. Econ. Entomol.* **1998,** *91*, 641–649.

3. Liu, H. X.; Huang, G. R.; Zhang, H. M.; Wu, J. R.; Yao, Z. J. Annonaceous acetogenin mimics bearing a terminal lactam and their cytotoxicity against cancer cells. *Bioorg. Med. Chem. Lett.* **2007,** *17*, 3426–3430.

4. Yuan, S. S.; Chang, H. L.; Chen, H. W.; Kuo, F. C.; Liaw, C. C.; Su, J. H.; Wu, Y. C. Selective cytotoxicity of squamocin on T24 bladder cancer cells at the S-phase via a Bax-, Bad-, and caspase-3-related pathways. *Life Sci.* **2006,** *78*, 869–874.

5. Pomper, K. W.; Lowe, J. D.; Crabtree, S. B.; Keller, W. Identification of Annonaceous acetogenins in the ripe fruit of the North American pawpaw (*Asimina triloba*). *J. Agric. Food Chem.* **2009,** *57*, 8339–8343.

6. Parmar, V. S.; Tyagi, O. D.; Malhotra, A.; Singh, S. K.; Bisht, K. S.; Jain, R. Novel constituents of *Uvaria* species. *Nat. Prod. Rep.* **1994,** *11*, 219–224.

7. Yang, X. N.; Chen, H. S. Advances in study on chemical constituents and pharmacology of *Uvaria*. *Yaoxue Shijian Zazhi* **2009,** *27*, 81–83.

8. Padma, P.; Khosa, R. L.; Sahai, M. Acetogenins from the genus *Annona*. *Indian J. Nat. Prod.* **1996,** *12*, 3–21.

9. Jolad, S. D.; Hoffmann, J. J.; Schram, K. H.; Cole, J. R.; Tempesta, M. S.; Kriek, G. R.; Bates, R. B. Uvaricin, a new antitumor agent from *Uvaria accuminata* (Annonaceae). *J. Org. Chem.* **1982,** *47*, 3151–3153.

10. Madagascar Catalogue, 2011. *Catalogue of the Vascular Plants of Madagascar*. http://www.tropicos.org/project/mada (Accessed Nov. 16, 2011).

11. Liaw, C. C.; Chang, F. R.; Chen, Y. Y.; Chiu, H. F.; Wu, M. J.; Wu, Y. C. New Annonaceous acetogenins from *Rollinia mucosa*. *J. Nat. Prod.* **1999,** *62*, 1613–1617.

12. Hui, Y. H.; Rupprecht, J. K.; Liu, Y. M.; Anderson, J. E.; Smith, D. L.; Chang, C. J.; McLaughlin, J. L. Bullatacin and bullatacinone: two highly potent bioactive acetogenins from *Annona bullata*. *J. Nat. Prod.* **1989,** *52*, 463–477.

13. Santos, L. A. R. D.; Boaventura, M. A. D.; Pimenta, L. P. S. Cornifolin, a new *bis*-tetrahydrofuran Annonaceous acetogenin from *Annona cornifolia*. *Biochem. System. Ecol.* **2006,** *34*, 78–82.

14. Chang, F. R.; Wu, Y. C. Novel cytotoxic Annonaceous acetogenins from *Annona muricata*. *J. Nat. Prod.* **2001,** *64*, 925–931.

15. Lima, L. A. R. S.; Pimenta, L. P. S.; Boaventura, M. A. D. Acetogenins from *Annona cornifolia* and their antioxidant capacity. *Food Chem.* **2010,** *122*, 1129–1138.

16. Fang, X. P.; Gu, Z. M.; Rieser, M. J.; Hui, Y. H.; McLaughlin, J. L.; Nonfon, M.; Lieb, F.; Moeschler, H. F.; Wendisch, D. Structural revisions of some non-adjacent *bis*-tetrahydrofuran

Annonaceous acetogenins. *J. Nat. Prod.* **1993,** *56*, 1095–1100.

17. Queiroz, E. F.; Roblot, F.; Cavé, A.; Hocquemiller, R.; Serani, L.; Laprévote, O.; Paulo, M. d. Q. A new *bis*-tetrahydrofuran acetogenin from the roots of *Annona salzmanii*. *J. Nat. Prod.* **1999,** *62*, 710–713.

18. Gu, Z. M.; Fang, X. P.; Zeng, L.; Kozlowski, J. F.; McLaughlin, J. L. Novel cytotoxic Annonaceous acetogenins: (2,4-*cis* and *trans*)-bulladecinones from *Annona bullata* (annonaceae). *Bioorg. Med. Chem. Lett.* **1994,** *4*, 473–478.

19. Rieser, M. J.; Hui, Y. H.; Rupprecht, J. K.; Kozlowski, J. F.; Wood, K. V.; McLaughlin, J. L.; Hanson, P. R.; Zhuang, Z.; Hoye, T. R. Determination of absolute configuration of stereogenic carbinol centers in Annonaceous acetogenins by proton and fluorine 19-NMR analysis of Mosher ester derivatives. *J. Am. Chem. Soc.* **1992,** *114*, 10203–10213.

20. Latypov, S. K.; Seco, J. M.; Quinoa, E.; Riguera, R. MTPA vs MPA in the determination of the absolute configuration of chiral alcohols by ^{1}H NMR. *J. Org. Chem.* **1996,** *61*, 8569–8577.

21. Su, B. N.; Park, E. J.; Mbwambo, Z. H.; Santarsiero, B. D.; Mesecar, A. D.; Fong, H. H. S.; Pezzuto, J. M.; Kinghorn, A. D. New chemical constituents of *Euphorbia quinquecostata* and absolute configuration assignment by a aonvenient mosher ester procedure carried out in NMR tubes. *J. Nat. Prod.* **2002,** *65*, 1278–1282.

22. Zhao, G. X.; Gu, Z. M.; Zeng, L.; Chao, J. F.; Kozlowski, J. F.; Wood, K. V.; McLaughlin, J. L. The absolute configuration of trilobacin and trilobin, a novel highly potent acetogenin from the stem bark of *Asimina triloba* (Annonaceae). *Tetrahedron* **1995,** *51*, 7149–7160.

23. Hopp, D. C.; Zeng, L.; Gu, Z. M.; McLaughlin, J. L. Squamotacin: An Annonaceous

acetogenin with cytotoxic selectivity for the human prostate tumor cell line (PC-3). *J. Nat. Prod.* **1996,** *59*, 97–99.

24. Lima, L. A. R. S.; Pimenta, L. P. S.; Boaventura, M. A. D. Two new adjacent *bis*-tetrahydrofuran Annonaceous acetogenins from seeds of *Annona cornifolia*. *Planta Med.* **2009,** *75*, 80–83.

25. Chahboune, N.; Barrachina, I.; Royo, I.; Romero, V.; Sáez, J.; Tormo, J. R.; De Pedro, N.; Estornell, E.; Zafra-Polo, M. C.; Peláez, F.; Cortes, D. Guanaconetins, new antitumoral acetogenins, mitochondrial complex I and tumor cell growth inhibitors. *Bioorg. Med. Chem.* **2006,** *14*, 1089–1094.

26. Hopp, D. C.; Alali, F. Q.; Gu, Z. M.; McLaughlin, J. L. Three new bioactive *bis*-adjacent THF-ring acetogenins from the bark of *Annona squamosa*. *Bioorg. Med. Chem.* **1998,** *6*, 569–575.

27. Royo, I.; DePedro, N.; Estornell, E.; Cortes, D.; Pelaez, F.; Tormo, J. R. In vitro antitumor SAR of *threo/cis/threo/cis/erythro bis*-THF acetogenins: correlations with their inhibition of mitochondrial complex I. *Oncology Res.* **2003,** *13*, 521–528.

28. Gonzalez-Coloma, A.; Guadano, A.; de Ines, C.; Martinez-Diaz, R.; Cortes, D. Selective action of acetogenin mitochondrial complex I inhibitors. *Z. Naturforsch. C* **2002,** *57*, 1028–1034.

29. Abe, M.; Kenmochi, A.; Ichimaru, N.; Hamada, T.; Nishioka, T.; Miyoshi, H. Essential structural features of acetogenins: role of hydroxy groups adjacent to the *bis*-THF rings. *Bioorg. Med. Chem. Lett.* **2004,** *14*, 779–782.

30. Kojima, N.; Tanaka, T. Medicinal chemistry of Annonaceous acetogenins: design, synthesis, and biological evaluation of novel analogues. *Molecules* **2009,** *14*, 3621–3661.

31. Cao, S.; Brodie, P. J.; Miller, J. S.; Randrianaivo, R.; Ratovoson, F.; Birkinshaw, C.; Andriantsiferana, R.; Rasamison, V. E.; Kingston, D. G. I. Antiproliferative xanthones of *Terminalia calcicola* from the Madagascar rain forest. *J. Nat. Prod.* **2007,** *70*, 679–681.

32. Louie, K. G.; Behrens, B. C.; Kinsella, T. J.; Hamilton, T. C.; Grotzinger, K. R.; McKoy, W. M.; Winker, M. A.; Ozols, R. F. Radiation survival parameters of antineoplastic drug-sensitive and -resistant human ovarian cancer cell lines and their modification by buthionine sulfoximine. *Cancer Res.* **1985,** *45*, 2110–2115.

33. Madagascar Catalogue. http://www.tropicos.org/Specimen/2822281 (Accessed Nov. 16, 2011).

Chapter 3: Isolation and Synthesis of Antiproliferative Calamenene-type Sesquiterpenoids from *Sterculia tavia* from the Madagascar Rain Forest

This chapter is a slightly expanded version of a published article. (Dai, Y.; Harinantenaina, L.; Brodie, P. J.; Callmander, M. W.; Randrianasolo, S.; Rakotobe, E.; Rasamison, V. E.; Kingston, D. G. I. Isolation and synthesis of two antiproliferative calamenene-type sesquiterpenoids from *Sterculia tavia* from the Madagascar rain forest. *Bioorg. Med. Chem.* **2012,** *20*, 6940–6944.) Attributions of co-authors of the articles are described as follows in the order of the names listed. The author of this dissertation (Mr. Yumin Dai) conducted the isolation and structural elucidation part of the titled compounds, and drafted the manuscript. Dr. Liva Harinantenaina was a mentor for this work, and in particular, he provided invaluable advice and hints for the structural elucidation of that compound, and he also proofread the manuscript before submission. Ms. Peggy Brodie performed the A2780 bioassay on the isolated fractions and compounds. Dr. Martin W. Callmander and Dr. Sennen Randrianasolo from Missouri Botanical Garden did the plant collections and identification. Dr. Etienne Rakotobe and Dr. Vincent E. Rasamison from Madagascar carried out the initial plant extraction. Dr. David G. I. Kingston was a mentor for this work and the corresponding author for the published article. He provided critical suggestions for this work and edited the final version of the manuscript.[1]

3.1 Introduction

Discovering antiproliferative natural products from both tropical dry forests and rainforests of Madagascar has been one of the objectives of our group's involvement for more than 15 years in the International Cooperative Biodiversity Group (ICBG) program.[2-5] As a part of this research, an

EtOH extract from the bark of *Sterculia tavia* (Malvaceae) from the rain forest of northern Madagascar was found to exhibit antiproliferative activity against the A2780 human ovarian cancer cell line, with an IC_{50} value of 14 μg/mL. The Malvaceae family is a family of flowering plants containing over 200 genera with close to 2,300 species.[6] *Sterculia*, one of the largest genera of this family, is a rich source of alkaloids, saponins and flavonoid glycosides, which are well-known for their broad range of bioactivity, including antimicrobial, antifungal, insecticidal, cytotoxic, antioxidant, and anti-inflammatory activities among others.[7-10] 2*n*-(octylcycloprop-*α*-enyl)octanoic acid (**3.1**) and taraxer-14-en-3-*β*-ol (**3.2**) listed are two examples of bioactive compounds isolated from the genus *Sterculia.* Although the genus *Sterculia* has been well investigated, the present species is endemic to Madagascar and has not been explored for its phytochemical composition and biological activity. The EtOH extract of *S. tavia* was thus selected for bioassay guided fractionation to isolate its antiproliferative components.

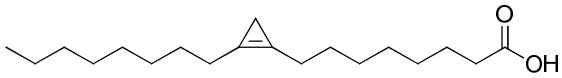

3.1

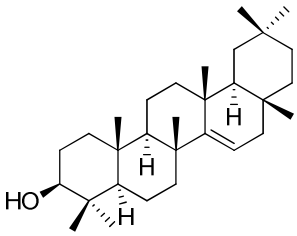

3.2

3.2 Results and Discussion

3.2.1 *Isolation of Active Compounds*

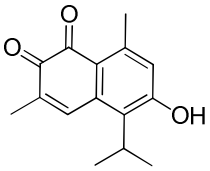

3.3

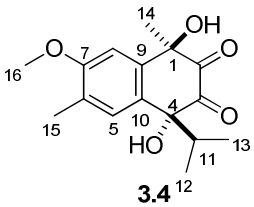

3.4

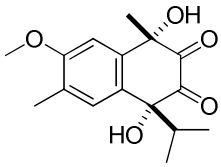

3.5

Figure 3.1 Chemical Structure of Compounds **3.4–3.5**

The EtOH extract of the bark part of the *S. tavia* was subjected to liquid–liquid partitioning to

give an active CH_2Cl_2 fraction with an IC_{50} value of 9.6 μg/mL. Bioassay guided separation, including LH-20 size exclusion, normal-phase silica gel chromatography, and C_{18} reverse-phase HPLC, was used to obtain the known cadinane-type sesquiterpenoid mansonone (**3.3**), and the two new calamenene-type sesquiterpenoids designated tavinin A (**3.4)** and *epi*-tavinin A (**3.5**) as the major antiproliferative constituents of the extract (**Scheme 3.1**). Herein, we report the structural elucidation and synthesis of the two new compounds.

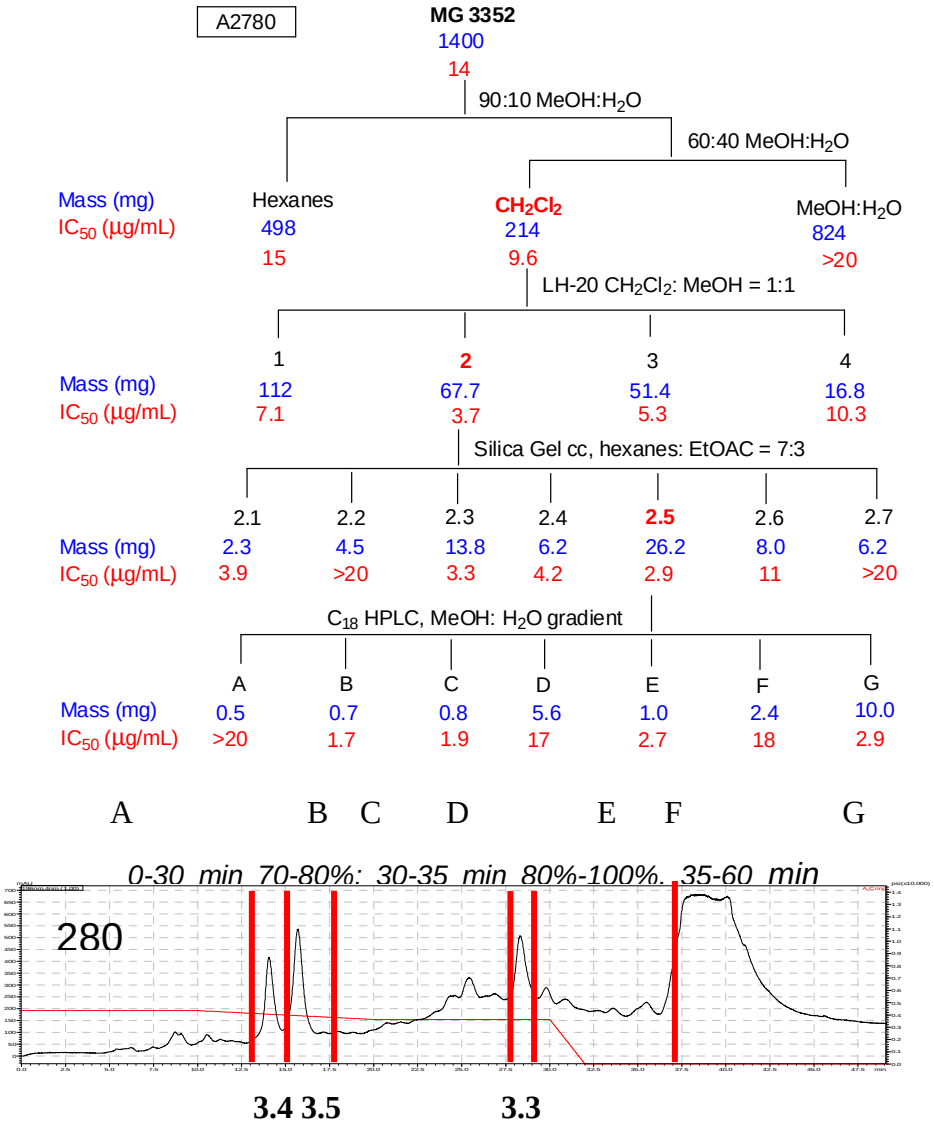

Scheme 3.1 Bioassay Guided Separation of the Extract of *Sterculia tavia* and HPLC Chromatogram of Fraction 2.5

3.2.2 *Structure Elucidation of Compound **3.3***

Compound **3.3** was identified as the cadinane-type sesquiterpenoid mansonone G (6-hydroxy-5-isopropyl-3,8-dimethyl-naphthalene-1,2-dione) by comparison of its physical and spectroscopic data with those reported in the literature.[11, 12]

Table 3.1 NMR Spectroscopic Data for **3.4** and **3.5** in acetone-d_6 (600 MHz)

	3.4		**3.5**	
position	δ_H (J in Hz)	δ_C,[a] type	δ_H (J in Hz)	δ_C[a], type
1	-	73.8, C	-	74.7, C
2	-	204.0, C	-	208.2, C
3	-	196.7, C	-	200.7, C
4	-	88.9, C	-	91.2, C
5	7.64 s	127.8, CH	7.68 s	128.1, CH
6	-	116.7, C	-	116.9, C
7	-	162.9, C	-	163.2, C
8	7.37 s	107.4, CH	7.33 s	108.0, C
9	-	145.3, C	-	144.8, C
10	-	123.1, C	-	122.8, C
11	2.52 sept	36.1, CH	2.35 sept	35.6, CH
12	0.67 d (6.7)	15.4, CH_3	0.81 d (6.7)	15.6, CH_3
13	0.88 d (6.7)	15.9, CH_3	0.90 d (6.7)	16.2, CH_3
14	1.62 s	28.1, CH_3	1.86 s	27.4, CH_3
15	2.27 s	15.1, CH_3	2.27 s	15.1, CH_3
16	4.04 s	55.5, CH_3	4.05 s	55.5, CH_3

[a]The ^{13}C NMR spectral data were generated from gHSQC and gHMBC spectra.

3.2.3 *Structure Elucidation of Compound **3.4***

Tavinin A (**3.4**), $[\alpha]^{21}_{D}$ +15 (*c* 0.12, MeOH), was isolated as a light yellow oil. Its positive ion HR–ESI–MS revealed quasi-molecular ion peaks at *m/z* 293.1399 $[M+H]^+$ and 315.1194 $[M+Na]^+$, corresponding to a molecular formula of $C_{16}H_{20}O_5$, with seven degrees of unsaturation. Based on the similarity of the NMR spectral data of **3.4** and those of compound **3.3**, compound **3.4** was identified as a sesquiterpenoid with a similar carbon skeleton. The six aromatic ^{13}C NMR resonances: δ_C 162.9, 145.3, 127.8, 123.1, 116.7 and 107.4, as well as the two singlet signals (**Table 3.1**) observed in the aromatic region of its ^1H NMR spectrum (δ_H 7.64 and 7.37) revealed the presence of a tetrasubstituted benzene ring with two protons located in the *para*-position.[13] The

presence of two deshielded carbon signals at δ_C 204.0 and 196.7, as well as the compound's IR absorption (ν_{max} = 1659 cm^{-1}), indicated the presence of two hydrogen-bonded carbonyl groups in the structure. Since the benzene ring and two carbonyl groups contribute four and two degrees of unsaturation, respectively, the remaining one was assigned to a ring. The above data indicated that the basic skeleton of **3.4** was that of an oxygenated calamenene-type sesquiterpenoid.[14] The methyl proton signal located at δ_H 2.27 and the methoxy proton at δ_H 4.04 (both singlets) were assignable to a C-6 methyl carbon and to the carbon of a C-7 methoxyl group of the benzene ring. This assignment was supported by HMBC correlations (**Fig. 3.2**) between H-15 (δ_H 2.27) and C-7 (δ_C 162.9) and the C-5 methine carbon (δ_C 127.8), and between H-16 (δ_C 4.04) and C-7. An oxygen-bearing quaternary carbon (δ_C 88.9, C-4) was determined to be attached to C-10 of the benzene ring (δ_C 123.1) due the presence of a ^3J HMBC crosspeak between the methine proton at H-5 and C-4. The ^{1}H NMR spectrum exhibited resonances at δ_H 0.67 (d, J = 6.7 Hz, H-12) and δ_H 0.88 (d, J = 6.7 Hz, H-13) for the two methyl groups of an isopropyl group, and these showed COSY correlations with a methine proton at δ_H 2.52 (sept, J = 6.7 Hz, H-11).

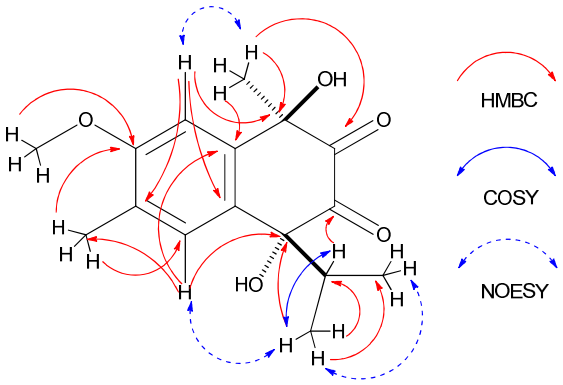

Figure 3.2 HMBC, COSY, and NOESY Correlations of Compound **3.4**

The ^3J HMBC correlation between the protons of one of the doublet methyl groups (H-12/H-13) and the carbon at δ_C 88.9 allowed us to determine the connection of the isopropyl unit to be at C-4. Moreover, the ^2J HMBC correlation observed between the protons at δ_H 1.62

(H-14) and C-1, the ^3J HMBC crosspeaks between H-14 and C-9 (δ_C 145.3) and between H-14 and one carbonyl carbon at δ_C 204.0 (C-2), as well as the ^3J HMBC correlations between the septet methine proton (H-11) and the carbon at δ_C 196.7 (C-3) allowed us to determine the location of a second oxygen-bearing quaternary carbon (δ_C 73.8) and the two carbonyl carbons to be at C-1, C-2 and C-3, respectively. The relative configuration of **3.4** (**Fig. 3.2**) as well as the assignment of the aromatic methyl and methoxy groups to C-6 and C-7 respectively, rather than the reverse, was deduced by the interpretation of the results of the 1D NOE-difference experiment. When the H-14 protons (δ_H 1.62) were irradiated, only the signal at δ_H 7.37 (H-8) was amplified (1.23%). Similarly, irradiation of H-11 (δ_H 2.52) only enhanced the aromatic signals at δ_H 7.64 (H-5) by 3.18%.

3.2.4 *Structure Elucidation of Compound **3.3***

The second compound isolated, *epi*-Tavinin A (**3.5**), $[\alpha]^{21}_D$ +8 (*c* 0.12, MeOH), had the same molecular formula ($C_{16}H_{20}O_5$) as **3.4** by interpretation of its HR–ESI–MS data. The NMR spectroscopic data of compound **3.5** were very similar to those of **3.4** except for the ^{1}H chemical shifts of H-11, H-12, H-13 and H-14. Compounds **3.4** and **3.5** were thus assigned as a pair of diastereomers differing in one of their two stereogenic centers (C-1 and C-4). The relative configuration of **3.5** was determined in the same manner as that of **3.4** (**Fig. 3.3**). Irradiation of H-14 in a 1D NOE-difference experiment enhanced the signals of *both* H-8 and H-11 by 1.32% and 1.35%, respectively, indicating a *syn* relationship between the methyl and isopropyl groups in **3.5**. Based on these observations, the relative configurations of C-1 and C-4 of compound **3.4** were assigned as *R** and *R** while those of C-1 and C-4 of **3.5** were assigned as *S** and *R**.

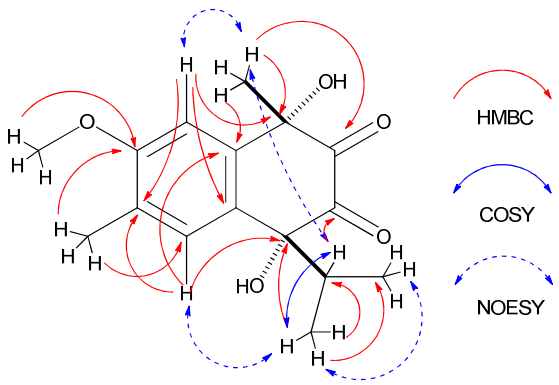

Figure 3.3 HMBC, COSY, and NOESY Correlations of Compound **3.5**

3.2.5 *Synthesis of Compound **3.4** and Compound **3.5***

The structures of compounds **3.4** and **3.5** were confirmed by synthesis (**Scheme 3.2**). The synthesis initially followed McCormick's method for the synthesis of lacinilene C methyl ether (**3.12**) from 2-methylanisole.[15] The literature procedure was modified by running the Grignard reaction to convert the known ketoester **3.6** into 5-isopropyl-5-(4-methoxy-3-methylphenyl)-dihydrofuran-2-one (**3.8**) at low temperature, which increased the yield of **3.8** from 20% to 42% and of the reduction byproduct **3.7** from 23% to 30%. Dihydrofuranone **3.8** was then converted to cycloalkene **3.9**, diol **3.10**, and ketone **3.11** as previously described,[15] except that conversion of **3.10** to **3.11** was carried out using the sulfur trioxide pyridine complex instead of the Swern oxidation originally used.[15] Oxidation of the carbon-carbon double bond of compound **3.11** to triol **3.15** could not be accomplished directly with osmium tetroxide in the presence of *N*-methylmorpholine-*N*-oxide (NMO) because of the electron deficient nature of the α,β-unsaturated double bond. The ketone **3.12** was thus reduced to alcohol **3.13**[16] by Luche reduction[17] in a yield of 90%. The product appeared to consist of a single compound as judged by HPLC and by the presence of only one singlet for H-2 in its ^{1}H NMR spectrum, presumably because the orientation of the hydride ion attack was governed by complexation of the borohydride

with the adjacent C-1 hydroxy group. Oxidation of **3.13** with osmium tetroxide in the presence of *N*-methylmorpholine-*N*-oxide afforded tetraol **3.14** as a mixture of stereoisomers. Without separation of this mixture, the tetraols **3.14** were further oxidized by the sulfur trioxide pyridine complex to give a mixture of four diones as two pairs of enantiomers in the relatively low yield of 23%. The diones were separated by HPLC to afford synthetic racemic **3.4** and synthetic racemic **3.5**. The structures of the natural products isolated were confirmed by comparison of their ^{1}H NMR, UV spectrometric and HR–ESI–MS data with those of their synthetic counterparts.

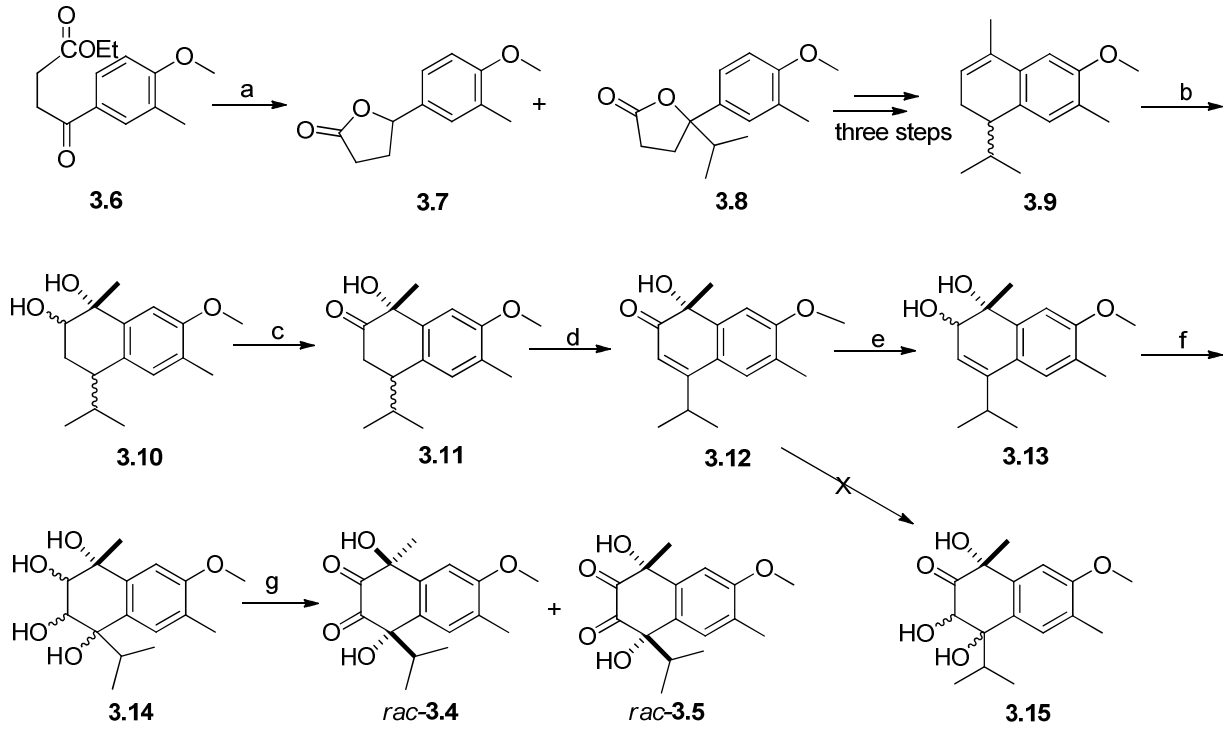

Conditions: a. $(CH_3)_2CHMgCl$, THF, –15 °C, 1 h, 42%; b. 2% OsO_4, NMO, CH_2Cl_2, RT, 48 h, 75%; c. SO_3-pyridine complex, CH_2Cl_2, 0 °C, 2 h, 92%; d. DDQ, benzene, reflux, 24 h, 58%; e. $NaBH_4$, $CeCl_3{\cdot}7H_2O$, RT, 5 min, 90%. f. 2% OsO_4, NMO, CH_2Cl_2, RT, 48 h; g. SO_3-pyridine complex, CH_2Cl_2, 0 °C, 2 h, 13% (*rac*-**3.4**) 10% (*rac*-**3.5**).

Scheme 3.2 Synthesis of Compounds **3.4** and **3.5**

3.2.6 *Antiproliferative Activity of the Isolated Compounds and Synthetic Intermediates.*

The isolated tavinin A (**3.4**) and *epi*-tavinin A (**3.5**), the synthetic compounds *rac*-**3.4** and *rac*-**3.5** as well as the intermediates involved in the synthetic route were tested for antiproliferative activity against the A2780 ovarian cancer. As listed in **Table 3.2**, both natural products **3.4** and **3.5** showed modest inhibition of the A2780 ovarian cancer cells, with IC_{50} values of 5.5 and 6.7 μM, respectively. The synthetic compounds *rac*-**3.4** and *rac*-**3.5** had identical values within experimental error, indicating that bioactivity is not dependent on stereochemistry in this series. Among the synthetic intermediates, only lacinilene C methyl ether (**3.12**, IC_{50} value of 4.0 μM) was of comparable potency to the natural products; the other calamenene-type sesquiterpenoid intermediates were less active or inactive. The cytotoxic activity of compound **3.12** may be due to the presence of an *α*,*β*-unsaturated ketone function in the molecule; such groups are electrophilic and are able to bind to receptors, leading to facile reactions with protein thiols, and ultimately to induction of apoptosis.[18]

Table 3.2 Cytotoxicity of Compound **3.3–3.5** and Synthetic Intermediates **3.9–3.14** against A2780 Ovarian Cancer Cells.

Compound	**3.3**	**3.4**	**3.5**	Rac-**3.4**	Rac-**3.5**	Paclitaxel
IC_{50} (μM)	10 ± 0.9	5.5 ± 0.9	6.7 ± 0.3	5.9 ± 0.7	6.3 ± 0.4	0.028 ± 0.003
Compound	**3.9**	**3.10**	**3.11**	**3.12**	**3.13**	**3.14**
IC_{50} (μM)	>50	>50	34 ± 2	4.0 ± 0.5	22 ± 3	36 ± 3

3.3 Experimental Section

3.3.1 *General Experimental Procedures.*

Optical rotations were recorded on a JASCO P-2000 polarimeter. IR spectroscopic data were measured on a MIDAC M-series FTIR spectrophotometer. NMR spectra were recorded in acetone-d_6 or $CDCl_3$ on Bruker Avance 500 or Bruker Avance 600 spectrometers. The chemical

shifts are given in δ (ppm), and coupling constants (J) are reported in Hz. Mass spectra were obtained on an Agilent 6220 LC–TOF–MS in the positive ion mode.

3.3.2 *Antiproliferative Bioassay*

Antiproliferative activities were obtained at Virginia Tech against the drug-sensitive A2780 human ovarian cancer cell line[19] as previously described.[4]

3.3.3 *Plant Material*

A sample of the bark parts of *Sterculia tavia* was collected in October 2005. The sample was collected from a tree 24 meters high, with yellowish seeds and light brown fruits. The collection was made in the rainforest 8 km from Ankijabe, in the Daraina region of Madagascar, at coordinates 13°16'12"S 049°36'40"E and elevation 617 m. Voucher specimens have been deposited at the Parc Botanique and Zoologique de Tsimbazaza (TAN), at the Centre National d'Application des Recherches Pharmaceutiques in Antananarivo, Madagascar (CNARP), the Missouri Botanical Garden in St. Louis, Missouri (MO), and the Muséum National d'Histoire Naturelle in Paris, France (P), voucher Sennen Randrianasolo et al. 533.

3.3.4 *Extraction and Isolation*

Dried bark parts of *S. tavia* (252 g) were ground in a hammer mill, then extracted with EtOH by percolation for 24 h at room temperature to give the crude extract MG 3532 (5.2 g), of which 1.42 g was shipped to Virginia Tech for bioassay-guided isolation. A 1.4 g sample of MG 3532 (IC_{50} 14 μg/mL) was suspended in aqueous MeOH (MeOH/H_2O, 9:1, 100 mL), and extracted with hexanes (3 × 100 mL portions). The aqueous layer was then diluted to 60% MeOH (v/v) with H_2O

and extracted with CH_2Cl_2 (3 × 150 mL portions). The hexanes fraction was evaporated in vacuo to leave 498 mg of material with IC_{50} = 15 μg/mL. The residue from the CH_2Cl_2 fraction (214 mg) had an IC_{50} of 9.6 μg/mL, and the remaining aqueous MeOH fraction had an IC_{50} > 20 μg/mL. LH-20 size exclusion open column chromatography (CH_2Cl_2/MeOH, 1:1) of the CH_2Cl_2 fraction was used to obtain six fractions, of which the two most active fractions F3 (67.7 mg) and F4 (51.4 mg) had IC_{50} values of 5.9 and 4.8 μg/mL, respectively. Fraction F4 was then applied to a silica gel column with elution by hexanes/EtOAc, 7:3 to give seventeen fractions, of which fraction F2-4 (2.3 mg) was the most active (IC_{50} 3.7 μg/mL), and yielded compound **3.3** (1.5 mg, IC_{50} 2.5 μg/mL) on chromatography on C_{18} HPLC with elution by 85% MeOH in water, with the retention time of 14.9 minute. Fraction F3 was also applied to a silica gel column with elution by hexanes/EtOAC, 4:1 to give six fractions, of which fraction F2-5 (26.2 mg) was the most active (IC_{50} 2.7 μg/mL). Compounds **3.4** (0.32 mg, IC_{50} 1.7 μg/mL) and **3.5** (0.28 mg, IC_{50} 1.9 μg/mL), with retention times of 14.7 and 15.2 minutes, respectively, were obtained by using C_{18} HPLC eluted by 70% MeOH in H_2O to purify fraction F2-5.

3.3.5 *(1R,4R)-1,4-dihydroxy-1-isopropyl-6-methoxy-4,7-dimethylnaphthalene-2,3(1H,4H)-dione (**3.4**, Tavinin A)*

Light yellow oil; $[\alpha]_D^{21}$ +15 (*c* 0.12, MeOH); UV (MeOH) λ_{max} (ε) 207 (3.20), 232 (2.35), 280 (1.62); IR ν_{max} cm^{-1}: 3418, 2926, 1659, 1463, 1052 cm^{-1}. ^1H NMR (600 MHz, acetone-d_6), and ^{13}C NMR spectra (125 MHz, acetone-d_6), see **Table 3.1**; HR–ESI–MS *m/z* 315.1194 $[M+Na]^+$ (calc. for $C_{16}H_{20}NaO_5^+$, 315.1203).

3.3.6 *(1R,4S)-1,4-dihydroxy-1-isopropyl-6-methoxy-4,7-dimethylnaphthalene-2,3(1H,4H)-dione (**3.5**, Epi-Tavinin A)*

Light yellow oil; $[\alpha]_D^{21}$ +8 (*c* 0.12, MeOH); UV (MeOH) λ_{max} (ε) 207 (3.20), 232 (2.35), 280 (1.62); IR ν_{max} cm^{-1}: 3432, 2932, 1671, 1459, 1078 cm^{-1}. ^1H NMR (600 MHz, acetone-d_6), and ^{13}C NMR spectra (125 MHz, acetone-d_6), see **Table 3.1**; HR–ESI–MS *m/z* 315.1201 $[M+Na]^+$ (calc. for $C_{16}H_{20}NaO_5^+$, 315.1203).

3.3.7 *Synthesis of 4-hydroxy-4-(4-methoxy-3-methylphenyl)-5-methylhexanoic acid lactone (**3.8**)*

Ketoester **3.6**[20] (500 mg) was dissolved in 50 mL of THF, and the solution cooled to –15 ^oC. Isopropylmagnesium chloride (1.5 mL of a 2.0 M solution in THF) was added during a 15 min period. After stirring for 2 h, the mixture was dried under reduced pressure, and 50 mL of saturated NH_4Cl solution was added. The aqueous solution was extracted with 50 mL Et_2O three times, and the extracts were washed with saturated NaCl solution, dried over Na_2SO_4 and concentrated to afford 468 mg brown oil, which was refluxed together with 500 mg KOH in 100 mL 95% EtOH for 4 h. The EtOH was removed from the mixture under reduced pressure, 100 mL of water was added, and the resulting mixture was extracted three times with 50 mL Et_2O. The aqueous portion was acidified to pH 1 with HCl and stirred at rt for 2 h. The acidified solution was extracted three times by another 50 mL of Et_2O, and the ethereal potion was washed with saturated Na_2CO_3 and NaCl solution, respectively, dried by Na_2SO_4 and concentrated under reduced pressure to afford 313 mg of a yellow oil. Chromatographic purification of the crude lactone (50 g of silica gel; eluted with hexanes/EtOAc, 7:3) afforded 167 mg (20%) of compound **3.8** (R_f 0.56, silica gel TLC, hexanes/EtOAc, 7:3) and 140 mg (42%) of compound **3.7** (R_f 0.40). The NMR and mass spectrometric data were consistent with the data reported.[15]

3.3.8 *Synthesis of 1,2,3,4-tetrahydro-1,2-dihydroxy-4-isopropyl-7-methoxy-1,6-dimethyl-naphthalenes (**3.10**)*

This compound was prepared from 4-hydroxy-4-(4-methoxy-3-methylphenyl)-5-methyl-hexanoic acid lactone (**3.8**) in four steps as previously described; its spectroscopic data matched the literature data.[15]

3.3.9 *Synthesis of l-Hydroxy-4-isopropyl-7-methoxy-1,6-dimethyl-2-naphthalenone (**3.12**).*

Diol mixture **3.10** (50 mg) was dissolved in 50 mL of CH_2Cl_2 and the solution cooled to 0 ^oC. Sulfur trioxide pyridine complex (150.6 mg) was added to the solution during a 5 min period. After stirring for 2 h, 50 mL of saturated Na_2CO_3 solution was added, and the layers were separated. The aqueous layer was extracted with 50 mL of CH_2Cl_2 three times, and the combined organic layers were washed with saturated NaCl solution, dried over Na_2SO_4, and concentrated under reduced pressure to afford 45.3 mg of ketone **3.11** as a yellow oil. The crude ketone and 56.6 mg dichlorodicyanobenzoquinone were stirred in 50 mL of benzene for 24 h at room temperature, after which the solvent was evaporated under reduced pressure. The resulting oil was purified by column chromatography (50 g of silica gel; eluted with hexanes/EtOAc, 3:2) to give 28.9 mg (58%) of compound **3.12** (R_f 0.40, hexanes/EtOAc, 3:2). The NMR and mass spectrometric data were consistent with the reported data.[15]

3.3.10 *Synthesis of 4-Isopropyl-7-methoxy-1,6-dimethyl-1,2-dihydronaphthalene-1,2-diol (**3.13**)*

Compound **3.12** (26.0 mg) was dissolved in 25 mL of 0.4 mM methanolic $CeCl_3 \cdot 7H_2O$ at room temperature, and 1 equivalent of $NaBH_4$ (3.8 mg) was added to the solution. After stirring for 5 min, the mixture was dried under reduced pressure, redissolved in 25 mL of water and extracted

three times with 25 mL of CH_2Cl_2. The organic portion was washed with saturated NaCl solution, dried over Na_2SO_4 and concentrated under reduced pressure. The resulting light yellow oil was purified by column chromatography (50 g of silica gel; eluted with hexanes/EtOAc, 3:2) to afford 23.7 mg (90%) of solid diol **3.13**. The product appeared to consist of a single compound as judged by HPLC and by the presence of only one singlet for H-2 in its ^{1}H NMR spectrum. HR–ESI–MS, *m/z* 285.1472 $[M+Na]^+$ (calc. for $C_{16}H_{22}NaO_3^+$, 285.1461); ^{1}H NMR ($CDCl_3$) δ_H 7.12 (H-8, s, 1H), 7.06 (H-5, s, 1H), 5.56 (H-3, br s, 1H), 4.48 (H-2, br s, 1H), 3.86 (H-16, s, 3H), 2.87 (H-11, sept, J = 6.7 Hz, 1H), 2.19 (H-15, s, 3H), 1.30 (H-14, s, 3H), 1.19 (H-12, d, J = 6.7 Hz, 3H), 1.06 (H-13, d, J = 6.7 Hz, 3H); ^{13}C-NMR ($CDCl_3$) δ_C 157.5 (C-7, C), 142.6 (C-4, C), 142.2 (C-9, C), 126.2 (C-5, CH), 125.2 (C-10, C), 125.2 (C-6, C), 121.7 (C-3, CH), 105.7 (C-8, CH), 77.1 (C-2, CH), 77.0 (C-1, C), 55.7 (C-16, CH_3), 28.2 (C-11, CH); 22.7 (C-14, CH_3), 21.6 (C-12, CH_3), 20.8 (C-13, CH_3), 16.4 (C-15, CH_3).

3.3.11 *Synthesis of 1,4-Dihydroxy-1-isopropyl-6-methoxy-4,7-dimethylnaphthalene-2,3-diones rac-**3.4** and rac-**3.5***.

Diol **3.13** (22.0 mg) was dissolved in 6 mL of acetone and 2.5 mL of water and the solution cooled to –25 ^{o}C. *N*-methylmorpholine-*N*-oxide (0.05 mL of a 50% solution in water) and 0.1 mL of 2% osmium tetroxide aqueous solution were then added under nitrogen. The mixture was allowed to warm to room temperature and stirred for an additional 48 h, and then 50 mg of $Na_2S_2O_4$ was added. The acetone was removed under reduced pressure, the pH was adjusted to 2 by HCl, and the solution was extracted with 20 mL CH_2Cl_2 three times. The combined extracts were washed with saturated NaCl solution, dried by Na_2SO_4 and concentrated under reduced pressure to afford product **3.14** as a light brown oil. The crude product was oxidized directly with sulfur

trioxide pyridine complex as described in the synthesis of compound **3.12** above. The resulting 6.6 mg of light brown oil was applied to C_{18} HPLC and eluted by 68% MeOH in water to afford 3.2 mg (13%) of light yellow oil (*rac*-**3.4)** and 2.5 mg (10%) of light yellow oil (*rac*-**3.5**), at retention times of 19.5 and 20.7 min, respectively. The NMR and mass spectrometric data of both compounds were identical to those of the corresponding natural products.

3.4 References and Notes

1. Dai, Y.; Harinantenaina, L.; Brodie, P. J.; Callmander, M. W.; Randrianasolo, S.; Rakotobe, E.; Rasamison, V. E.; Kingston, D. G. I. Isolation and synthesis of two antiproliferative calamenene-type sesquiterpenoids from *Sterculia tavia* from the Madagascar rain forest. *Bioorg. Med. Chem.* **2012,** *20*, 6940–6944.

2. Zhou, B. N.; Baj, N. J.; Glass, T. E.; Malone, S.; Werkhoven, M. C. M.; van Troon, F.; David, M.; Wisse, J. H.; Kingston, D. G. I. Bioactive labdane diterpenoids from *Renealmia alpinia* from the Suriname rain forest. *J. Nat. Prod.* **1997,** *60*, 1287–1293.

3. Dai, Y.; Harinantenaina, L.; Brodie, P. J.; Birkinshaw, C.; Randrianaivo, R.; Applequist, W.; Ratsimbason, M.; Rasamison, V. E.; Shen, Y.; TenDyke, K.; Kingston, D. G. Two antiproliferative triterpene saponins from *Nematostylis anthophylla* from the highlands of central Madagascar. *Chem Biodivers* **2013,** *10*, 233–240.

4. Pan, E.; Harinantenaina, L.; Brodie, P. J.; Callmander, M.; Rakotonandrasana, S.; Rakotobe, E.; Rasamison, V. E.; TenDyke, K.; Shen, Y.; Suh, E. M.; Kingston, D. G. I. Cardenolides of *Leptadenia madagascariensis* from the Madagascar dry forest. *Bioorg. Med. Chem.* **2011,** *19*, 422–428.

5. Pan, E.; Gorka, A. P.; Alumasa, J. N.; Slebodnick, C.; Harinantenaina, L.; Brodie, P. J.; Roepe, P. D.; Randrianaivo, R.; Birkinshaw, C.; Kingston, D. G. I. Antiplasmodial and antiproliferative pseudoguaianolides of *Athroisma proteiforme* from the Madagascar dry forest. *J. Nat. Prod.* **2011,** *74*, 2174–2180.

6. Judd, W.; Manchester, S. Circumscription of Malvaceae (Malvales) as determined by a

preliminary cladistic analysis of morphological, anatomical, palynological, and chemical characters. *Brittonia* **1997,** *49*, 384–405.

7. Lopez-Feria, S.; Cardenas, S.; Garcia-Mesa, J. A.; Valcarcel, M. Usefulness of the direct coupling headspace-mass spectrometry for sensory quality characterization of virgin olive oil samples. *Anal. Chim. Acta* **2007,** *583*, 411–417.

8. Reid, K. A.; Jäger, A. K.; Light, M. E.; Mulholland, D. A.; Staden, J. V. Phytochemical and pharmacological screening of *Sterculiaceae* species and isolation of antibacterial compounds. *J. Ethnopharmacol.* **2005,** *97*, 285–291.

9. Rani, P.; Rajasekharreddy, P. Insecticidal activity of (2*n*-octylcycloprop-1-enyl)-octanoic acid (I) against three coleopteran stored product insects from *Sterculia foetida* (L.). *J. Pest Sci.* **2010,** *83*, 273–279.

10. Naik, D. G.; Mujumdar, A. M.; Waghole, R. J.; Misar, A. V.; Bligh, S. W.; Bashall, A.; Crowder, J. Taraxer-14-en-3β-ol, an anti-inflammatory compound from *Sterculia foetida* L. *Planta Med.* **2004,** *70*, 68–69.

11. Tiew, P.; Puntumchai, A.; Kokpol, U.; Chavasiri, W. Coumarins from the heartwoods of *Mansonia gagei* Drumm. *Phytochemistry* **2002,** *60*, 773–776.

12. Tanaka, N.; Yasue, M.; Imamura, H. The quinonoid pigments of *Mansonia altissima* wood. *Tetrahedron Lett.* **1966,** *7*, 2767–2773.

13. Nabeta, K.; Katayama, K.; Nakagawara, S.; Katoh, K. Sesquiterpenes of cadinane type from cultured cells of the liverwort, *Heteroscyphus planus*. *Phytochemistry* **1992,** *32*, 117–122.

14. Kashman, Y. 8-Methoxy and 5-hydroxy-8-methoxy-calamenenes from the marine gorgonian

Subergorgia hicksoni. *Tetrahedron* **1979,** *35*, 263–266.

15. McCormick, J. P.; Shinmyozu, T.; Pachlatko, J. P.; Schafer, T. R.; Gardner, J. W.; Stipanovic, R. D. Gossypium cadinanes and their analogs: synthesis of lacinilene C, 2,7-dihydroxycadalene, and their methyl ethers. *J. Org. Chem.* **1984,** *49*, 34–40.

16. Jeffs, P. W.; Lynn, D. G. Isolation and structure of 1-hydroxy-7-methoxy-4-isopropyl-1,6-dimethyl-2(1H)-naphthalenone from cotton. *J. Org. Chem.* **1975,** *40*, 2958–2960.

17. Gemal, A. L.; Luche, J. L. Lanthanoids in organic synthesis. 6. Reduction of alpha-enones by sodium borohydride in the presence of lanthanoid chlorides: synthetic and mechanistic aspects. *J. Am. Chem. Soc.* **1981,** *103*, 5454–5459.

18. Nakayachi, T.; Yasumoto, E.; Nakano, K.; Morshed, S. R.; Hashimoto, K.; Kikuchi, H.; Nishikawa, H.; Kawase, M.; Sakagami, H. Structure–activity relationships of *α,β*-unsaturated ketones as assessed by their cytotoxicity against oral tumor cells. *Anticancer Res.* **2004,** *24*, 737–742.

19. Louie, K. G.; Behrens, B. C.; Kinsella, T. J.; Hamilton, T. C.; Grotzinger, K. R.; McKoy, W. M.; Winker, M. A.; Ozols, R. F. Radiation survival parameters of antineoplastic drug-sensitive and -resistant human ovarian cancer cell lines and their modification by buthionine sulfoximine. *Cancer Res.* **1985,** *45*, 2110–2115.

20. Bell, A. A.; Stipanovic, R. D.; Zhang, J.; Mace, M. E.; Reibenspies, J. H. Identification and synthesis of trinorcadalene phytoalexins. *Phytochemistry* **1998,** *49*, 431–440.

Chapter 4: Antiproliferative Triterpene Saponins from *Nematostylis anthophylla* from the Madagascar Rain Forest

This chapter is a slightly expanded version of a published article. (Dai, Y.; Harinantenaina, L.; Brodie, P. J.; Birkinshaw, C.; Randrianaivo, R.; Applequist, W.; Ratsimbason, M.; Rasamison, V. E.; Shen, Y.; TenDyke, K.; Kingston, D. G. I. Two antiproliferative triterpene saponins from *Nematostylis anthophylla* from the highlands of central Madagascar. *Chem. Biodivers.* **2013,** *10*, 233–240.) Attributions of co-authors of the articles are described as follows in the order of the names listed. The author of this dissertation (Mr. Yumin Dai) conducted the isolation and structural elucidation part of the titled compounds, and drafted the manuscript. Dr. Liva Harinantenaina was a mentor for this work, and in particular, he provided invaluable advice and hints for the structural elucidation of those compound, and he also proofread the manuscript before submission. Ms. Peggy Brodie performed the A2780 bioassay on the isolated fractions and compounds. Dr. Chris Birkinshaw, Dr. Richard Randrianaivo, and Dr. Wendy Applequist from Missouri Botanical Garden did the plant collections and identification. Dr. Michel Ratsimbason and Dr. Vincent E. Rasamison from Madagascar carried out the initial plant extraction. Dr. Yongchun Shen, Dr. Karen TenDyke, and Dr. Edward M. Suh from Eisai Inc. performed the A2058 and H522 bioassays on the compounds isolated. Dr. David G. I. Kingston was a mentor for this work and the corresponding author for the published article. He provided critical suggestions for this work and edited the final manuscript.[1]

4.1 Introduction

As part of our engagement in an International Cooperative Biodiversity Group (ICBG) program, we are focusing on the search for antiproliferative natural products from both the tropical dry forests and the rainforests of Madagascar. [2-4] The A2780 human ovarian cancer cell line is used as the primary screen because it is a relatively sensitive cell line and gives reproducible results. As a part of this research, an EtOH extract from the roots of *Nematostylis anthophylla* (Rubiaceae) from the dry forest of northern Madagascar exhibited antiproliferative activity against the A2780 cell line, with an IC_{50} value of 6.9 μg/mL. The Rubiaceae family is a large family of 630 genera and about 13,000 species found worldwide. [5] This family is a rich source of indole alkaloids, terpenoids and anthraquinones, all of which are well-known for their broad range of bioactivity, including antimicrobial, antimalarial, antidiabetic, vasorelaxant, cytotoxic, antioxidant, and anti-inflammatory activities among others. [6-10] Nauclearorine (**4.1**), virdiflorol (**4.2**) and geranylacetone (**4.3**) listed are the examples of bioactive compounds isolated from the Rubiaceae family. Since *Nematostylis* is one of the many genera of the Rubiaceae family that have not been systematically investigated for their phytochemical composition, the ethanol extract of *Nematostylis anthophylla* was selected for bioassay guided fractionation to isolate its active components.

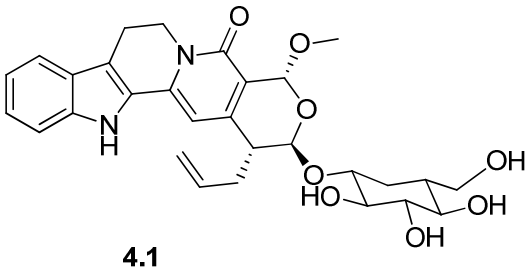

4.1

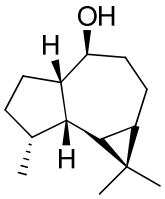

4.2

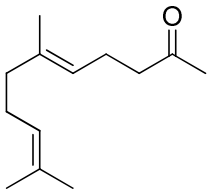

4.3

4.2 Results and Discussion

4.2.1 *Isolation of Active Compounds*

An EtOH extract of the roots of *Nematostylis anthophylla* was subjected to liquid–liquid partitioning to give an active *n*-BuOH fraction with an IC_{50} value of 2.2 μg/ml. Bioassay guided separation (**Scheme 4.1**), including LH-20 size exclusion, HP-20 diaion and silica gel normal-phase chromatography, was used to obtain three new bioactive compounds comprising the known triterpene saponin randianin (**4.4**) and the two new related glycosides designated 2"-*O*-acetylrandianin (**4.5**) and 6"-*O*-acetylrandianin (**4.6**). Herein, we report the structural elucidation and antiproliferative properties of the two new isolates.

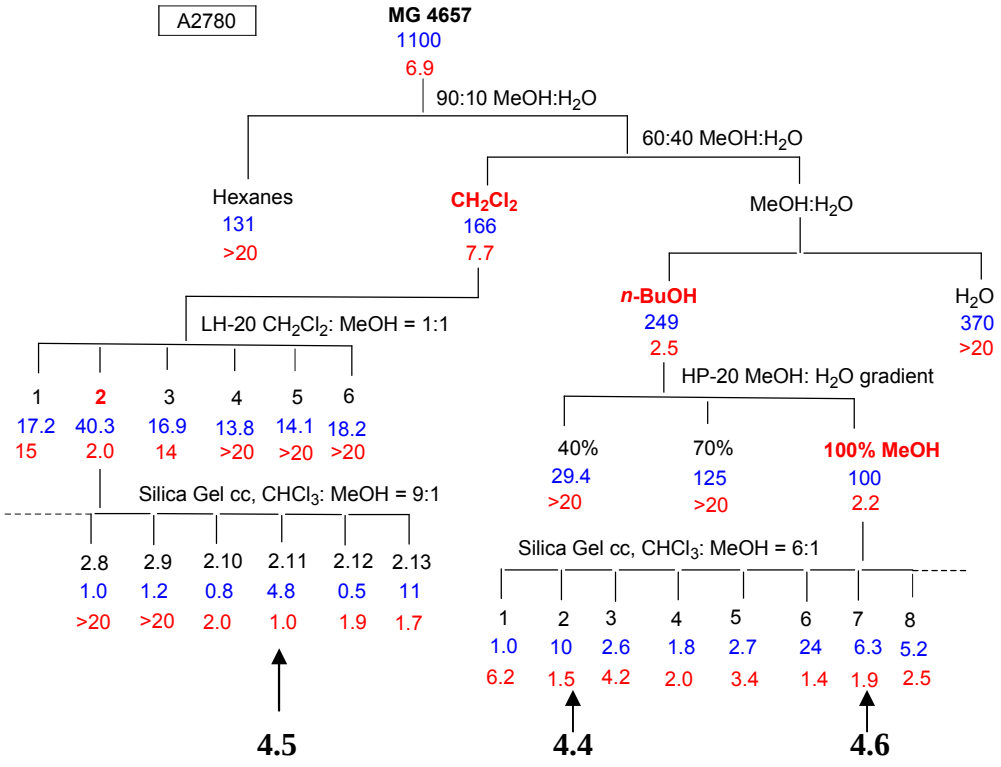

Scheme 4.1 Bioassay Guided Separation of the Extract of *Nematostylis anthophylla*

(The first number under each fraction is the weight in mg,and the second number is the IC50 value of the A2780 cells in μg/mL)

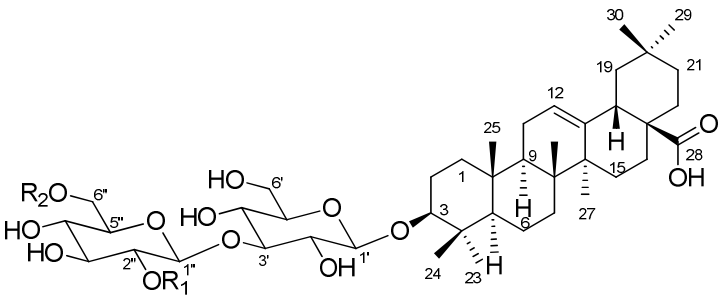

Compound	R_1	R_2
4.4	H	H
4.5	Ac	H
4.6	H	Ac

Figure 4.1 Chemical Structure of Compounds **4.4**–**4.6**

4.2.2 *Structure Elucidation of Compound **4.4***

Compound **4.4** was identified as randianin (oleanolic acid-3-*O*-*β*-D-glucopyranosyl-(1→3)-*β*-D-glucopyranoside) by comparison of its chemical and spectroscopic data with those reported in the literature for the aglycone[11] and the glycoside. [12]

4.2.3 *Structure Elucidation of Compound **4.5***

Compound **4.5**, $[\alpha]^{21}_{D}$ +12 (*c* 1.2, MeOH), was isolated as a light yellow solid. Its positive ion HR–ESI–MS revealed pseudo-molecular ion peaks at *m/z* 845.4692 $[M+Na]^+$ and 861.4618 $[M+K]^+$, corresponding to a molecular formula of $C_{44}H_{70}O_{14}$. The observation of a carbonyl absorption at 1734 cm^{-1} in the IR spectrum, a ^{13}C NMR resonance at δ_C 170.7, and a singlet signal at δ_H 1.98 in the ^1H NMR spectrum suggested the presence of an acetyl group. Meanwhile, its glycosidic nature was corroborated by the presence of two anomeric proton signals at δ_H 4.83 and 5.43. In addition to the methyl and carbonyl carbons of the acetyl group, there were 42 carbon

signals in the ^{13}C NMR spectrum, among which 30 carbon signals were assigned to a triterpenoid aglycone and the remaining 12 carbons to a disaccharide moiety. The ^{1}H NMR spectrum of **4.5** indicated that the aglycone had seven methyl groups, with three-proton singlets at δ_H 0.80, 0.89, 0.97, 1.00, 1.03, 1.27 and 1.33, and one olefinic proton at δ_H 5.49. Correspondingly, signals for seven methyl carbons at δ_C 15.8, 17.2, 17.8, 24.1, 26.6, 28.5 and 33.7 ppm, and for two olefinic carbons at δ_C 122.9 and 145.2 ppm, were observed in the ^{13}C NMR spectrum (**Table 4.1**). The presence of a carbonyl absorption at 1689 cm^{-1} and a broad hydroxy absorption at 3453 cm^{-1} in its IR spectrum, together with a ^{13}C NMR resonance at δ_C 180.6 ppm, supported the presence of a carboxylic acid group.

Inspection of the ^{1}H and ^{13}C NMR spectra of compound **4.5** indicated that it had the same oleanolic acid aglycone as compound **4.4**. The HMBC correlation between H-18 (dd, J = 4.1, 14.0 Hz) and C-28 confirmed that the carboxylic carbon was connected to C-17.[13] HMBC correlations between the H-1' anomeric proton and C-3, as well as between H-3 and the anomeric carbon C-1', confirmed that the disaccharide moiety was connected to C-3 (**Fig. 4.2**).

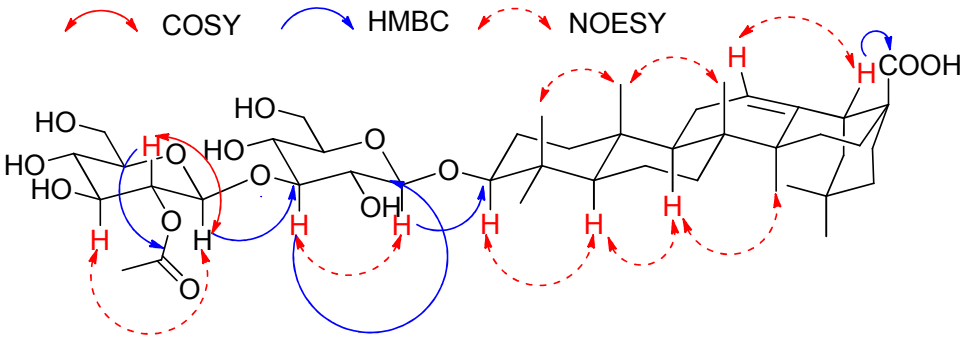

Figure 4.2 HMBC, COSY and NOESY Correlations of Compound **4.5**

Table 4.1 NMR Spectroscopic Data for **4.4–4.6** in Pyridine-d_5 (^{1}H-500 MHz, ^{13}C-125 MHz)

	4.4		**4.5**		**4.6**	
	δ_H (J in Hz)	δ_C, type	δ_H (J in Hz)	δ_C, type	δ_H (J in Hz)	δ_C, type
1a	1.21–1.25	39.0, CH_2	1.21–1.25	39.0, CH_2	1.22–1.26	39.0, CH_2
1b	1.39–1.42		1.37–1.40		1.39–1.42	
2a	1.75–1.78	26.8, CH_2	1.76–1.79	26.9, CH_2	1.74–1.77	26.8, CH_2
2b	2.14–2.18		2.15–2.19		2.14–2.18	
3	3.36 dd (4.4, 11.9)	89.3, CH	3.36 dd (4.4, 11.9)	89.3, CH	3.36 dd (4.4, 11.7)	89.4, CH
4	-	40.1, C	-	40.1, C	-	40.1, C
5	0.76–0.80	56.1, CH	0.76–0.79	56.1, CH	0.78–0.82	56.1, CH
6a	1.21–1.25	18.8, CH_2	1.22–1.25	18.8, CH_2	1.23–1.26	18.8, CH_2
6b	1.45–1.49		1.46–1.50		1.46–1.50	
7a	1.78–1.82	33.6, CH_2	1.78–1.82	33.6, CH_2	1.78–1.82	33.6, CH_2
7b	1.85–1.87		1.85–1.87		1.85–1.87	
8	-	39.8, C	-	39.8, C	-	39.8, C
9	1.65 brt (8.9)	48.3, CH	1.64 brt (8.9)	48.4, CH	1.65 brt (8.9)	48.3, CH
10	-	37.3, C	-	37.3, C	-	37.3, C
11	1.88–1.92	24.1, CH_2	1.88–1.92	24.1, CH_2	1.88–1.92	24.1, CH_2
12	5.50 t (3.3)	122.8, CH	5.49 t (3.3)	122.9, CH	5.50 t (3.3)	122.8, CH
13	-	145.3, C	-	145.2, C	-	145.3, C
14	-	42.5, C	-	42.6, C	-	42.5, C
15a	1.18–1.21	28.7, CH_2	1.18–1.21	28.7, CH_2	1.18–1.21	28.7, CH_2
15b	2.02–2.05		2.02–2.05		2.02–2.05	
16a	1.76–1.79	24.1, CH_2	1.75–1.78	24.1, CH_2	1.76–1.79	24.1, CH_2
16b	2.18–2.21		2.17–2.20		2.18-2.21	
17	-	47.0, C	-	47.1, C	-	47.0, C
18	3.32 dd (4.1, 14.0)	42.4, CH	3.32 dd (4.1, 14.0)	42.4, CH	3.32 dd (4.0, 13.9)	42.4, CH
19a	1.28–1.31	46.9, CH_2	1.28–1.31	46.9, CH_2	1.28–1.31	46.9, CH_2
19b	1.82–1.84		1.82–1.84		1.82–1.84	
20	-	31.3, C	-	31.3, C	-	31.3, C
21a	1.49–1.52	34.6, CH_2	1.49–1.52	34.6, CH_2	1.49–1.52	34.6, CH_2
21b	1.82–1.84		1.82–1.84		1.82–1.84	
22a	1.45–1.49	33.6, CH_2	1.45–1.49	33.6, CH_2	1.46–1.50	33.5, CH_2
22b	2.05–2.08		2.05–2.08		2.05–2.08	
23	1.27 s	17.8, CH_3	1.27 s	17.8, CH_3	1.32 s	17.8, CH_3
24	0.89 s	28.5, CH_3	0.89 s	28.5, CH_3	1.01 s	28.5, CH_3
25	0.82 s	15.8, CH_2	0.80 s	15.8, CH_2	0.82 s	15.8, CH_2
26	1.00 s	17.4, CH_3	1.00 s	17.2, CH_3	1.00 s	17.3, CH_3
27	1.33 s	26.5, CH_3	1.33 s	26.6, CH_3	1.33 s	26.5, CH_3
28	-	180.7, C	-	180.6, C	-	180.7, C
29	1.03 s	24.1, CH_3	1.03 s	24.1, CH_3	1.02 s	24.1, CH_3
30	0.97 s	33.7, CH_3	0.97 s	33.7, CH_3	0.97 s	33.6, CH_3
	C-3-Glucose					
1'	4.91 d (7.8)	106.7, CH	4.83 d (7.8)	107.1, CH	4.91 d (7.6)	106.7, CH
2'	4.09–4.11	74.8, CH	3.96–4.02	74.4, CH	4.05–4.08	74.7, CH
3'	4.23 t (8.8)	89.3, CH	4.15 t (8.8)	89.3, CH	4.18 t (8.9)	89.7, CH
4'	4.11–4.14	70.2, CH	4.04–4.08	70.7, CH	4.11 t (8.9)	70.0, CH
5’	3.92–3.98	78.3, CH	3.89–3.93	78.1, CH	3.92–3.98	78.3, CH
6'a	4.32 d (11.0)	62.9, CH	4.26 d (11.4)	63.1, CH	4.32 dd (6.2, 11.8)	62.9, CH
6'b	4.51 d (11.0)		4.48 dd (2.1, 11.4)		4.52 dd (2.2, 11.8)	
	C-3'-Glucose					
1"	5.32 d (7.8)	106.3, CH	5.43 d (8.1)	103.7, CH	5.25 d (7.9)	106.3, CH
2"	4.02–4.05	75.9, CH	5.66 dd (8.1, 9.1)	75.7, CH	4.03–4.05	75.7, CH
3"	4.26 t (9.2)	75.8, CH	4.31 t (9.1)	76.6, CH	4.22 t (9.1)	75.7, CH
4"	4.20 t (9.2)	72.0, CH	4.20 t (9.1)	72.3, CH	4.01 t (9.1)	71.9, CH
5"	4.07–4.09	79.1, CH	4.07–4.10	79.1, CH	4.23–4.26	78.3, CH
6"a	4.34 d (11.1)	62.8, CH	4.28 d (11.5)	62.7, CH	4.67 dd (6.8, 11.8)	64.9, CH
6"b	4.56 d (11.1)		4.58 dd (2.1, 11.5)		4.95 dd (2.2, 11.8)	
2"- Acetyl						
CO				170.7, C		
CH_3			1.98 s	21.5, CH_3		
6"-Acetyl						
CO						171.2, C
CH_3					2.00 s	21.0, CH_3

Both sugar molecules, which were represented by the of two sets of anomeric signals at δ_H 4.83/δ_C 107.1 ppm and δ_H 5.43/δ_C 103.7 ppm, respectively, were identified as glucose, based on the similarity of their ^{13}C NMR chemical shifts with those of the sugar moiety of **4.4**. The linkage between the two glucopyranosyl units was concluded to be 1→3 by the observation of HMBC correlations between H-3' and two anomeric carbons (C-1' and C-1"), as well as the cross-peak between H-3' and H-2' in the COSY spectrum (**Fig. 4.2**). The coupling constants between H-1' and H-2', and H-1" and H-2" (J = 7.8 and 8.1 Hz, respectively) indicated their axial-axial conformation and thus the β-configuration of the two sugar units. The location of the acetyl group was deduced to be at the hydroxy group of C-2" of a glucopyranosyl residue, based on the comparison of the ^{1}H and ^{13}C NMR spectra of **4.5** with those of **4.4**. Due to this acetylation, the chemical shift of H-2" of compound **4.5** was δ_H 5.66 as compared to δ_H 4.04 for compound **4.4**, while other protons in the distal glucose had chemical shifts similar to those of compound **4.4**. The position of the acetyl group was confirmed by the COSY cross-peak between the downfield H-2" (δ_H 5.66) and the corresponding anomeric proton H-1", and a three-bond HMBC correlation between H-2" and the carbonyl carbon of the acetyl group (**Fig. 4.2**).

In order to determine the absolute configuration of the two glucoses and to confirm the overall structure assignment, compound **4.5** was hydrolyzed with 6 M ammonium hydroxide to yield a product identified as randiadin (**4.4**) by its ^{1}H and ^{13}C NMR spectra. Further hydrolysis of **4.4** with 3 M hydrochloric acid yielded oleanolic acid, identified by its ^{1}H and ^{13}C NMR spectra, and a single monosaccharide, as indicated by a single TLC spot with the same R_f value as standard D-glucose. Its absolute configuration was determined to be D based on its positive optical rotation.

Based on this evidence, the structure of **4.5** was assigned as oleanolic acid-3-*O*-*β*-D-glucopyranosyl-(1→3)-(2"-*O*-acetyl)-*β*-D-glucopyranoside, or 2"-*O*-acetylrandia-nin.

4.2.4 *Structure Elucidation of Compound **4.6***

Compound **4.6**, isolated as light yellowish solid, $[\alpha]^{21}_{D}$ +17 (*c* 1.2, MeOH), had the same molecular formula as compound **4.5** as determined by HR–ESI–MS (*m/z* 845.4643 $[M+Na]^+$ and 861.4569 $[M+K]^+$), corresponding to a molecular formula of $C_{44}H_{70}O_{14}$. Due to the similarity of its NMR spectroscopic data with those of compounds **4.4** and **4.5**, the aglycone portion of **4.6** was also assigned as oleanolic acid, with the disaccharide moiety connected to C-3 of the aglycone.

As in compound **4.5**, the presence of two sugar molecules was suggested by the NMR spectra, which showed two sets of anomeric signals at δ_H 4.91/δ_C 106.7 and δ_H 5.25/δ_C 106.3, respectively. The two sugars were determined to be glucose, as corroborated by the similarity of the ^{13}C NMR chemical shifts of all carbons compared to those of compound **4.4**. The linkage between the two glucopyranosyl units was determined to be 1→3 by the observation of the HMBC correlations between H-3' and two anomeric carbons (C-1' and C-1"), as well as the cross-peak between H-3' and H-2' in the COSY spectrum (**Fig. 4.3**). The coupling constants between H-1' and H-2', and H-1" and H-2" (*J* = 7.8 and 7.8 Hz, respectively) indicated their axial-axial orientation and thus the *β*-configuration of the two sugar units. The presence of an acetyl group was indicated by a carbonyl absorption at 1727 cm^{-1} in its IR spectrum, ^{13}C NMR resonances at δ_C 171.2 ppm, and a singlet signal at 2.00 ppm in its ^{1}H NMR spectrum. The C-6" hydroxy group of the outer glucose of **4.6** was acetylated, as opposed to the C-2" of compound **4.5**. This was determined by comparing

the NMR spectral data of the outer glucose of **4.6** with those of **4.4**. The chemical shift of the two diastereotopic protons H-6'' of **4.4** were shifted from δ_H 4.54 and 4.58 ppm to δ_H 4.67 and 4.95 ppm in **4.6**, while the resonances of the other protons of the outer glucose are similar to those of compound **4.4**. Furthermore, the location of the acetyl group at C-6'' was confirmed by the COSY cross-peak between H-6'' and H-5'', and a three-bond HMBC correlation between H-6'' and the acetyl carbonyl carbon at 171.2 ppm, and between H-5'' and the anomeric carbon C-1'' (**Fig. 4.3**).

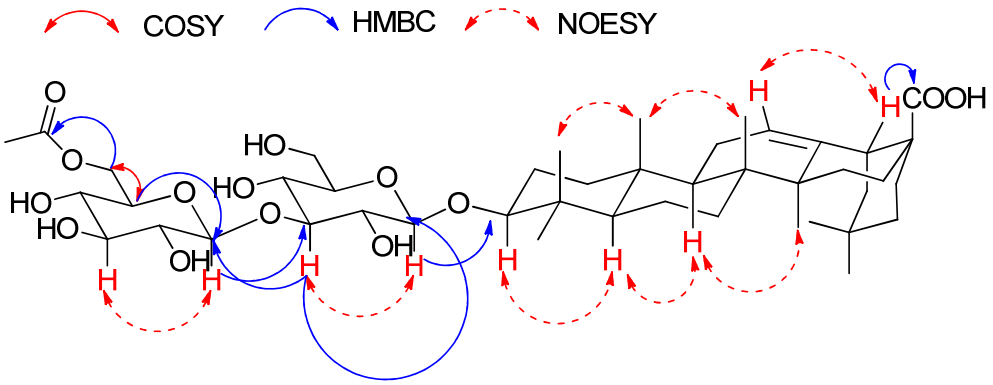

Figure 4.3 HMBC, COSY and NOESY Correlations of Compound **4.6**

As with compound **4.5**, the absolute configuration of the two glucoses and the overall structure assignment were confirmed by successive basic hydrolysis of **4.6** to randiadin and then acidic hydrolysis to oleanolic acid and D-glucose. Based on this evidence, the structure of **4.6** was elucidated as oleanolic acid-3-*O*-*β*-D-glucopyranosyl-(1→3)-(6''-*O*-acetyl)-*β*-D-glucopyranoside, or 6''-*O*-acetylrandianin.

4.2.5 *Antiproliferative Activities of the Isolated Compounds.*

Compounds **4.4**–**4.6** were tested for antiproliferative activity against the A2780 ovarian cancer, the A2058 melanoma, and the H522 lung cancer cell lines. All three compounds showed modest inhibition of the proliferation of A2780 ovarian cancer cell, with IC_{50} values in the low micromolar range. However, they showed only weak inhibition of the proliferation of A2058 melanoma and the H522 lung cancer cell lines (**Table 4.2**). Several hundred cytotoxic triterpene saponins have been identified from plants, but only a few of them showed selective antiproliferative activity.[14] 2"-*O*-Acetylrandianin (**4.5**) and 6"-*O*-acetylrandianin (**4.6**) are examples of compounds that selectively inhibit the proliferation of A2780 ovarian cancer cells. Furthermore, in the A2780 assay, the cytotoxicity of the two acetylated saponins is stronger than that of randianin (**4.4**), which has no acetyl group in its structure. This suggests that the increase in activity on acetylation may be due to an increase in lipophilicity, facilitating cellular uptake.[15]

Table 4.2 Antiproliferative Activities of Compounds **4.4–4.6**.

Compound	IC_{50} (μM)		
	A2780	A2058	H522
4.4	2.2 ± 0.2	7.63	7.32
4.5	1.7 ± 0.1	>3.3, <10	>10
4.6	1.2 ± 0.3	>3.3, <10	>10
Paclitaxel	0.028± 0.003	ND	ND
Vinblastine	ND	0.004	0.009

ND = not determined

4.3 Experimental Section

4.3.1 *General Experimental Procedures.*

Optical rotations were recorded on a JASCO P-2000 polarimeter. IR spectroscopic data were measured on a MIDAC M-series FTIR spectrophotometer. NMR spectra were recorded in pyridine-d_5 on a Bruker Avance 500 spectrometer. The chemical shifts are given in δ (ppm), and coupling constants (J) are reported in Hz. Mass spectra were obtained on an Agilent 6220 LC–TOF–MS in the positive ion mode.

4.3.2 *Antiproliferative Bioassay*

Antiproliferative activities were obtained at Virginia Polytechnic Institute and State University against the drug-sensitive A2780 human ovarian cancer cell line as previously described. [16] The values reported are the mean of three replicates. Antiproliferative activities against the A2058 melanoma and the H522 lung cancer cell lines were determined at Eisai Inc. by similar procedures to those used for the H460 cell line. [17]

4.3.3 *Plant Material*

A sample of the roots of *Nematostylis anthophylla* (A. Rich.) Baill. was collected in March 2011. The sample was a shrub of 60 cm with red flowers and succulent leaves, growing in rocky habitat in the Vakinakaratra region of the Antsirabe II district, Madagascar at an elevation of 1650 m., and coordinates 20°03'59"S 047°00'01"E (–20.0663889, 47.0002778). Duplicate voucher specimens (*Richard Randrianaivo et al. 1803)* have been deposited at the Parc Botanique et

Zoologique de Tsimbazaza (TAN), at the Centre National d'Application des Recherches Pharmaceutiques in Antananarivo, Madagascar (CNARP), the Missouri Botanical Garden in St. Louis, Missouri (MO), and the Muséum National d'Histoire Naturelle in Paris, France (P).

4.3.4 *Extraction and Isolation*

Dried root parts of *N. anthophylla* (273 g) were ground in a hammer mill, then extracted with EtOH by percolation for 24 h at room temperature to give the crude extract MG 4657 (12.4 g), of which 3.2 g was shipped to Virginia Tech for bioassay-guided isolation. A 1.1 g sample of MG 4657 (IC_{50} 6.9 μg/mL) was suspended in aqueous MeOH (MeOH/H_2O, 9:1, 100 mL), and extracted with hexanes (3 × 100 mL portions). The aqueous layer was then diluted to 60% MeOH (v/v) with H_2O and extracted with CH_2Cl_2 (3 × 150 mL portions). The remaining aqueous layer was further extracted with *n*-BuOH (3 × 100 mL portions). The hexanes fraction was evaporated in vacuo to leave 131 mg of material with IC_{50} > 20 μg/ml. The residue from the CH_2Cl_2 fraction (166 mg) had an IC_{50} of 7.7 μg/ml, the residue from the *n*-BuOH fraction (248.6 mg) had an IC_{50} of 2.5 μg/mL and the remaining aqueous MeOH fraction had an IC_{50} > 20 μg/ml. Chromatography of the CH_2Cl_2 fraction over a Sephadex® LH-20 size exclusion column with elution by CH_2Cl_2/MeOH, 1:1 was used to obtain six fractions, of which the most active fraction (40.3 mg) had an IC_{50} of 2.0 μg/mL. This fraction was then applied to a silica gel column with elution by $CHCl_3$/MeOH, 9:1 to give fourteen fractions, of which fraction 11 (4.8 mg) was the most active (IC_{50} 1.0 μg/mL) and yielded compound **4.6**. The *n*-BuOH fraction was applied to an open column of Diaion HP-20 resin and eluted with a step MeOH/H_2O gradient of 40%, 70% and 100% MeOH. The 100% MeOH fraction

was the most active fraction (100 mg) with an IC_{50} of 2.2 μg/mL. This fraction was applied to a silica gel column and eluted with $CHCl_3$/MeOH, 6:1 to give thirteen fractions, of which fraction 4 (1.8 mg) yielded compound **4.5**, with an IC_{50} of 1.5 μg/mL, and fraction 7 (6.3 mg) yielded compound **4.4**, with an IC_{50} of 1.9 μg/mL.

4.3.5 *Hydrolysis of Compounds **4.5** and **4.6**.*

Compound **4.6** (3.0 mg) was hydrolyzed with 10 mL 6 M NH_4OH for 2 h at 110 °C. The solution was evaporated to dryness under reduced pressure, and then dissolved in H_2O and extracted three times with *n*-BuOH. [18, 19] The *n*-BuOH extract was evaporated to dryness and yielded a light-yellow powder (2.6 mg) identified as compound **4.4** by its ^1H and ^{13}C NMR spectra. The light-yellow powder was further hydrolyzed with 10mL 3 M HCl for 4 h at 100 °C. The solution was extracted three times with EtOAc, and both the organic and the H_2O layers were evaporated to dryness under reduced pressure. The structure of the white powder (1.4 mg) derived from the organic layer was determined to be oleanolic acid by ^1H and ^{13}C NMR spectroscopy. The semi-solid carbohydrate mixture from the water layer (0.9 mg) was dissolved in 2 mL of water and kept overnight before TLC analysis and determination of its optical rotation. The same procedure was also applied to compound **4.5**. The sugar from both **4.5** and **4.6** had an R_f value identical to glucose by TLC on a silica gel plate with $CHCl_3$/MeOH/H_2O,15:6:1, and they had $[\alpha]_D^{21}$ +53.9 and 54.2, respectively, *c* 0.1, H_2O.

4.3.6 *2''-O-Acetylrandianin (**4.5**)*.

Light yellow solid; $[\alpha]_D^{21}$ +12 (*c* 1.2, MeOH); IR ν_{max} cm^{-1}: 3453, 2935, 1734, 1689, 1027 cm^{-1}. ^1H NMR (500 MHz, pyridine-d_5), and ^{13}C NMR (125 MHz, pyridine-d_5), see **Table 4.1**; HR–ESI–MS *m/z* 845.4692 $[M+Na]^+$ (calc. for $C_{44}H_{70}NaO_{14}^+$, 845.4658)

4.3.7 *6''-O-Acetylrandianin (**4.6**)*.

Light yellow solid; $[\alpha]_D^{21}$ +17 (*c* 1.2, MeOH); IR ν_{max} cm^{-1}: 3439, 2935, 1727, 1689, 1027 cm^{-1}. ^1H NMR (500 MHz, pyridine-d_5), and ^{13}C NMR (125 MHz, pyridine-d_5), see **Table 4.1**; HR–ESI–MS *m/z* 845.4643 $[M+Na]^+$ (calc. for $C_{44}H_{70}NaO_{14}^+$, 845.4658).

4.4 References and Notes

1. Dai, Y.; Harinantenaina, L.; Brodie, P. J.; Birkinshaw, C.; Randrianaivo, R.; Applequist, W.; Ratsimbason, M.; Rasamison, V. E.; Shen, Y.; TenDyke, K.; Kingston, D. G. I. Two antiproliferative triterpene saponins from *Nematostylis anthophylla* from the highlands of central Madagascar. *Chem. Biodivers.* **2013,** *10*, 233–240.

2. Harinantenaina, L.; Brodie, P. J.; Callmander, M. W.; Razafitsalama, L. J.; Rasamison, V. E.; Rakotobe, E.; Kingston, D. G. I. Two Antiproliferative saponins of *Tarenna grevei* from the Madagascar dry forest. *Nat. Prod. Commun.* **2012,** *7*, 705–708.

3. Kingston, D. G. I. Modern natural products drug discovery and its relevance to biodiversity conservation. *J. Nat. Prod.* **2011,** *74*, 496–511.

4. Pan, E.; Cao, S.; Brodie, P. J.; Callmander, M.; Rakotonandrasana, S.; Rakotobe, E.; Rasamison, V.; TenDyke, K.; Shen, Y.; Suh, E. M.; Kingston, D. G. I. Alkaloids of *Ambavia gerrardii* from the Madagascar dry forest and the synthesis of 9-hydroxyeupolauridine. *J. Nat. Prod.* **2011,** *74*, 1169–1174.

5. Karou, S. D.; Tchacondo, T.; Ilboudo, D. P.; Simpore, J. Sub-Saharan Rubiaceae: A review of their traditional uses. phytochemistry and biological activities. *Pak. J. Biol. Sci.* **2011,** *14*, 149–169.

6. Comini, L. R.; Fernandez, I. M.; Vittar, N. B. R.; Montoya, S. C. N.; Cabrera, J. L.; Rivarola, V. A. Photodynamic activity of anthraquinones isolated from *Heterophyllaea pustulata* Hook f. (Rubiaceae) on MCF-7c3 breast cancer cells. *Phytomedicine* **2011,** *18*, 1093–1095.

7. Mukhtar, M. R.; Osman, N.; Awang, K.; Hazni, H.; Qureshi, A. K.; Hadi, A. H. A.; Zaima, K.;

Morita, H.; Litaudon, M. Neonaucline, a new indole alkaloid from the leaves of *Ochreinauclea maingayii* (Hook. f.) Ridsd. (Rubiaceae). *Molecules* **2012,** *17*, 267–274.

8. Nazari, A. S.; Dias, S. A.; Costa, W. F. d.; Bersani-Amado, C. A.; Vidotti, G. J.; Souza, M. C. d.; Sarragiotto, M. H. Anti-inflammatory and antioxidant activities of *Randia hebecarpa* and major constituents. *Pharm. Biol.* **2006,** *44*, 7–9.

9. Rasoarivelo, S. T. R.; Grougnet, R.; Vérité, P.; Lecsö, M.; Butel, M.-J.; Tillequin, F.; Guillou, C. R.; Deguin, B. Chemical composition and antimicrobial activity of the essential oils of *Anthospermum emirnense* and *Anthospermum perrieri* (Rubiaceae). *Chem. Biodivers.* **2011,** *8*, 145–154.

10. He, Z. D.; Ma, C.Y. ; Zhang, H. J.; Tan, G. T.; Tamez, P.; Sydara, K.; Bouamanivong, S.; Southavong, B.; Soejarto, D. D.; Pezzuto, J. M.; Fong, H. H. S. Antimalarial constituents from *Nauclea orientalis* (L.) L. *Chem. Biodivers.* **2005,** *2*, 1378–1386.

11. Abdel-Kader, M. S.; Bahler, B. D.; Malone, S.; Werkhoven, M. C. M.; Wisse, J. H.; Neddermann, K.; Bursuker, I.; Kingston, D. G. I. Bioactive saponins from *Swartzia schomburgkii* from the Suriname rain forest. *J. Nat. Prod.* **2000,** *63*, 1461–1464.

12. Sotheeswaran, S.; Bokel, M.; Kraus, W. A hemolytic saponin, Randianin, from *Randia dumetorum*. *Phytochemistry* **1989,** *28*, 1544–1546.

13. Tori, K.; Seo, S.; Shimaoka, A.; Tomita, Y. Carbon-13 NMR spectra of olean-12enes. *Tetrahedron Lett.* **1974,** *48*, 4227–4230.

14. Arai, M.; Hayashi, A.; Sobou, M.; Ishida, S.; Kawachi, T.; Kotoku, N.; Kobayashi, M. Anti-angiogenic effect of triterpenoidal saponins from *Polygala senega*. *J. Nat. Med.* **2011,** *65*,

149–156.

15. Colin, D.; Gimazane, A.; Lizard, G.; Izard, J. C.; Solary, E.; Latruffe, N.; Delmas, D. Effects of resveratrol analogs on cell cycle progression, cell cycle associated proteins and 5-fluoro-uracil sensitivity in human derived colon cancer cells. *Int. J. Cancer* **2009,** *124*, 2780–2788.

16. Cao, S.; Brodie, P. J.; Miller, J. S.; Randrianaivo, R.; Ratovoson, F.; Birkinshaw, C.; Andriantsiferana, R.; Rasamison, V. E.; Kingston, D. G. I. Antiproliferative xanthones of *Terminalia calcicola* from the Madagascar rain forest. *J. Nat. Prod.* **2007,** *70*, 679–681.

17. Pan, E.; Harinantenaina, L.; Brodie, P. J.; Callmander, M.; Rakotonandrasana, S.; Rakotobe, E.; Rasamison, V. E.; TenDyke, K.; Shen, Y.; Suh, E. M.; Kingston, D. G. I. Cardenolides of *Leptadenia madagascariensis* from the Madagascar dry forest. *Bioorg. Med. Chem.* **2011,** *19*, 422–428.

18. Tchacondo, T.; Karou, S. D.; Batawila, K.; Agban, A.; Ouro-Bang'na, K.; Anani, K. T.; Gbeassor, M.; de Souza, C. Herbal remedies and their adverse effects in tem tribe traditional medicine in togo. *Afr. J. Tradit. Complement Altern. Med.* **2011,** *8*, 45–60.

19. Karou, S. D.; Tchacondo, T.; Djikpo Tchibozo, M. A.; Abdoul-Rahaman, S.; Anani, K.; Koudouvo, K.; Batawila, K.; Agbonon, A.; Simpore, J.; de Souza, C. Ethnobotanical study of medicinal plants used in the management of diabetes mellitus and hypertension in the central region of Togo. *Pharm. Biol.* **2011,** *49*, 1286–1297.

Chapter 5: Antiproliferative Homoisoflavonoids and Bufatrienolides from *Urginea depressa*

This chapter is a slightly expanded version of a published article. (Dai, Y.; Harinantenaina, L.; Brodie, P. J.; Goetz, M.; Shen, Y.; Tendyke, K.; Kingston, D. G. I. Antiproliferative homoisoflavonoids and bufatrienolides from *Urginea depressa*. *J. Nat. Prod.* **2013,** *76*, 865–872.) Attributions of co-authors of the articles are described as follows in the order of the names listed. The author of this dissertation (Mr. Yumin Dai) conducted the isolation and structural elucidation part of the titled compounds, and drafted the manuscript. Dr. Liva Harinantenaina was a mentor for this work, and in particular, he provided invaluable advice and hints for the structural elucidation of that compound, and he also proofread the manuscript before submission. Ms. Peggy Brodie performed the A2780 bioassay on the isolated fractions and compounds. Dr. Michael Goetz from Natural Products Discovery Institute did the plant collections and identification. Dr. Yongchun Shen, Dr. Karen TenDyke, and Dr. Edward M. Suh from Eisai Inc. performed the A2058 and H522 bioassay on the compounds isolated. Dr. David G. I. Kingston was a mentor for this work and the corresponding author for the published article. He provided critical suggestions for this work and edited the final version of manuscript.[1]

5.1 Introduction

Natural products have been a major source of new drugs for the last 70 years, with almost 50% of all anticancer drugs discovered since 1940 being natural products or modified natural products.[2] Until recently the Merck pharmaceutical company maintained a strong program in natural products research, which resulted in the discovery of the antifungal agent CANCIDAS®, the antibacterial

MEFOXIN® (cefoxitin), and the statin MEVACOR®, among others, but the company halted in-house natural products research in 2008.[3] The superb Merck natural products library, which is considered to be one of the most diverse and best curated natural products libraries in the world, was donated to The Institute for Hepatitis and Virus Research (IHVR) and its Natural Products Discovery Institute (NPDI) in 2011.[4] A collaborative research project was then established between Virginia Tech and the NPDI to interrogate this library for potential antiproliferative and antimalarial activities.

Screening of several thousand extracts from the NPDI collection indicated that a CH_2Cl_2 extract of the whole plant *Urginea depressa* (Asparagaceae, formerly Hyacinthaceae)[5] exhibited antiproliferative activity against the A2780 human ovarian cancer cell line, with an IC_{50} value of 2.4 μg/mL. The Asparagaceae family is a family of herbaceous perennial bulbous flowering plants, which are distributed predominantly in Mediterranean climates including South Africa, Central Asia, and South America. *Urginea*, a genus of this family, is a rich source of stilbenoids, homoisoflavonoids (*eg.* 4'-O-demethyleucomol, **5.1**), bufadienolides, sesquiterpenoids (*eg.* 6*α*-hydroxyl-4-endesmen-1-one, **5.2**), and alkaloids (*eg.* Steviamine, **5.3**), which are well-known for their broad range of bioactivities, including antimicrobial, antioxidant, cytotoxic, and anti-inflammatory activities, etc.[6-10] The genus *Urginea* has been explored by other investigators, and in addition four bufadienolides were isolated from *Drimia depressa*, a botanical synonym of *Urginea depressa*.[11, 12] These previous studies did not however report any biological data and the extract of *U. depressa* was selected for bioassay guided fractionation to isolate its bioactive components.

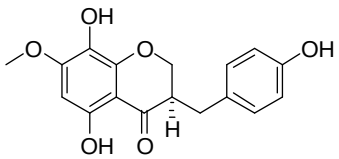

5.1

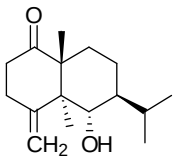

5.2

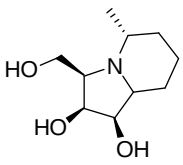

5.3

5.2 Results and Discussion

5.2.1 *Isolation of Active Compounds*

An EtOH extract of the whole plant of *Urginea depressa* was subjected to liquid–liquid partitioning to give active hexanes, CH_2Cl_2, and aqueous MeOH fractions with the IC_{50} values to the A2780 ovarian cancer cell line of 2.6, 0.68, and 0.72 μg/mL, respectively. Bioassay guided separation of the hexanes and CH_2Cl_2 fractions, including Sephadex LH-20 size exclusion, silica gel normal-phase chromatography and C_{18} reverse-phase HPLC, yielded six new homoisoflavonoids which were named urgineanins A–F (**5.4** – **5.9**); urgineanins C and F (**5.6** and **5.9**) are enantiomers of known compounds（**Scheme 5.1**）. In addition, the bioactive aqueous methanol fraction from the initial liquid–liquid partition described above was subjected to bioassay-guided separation using diaion HP-20, size exclusion Sephadex LH-20, C_{18} flash chromatography, and C_{18} reverse-phase HPLC to afford the two known compounds **5.10** and **5.12**, and the two new bioactive bufatrienolides, named urginin B (**5.11**) and urginin C (**5.13**). Herein, we report the structural elucidation of these compounds.

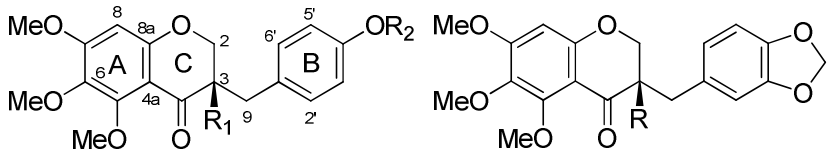

	R_1	R_2
5.4	OH	CH_3
5.5	OH	H
5.6	H	CH_3

	R
5.7	OH
5.8	H

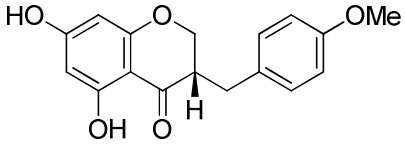

5.9

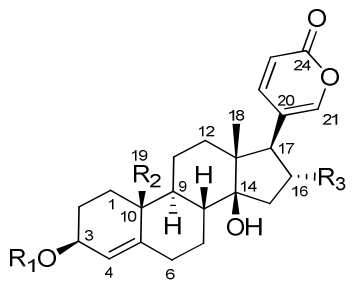

	R_1	R_2	R_3
5.10	Glc	CHO	H
5.11	Glc	CHO	OAc
5.12	4'-Glc-Rha-3'-Rha	CH_3	H
5.13	4'-Glc-Rha-3'-Rha	CHO	H

Figure 5.1 Chemical Structure of Compounds **5.4–5.13**

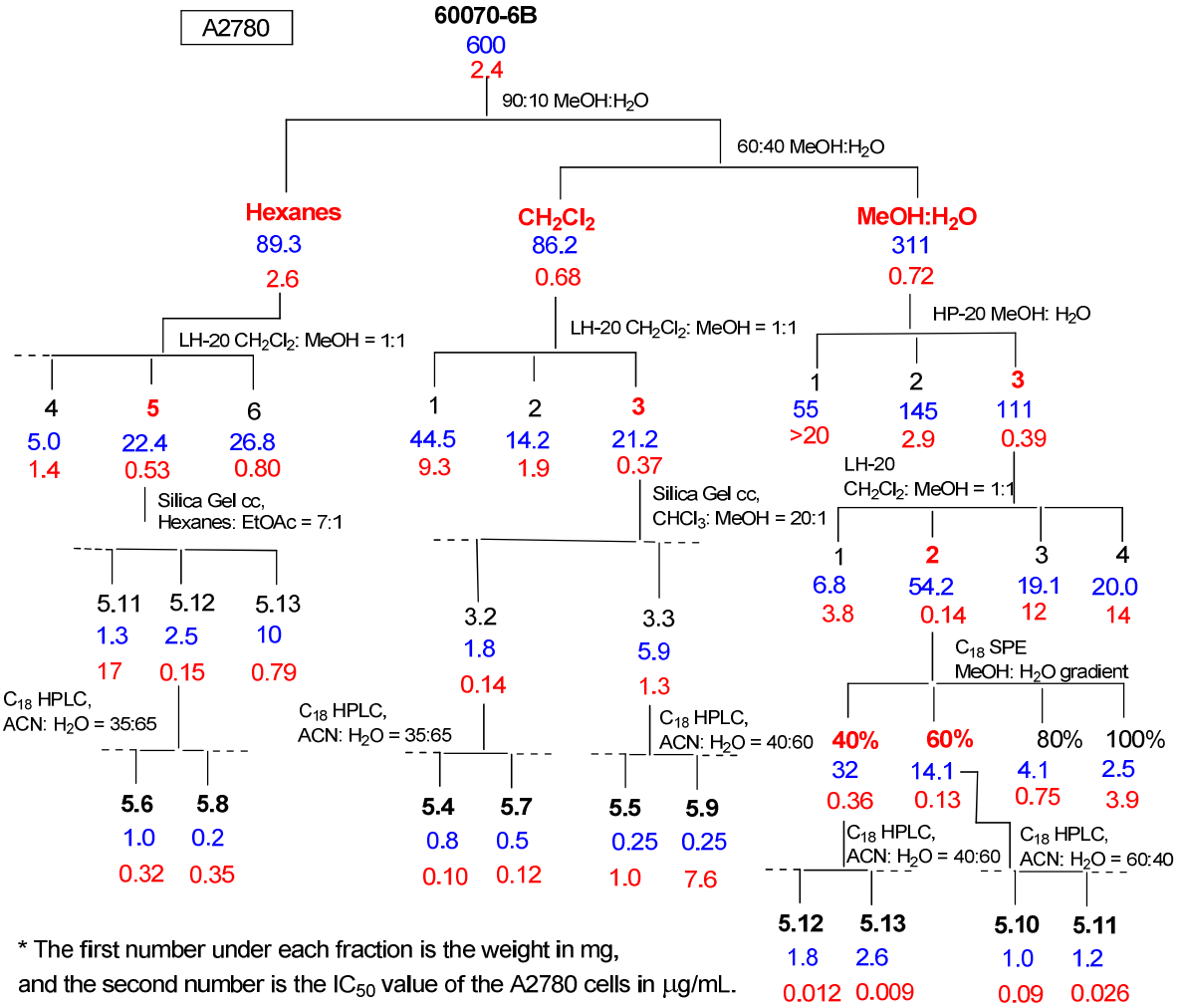

Scheme 5.1 Bioassay Guided Separation of the Extract of *Urginea depressa*

5.2.2 *Structure Elucidation of Compound* ***5.4***

Urgineanin A (**5.4**), $[\alpha]^{21}_{D}$ +26 (*c* 0.12, MeOH), was isolated as a light yellow oil. Its composition was established as $C_{20}H_{22}O_7$ by positive ion HR–ESI–MS. Its IR spectrum exhibited absorption bands at 3464 and 1678 cm^{-1}, indicating the presence of hydroxy and conjugated carbonyl groups. Its ^{1}H NMR spectrum displayed the typical splitting pattern of an eucomol-type homoisoflavonoid, with two pairs of geminal coupled proton signals at δ_H 3.93 and 3.96 (each a doublet, J = 11.4 Hz), and δ_H 2.79 and 2.83 (each a doublet, J = 10.8 Hz).[13] The observation of 12 aromatic carbon signals, a carbonyl carbon resonance at δ_C 191.8, as well as a methylene carbon signal at δ_C 38.6 in the ^{13}C NMR spectrum, corroborated the homoisoflavonoid structure (**Table 5.1**). The basic skeleton of 3-hydroxy-3-benzyl-4-chromanone was confirmed by the HMBC correlations between H-2 and C-3, H-9 and C-3, H-9 and C-2, H-2 and C-4, H-9 and C-4, and H-9 and C-1'. The presence of four proton singlets (each 3H) located at δ_H 3.69, 3.72, 3.74, and 3.85 in the ^{1}H NMR spectrum, corresponding by HMQC to the four aromatic carbon resonances located at δ_C 60.8, 54.9, 61.2, and 56.2, indicated the presence of four methoxy groups. Two doublets at δ_H 6.84 and 7.13 (2H each, J = 8.7 Hz) indicated a *para*-disubstituted B−ring. A singlet at δ_H 6.49 was assigned to H-8 of the A-ring, based on the HMBC correlations between H-8 and C-8a and between H-8 and C-4a (**Fig. 5.2**).

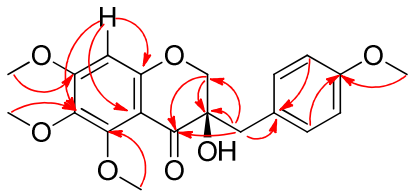

Figure 5.2 HMBC Correlation of Compound **5.4**

The stereochemistry at C-3 was determined by comparison of its electronic circular dichroism (ECD) spectrum with those of previously reported homoisoflavonoids. Thus the positive π–π*

Cotton effect ($\Delta\varepsilon$ = 10.8) at 280 nm and the negative n–π* Cotton effect ($\Delta\varepsilon$ = –7.2) at 315 nm indicated the *R* configuration, in analogy to caesalpiniaphenol A,[14] and in agreement with the statement that a positive Cotton effect in the 287–295 nm region of the ECD curves of homoisoflavonoids is indicative of a 3*S*-configuration for compounds lacking a C-3 hydroxy group,[15] corresponding to the 3*R* configuration for C-3 hydroxylated compounds.

Hence, the structure of compound **5.4** was assigned as *(3R)*–3-hydroxy-3-(4'-methoxybenzyl)-5,6,7-trimethoxychroman-4-one.

Table 5.1 NMR Spectroscopic Data for Compounds **5.4**, **5.5**, **5.7** and **5.8** in DMSO-d_6 (600 MHz)

	5.4		**5.5**		**5.7**		**5.8**	
position	δ_H (*J* in Hz)	δ_C, type	δ_H (*J* in Hz)	δ_C, type	δ_H (*J* in Hz)	δ_C, type	δ_H (*J* in Hz)	δ_C, type
2a	3.96 d (11.4)	71.5, CH_2	3.96 d (11.3)	71.2, CH_2	3.99 d (10.6)	71.4, CH_2	4.27 dd (11.3, 4.5)	69.4, CH_2
2b	3.93 d (11.4)		3.92 d (11.3)		3.95 d (10.6)		4.08 dd (11.3, 8.8)	
3	-	72.1, C	-	72.7, C	-	72.1, C	2.85 m	47.7, CH
4	-	191.8, C	-	191.9, C	-	191.7, C	-	190.8, C
4a	-	106.8, C	-	106.8, C	-	107.7, C	-	108.7, C
5		153.6, C	-	153.7, C	-	153.6, C	-	154.0, C
6	-	137.1, C	-	137.3, C	-	137.1, C	-	137.4, C
7	-	159.0, C	-	159.1, C	-	159.0, C	-	159.2, C
8	6.49 s	96.5, CH	6.49 s	96.6, CH	6.49 s	96.5, CH	6.45 s	96.9, CH
8a	-	158.8, C	-	158.7, C		158.8, C	-	158.9, C
9a	2.83 d (10.8)	38.6, CH_2	2.77 d (10.7)	38.7, CH_2	2.83 d (10.5)	38.7, CH_2	3.01 dd (14.1, 5.1)	32.3, CH_2
9b	2.79 d (10.8)		2.73 d (10.7)		2.79 d (10.5)		2.57 dd (14.1, 9.4)	
1'	-	127.2, C	-	125.8, C	-	129.0, C	-	132.1, C
2'	7.13 d (8.7)	131.5, CH	7.00 d (8.5)	131.4, CH	6.79 d (1.6)	114.9, CH	6.84 d (1.6)	108.6, CH
3'	6.84 d (8.7)	113.2, CH	6.66 d (8.5)	114.6, CH	-	145.8, C	-	145.7, C
4'	-	157.9, C	-	156.3, C	-	146.9, C	-	146.4, C
5'	6.84 d (8.7)	113.2, CH	6.66 d (8.5)	114.6, CH	6.81 d (7.9)	110.6, CH	6.83 d (8.0)	109.8, CH
6'	7.13 d (8.7)	131.5, CH	7.00 d (8.5)	131.4, CH	6.65 dd (7.9, 1.6)	123.4,CH	6.68 dd (8.0, 1.6)	122.0, CH
5-OMe	3.74 s	61.2, CH_3	3.74 s	61.2, CH_3	3.74 s	61.2, CH_3	3.74 s	61.2, CH_3
6-OMe	3.69 s	60.8, CH_3	3.68 s	60.8, CH_3	3.69 s	60.8, CH_3	3.66 s	60.8, CH_3
7-OMe	3.85 s	56.2, CH_3	3.86 s	56.2, CH_3	3.85 s	56.2, CH_3	3.84 s	56.2, CH_3
4'-OMe	3.72 s	54.9, CH_3						
3'-OCH_2 O-4'					5.97 d (1.0) 5.98 d (1.0)	100.6, CH_2	5.97 d (1.0) 5.98 d (1.0)	100.6, CH_2

* Carbon-NMR data for compound **5.5** and **5.8** were obtained from HMBC and HSQC or HMQC spectra.

5.2.3 *Structure Elucidation of Compound* ***5.5***

Urgineanin B (**5.5**), $[\alpha]^{21}_{D}$ +18 (*c* 0.12, MeOH), was also isolated as a light yellow oil; its composition was established as $C_{19}H_{20}O_7$ by positive ion HR–ESI–MS. Comparison of ^{1}H and ^{13}C NMR spectroscopic data of **5.5** with those of **5.4** (**Table 5.1**) indicated that both compounds had the same skeleton and substitution pattern, and differed only in that **5.5** had a hydroxy group in place of one of the *O*-methyl groups of **5.4**. The ^{1}H NMR spectrum of compound **5.5** showed three singlets at δ_H 3.68, 3.74 and 3.86 (each 3H) for the three methoxy groups of ring A. The presence of a hydroxy group instead of an *O*-methyl group at C-4' was confirmed by the absence of the NMR resonances (δ_H 3.72/ δ_C 54.9) and 2D correlations of the 4'-*O*-methyl methoxy group of **5.4** (**Fig. 5.3**). Similar to compound **5.4**, a positive π–π* Cotton effect ($\Delta\varepsilon$ = 10.4) at 281 nm and a negative n–π* Cotton effect ($\Delta\varepsilon$ = –7.3) at 316 nm indicated the *R* configuration of C-3. Thus, the structure of compound **5.5** was concluded to be *(3R)*–3-hydroxy-3-(4'-hydroxybenzyl)-5,6,7-trimethoxychroman-4-one.

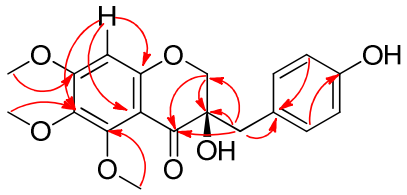

Figure 5.3 HMBC Correlation of Compound **5.5**

5.2.4 *Structure Elucidation of Compound* ***5.6***

Urgineanin C (**5.6**), $[\alpha]^{21}_{D}$ +9, was identified as the enantiomer of the known homoisoflavonoid (3*S*)–5,6,7-trimethoxy-3-(4-methoxybenzyl)chroman-4-one by comparison of its experimental and reported physical and spectroscopic data.[15, 16] Based on the positive π–π* Cotton effect ($\Delta\varepsilon$ = 5.6) at 286 nm and a negative n–π* Cotton effect ($\Delta\varepsilon$ = –2.8) at 251 nm, the

absolute configuration of C-3 was assigned as *S*, enantiomeric with the reported compound.[15]

5.2.5 *Structure Elucidation of Compound* ***5.7***

Urgineanin D (**5.7**, $[\alpha]^{21}_{D}$ +23, light yellow oil) had the molecular formula $C_{20}H_{20}O_8$ as determined by the HR–ESI–MS. Comparison of the NMR spectroscopic data of **5.7** with those of **5.4** indicated that the only difference was the B-ring substitution pattern. The ^{1}H NMR spectrum of **5.7** had signals for three aromatic protons of the B-ring with an ABX-type spin system [δ_H 6.79 (1H, d, J = 1.6 Hz), 6.81 (1H, d, J = 7.9 Hz) and 6.65 (1H, dd, J = 7.9, 1.6 Hz)]. The presence of a methylenedioxy group (-OCH_2O-) in **5.7** was confirmed by the typical methylene carbon signal at δ_C 100.6 and two proton resonances at δ_H 5.97 and 5.98 (2H, d, J = 1.0 Hz).[17] This group was assigned to C-3' and C-4' based on HMBC correlations between the methylene protons and C-3'/C-4', and between H-2' and C-4' (**Fig. 5.4**). As with compounds **5.4** and **5.5**, the absolute configuration of C-3 was determined to be *R* based on the positive π–π* Cotton effect ($\Delta\varepsilon$ = 6.8) at 280 nm and a negative n–π* Cotton effect ($\Delta\varepsilon$ = –5.2) at 316 nm. The structure of compound **5.7** was thus assigned as *(3R)*–3-hydroxy-3-(3',4'-methylenedioxy)-5,6,7-trimethoxychroman-4-one.

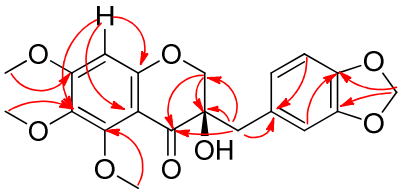

Figure 5.4 HMBC Correlation of Compound **5.7**

5.2.6 *Structure Elucidation of Compound* ***5.8***

Urgineanin E (**5.8**) was obtained as a light yellow oil with $[\alpha]^{21}_{D}$ +12 (*c* 0.12, MeOH). Its molecular formula was deduced as $C_{20}H_{20}O_7$ by HR–ESI–MS. Comparison of the ^{1}H NMR

spectroscopic data of compound **5.8** with those of compound **5.7** indicated that both compounds possessed the same A- and B-ring substitutions but differed in the C-ring. The ^{1}H NMR spectrum of compound **5.8** displayed the typical splitting pattern of eucomin-type homoisoflavonoids, characterized by two sets of doublet of doublets (δ_H 4.08/4.27 and δ_H 2.57/3.01) assignable to the two protons of C-2 and C-9, respectively; and the prominent complex multiplet (δ_H 2.85) signal of the proton at C-3.[18] The absence of an OH group at C-3 was confirmed by the upfield shift of the C-3 resonance (δ_C 47.7 ppm). The basic skeleton of 3-benzyl-4-chromanone was corroborated by HMBC correlations between H-2 and C-3, H-3 and C-9, H-9 and C-3, H-9 and C-2, H-2 and C-4, and H-9 and C-1' (**Fig. 5.5**). The absolute configuration of compound **5.8** was determined to be *S*, based on its positive π–π* Cotton effect ($\Delta\varepsilon$ = 5.9) at 288 nm and the negative n–π* Cotton effect ($\Delta\varepsilon$ = –0.1) at 309 nm.[19] The structure of compound **5.8** was thus assigned as *(3S)*–3-(3',4'-methylenedioxy)-5,6,7-trimethoxychroman-4-one.

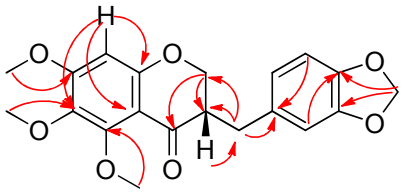

Figure 5.5 HMBC Correlation of Compound **5.8**

5.2.7 *Structure Elucidation of Compound* ***5.9***

Urgineanin F (**5.9**), [α] $^{21}_{D}$ +6, was identified as the enantiomer of the known homoisoflavonoid (3*S*)–5,7-dihydroxy-3-(4-methoxybenzyl)chroman-4-one by comparison of its experimental and reported physical and spectroscopic data.[20, 21] As with **5.6**, compound **5.9** differs from the known compound by its configuration at C-3. A positive π–π* Cotton effect ($\Delta\varepsilon$ = 5.8) at 288 nm and a negative n–π* Cotton effect ($\Delta\varepsilon$ = –2.2) at 251 nm indicated the 3*S* configuration.

5.2.8 *Structure Elucidation of Compound* ***5.10***

Compound **5.10** was identified as altoside (14*β*-hydroxy-19*β*-oxobufa-4,20,22-trienolide -3*β*-*O*-*β*-D-glucopyranoside), a known bufatrienolide isolated in 1959 from *Urginea altissima*.[22] To complete the partially reported NMR spectroscopic data reported in the literature, and to enable comparison with the NMR data of **5.11** and **5.13**, its complete ^{1}H and ^{13}C NMR spectroscopic data (**Table 5.2**), as well as its key HMBC correlations are recorded here (**Fig. 5.6**).

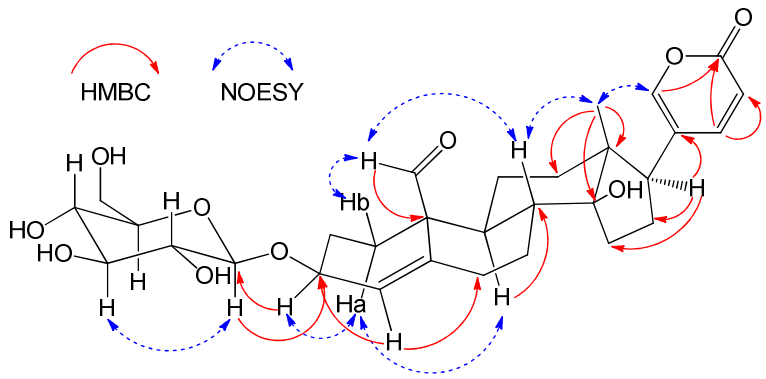

Figure 5.6 HMBC and NOESY Correlations of Compound **5.10**

Table 5.2 NMR Spectroscopic Data for **5.10**–**5.11**, **5.13** in Methanol-d_4 (600 MHz)

	5.10		**5.11**		**5.13**	
Position	δ_H (J in Hz)	δ_C, type	δ_H (J in Hz)	δ_C, type	δ_H (J in Hz)	δ_C, type
1a	2.13 m	28.1, CH_2	2.16 m	27.7, CH_2	2.16 m	29.6, CH_2
1b	1.08 m		1.04 m		1.10 m	
2a	1.99 m	27.6, CH_2	2.00 m	27.2, CH_2	2.08 m	28.5, CH_2
2b	1.28 m		1.36 m		1.30 m	
3	4.18 m	74.2, CH	4.19 m	74.1, CH	4.05 m	74.1, CH
4	5.74 brs	126.2, CH	5.76 brs	126.4, CH	5.63 brs	127.2, CH
5	-	138.2, C	-	138.4, C	-	139.7, C
6a	2.29 m	32.9, CH_2	2.31 m	32.7, CH_2	2.33 m	34.2, CH_2
6b	2.23 m		2.25 m		2.24 m	
7a	2.35 m	28.4, CH_2	2.34 m	28.3, CH_2	2.36 m	29.4, CH_2
7b	1.27 m		1.30 m		1.29 m	
8	1.78 m	43.0, CH	1.81 m	42.9, CH	1.80 m	44.4, CH
9	1.23 m	49.4, CH	1.21 m	49.3, CH	1.25 m	51.0, CH
10	-	53.6, C	-	53.4, C	-	55.0, C
11a	1.60 m	21.5, CH_2	1.62 m	21.3, CH_2	1.63 m	23.1, CH_2
11b	1.30 m		1.32 m		1.32 m	
12a	1.44 m	40.2, CH_2	1.50 m	39.0, CH_2	1.46 m	41.5, CH_2

12b	1.31 m		1.28 m		1.33 m	
13	-	47.7, C	-	49.2, C	-	49.0, C
14	-	84.0, C	-	82.9, C	-	85.8, C
15a	1.88 m	31.4, CH_2	1.67 d (15.6)	39.5, CH_2	1.91 m	32.8, CH_2
15b	1.53 m		2.43 dd (15.6, 8.8)		1.55 m	
16a	2.07 m	28.2, CH_2	5.38 t (8.8)	74.2, CH	1.91 m	29.7, CH_2
16b	1.65 m				1.66 m	
17	2.45 dd (9.5, 6.9)	50.6, CH	2.87 d (8.8)	56.6, CH	2.47 dd (9.5, 7.0)	52.0, CH
18	0.62 s	15.7, CH_3	0.70 s	15.5, CH_3	0.64 s	17.1, CH_3
19	9.72 s	204.1, C	9.72 s	203.9, C	9.75 s	204.4, C
20	-	123.7, C	-	117.6, C	-	123.6, C
21	7.33 d (1.7)	149.1, CH	7.34 d (1.7)	151.3, CH	7.34 d (1.7)	150.6, CH
22	7.90 dd (9.5, 1.7)	147.8, CH	8.15 dd (9.5, 1.7)	150.6, CH	7.90 dd (9.5, 1.7)	149.3, CH
23	6.19 d (9.5)	114.0, CH	6.10 d (9.5)	111.8, CH	6.20 d (9.5)	115.5, CH
24	-	163.5, C	-	163.6, C	-	163.1, C
Acetyl						
CO				170.2, C		
CH_3			1.75 s	19.6, CH_3		
	C-3-*O*-Glucopyranosyl		C-3-*O*-Glucopyranosyl		C-3-*O*-Rhamnopyranosyl	
1'	4.32 d (7.9)	102.0, CH	4.33 d (7.8)	102.1, CH	4.72 overlapped	100.9, CH
2'	3.04 dd (9.1, 7.9)	73.6, CH	3.05 dd (9.2, 7.8)	73.7, CH	3.78 dd (3.2, 2.0)	72.5, CH
3'	3.17 m	76.6, CH	3.18 m	76.6, CH	3.84 dd (9.3, 3.2)	81.5, CH
4'	3.15 m	70.2, CH	3.16 m	70.3, CH	3.67 t (9.3)	78.1, CH
5'	3.26 m	76.7, CH	3.26 m	76.7, CH	3.64 dq (9.3, 6.2)	69.1, CH
6'a	3.55 dd (4.7, 11.1)	61.5, CH	3.56 dd (6.5, 11.4)	61.4, CH	1.21 d (6.2)	18.2, CH_3
6'b	3.76 dd (2.1, 11.1)		3.77 dd (2.1, 11.4)			
					C-3'-*O*-Rhamnopyranosyl	
1"					4.89 d (1.7)	104.6, CH
2"					3.94 dd (3.4, 1.7)	70.0, CH
3"					3.64 dd (9.5, 3.4)	72.2, CH
4"					3.30 t (9.5)	74.1, CH
5"					3.73 dq (9.5, 6.2)	70.2, CH
6"					1.20 d (6.2)	17.9 CH_3
					C-4'-*O*-Glucopyranosyl	
1'''					4.48 d (7.9)	104.4, CH
2'''					3.07 dd (9.1, 7.9)	75.3, CH
3'''					3.26 dd (9.1, 8.8)	77.9, CH
4'''					3.21 t (8.8)	71.9, CH
5'''					3.13 ddd (2.4, 5.5, 8.8)	78.0, CH
6'''					3.58 dd (5.5, 11.8)	62.9, CH
6'''					3.75 dd (2.4, 11.8)	

* ^{13}C-NMR data for compound **5.10** were obtained from HMBC and HSQC spectra.

5.2.9 *Structure Elucidation of Compound* ***5.11***

Urginin B (**5.11**), $[\alpha]^{21}_{D}$ +27 (*c* 1.2, MeOH), was isolated as a light yellow powder, and its composition was determined as $C_{32}H_{42}O_{12}$ by HR–ESI–MS. A ^{13}C NMR resonance at δ_C 170.2 ppm, and a singlet at δ_H 1.75 (3H) in the ^{1}H NMR spectrum suggested the presence of an *O*-acetyl group. In addition, a formyl group was revealed by the observation of a carbonyl absorption (1710 cm^{-1}), a ^{13}C NMR resonance at δ_C 203.9, and a singlet signal at δ_H 9.72 in the ^{1}H NMR spectrum. Meanwhile, the glycosidic nature of compound **5.11** was indicated by the presence of a proton signal at δ_H 4.33 (d, J = 7.8 Hz, H-1'), as well as six resonances observed in the range of δ_H 2.90–3.80. In addition to the methyl and carbonyl carbons of the *O*-acetyl group, there were 30 carbon signals in the ^{13}C NMR spectrum, among which 24 (including a formyl carbon) were assigned to a bufatrienolide aglycone, and the remaining six to a monosaccharide moiety.[23]

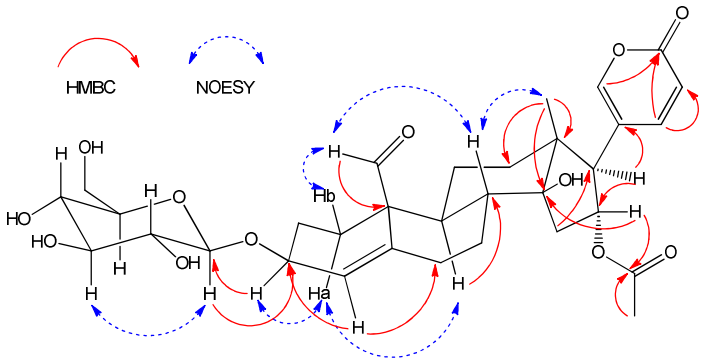

Figure 5.7 HMBC and NOESY Correlations of Compound **5.11**

The ^{1}H and ^{13}C NMR spectra of compounds **5.11** and **5.10** were similar except that the spectra of **5.11** contained signals for an *O*-acetyl group and one additional oxygen-bearing carbon (δ_H 5.38, δ_C 74.2), indicating that **5.11** is a bufatrienolide. The three oxygen-bearing carbons C-3 (δ_C 74.1), C-16 (δ_C 74.2) and C-14 (δ_C 82.9) were assigned based on the interpretation of the HSQC, COSY and HMBC spectra (**Fig. 5.7**), indicating the additional group to be at C-16. The *O*-acetyl group was deduced to be attached to C-16, as indicated by the HMBC correlations between H-17

and C-16, H-17 and C-20, as well as between H-16 (δ_H 2.87) and the carbonyl carbon of the *O*-acetyl group.

The coupling constant between H-17 and H-16 (J = 8.8 Hz) indicated a *trans* configuration of the two protons, and thus an α-orientation of the *O*-acetyl group.[24] The orientation of H-3 was also determined to be α, based on the NOESY crosspeaks between H-1b and H-19, and H-3 and H-1a. (**Fig. 5.7**). The absolute configuration at C-14 was assigned as *S* based on the similarities of structure and origin of **5.10** and **5.11**, and on the common occurrence of this configuration for 14-hydroxybufadienolides.[25]

The anomeric signals at δ_H 4.33 (d, J = 7.8 Hz)/δ_C 102.1 were assigned to a β-glucopyranosyl unit, based on their similarity with those of the sugar moiety of **5.10** (**Table 5.2**). In order to determine the absolute configuration of the glucose, compound **5.11** was hydrolyzed with 3 M hydrochloric acid to yield D-glucose, as indicated by its identical R_f value compared to the D-glucose standard in TLC-analysis and its positive optical rotation. Based on the above evidence, the structure of compound **5.11** was assigned as14β-hydroxy-19β-oxobufa-4,20,22-trienolide-16α-*O*-acetyl-3β-*O*-β-D-glucopyranoside.

5.2.10 *Structure Elucidation of Compound **5.9***

Compound **5.12** was identified as urginin, (14β-hydroxybufa-4,20,22-trienolide-3β-*O*-{α-L-rhamnopyranosyl-[(1→4)-β-D-glucopyranosyl]-(1→3)-α-L-rhamnopyranoside}), by comparison of its experimental and reported physical and spectroscopic data.[26]

5.2.11 *Structure Elucidation of Compound **5.13***

Urginin C (**5.13**), $[\alpha]^{21}_{D}$ −14 (*c* 1.2, MeOH), was obtained as a light yellow powder. Its

composition was assigned as $C_{42}H_{60}O_{18}$, based on its positive ion HR–ESI–MS spectrum. Comparison of the ^{1}H and ^{13}C NMR spectroscopic data of compound **5.13** with those of compounds **5.10** and **5.12** indicated that compounds **5.10** and **5.13** possessed the same 3*β*,14*β*-dihydroxy-19*β*-oxobufa-4,20,22-trienolide aglycone,[27, 28] and that compounds **5.12** and **5.13** had identical sugar moieties at C-3.

The presence of trisaccharide units was suggested by the three sets of anomeric signals at δ_H 4.72/δ_C 100.9, δ_H 4.89 (d, J = 1.7 Hz)/δ_C 104.6, and δ_H 4.48 (d, J = 7.9 Hz)/δ_C 104.4, respectively. In addition, the two doublets in the ^{1}H NMR spectrum at δ_H 1.20 (3H, J = 6.2 Hz) and δ_H 1.21 (3H, J = 6.2 Hz) indicated the presence of two rhamnose units. The third sugar moiety was identified as glucose, based on the proton splitting patterns of the seven proton resonances of H-1''' to H-6'''ab in the ^{1}H NMR spectrum (**Table 5.2**). 2D NMR spectroscopic data, including HMBC, HSQC, and NOESY, were employed to determine the linkages between the sugars and the aglycone and between the sugars. One of the rhamnopyranosyl units was connected to C-3, as indicated by ^{3}J-HMBC correlations between H-1' and C-3. The HMBC crosspeaks between H-1'' and C-3', and H-3' (δ_H 3.64, dd, J = 9.5, 3.4 Hz) and C-1' indicated that the second rhamnopyranosyl unit was connected to C-3'. The glucopyranosyl unit was determined to be connected to C-4', based on the HMBC correlation between H-1''' and C-4', as well as H-6' and C-4' (**Fig. 5.8**).

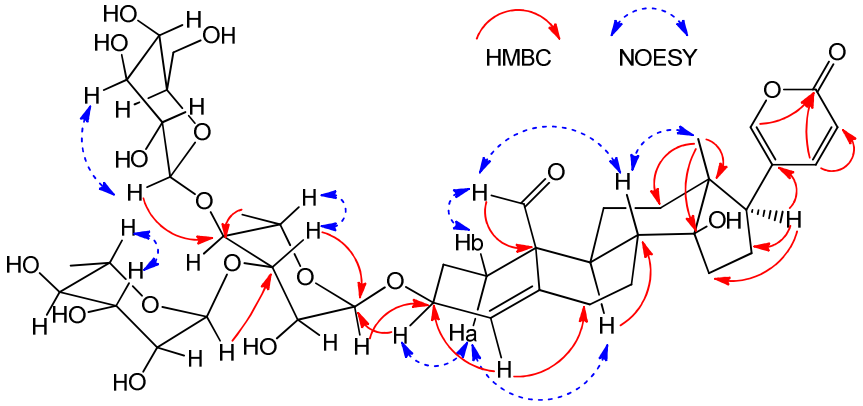

Figure 5.8 HMBC and NOESY Correlations of Compound **5.13**.

The coupling constant between H-1''' and H-2''' (J = 7.9 Hz) of the glucose indicated the β-configuration of the glucopyranosyl unit, and the configurations of the two rhamnopyranosyl units were both deduced to be α, as indicated by the coupling constants between H-1' and H-2', and H-1'' and H-2'' (both J = 1.7 Hz). Compound **5.13** was hydrolyzed with 3 M hydrochloric acid to yield L-rhamnose and D-glucose, as indicated by the identical R_f values compared to the L-rhamnose and D-glucose standards, respectively, in the TLC-analysis, the positive optical rotation of the glucose, and the negative optical rotation of the rhamnose.

Compound **5.13** was thus assigned as 14β-hydroxy-19β-oxobufa-4,20,22-trienolide-3β-*O*-{α-L-rhamnopyranosyl-[(1→4)-β-D-glucopyranosyl]-(1→3)-α-L-rhamnopyranoside}.

5.2.12 *Antiproliferative Activities of the Homoisoflavanones.*

The isolated compounds were tested for antiproliferative activity against the A2780 ovarian cancer, the A2058 melanoma, and the H522-T1 human non-small cell lung cancer cells lines.

Table 5.3 Bioactivities of Homoisoflavonoids **5.4–5.9**

	Compounds							
	5.4	**5.5**	**5.6**	**5.7**	**5.8**	**5.9**	Vinblastine	Taxol
A2780 IC_{50} (μM)	0.32 ± 0.05	3.4 ± 0.16	1.3 5 ± 0.10	0.35 ± 0.06	1.44 ± 0.08	23 ± 1.2	NT	0.028 ± 0.002
A2058 IC_{50} (μM)	0.068	>10	0.69	0.38	>10	>10	0.0037	NT
H522-T1 IC_{50} (μM)	0.071	6.78	0.74	0.43	>10	>10	0.0052	NT

As listed in **Table 5.3**, the five homoisoflavonoids urgineanins A–E (**5.4** – **5.8**) showed strong antiproliferative activity against the A2780 ovarian cancer cell line with IC_{50} values of 0.32, 3.4, 1.35, 0.35 and 1.44 μM, respectively, while the less oxygenated analogue **5.9** had a much lower activity. Additional testing against the A2058 melanoma and H522-T1 human non-small cell lung cancer cells lines showed some interesting differential activities, with compound **5.4** being about five fold more potent to the A2058 and H522-T1 cell lines than to the A2780 line, compound **5.7** being approximately equipotent to all three cell lines, and compounds **5.5** and **5.8** being

significantly less potent to the A2058 and H522-T1 cell lines than to the A2780 cell line.

To date, more than 110 homoisoflavonoids distributed between eight different structural types have been isolated from plants, varying by the number and position of oxygenation of the A- and/or B- rings.[29] Previous work showed that not all homoisoflavonoids are cytotoxic to cancer cells,[30] and the present results suggest two factors that contribute to increased antiproliferative activity. The first is the degree of methylation. This is suggested by the observation that the two compounds with the highest overall antiproliferative activities are **5.4**, with four methoxy groups, and **5.7**, with three methoxy and one methylenedioxy group. This result may be due to the fact that methylation increases lipophilicity, which facilitates cellular uptake.[31, 32] The second factor is that hydroxylation at C-3 increases activity; higher antiproliferative activity was observed for the eucomol-type homoisoflavonoids **5.4** and **5.7**, with a hydroxy group at C-3, than for the corresponding eucomin-type homoisoflavonoids **5.6** and **5.8**, lacking a hydroxy group at C-3.

5.2.13 *Antiproliferative Activities of the Bufatrinolides.*

The bufatrienolides were also tested for antiproliferative activity against the A2780 ovarian cancer, the A2058 melanoma, and the H522-T1 human non-small cell lung cancer cells lines.

Table 5.4 Bioactivities of Bufatrienolides **5.10–5.13**

	Compounds					
	5.10	**5.11**	**5.12**	**5.13**	Vinblastine	Taxol
A2780 IC_{50} (μM)	0.024 ± 0.006	0.011 ± 0.002	0.111 ± 0.008	0.041 ± 0.003	NT	0.028 ± 0.002
A2058 IC_{50} (μM)	0.048	0.060	0.18	0.076	0.0037	NT
H522-T1 IC_{50} (μM)	0.034	0.044	0.11	0.051	0.0052	NT

As listed in **Table 5.4**, the four bufatrienolides, altoside (**5.10**), urginin B (**5.11**), urginin (**5.12**), and urginin C (**5.13**) all showed strong antiproliferative activity, with IC_{50} values of 24, 11, 111,

and 41 nM, respectively. Bufadienolides are polyhydroxy C-24 steroids and their glycosides which have been found in both plant and animal sources.[25, 33] They inhibit the α-unit of the enzyme Na^+, K^+–ATPase to further induce cell apoptosis.[34] Previous research on the structure-activity relationship of the bufadienolides indicated that the presence of the 19-oxo group increases the antiproliferative activity against primary liver carcinoma PLC/PRF/5 cells compared to those bufadienolides with 19-CH_3.[35] Our data corroborate this statement since urginin C (**5.13**) showed a higher activity compared to urginin (**5.12**), and the two compounds only differ in their C-10 substitution. Moreover, urginin B (**5.11**) displayed a higher cytotoxicity than altoside (**5.10)**, indicating that the introduction of an *O*-acetyl group increases the potency, as previously described.[36] In addition, the number of sugars attached to the aglycone affects the cytotoxicity of the bufatrienolide, since the monoglucosides **5.10** and **5.11** were more potent than the trisaccharide bufatrienolides **5.12** and **5.13**. It is possible that the greater number of hydroxy groups from the sugars causes decreased lipophilicity, reducing cellular uptake.[37]

5.3 Experimental Section

5.3.1 *General Experimental Procedures.*

Optical rotations were recorded on a JASCO P-2000 polarimeter. UV and IR spectroscopic data were measured on a Shimadzu UV-1201 spectrophotometer and a MIDAC M-series FTIR spectrophotometer, respectively. ECD spectra were obtained on a JASCO J-815 circular dichroism spectrometer. NMR spectra were recorded in DMSO-d_6 on Bruker Avance 500 or 600 spectrometers. The chemical shifts are given in δ (ppm), and coupling constants (J) are reported in Hz. Mass spectra were obtained on an Agilent 6220 LC–TOF–MS in the positive ion mode.

5.3.2 *Antiproliferative Bioassay*

Antiproliferative activities were obtained at Virginia Polytechnic Institute and State University against the drug-sensitive A2780 human ovarian cancer cell line as previously described.[38] Antiproliferative activities against the A2058 melanoma and the H522-T1 lung cancer cell lines were determined at Eisai Inc. by similar procedures to those used for the H460 cell line. [39]

5.3.3 *Plant Material*

Plant collection was made in the Pilgrims Rest district, State of Mpumalanga, South Africa, by Prof. P. C. Zietsman under the auspices of the New York Botanical Garden, accession number Z03749a. A voucher specimen is deposited in the New York Botanical Garden.

5.3.4 *Extraction and Isolation*

The dried and powdered whole plant (100 g) of *Urginea depressa* was exhaustively extracted with EtOH (1L × 2) in two 24-hour percolation steps; successive partition of the concentrated extract with hexanes and CH_2Cl_2 gave an active CH_2Cl_2 extract. For purposes of fractionation and purification, 0.75 grams of the original EtOH extract designated 60070-6B was shipped to Virginia Tech for bioassay-guided isolation. A 0.60 g sample of 60070-6B (IC_{50} 2.4 μg/mL) was suspended in aqueous MeOH (MeOH/H_2O, 9:1, 100 mL), and extracted with hexanes (3 × 100 mL). The aqueous layer was diluted to 60% MeOH (v/v) with H_2O and extracted with CH_2Cl_2 (3 × 150 mL). The hexanes fraction was evaporated in vacuo to leave 89.3 mg of material with IC_{50} = 2.6 μg/mL. The residue from the CH_2Cl_2 fraction (86.2 mg) had an IC_{50} of 0.68 μg/mL, and the remaining aqueous MeOH fraction was centrifuged to give a supernatant (311 mg) with an IC_{50} of 0.72 μg/mL.

The CH_2Cl_2 fraction was subjected to size exclusion open column chromatography on Sephadex LH-20 to yield three fractions, of which the most active fraction F3 (21.2 mg) had an IC_{50} value of 0.37 μg/mL. Fraction F3 was applied to a silica gel column with elution by $CHCl_3$/MeOH, 20:1 to give 14 fractions. Fraction F3-2 (1.8 mg), the most active fraction (IC_{50} 0.14 μg/mL), was further applied on C_{18} HPLC and eluted by 35% MeCN in H_2O to yield compound **5.4** (0.8 mg) and compound **5.7** (0.5 mg), with retention times of 20.3 and 19.2 minutes, respectively. Using the same C_{18} HPLC column, fraction F3-3 (5.9 mg, IC_{50} 1.3 μg/mL) was eluted with 40% MeCN in H_2O to give compound **5.5** (0.25 mg) and compound **5.9** (0.25 mg), with retention times of 9.8 and 20.4 minutes, respectively. In the same manner, Sephadex LH-20 size exclusion open column chromatography of the hexanes fraction yielded six fractions, of which the most active fraction F5 (22.4 mg) had an IC_{50} values of 0.53 μg/mL. Fraction F5 was applied to a silica gel column and eluted with hexanes/EtOAc, 7:1 to give 13 fractions. Fraction F5-12 (2.5 mg), the most active fraction (IC_{50} 0.15 μg/mL), was further separated on C_{18} HPLC eluted by 35% MeCN in H_2O to yield compound **5.8** (0.2 mg) and compound **5.6** (1.0 mg), with retention times of 26.2 and 27.4 minutes, respectively.

The MeOH-soluble fraction was separated on an HP-20 Diaion open column to give three fractions, of which the most active fraction F3 (111.1 mg) had an IC_{50} value of 0.39 μg/mL. F3 was applied to a Sephadex LH-20 size exclusion open column with elution by CH_2Cl_2/MeOH,1:1 to give four fractions. Fraction 3-2 (54.2 mg), the most active (IC_{50} 0.14 μg/mL) fraction, was applied on C_{18} SPE eluted by 40, 60, 80 and 100% MeOH in H_2O to give a 40% fraction (IC_{50} 0.12 μg/mL), and a 60% fraction (IC_{50} 0.36 μg/mL). The 40% fraction was subjected to C_{18} HPLC eluted by 40% MeOH in H_2O and yielded compound **5.12** (1.8 mg) and compound **5.13** (2.6 mg), with retention times of 13.9 and 7.2 minutes, respectively. In the same manner, the 60% fraction was subjected to C_{18} HPLC eluted by 60% MeOH in H_2O to yield compound **5.10** (1.0 mg) and compound **5.11** (1.2

mg), with retention times of 20.6 and 6.2 minutes, respectively.

5.3.5 *Hydrolysis of Compounds **5.10**, **5.11** and **5.13**.*

Compound **5.13** (2.0 mg) was hydrolyzed with 10 mL 3 M HCl for 4 h at 100 °C. The solution was extracted with EtOAc (3 × 50 mL), and both the organic and the water layers were evaporated to dryness under reduced pressure. The structure of the white powder (1.4 mg) derived from the organic layer was determined to be 3*β*,14*β*-dihydroxy-19*β*-oxobufa-4,20,22-trienolide by ^{1}H and ^{13}C NMR spectroscopy. The semi-solid carbohydrate mixture from the water layer (0.45 mg) was applied to a silica gel column, eluted by $CHCl_3$/MeOH/H_2O,15:7:2 (lower phase). Two fractions (monosaccharide 1 and monosaccharide 2) were obtained; each of which was dissolved in 1 mL of H_2O and kept overnight before TLC analysis and determination of optical rotations. On the silica gel TLC plate, monosaccharide 1 (R_f = 0.36) had an identical R_f value to L-rhamnose, developed by $CHCl_3$/MeOH/H_2O,13:7:2 (lower phase). Moreover, it had an $[\alpha]_D^{22}$ –7.0, (*c* 0.1, H_2O). Monosaccharide 2 (R_f = 0.20) had an identical R_f value to D-glucose on the same TLC system as that of monosaccharide 1, with $[\alpha]_D^{22}$ +54, *c* 0.1, H_2O. Both of the optical rotation values are similar to the ones reported in the literature.

Compounds **5.10** and **5.11** were hydrolyzed and analyzed in the same manner, and D-glucose was obtained from both of the aqueous portions of the hydrolytes, with $[\alpha]_D^{22}$ +53 and +52, (*c* 0.1, H_2O)

5.3.6 *Urgineanin A (**5.4**): (3R)–3-hydroxy-3-(4'-methoxybenzyl)-5,6,7-trimethoxychroman-4-one*

Light yellow oil; $[\alpha]_D^{21}$ +26 (*c* 0.12, MeOH); UV (MeOH) λ_{max} (ε) 229 (1.6), 274 (1.2); IR ν_{max} cm^{-1}: 3464, 2932, 1678, 1600, 1483, 1265, 1121 cm^{-1}; ECD (c 0.031 mM, MeOH) $\Delta\varepsilon_{280}$ +10.8,

$\Delta\varepsilon_{315}$ –7.2; ^{1}H NMR (600 MHz, DMSO-d_6), and ^{13}C NMR (150 MHz, DMSO-d_6), see **Table 5.1**; HR–ESI–MS *m/z* 397.1258 $[M+Na]^+$ (calc. for $C_{20}H_{22}NaO_7^+$, 397.1263) and 375.1438 $[M+H]^+$ (calcd for $C_{20}H_{23}O_7^+$, 375.1438).

5.3.7 *Urgineanin B (**5.5**): (3R)–3-hydroxy-3-(4'-hydroxybenzyl)-5,6,7-trimethoxychroman-4-one*

Light yellow oil; $[\alpha]_D^{21}$ +23 (*c* 0.12, MeOH); UV (MeOH) λ_{max} (ε) 229 (1.2), 274 (0.9); IR ν_{max} cm^{-1}: 3485, 2924, 1677, 1598, 1477, 1263, 1119 cm^{-1}; ECD (c 0.031 mM, MeOH) $\Delta\varepsilon_{281}$ +10.4, $\Delta\varepsilon_{316}$ –7.3; ^{1}H NMR (600 MHz, DMSO-d_6), and ^{13}C NMR (150 MHz, DMSO-d_6), see **Table 5.1**; HR–ESI–MS *m/z* 383.1102 $[M+Na]^+$ (calcd for $C_{19}H_{20}NaO_7^+$, 383.1107) and 361.1277 $[M+H]^+$ (calc. for $C_{19}H_{21}O_7^+$, 361.1282).

5.3.8 *Urigineanin C (**5.7**): (3R)–3-hydroxy-3-(3',4'-methylenedioxy)-5,6,7-trimethoxychroman-4-one*

Light yellow oil; $[\alpha]_D^{21}$ +18 (*c* 0.12, MeOH); UV (MeOH) λ_{max} (ε) 229 (1.2), 274 (0.9); IR ν_{max} cm^{-1}: 3497, 2897, 1679, 1600, 1479, 1246, 1111 cm^{-1}; ECD (c 0.031 mM, MeOH) $\Delta\varepsilon_{280}$ +6.8, $\Delta\varepsilon_{316}$ –5.2; ^{1}H NMR (600 MHz, DMSO-d_6), and ^{13}C NMR (150 MHz, DMSO-d_6), see **Table 5.1**; HR–ESI–MS *m/z* 411.1053 $[M+Na]^+$ (calcd for $C_{20}H_{20}NaO_8^+$, 411.1056), and $[M+H]^+$ *m/z* 389.1231 (calc. for $C_{20}H_{21}O_8^+$, 389.1231).

5.3.9 *Urigineanin D (**5.8**): (3S)–3-(3',4'-methylenedioxy)-5,6,7-trimethoxychroman-4-one*

Light yellow oil; $[\alpha]_D^{21}$ +12 (*c* 0.12, MeOH); UV (MeOH) λ_{max} (ε) 229 (1.8), 280 (1.3); IR ν_{max} cm^{-1}: 2898, 1646, 1591, 1483, 1251, 1028 cm^{-1}; ECD (c 0.031 mM, MeOH) $\Delta\varepsilon_{288}$ +5.9, $\Delta\varepsilon_{309}$ –0.1; ^{1}H NMR (600 MHz, DMSO-d_6), and ^{13}C NMR (150 MHz, DMSO-d_6), see **Table 5.1**;

HR–ESI–MS *m/z* 395.1100 $[M+Na]^+$ (calcd for $C_{20}H_{20}NaO_7^+$, 395.1107) and 373.1279 $[M+H]^+$ (calc. for $C_{20}H_{21}O_7^+$, 373.1282).

5.3.10 *Altoside (**5.10**):*

Light yellow powder; $[\alpha]_D^{21}$ +23 (*c* 0.12, MeOH); UV (MeOH) λ_{max} (ε) 208 (1.8), 298 (0.6); IR ν_{max} cm^{-1}: 3385, 2924, 2855, 1738, 1710, 1455, 1250, 1064 cm^{-1}. ^1H NMR (600 MHz, MeOH-d_4), and ^{13}C NMR (150 MHz, MeOH-d_4), see **Table 5.2**; HR–ESI–MS *m/z* 583.2482 $[M+Na]^+$ (calc. for $C_{30}H_{40}NaO_{10}^+$, 583.2514).

5.3.11 *Urginin B (**5.11**):*

Light yellow powder; $[\alpha]_D^{21}$ +27 (*c* 0.12, MeOH); UV (MeOH) λ_{max} (ε) 211 (1.9), 288 (0.6); IR ν_{max} cm^{-1}: 3362, 2924, 2850, 1735, 1710, 1450, 1245, 1068 cm^{-1}. ^1H NMR (600 MHz, MeOH-d_4), and ^{13}C NMR (150 MHz, MeOH-d_4), see **Table 5.2**; HR–ESI–MS *m/z* 641.2646 $[M+Na]^+$ (calc. for $C_{32}H_{42}NaO_{12}^+$, 641.2568).

5.3.12 *Urginin C (**5.13**):*

Light yellow powder; $[\alpha]_D^{21}$ −14 (*c* 0.12, MeOH); UV (MeOH) λ_{max} (ε) 211 (1.9), 296 (0.7); IR ν_{max} cm^{-1}: 3348, 2925, 2860, 1734, 1710, 1459, 1268, 1124 cm^{-1}. ^1H NMR (600 MHz, MeOH-d_4), and ^{13}C NMR (150 MHz, MeOH-d_4), see **Table 5.2**; HR–ESI–MS *m/z* 875.3738 $[M+Na]^+$ (calc. for $C_{42}H_{60}NaO_{18}^+$, 875.3672).

5.4 References and Notes

1. Dai, Y.; Harinantenaina, L.; Brodie, P. J.; Goetz, M.; Shen, Y.; Tendyke, K.; Kingston, D. G. I. Antiproliferative homoisoflavonoids and bufatrienolides from *Urginea depressa*. *J. Nat. Prod.* **2013,** *76*, 865–872.

2. Newman, D. J.; Cragg, G. M. Natural products as sources of new drugs over the 30 years from 1981 to 2010. *J. Nat. Prod.* **2012,** *75*, 311–335.

3. Mullin, R. Merck cuts sales jobs and halts natural products research. In *Chem. Eng. News*, 2008.

4. Anonymous. Institute for hepatitis and virus research receives one of world's largest natural products library from Merck. In 2011.

5. Chase, M. W.; Reveal, J. L.; Fay, M. F. A subfamilial classification for the expanded asparagalean families Amaryllidaceae, Asparagaceae and Xanthorrhoeaceae. *Bot. J. Linn. Soc.* **2009,** *161*, 132–136.

6. Koorbanally, C.; Mulholland, D. A.; Crouch, N. R. Eudesmane-type sesquiterpenoids from *Urginea epigea* (Urgineoideae; Hyacinthaceae). *Biochem. Syst. Ecol.* **2005,** *33*, 295–299.

7. Koorbanally, N. A.; Crouch, N. R.; Harilal, A.; Pillay, B.; Mulholland, D. A. Coincident isolation of a novel homoisoflavonoid from *Resnova humifusa* and *Eucomis montana* (Hyacinthoideae: Hyacinthaceae). *Biochem. Syst. Ecol.* **2006,** *34*, 114–118.

8. Michalik, A.; Hollinshead, J.; Jones, L.; Fleet, G. W. J.; Yu, C. Y.; Hu, X. G.; van Well, R.; Horne, G.; Wilson, F. X.; Kato, A.; Jenkinson, S. F.; Nash, R. J. Steviamine, a new indolizidine alkaloid from *Stevia rebaudiana*. *Phytochem. Lett.* **2010,** *3*, 136–138.

9. Moodley, N.; Crouch, N. R.; Mulholland, D. A. Bufadienolides from *Drimia macrocentra* and *Urginea riparia* (Hyacinthaceae: Urgineoideae). *Phytochemistry* **2007,** *68*, 2415–2419.

10. Toit, K. D.; Kweyama, A.; Bodenstein, J. Anti-inflammatory and antimicrobial profiles of *Scilla nervosa* (Burch.) Jessop (Hyacinthaceae). *S. Afr. J. Sci.* **2011,** *107*, 96–100.

11. Crouch, N. R.; Langlois, A.; Mulholland, D. A. Bufadienolides from the southern African *Drimia depressa* (Hyacinthaceae: Urgineoideae). *Phytochemistry* **2007,** *68*, 1731–1734.

12. Rees, R.; Schindler, O.; Reichstein, T. Teilsynthese von hellebrigenin-*β*-D-glucosid-(1,5) und Hellebrigenol-*β*-D-glucosid-(1,5), sowie Nachweis dieser zwei Glykoside in den Zwiebeln von *Urginea depressa* Baker. Glykoside und Aglykone, 202. Mitteilung. *Helv. Chim. Acta* **1959,** *42*, 1052–1065.

13. Böhler, P.; Tamm, C. The homoisoflavones, a new class of natural product. Isolation and structure of eucomin and eucomol. *Tetrahedron Lett.* **1967,** *8*, 3479–3483.

14. Cuong, T. D.; Hung, T. M.; Kim, J. C.; Kim, E. H.; Woo, M. H.; Choi, J. S.; Lee, J. H.; Min, B. S. Phenolic compounds from *Caesalpinia sappan* heartwood and their anti-inflammatory activity. *J. Nat. Prod.* **2012,** *75*, 2069–2075.

15. Adinolfi, M.; Barone, G.; Corsaro, M. M.; Mangoni, L.; Lanzetta, R.; Parrilli, M. Absolute configuration of homoisoflavanones from *Muscari* species. *Tetrahedron* **1988,** *44*, 4981–4988.

16. Borgonovo, G.; Caimi, S.; Morini, G.; Scaglioni, L.; Bassoli, A. Taste-active compounds in a traditional Italian food: 'Lampascioni'. *Chem. Biodivers.* **2008,** *5*, 1184–1194.

17. Wang, Y.; Xu, J.; Zhang, L.; Qu, H. Three new homoisoflavanones from the *Ophiopogon japonicus* (Liliaceae). *Helv. Chim. Acta* **2010,** *93*, 980–984.

18. Böhler, P.; Tamm, C. The homo-isoflavones, a new class of natural product. Isolation and structure of eucomin and eucomol. *Tetrahedron Lett.* **1967,** *8*, 3479–3483.

19. Locniskar, M.; Belury, M. A.; Cumberland, A. G.; Patrick, K. E.; Fischer, S. M. The effect of the level of dietary corn oil on mouse skin carcinogenesis. *Nutr. Cancer* **1991,** *16*, 1–11.

20. Morales-Serna, J. A.; Jiménez, A.; Estrada-Reyes, R.; Marquez, C.; Cárdenas, J.; Salmón, M. Homoisoflavanones from *Agave tequilana* Weber. *Molecules* **2010,** *15*, 3295–3301.

21. Moodley, N.; Crouch, N. R.; Mulholland, D. A.; Slade, D.; Ferreira, D. 3-Benzyl-4-chromanones (homoisoflavanones) from bulbs of the ethnomedicinal geophyte *Ledebouria revoluta* (Hyacinthaceae). *S. Afr. J. Bot.* **2006,** *72*, 517–520.

22. Lichti, H.; von Wartburg, A.; Renz, J. Altoside, a cardioactive glycoside from *Urginea altissima. Planta Med.* **1959,** *7*, 451–455.

23. Iizuka, M.; Warashina, T.; Noro, T. Bufadienolides and a new lignan from the bulbs of *Urginea maritima*. *Chem. Pharm. Bull.* **2001,** *49*, 282–286.

24. Crouch, N. R.; Toit, K. d.; Mulholland, D. A.; Drewes, S. E. Bufadienolides from bulbs of *Urginea lydenburgensis* (Hyacinthaceae: Urgineoideae). *Phytochemistry* **2006,** *67*, 2140–2145.

25. Gao, H.; Popescu, R.; Kopp, B.; Wang, Z. Bufadienolides and their antitumor activity. *Nat. Prod. Rep.* **2011,** *28*, 953–969.

26. Pohl, T.; Koorbanally, C.; Crouch, N. R.; Mulholland, D. A. Bufadienolides from *Drimia robusta* and *Urginea altissima* (Hyacinthaceae). *Phytochemistry* **2001,** *58*, 557–561.

27. Shimada, K.; Umezawa, E.; Nambara, T.; Kupchan, S. M. Isolation and characterization of cardiotonic steroids from the bulb of *Urginea altissima* Baker. *Chem. Pharm. Bull.* **1979,** *27*,

3111–3114.

28. Kupchan, S. M.; Moniot, J. L.; Sigel, C. W.; Hemingway, R. J. Tumor inhibitors. LXV. Bersenogenin, berscillogenin, and 3-epiberscillogenin, three new cytotoxic bufadienolides from *Bersama abyssinica*. *J. Org. Chem.* **1971,** *36*, 2611–2616.

29. Jiang, H. B.; Huang, J.; Guo, M. J.; Zou, P.; Tian, X. Q. Recent advances in the study of natural homoisoflavonoids. *Yao Xue Xue Bao* **2007,** *42*, 118–126.

30. Yan, J.; Sun, L. R.; Zhou, Z. Y.; Chen, Y. C.; Zhang, W. M.; Dai, H. F.; Tan, J. W. Homoisoflavonoids from the medicinal plant *Portulaca oleracea*. *Phytochemistry* **2012,** *80*, 37–41.

31. Walle, T. Methylation of dietary flavones greatly improves their hepatic metabolic stability and intestinal absorption. *Mol. Pharm.* **2007,** *4*, 826–832.

32. Walle, T. Methylation of dietary flavones increases their metabolic stability and chemopreventive effects. *Int. J. Mol. Sci.* **2009,** *10*, 5002–5019.

33. Steyn, P.; van Heerden, F. R. Bufadienolides of plant and animal origin. *Nat. Prod. Rep.* **1998,** *15*, 397–413.

34. Numazawa, S.; Shinoki, M. A.; Ito, H.; Yoshida, T.; Kuroiwa, Y. Involvement of Na^+, K^+–ATPase inhibition in K562 cell differentiation induced by bufalin. *J. Cell. Physiol.* **1994,** *160*, 113–120.

35. Kamano, Y.; Kotake, A.; Hashima, H.; Inoue, M.; Morita, H.; Takeya, K.; Itokawa, H.; Nandachi, N.; Segawa, T.; Yukita, A.; Saitou, K.; Katsuyama, M.; Pettit, G. R. Structure–cytotoxic activity relationship for the toad poison bufadienolides. *Bioorg. Med. Chem.* **1998,** *6*, 1103–1115.

36. Ye, M.; Qu, G.; Guo, H.; Guo, D. Novel cytotoxic bufadienolides derived from bufalin by microbial hydroxylation and their structure–activity relationships. *J. Steroid Biochem. Mol. Biol.* **2004,** *91*, 87–98.

37. Braca, A.; Autore, G.; De Simone, F.; Marzocco, S.; Morelli, I.; Venturella, F.; Tommasi, N. D. Cytotoxic saponins from *Schefflera rotundifolia*. *Planta Med.* **2004,** *70*, 960–966.

38. Dai, Y.; Harinantenaina, L.; Brodie, P. J.; Callmander, M. W.; Randrianaivo, R.; Rakotonandrasana, S.; Rakotobe, E.; Rasamison, V. E.; Shen, Y.; TenDyke, K.; Suh, E. M.; Kingston, D. G. I. Antiproliferative acetogenins from a *Uvaria sp.* from the Madagascar dry forest. *J. Nat. Prod.* **2011,** *75*, 479–483.

39. Pan, E.; Harinantenaina, L.; Brodie, P. J.; Callmander, M.; Rakotonandrasana, S.; Rakotobe, E.; Rasamison, V. E.; TenDyke, K.; Shen, Y.; Suh, E. M.; Kingston, D. G. I. Cardenolides of *Leptadenia madagascariensis* from the Madagascar dry forest. *Bioorg. Med. Chem.* **2011,** *19*, 422–428.

Chapter 6: Isolation of Antiplasmodial Anthraquinones from *Kniphofia ensifolia*, and Synthesis and Structure–activity Relationships of Related Compounds

This chapter is a slightly expanded version of a submitted manuscript.[1] Attributions of co-authors of the articles are described as follows in the order of the names listed. The author of this dissertation (Mr. Yumin Dai) conducted the isolation, structural elucidation and synthesis of the titled compounds, and drafted the manuscript. Dr. Liva Harinantenaina was a mentor for this work, and in particular, he provided invaluable advice and hints for the structural elucidation of these compounds, and he also proofread the manuscript before submission. Ms. Jessica Bowman performed the Dd2 bioassay on the isolated fractions and compounds, under the guidance of Dr. Maria B. Cassera. Ms. Peggy Brodie performed the A2780 bioassay on the isolated fractions and compounds. Dr. Michael Goetz from Natural Products Discovery Institute did the plant collections and identification. Dr. David G. I. Kingston was the mentor for this work and the corresponding authors for the published article. He provided critical suggestions for this work and edited the final version of the manuscript.

6.1 Introduction

As part of a collaborative research project established between Virginia Tech and the Institute for Hepatitis and Virus Research (IHVR) and its the Natural Products Discovery Institute (NPDI),[2] we are searching for antiproliferative and antimalarial natural products in the plant extract library of the NPDI. An investigation for antiproliferative compounds from this library yielded several

homoisoflavonones and bufadienolides with strong antiproliferative activity,[3] and this paper reports the first results from our investigation of extracts with antimalarial activity.

Screening of over 6,900 extracts from the NPDI collection led to the identification of a CH_2Cl_2 extract of *Kniphofia ensifolia* Baker (Asphodelaceae)[4] with promising antiplasmodial activity against the drug-resistant Dd2 strain of *Plasmodium falciparum*, with an IC_{50} around 6 μg/mL. Members of the Asphodelaceae family are widely distributed in Africa, central and western Europe, the Mediterranean basin, Central Asia, and Australia.[5] The genus *Kniphofia* is a rich source of anthraquinones, flavonoids and alkaloids, which are well-known for their broad range of bioactivities, including anticancer and antimalarial activities.[6-8] 1-(1-Hydroxy-8-methoxy-3-methylnaphthalen-2-yl)ethanone (**6.1**), *N*-4'-chlorobutyl butyramide (**6.2**) and *N*, *N*-dimethylconiine (**6.3**) listed are the examples of bioactive compounds isolated from the genus *Kniphofia*. Although the genus *Kniphofia* has been well explored, the phytochemistry of *K. ensifolia* has not previously been investigated, and its extract was thus selected for bioassay guided fractionation to isolate its bioactive components.

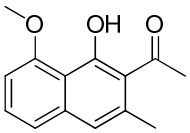

6.1

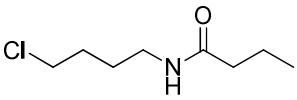

6.2

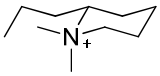

6.3

6.2 Results and Discussion

6.2.1 *Isolation of Active Compounds*

An EtOH extract of the whole plant of *K. ensifolia* was subjected to liquid–liquid partitioning to give an antiplasmodial CH_2Cl_2 fraction (IC_{50} ~ 6.0 μg/mL). Bioassay guided separation (Scheme **6.1**) of the CH_2Cl_2 fraction, including Sephadex LH-20 size exclusion chromatography,

normal-phase silica gel chromatography, and C_{18} reverse-phase HPLC, yielded two new anthraquinones, named kniphofiones A and B (**6.6**, **6.7**), two known strongly active anthraquinones (**6.9**, **6.10**), and five other known anthraquinones (**6.4**, **6.5**, **6.7**, **6.11**, **6.12**). The structure elucidation of the new compounds is reported herein.

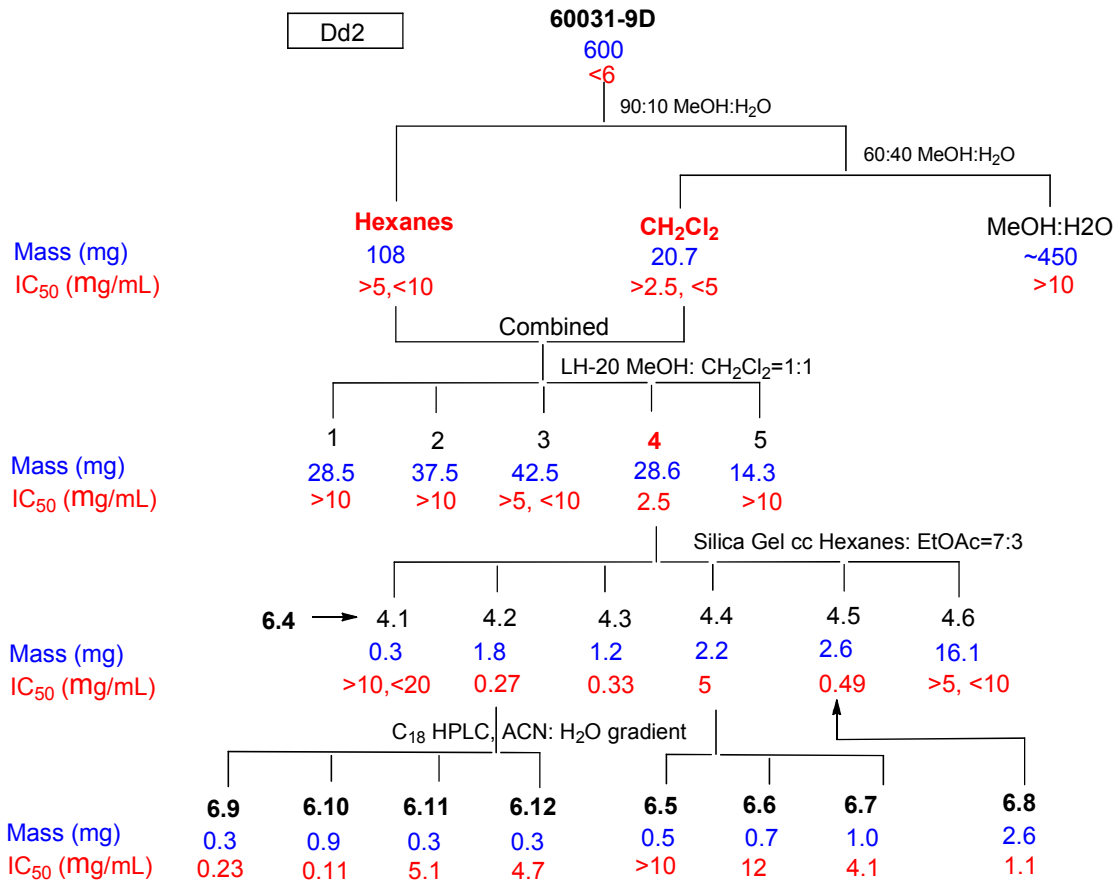

Scheme 6.1 Bioassay Guided Separation of the Extract of *Kniphofia ensifolia*

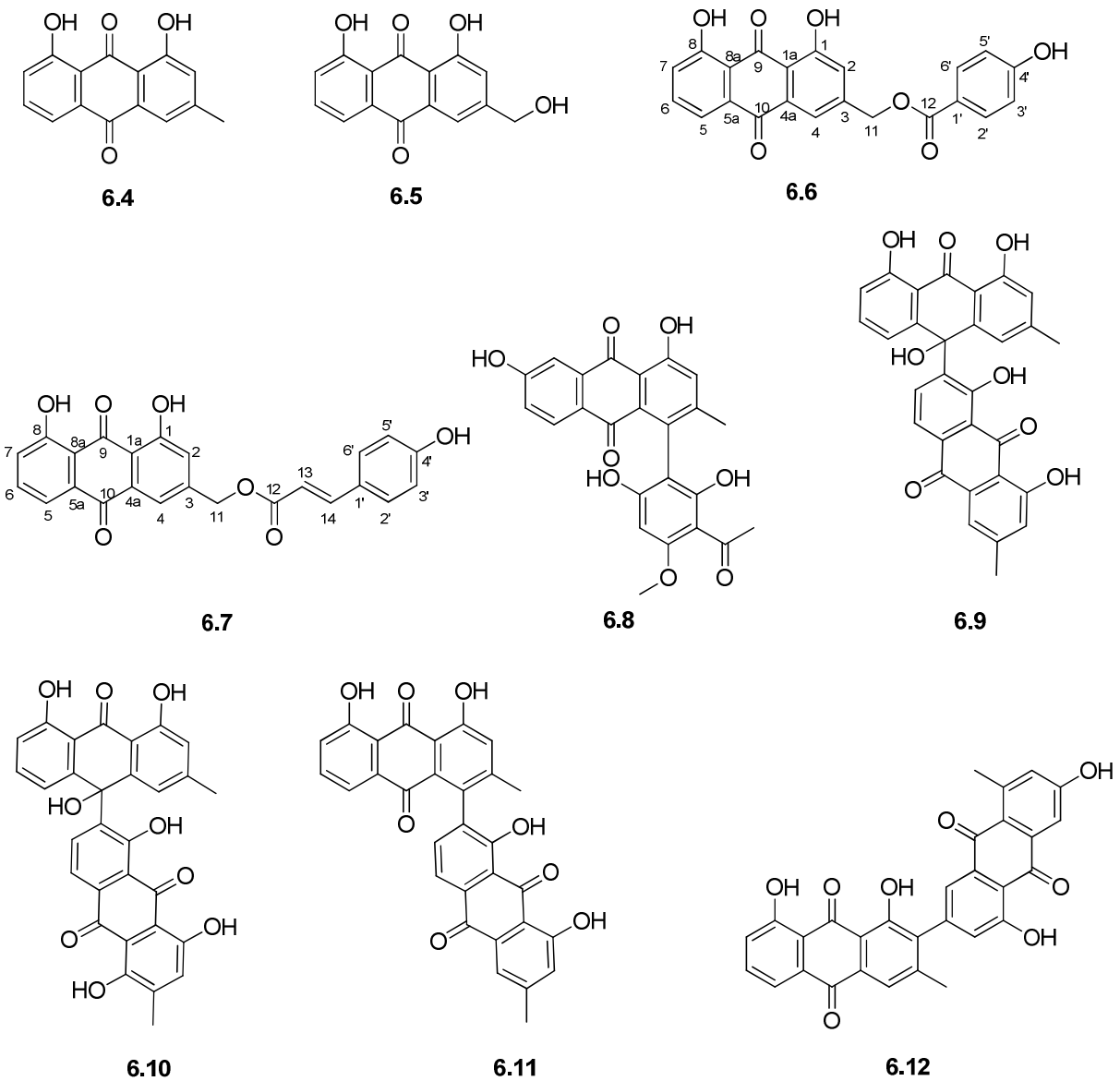

Figure 6.1 Chemical Structure of Compounds **6.4–6.12**

6.2.2 *Structure Elucidation of the Known Compounds **6.4–6.5**, and **6.8–6.12***.

Compounds **6.4**, **6.5** and **6.8–6.12** were identified as chrysophanol (**6.4**),[9] aloe-emodin (**6.5**),[10] knipholone (**6.8**),[11] 10-(chrysophanol-7'-yl)-10-hydroxylchrysophanol-9-anthrone (**6.9**),[7] chryslandicin (**6.10**),[12] asphodeline (**6.11**),[13] and microcarpin (**6.12**)[14] respectively, by comparison of their experimental and reported physical and spectroscopic data with literature data.

6.2.3 *Structure Elucidation of Compound* ***6.6***.

Kniphofione A (**6.6**) was isolated as a yellow-orange powder. Its negative ion HR–ESI–MS revealed a peak for a deprotonated molecular ion at *m/z* 389.0688 $[M–H]^–$, corresponding to a molecular formula of $C_{22}H_{14}O_7$. Its IR spectrum exhibited absorption bands at 3390 and 1673 cm^{-1}, indicating the presence of hydroxy and conjugated carbonyl groups. The presence of two chelated hydroxy groups was further confirmed by two singlet signals located at δ_H 12.09 and 12.12 in the ^1H NMR spectrum (**Table 6.1**). In addition, a set of three coupled aromatic protons in the ABC-type spin system [δ_H 7.90 (1H, dd, J = 7.9, 1.6 Hz), 7.73 (1H, dd, J = 8.0, 7.9 Hz) and 7.39 (1H, dd, J = 8.0, 1.6 Hz)], two *meta*-coupled doublets located at δ_H 7.87 and 7.34 (both, 1H, J = 1.6), as well as methylene protons on an oxygen-bearing carbon at δ_H 5.44 (2H, singlet), were similar to the corresponding signals of aloe-emodin (**6.5**) and of aloe-emodin-type anthraquinones.[10, 15] The observation of two carbonyl carbon resonances located at δ_C 192.7 and 181.6, as well as a methylene carbon signal at δ_C 64.9 (C-11) in the ^{13}C NMR spectrum, corroborated its structure as an aloe-emodin derivative. The basic skeleton of 1,8-dihydroxy-3-(hydroxymethyl) anthracene-9,10-dione was confirmed by the HMBC correlations between H-2 and C-1a, H-4 and C-10, H-6 and C-8, H-7 and C-8a, and H-11 and C-2 (**Fig. 6.2**).

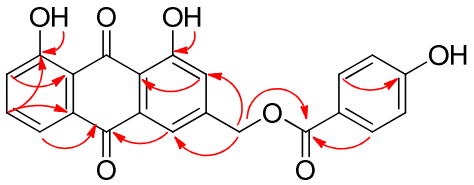

Figure 6.2 HMBC Correlation of Compound **6.6**

Furthermore, the presence of a *para*-hydroxybenzoate group was suggested by the presence of two doublets at δ_H 8.07 and 6.92 (2H each, J = 8.8 Hz) in the ^1H NMR spectrum, and a set of five carbon signals at δ_C 165.8 (C-12), 159.6 (C-4'), 132.0 (C-2'/6'), 122.4 (C-1'), and 113.9 (C-3'/5'), in

the ^{13}C NMR spectrum.[16] The structure of the *para*-hydroxybenzoate group and its connection to C-11 was further confirmed by the HMBC correlations between H-2'/H-6' and C-12, H-6'/H-2' and C-4', and H_2-11 and C-12. Hence, the structure of compound **6.6** was assigned as (1,8-dihydroxy-9,10-dioxo-9,10-dihydroanthracen-3-yl)methyl 4-hydroxybenzoate.

Table 6.1 NMR Spectroscopic Data for **6.6** and **6.7** in $CDCl_3$ (500 MHz)

	6.6		**6.7**	
position	δ_H (*J* in Hz)	δ_C, type	δ_H (*J* in Hz)	δ_C, type
1	-	162.9, C	-	162.8, C
1a	-	115.3, C	-	115.2, C
2	7.87 d (1.6)	118.6, CH	7.87 d (1.6)	118.5, CH
3	-	147.0, C	-	146.9, C
4	7.34 d (1.6)	122.4, CH	7.36 d (1.6)	122.4, CH
4a	-	133.6, C	-	133.6, C
5	7.90 dd (7.9, 1.6)	120.2, CH	7.87 dd (7.9, 1.6)	120.2, CH
5a	-	134.1, C	-	133.9, C
6	7.73 dd (8.0, 7.9)	137.4, CH	7.73 dd (8.0, 7.9)	137.3, CH
7	7.39 dd (8.0, 1.6)	124.8, CH	7.35 dd (8.0, 1.6)	124.8, CH
8	-	162.7, C	-	162.8, C
8a	-	115.9, C	-	115.8, C
9	-	192.7, C	-	192.7, C
10	-	181.6, C	-	181.6, C
11	5.44 s	64.9, CH_2	5.35 s	64.6, CH_2
12	-	165.8, C	-	166.7, C
13	-	-	6.43 d (15.9)	114.4, CH
14	-	-	7.75 d (15.9)	145.8, CH
1'	-	121.8, C	-	126.9, C
2'	8.07 brd (8.8)	132.0, CH	7.50 brd (8.5)	130.0, CH
3'	6.92 brd (8.8)	113.9, CH	6.88 brd (8.5)	114.4, CH
4'	-	159.6, C	-	159.5, C
5'	6.92 brd (8.8)	113.9, CH	6.88 brd (8.5)	114.4, CH
6'	8.07 brd (8.8)	132.0, CH	7.50 brd (8.5)	130.0, CH
1-OH	12.12 s	-	12.11 s	-
8-OH	12.09 s	-	12.09 s	-

6.2.4 *Structure Elucidation of Compound **6.7***.

Kniphofione B (**6.7**) was obtained as a light yellow oil. Its molecular formula was deduced to be $C_{24}H_{16}O_7$, based on its protonated molecular ion peak at *m/z* 417.0986 $[M+H]^+$ and a sodiated

molecular ion peak at *m/z* 439.0806 $[M+Na]^+$ in its positive ion HR–ESI–MS. The ^{1}H NMR spectrum of compound **6.7** displayed splitting patterns in the aromatic region similar to that of compound **6.6**, suggesting they have related structures. Comparison of the ^{13}C NMR spectroscopic data of **6.7** with those of **6.6** (**Table 6.1**) indicated that both compounds shared the same aloe-emodin-type anthraquinone skeleton, but differed in the acyl group attached to C-11. The presence of a *trans para*-hydroxycinnamate group in **6.7**, as opposed to the *para*-hydroxybenzoate group in **6.6**, was indicated by the presence of two doublets at δ_H 7.50 and 6.88 (2H each, J = 8.8 Hz) in the ^{1}H NMR spectrum, a set of five carbon signals at δ_C 166.7 (C-12), 159.5 (C-4'), 130.0 (C-2'/6'), 126.9 (C-1'), and 114.4 (C-3'/5') in the ^{13}C NMR spectrum, and *trans*-coupled doublet proton signals at δ_H 6.43 and 7.75 (both, 1H, J = 15.9 Hz). The latter signals corresponded by HMQC to the two methine carbon resonances at δ_C 114.4 (C-13) and 145.8 (C-14).[17] The two carbons of the carbon-carbon double bond in the cinnamate group were assigned to C-13 and C-14, based on the HMBC crosspeaks between H-13 and C-1', H-6' and C-14, and H-14 and C-12 (**Fig. 6.3**). The structure of compound **6.7** was thus determined as (*E*)–(1,8-dihydroxy-9,10-dioxo-9,10-dihydroanthracen-3-yl)-methyl 3-(4-hydroxyphenyl) acrylate.

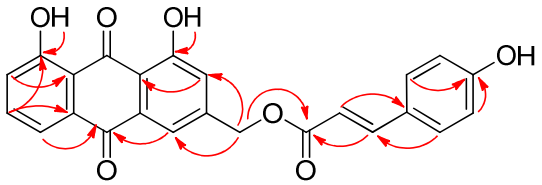

Figure 6.3 HMBC Correlation of Compound **6.7**

6.2.5 *Biological Activities and Structure–Activity Relationship Study*

All the isolated compounds were tested for antiproliferative activity against the A2780 ovarian cancer cell line and for antiplasmodial activity against the Dd2 chloroquine-resistant strain of *P. falciparum*.

Table 6.2 Bioactivities of the Isolated Anthraquinones (**6.4–6.12**)

	Compounds								
	6.4	**6.5**	**6.6**	**6.7**	**6.8**	**6.9**	**6.10**	**6.11**	**6.12**
Dd2 IC_{50} (μM)	58	55	26 ± 4	9 ± 1	1.1 ± 0.2	0.4 ± 0.1	0.2 ± 0.1	10 ± 2	10 ± 2
A2780 IC_{50} (μM)	> 60	26 ± 2	> 60	> 60	8.0 ± 1.5	6.2 ± 0.9	4.3 ± 1.1	> 60	> 60

As listed in **Table 6.2**, the known dimeric compounds (**6.9** and **6.10**) displayed the highest antiplasmodial activity, with IC_{50} values of 0.4 ± 0.1 and 0.2 ± 0.1 μM, respectively. In addition, both of these dimeric compounds showed modest antiproliferative activity against the A2780 human ovarian cancer cell line, with IC_{50} values of 6.2 ± 0.9 and 4.3 ± 1.1 μM, respectively. However, their modest antiproliferative activity, which implied cytotoxicity, and lack of synthetic accessibility decreased their appeal as lead compounds for potential antimalarial agents. For these reasons, the two modestly active new compounds (**6.6** and **6.7**, IC_{50} = 26 ± 4 and 9 ± 1 μM, respectively) were more attractive for a study of structure-activity relationships due to their low cytotoxicities (IC_{50} > 60 μM) and synthetic accessibility. Both compounds are C-11 acylated derivatives of aloe-emodin (**6.5**), and so a number of C-11 acylated aloe-emodin derivatives were prepared by standard methods to determine the feasibility of developing derivatives with improved antiplasmodial activity.

Antiplasmodial activity data on the isolated natural products showed that compound **6.7**, the *para*-hydroxycinnamate derivative of aloe-emodin (**6.5**), is 6.7 times more potent than **6.5**, and this compound was thus selected as the lead compound for the present SAR study. Various acyl derivatives of aloe-emodin were then prepared by reaction of the commercially available natural product aloe-emodin (**6.5**) with a variety of organic acids, with 1-ethyl-3-(3-dimethylaminopropyl) carbodiimide (EDCI) as the coupling reagent. The reaction products were purified by column chromatography and their structures were confirmed by ^{1}H and ^{13}C NMR spectroscopy, and by HR–ESI–MS. The resulting compounds and their antiplasmodial activities are listed in **Table 6.3**.

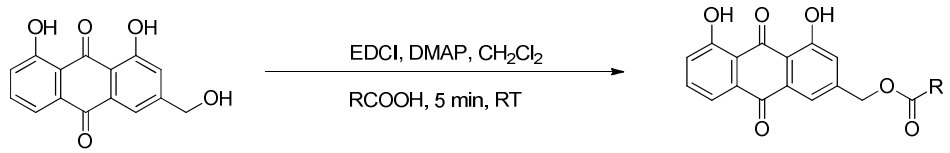

Scheme 6.2 Synthetic routes of aloe-emodin derivatives

Table 6.3 Antiplasmodial Activity of Natural and Synthetic Aloe-emodin Derivatives

Cpd	Structure	IC_{50} (μM)	Cpd	Structure	IC_{50} (μM)
6.4	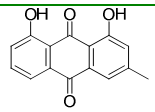	~ 58	**6.21**	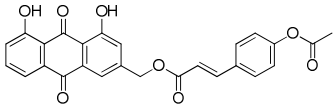	12 ± 2
6.5	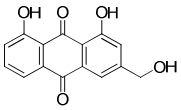	~ 55	**6.22**	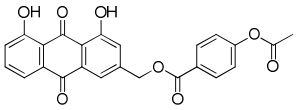	30 ± 2
6.6	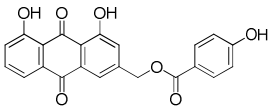	26 ± 4	**6.23**	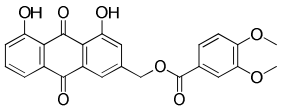	14 ± 2
6.7	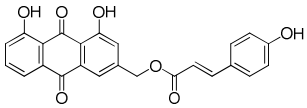	9 ± 1	**6.24**	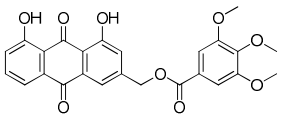	16 ± 2
6.13	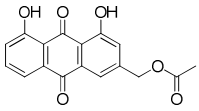	~ 42	**6.25**	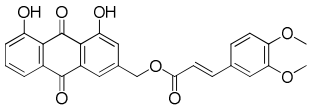	**1.3 ± 0.2**
6.14	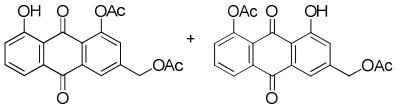	~ 60	**6.26**	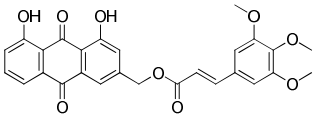	2.7 ± 0.4
6.15	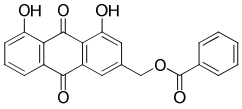	32 ± 2	**6.27**	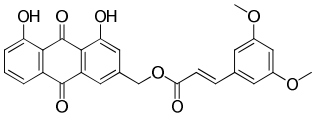	2.5 ± 0.9
6.16	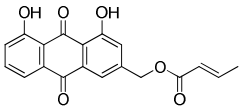	~ 45	**6.28**	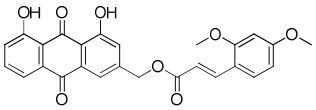	6.2 ± 2.1
6.17	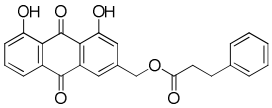	~ 36	**6.29**	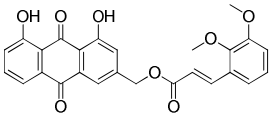	8.2 ± 1.9
6.18	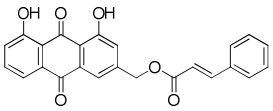	18 ± 2	**6.30**	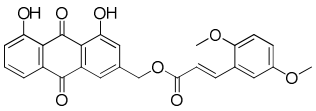	8.6 ± 1.9
6.19	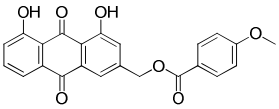	22 ± 2	**6.31**	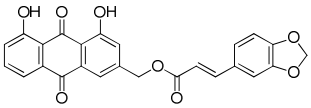	1.9 ± 0.3
6.20	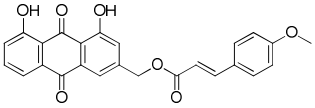	4.9 ± 0.7			

Inspection of the results of this study led to the following conclusions:

(i) Acetylation of the primary alcohol of aloe-emodin slightly increased antiplasmodial activity, while acetylation of the hydrogen-bonded hydroxy group might have a reverse effect.

The C-11 monoacetate (**6.13**, IC_{50} = ~ 42 μM) displayed slightly better antiplasmodial activity than aloe-emodin (IC_{50} = ~ 42 μM), while the mixture of the C-1, C-11 and C-8, C-11 diacetates (**6.14**, IC_{50} = ~ 60 μM) was slightly less potent than aloe-emodin. This result suggested that the presence of the hydrogen-bonded hydroxy groups might be important for antiplasmodial activity, and so acylation of the primary alcohol (C-11) of aloe-emodin was selected as the modification of choice for investigation.

(ii) The phenyl group and the non-aromatic carbon-carbon double bond are both important functional groups for increasing the antiplasmodial activity.

To explore whether acylation of the primary alcohol might increase potency, the C-11 crotonate, benzoate, phenylpropionate and cinnamate derivatives were synthesized. Cinnamate **6.18** (IC_{50} 18 ± 2 μM) displayed the highest activity among the four; benzoate **6.15** (IC_{50} = 32 ± 2 μM), phenylpropionate **6.17** (IC_{50} ~ 36 μM), and crotonate **6.16**, (IC_{50} ~ 45 μM) were all less potent. Although cinnamate **6.18** displayed the highest activity among all four acylated derivatives, it was only approximately half as potent as the 4-hydroxy-cinnamate **6.7** (kniphofione B), indicating that the hydroxy group at the C-4' of the phenyl group is a contributor to the higher activity.

(iii) The position and number of oxygenations on the phenyl group influences antiplasmodial activity.

The influence of the type of oxygenation at C-4' of the phenyl ring on antiplasmodial activity was investigated by the synthesis of 4-methoxybenzoate **6.19** (IC_{50} = 22 ± 2 μM), 4-methoxycinnamate **6.20** (IC_{50} = 4.9 ± 0.7 μM), 4-acetoxycinnamate **6.21** (IC_{50} = 12 ± 2 μM), and 4-acetoxybenzoate **6.22** (IC_{50} = 30 ± 2 μM). 4-Methoxycinnamate derivative **6.20** was more potent

than kniphofione B (**6.7**) and **6.21**, with hydroxycinnamate and acetoxycinnamate groups, respectively. Similar results were observed for the corresponding benzoate derivatives. The methoxy group is thus important for activity and was selected as the oxygenated moiety for further study.

Compounds **6.25** and **6.26** were then synthesized to investigate the influence of the number of methoxy groups on the phenyl ring of the cinnamate on potency. The 3,4-dimethoxycinnamate **6.25** (IC_{50} = 1.3 ± 0.2 μM) was more potent than both the 4-methoxycinnamate **6.20** (IC_{50} = 4.9 ± 0.7 μM) and the 3,4,5-trimethoxycinnamate **6.26** (IC_{50} = 2.7 ± 0.4 μM), suggesting that two methoxy groups on the cinnamate provided the best potency.

Finally, to understand what effect the positions of the methoxy groups on the cinnamate phenyl ring might have, 2,3-dimethoxycinnamate (**6.29**), 2,4-dimethoxycinnamate (**6.28**), 2,5-dimethoxycinnamate (**6.30**), and 3,5-dimethoxycinnamate (**6.27**) were synthesized and evaluated. 3,4-Dimethoxycinnamate (**6.25**) was the most potent of these compounds, and a similar response was observed from 3,4-methylenedioxycinnamate (**6.31**, IC_{50} = 1.9 ± 0.3 μM), suggesting that alkoxylation on the 3' and 4' positions of the phenyl group favorably influences antiplasmodial activity.

In summary, this SAR study showed that esterification of the primary hydroxyl group of aloe-emodin (**6.5**) with various carboxylic acids increased its antiplasmodial activity, with the most potent analogue being the 3,4-dimethylcaffeic acid derivative (**6.25**), with an IC_{50} value of 1.3 ± 0.2 μM (**Table 6.3**). This analogue displays 7 and 20 times the potency of the two new natural products isolated (**6.6** and **6.7**), and 42 times than that of aloe-emodin (**6.5**).

Although aloe-emodin (**6.5**) has previously been identified as an anticancer agent,[18, 19] and might thus be thought to have little potential for development as an antiplasmodial agent, our

bioassay data indicated that the acylation of the primary alcohol of aloe-emodin resulted in the increase of antiplasmodial activity (Dd2 assay), accompanied by a decrease of antiproliferative activity (A2780 assay). This observation indicates that further modifications of the C-11 hydroxyl group of aloe-emodin have the potential to yield antiplasmodial agents with little or no antiproliferative activity.

6.3 Experimental Section

6.3.1 *General Experimental Procedures.*

UV and IR spectroscopic data were measured on a Shimadzu UV-1201 spectrophotometer and a MIDAC M-series FTIR spectrophotometer, respectively. NMR spectra were recorded in $CDCl_3$ on Bruker Avance 500 or 600 spectrometers. The chemical shifts are given in δ (ppm), and coupling constants (J) are reported in Hz. Mass spectra were obtained on an Agilent 6220 LC−TOF−MS in the positive and negative ion mode.

6.3.2 *Antiproliferative Bioassay*

Antiproliferative activities were obtained at Virginia Polytechnic Institute and State University against the drug-sensitive A2780 human ovarian cancer cell line as previously described.[20]

6.3.3 *Antiplasmodial Bioassay*

The effect of each fraction and pure compound on parasite growth of the *P. falciparum* Dd2 strain was measured in a 72 h growth assay in the presence of drug as described previously with minor modifications.[21-23] Briefly, ring stage parasite cultures (200 μL per well, with 1%

hematocrit and 1% parasitemia) were grown for 72 h in the presence of increasing concentrations of the drug in a 5.05% CO_2, 4.93% O_2, and 90.2% N_2 gas mixture at 37 °C. After 72 h in culture, parasite viability was determined by DNA quantitation using SYBR Green I (50 μL of SYBR Green I in lysis buffer at 0.4 μL of SYBR Green I /mL of lysis buffer). The half-maximum inhibitory concentration (IC_{50}) calculation was performed with GraFit software using nonlinear regression curve fitting. IC_{50} values are the average of three independent determinations with each determination in duplicate and are expressed ± SEM.

6.3.4 *Plant Material*

Plant collection of *K. ensifolia* Baker (Asphodelaceae) was made in April 1999 on top of Mariepskop in the Pilgrims Rest district, State of Mpumalanga, South Africa, by Prof. P. C. Zietsman under the auspices of the New York Botanical Garden, accession number Z03796a. A voucher specimen is deposited in the New York Botanical Garden and also at BLFU (Bloemfontein Free University, South Africa).

6.3.5 *Extraction and Isolation*

The dried and powdered whole plant (100 g) of *Kniphofia ensifolia* was exhaustively extracted with EtOH (2 × 1 L) in two 24-hour percolation steps; successive partition of the concentrated extract with hexanes and CH_2Cl_2 gave an active CH_2Cl_2 fraction. 0.75 g of the original EtOH extract, designated 60031-9D, was shipped to Virginia Tech for bioassay-guided isolation. A 0.60 g sample of 60031-9D (IC_{50} 6.0 μg/mL) was suspended in aqueous MeOH (MeOH/H_2O, 9:1, 100 mL), and extracted with hexanes (3 × 100 mL). The aqueous layer was diluted to 60% MeOH (v/v) with H_2O and extracted with CH_2Cl_2 (3 × 150 mL). The hexanes

fraction was evaporated in vacuo to leave 108 mg of material with IC_{50} value between 5 and 10 μg/mL. The residue from the CH_2Cl_2 fraction (20.7 mg) was the most active fraction having an IC_{50} value between 2.5 and 5 μg/mL. The remaining aqueous MeOH fraction had an IC_{50} value of more than 10 μg/mL. The hexanes and CH_2Cl_2 fractions were combined due to the similarity of their TLC pattern.

The combined hexanes and CH_2Cl_2 fractions were divided into five fractions by Sephadex LH-20 size exclusion open column chromatography. The most active fraction (F4, 28.6 mg) had an IC_{50} value of 2.5 μg/mL. Fraction F4 was then applied to a silica gel column eluted with hexanes/EtOAc, 7:3 to give six fractions. Fraction 4-1 is the compound **6.4** (0.3 mg, IC_{50} ~ 58 μM) and fraction 4-5 is the compound **6.8** (2.6 mg, IC_{50} 1.1 ± 0.2 μM). The most active fraction 4-2 (1.8 mg, IC_{50} 0.27 μg/mL), was subjected to C_{18} HPLC using a MeCN and H_2O gradient as the solvent system to yield four known active compounds: compound **6.9** (0.3 mg, IC_{50} 0.4 ± 0.1 μM), compound **6.10** (0.9 mg, IC_{50} 0.2 ± 0.1 μM), compound **6.11** (0.3 mg, IC_{50} 10 ± 2 μM) and compound **6.12** (0.3 mg, IC_{50} 10 ± 2 μM), with retention times of 21.3, 26.0, 28.5 and 31.2 minutes, respectively. C_{18} HPLC of fraction 4-3 (2.2 mg, IC_{50} 5 μg/mL) gave compound **6.5** (0.5 mg, IC_{50} ~ 55 μM), as well as compounds **6.6** (0.7 mg, IC_{50} 26 ± 4 μM) and **6.7** (1.0 mg, IC_{50} 9 ± 1 μM), with retention times of 8.5, 18.0 and 21.2 minutes, respectively.

6.3.6 *(1,8-dihydroxy-9,10-dioxo-9,10-dihydroanthracen-3-yl)methyl 4-hydroxybenzoate (**6.6**, kniphofione A)*

Yellow-orange powder; UV (MeOH) λ_{max} (ε) 257 (1.6), 289 (0.5), 432 (0.5); IR ν_{max} cm^{-1}: 3390, 2915, 2343, 1673, 1621, 1450, 1277, 1110 cm^{-1}; ^1H NMR (600 MHz, $CDCl_3$), and ^{13}C NMR (150 MHz, $CDCl_3$), see **Table 6.1**; HR–ESI–MS *m/z* 425.0451 $[M+Cl]^-$ (calc. for $C_{22}H_{14}ClO_7^-$,

425.0434) and 389.0688 $[M–H]^–$ (calcd for $C_{22}H_{13}O_7^–$, 389.0667).

6.3.7 *(E)-(1,8-dihydroxy-9,10-dioxo-9,10-dihydroanthracen-3-yl)methyl 3-(4-hydroxyphenyl) acrylate (**6.7**, kniphofione B)*

Yellow-orange powder; UV (MeOH) λ_{max} (ε) 259 (1.2), 289 (1.4), 310 (0.9), 433 (0.6); IR ν_{max} cm^{-1}: 3390, 2916, 2362, 1706, 1627, 1603, 1450, 1268, 1161 cm^{-1}; ^1H NMR (600 MHz, $CDCl_3$), and ^{13}C NMR (150 MHz, $CDCl_3$), see **Table 6.1**; HR–ESI–MS *m/z* 439.0806 $[M+Na]^+$ (calcd for $C_{24}H_{16}NaO_7^+$, 439.0788) and 417.0986 $[M+H]^+$ (calc. for $C_{24}H_{17}O_7^+$, 417.0969).

6.3.8 *General Procedure for Synthesis of Ester Derivatives of Aloe-emodin* [24]

Substituted benzoic acids or cinnamic acids (0.1 mmol) in dry CH_2Cl_2 (0.2 mL) were treated with 1-ethyl-3-(3-dimethylaminopropyl) carbodiimide (EDCI, 20.6 mg, 0.1 mmol) and DMAP (1.0 mg, 0.006 mmol). The mixtures were stirred at room temperature for 5 minutes. Aloe-emodin (**2**, 5.4 mg, 0.02 mmol) was added, and stirring was continued at room temperature until the starting compound was consumed. The resulting solution was diluted with EtOAc (10 mL) and concentrated on a rotary evaporator. The final benzoate and cinnamate derivatives of aloe-emodin were purified by using preparative TLC (silica gel, 1000 μm; hexanes/EtOAc, 4:1).

6.3.9 *(1,8-dihydroxy-9,10-dioxo-9,10-dihydroanthracen-3-yl)methyl acetate **(6.13):***

Yellow-orange powder, 4.5 mg, yield 72%, R_f = 0.36 (hexanes/EtOAc, 4:1); HR–ESI–MS *m/z* 313.0711 $[M+H]^+$ (calc. for $C_{17}H_{13}O_6^+$, 313.0707); ^1H NMR (500 MHz, $CDCl_3$) δ_H 12.01 (s, 1H), 11.98 (s, 1H), 7.78 (dd, *J* = 7.5, 1.1 Hz, 1H), 7.72 (d, *J* = 1.6 Hz, 1H), 7.63 (dd, *J* = 8.2, 7.6 Hz, 1H), 7.25 (dd, *J* = 8.4, 1.1 Hz, 1H), 7.20 (d, *J* = 1.6 Hz, 1H), 5.12 (s, 2H), 2.12 (s, 3H); ^{13}C NMR

(126 MHz, $CDCl_3$) δ_C 192.7, 181.5, 170.5, 162.8, 162.6, 146.4, 137.3, 133.9, 133.51, 124.8, 122.4, 120.2, 118.5, 115.8, 115.3, 64.7, 20.8.

6.3.10 *Mixture of (1-acetoxy-8-hydroxy-9,10-dioxo-9,10-dihydroanthracen-3-yl)methyl acetate and (8-acetoxy-1-hydroxy-9,10-dioxo-9,10-dihydroanthracen-3-yl)methyl acetate* ***(6.14):***

Yellow-orange powder, 6.9 mg, yield 95%, R_f = 0.46 (hexanes/EtOAc, 4:1); HR–ESI–MS *m/z* 355.0815 $[M+H]^+$ (calc. for $C_{19}H_{15}O_7^+$, 355.0812); ^{1}H NMR (500 MHz, $CDCl_3$) δ_H 12.57 (s, 1H), 12.55 (s, 1H), 8.28 (dd, *J* = 7.8, 1.3 Hz, 1H), 8.22 (d, *J* = 1.0 Hz, 1H), 7.82 (dd, *J* = 8.0, 7.9 Hz, 1H), 7.81 (dd, *J* = 7.5, 1.2 Hz, 1H), 7.75(d, *J* = 1.6 Hz, 1H), 7.66 (dd, *J* = 8.3, 7.6 Hz, 1H), 7.43 (dd, *J* = 8.0, 1.3 Hz, 1H), 7.40 (d, *J* = 1.8 Hz, 1H), 7.26 (d, *J* =1.0 Hz, 1H), 5.24 (s, 2H), 5.17 (s, 2H), 2.48 (s, 3H), 2.48 (s, 3H), 2.19 (s, 3H), 2.18 (s, 3H).

6.3.11 *(1,8-dihydroxy-9,10-dioxo-9,10-dihydroanthracen-3-yl)methyl benzoate* ***(6.15):***

Yellow-orange powder, 4.0 mg, yield 53%, R_f = 0.32 (hexanes/EtOAc, 4:1); HR–ESI–MS *m/z* 375.0866 $[M+H]^+$ (calc. for $C_{22}H_{15}O_6^+$, 375.0863); ^{1}H NMR (500 MHz, $CDCl_3$) δ_H 12.11 (s, 1H), 12.06 (s, 1H), 8.12 (dd, *J* = 8.4, 1.3 Hz, 2H), 7.89 (d, *J* = 1.6 Hz, 1H), 7.85 (dd, *J* = 7.5, 1.1 Hz, 1H), 7.71 (dd, *J* = 8.2, 7.6 Hz, 1H), 7.61 (tt, *J* = 7.5, 1.3 Hz, 1H), 7.49 (t, *J* = 7.8, 2H), 7.32 (dd, *J* = 8.4, 1.0 Hz, 1H),, 5.46 (s, 2H); ^{13}C NMR (125 MHz, $CDCl_3$) δ_C 192.7, 181.5, 166.0, 162.8, 162.6, 146.6, 137.3, 133.9, 133.8, 133.5, 130.1, 129.8, 128.6, 124.8, 122.4, 120.2, 118.5, 115.8, 115.3, 65.1.

6.3.12 *(E)–(1,8-dihydroxy-9,10-dioxo-9,10-dihydroanthracen-3-yl)methyl-but-2-enoate* ***(6.16):***

Yellow-orange powder, 3.8 mg, yield 56%, R_f = 0.48 (hexanes/EtOAc, 4:1); HR–ESI–MS

m/z 339.0865 $[M+H]^+$ (calc. for $C_{19}H_{15}O_6^+$, 339.0863); ^{1}H NMR (500 MHz, $CDCl_3$) δ_H 12.09 (s, 1H), 12.07 (s, 1H), 7.85 (dd, *J* = 7.6, 1.1 Hz, 1H), 7.80 (d, *J* = 1.6 Hz, 1H), 7.70 (dd, *J* = 8.2, 7.8 Hz, 1H), 7.32 (dd, *J* = 8.4, 1.1 Hz, 1H), 7.29 (d, *J* = 1.6 Hz, 1H), 7.10 (dd, *J* = 15.5, 7.0 Hz, 1H), 5.96 (dd, *J* = 15.6, 1.6 Hz, 1H), 1.94 (dd, *J* = 6.9, 1.6 Hz, 3H); ^{13}C NMR (125 MHz, $CDCl_3$) δ_C 192.7, 181.6, 166.4, 162.8, 162.6, 146.8, 146.4, 137.3, 133.8, 133.6, 124.8, 122.3, 121.9, 120.2, 118.4, 115.8, 115.2, 64.4, 18.2.

6.3.13 *(1,8-dihydroxy-9,10-dioxo-9,10-dihydroanthracen-3-yl)methyl-3-phenylpropanoate* ***(6.17):***

Yellow-orange powder, 2.9 mg, yield 36%, R_f = 0.42 (hexanes/EtOAc, 4:1); HR–ESI–MS *m/z* 403.1146 $[M+H]^+$ (calc. for $C_{24}H_{19}O_6$, 403.1176); ^{1}H NMR (500 MHz, $CDCl_3$) δ_H 12.07 (s, 1H), 12.06 (s, 1H), 7.85 (dd, *J* = 7.6, 1.1 Hz, 1H), 7.76 (d, *J* = 1.6 Hz, 1H), 7.70 (dd, *J* = 8.3, 7.8 Hz, 1H), 7.32 (dd, *J* = 8.4, 1.1 Hz, 1H), 7.29 (d, *J* = 1.6 Hz, 1H), 7.28 (m, 2H), 7.21 (m, 3H), 5.18 (s, 2H), 3.01 (d, *J* = 7.8 Hz, 2H), 2.77 (d, *J* = 7.8 Hz, 2H); ^{13}C NMR (125 MHz, $CDCl_3$) δ_C 192.7, 181.5, 172.4, 162.8, 162.6, 146.4, 140.1, 137.3, 133.9, 133.5, 128.6, 128.3, 126.4, 124.8, 122.5, 120.2, 118.6, 115.8, 115.3, 64.7, 35.7, 30.9.

6.3.14 *(1,8-dihydroxy-9,10-dioxo-9,10-dihydroanthracen-3-yl)methyl cinnamate* ***(6.18):***

Yellow-orange powder, 3.5 mg, yield 44%, R_f = 0.38 (hexanes/EtOAc, 4:1); HR–ESI–MS *m/z* 401.1031 $[M+H]^+$ (calc. for $C_{24}H_{17}O_6^+$, 401.1020); ^{1}H NMR (500 MHz, $CDCl_3$) δ_H 12.03 (s, 1H), 12.00 (s, 1H), 7.79 (dd, *J* = 7.5, 1.1 Hz, 1H), 7.79 (d, *J* = 1.6 Hz, 1H), 7.73 (d, *J* = 16.0 Hz, 1H), 7.64 (dd, *J* = 8.3, 7.6 Hz, 1H), 7.50 (m, 2H), 7.35 (m, 3H), 7.27 (d, *J* = 1.6 Hz, 1H), 7.25 (dd, *J* = 8.4, 1.1 Hz, 1H), 6.48 (d, *J* = 16.0 Hz, 1H), 5.27 (s, 2H); ^{13}C NMR (125 MHz, $CDCl_3$) δ_C 192.7, 181.6, 166.4, 162.8, 162.6, 146.7, 146.2, 137.3, 134.1, 133.9, 133.6, 130.6, 129.0, 128.3, 124.8, 122.4,

120.2, 118.6, 117.0, 115.4, 115.3, 64.7.

6.3.15 *(1,8-dihydroxy-9,10-dioxo-9,10-dihydroanthracen-3-yl)methyl 4-methoxybenzoate* ***(6.19):***

Yellow-orange powder, 4.4 mg, yield 54%, R_f = 0.40 (hexanes/EtOAc, 4:1); HR–ESI–MS *m/z* 405.0971 $[M+H]^+$ (calc. for $C_{23}H_{17}O_7^+$, 405.0969); ^{1}H NMR (500 MHz, $CDCl_3$) δ_H 12.10 (s, 1H), 12.07 (s, 1H), 8.08 (d, *J* = 8.9 Hz, 2H), 7.88 (d, *J* = 1.5 Hz, 1H), 7.85 (dd, *J* = 7.5, 1.0 Hz, 1H), 7.70 (dd, *J* = 8.1, 7.8 Hz, 1H), 7.37 (d, *J* = 1.5 Hz, 1H), 7.32 (dd, *J* = 8.4, 1.0 Hz, 1H), 6.96 (d, *J* = 8.9 Hz, 2H), 5.42 (s, 2H), 3.88 (s, 3H); ^{13}C NMR (125 MHz, $CDCl_3$) δ_C 192.7, 181.6, 165.7, 164. 9, 162.8, 162.6, 146.9, 137.3, 134.1, 133.6, 131.9, 124.8, 122.3, 121.7, 120.2, 118.5, 115.8, 115.3, 113.8, 64.8, 55.5.

6.3.16 (*E*)-(1,8-dihydroxy-9,10-dioxo-9,10-dihydroanthracen-3-yl)methyl 3-(4-methoxyphenyl) acrylate ***(6.20):***

Yellow-orange powder, 3.5 mg, yield 41%, R_f = 0.36 (hexanes/EtOAc, 4:1); HR–ESI–MS *m/z* 431.1133 $[M+H]^+$ (calc. for $C_{25}H_{19}O_7^+$, 431.1125); ^{1}H NMR (500 MHz, $CDCl_3$) δ_H 12.02 (s, 1H), 12.00 (s, 1H), 7.79 (dd, *J* = 7.4, 1.1 Hz, 1H), 7.78 (d, *J* = 1.6 Hz, 1H), 7.68 (d, *J* = 16.0 Hz, 1H), 7.63 (dd, *J* = 8.3, 7.7 Hz, 1H), 7.45 (d, *J* = 8.8 Hz, 2H), 7.27 (d, *J* = 1.6 Hz, 1H), 7.25 (dd, *J* = 8.4, 1.1 Hz, 1H), 6.86 (d, *J* = 8.8 Hz, 2H), 6.34 (d, *J* = 16.0 Hz, 1H), 5.26 (s, 2H), 3.78 (s, 3H); ^{13}C NMR (125 MHz, $CDCl_3$) δ_C 192.7, 181.6, 166.7, 162.8, 161.7, 159.8, 146.9, 145.8, 137.3, 133.9, 133.6, 130.0, 126.9, 124.8, 122.4, 120.2, 118.5, 118.2, 115.8, 115.3, 114.4, 64.6, 55.5.

6.3.17 (*E*)- *(1,8-dihydroxy-9,10-dioxo-9,10-dihydroanthracen-3-yl)methyl 3-(4-acetoxyphenyl) acrylate* ***(6.21):***

Yellow-orange powder, 3.8 mg, yield 41%, R_f = 0.34 (hexanes/EtOAc, 4:1); HR–ESI–MS *m/z* 459.1079 $[M+H]^+$ (calc. for $C_{26}H_{19}O_8^+$, 459.1074); ^{1}H NMR (600 MHz, $CDCl_3$) δ_H 12.09 (s, 1H), 12.06 (s, 1H), 7.86 (dd, *J* = 7.4, 1.1 Hz, 1H), 7.85 (d, *J* = 1.6 Hz, 1H), 7.76 (d, *J* = 16.0 Hz, 1H), 7.70 (dd, *J* = 8.3, 7.7 Hz, 1H), 7.58 (d, *J* = 8.7 Hz, 2H), 7.35 (d, *J* = 1.6 Hz, 1H), 7.32 (dd, *J* = 8.4, 1.1 Hz, 1H), 7.15 (d, *J* = 8.6 Hz, 2H), 6.50 (d, *J* = 16.0 Hz, 1H), 5.33 (s, 2H), 2.32 (s, 3H); ^{13}C NMR (150 MHz, $CDCl_3$) δ_C 192.8, 181.6, 169.2, 166.3, 162.9, 162.7, 152.5, 146.7, 145.1, 137.4, 134.0, 133.7, 132.0, 129.5, 124.9, 122.6, 122.3, 120.3, 118.7, 117.3, 115.9, 115.4, 64.9, 21.2.

6.3.18 *(1,8-dihydroxy-9,10-dioxo-9,10-dihydroanthracen-3-yl)methyl 4-acetoxybenzoate* ***(6.22):***

Yellow-orange powder, 4.2 mg, yield 49%, R_f = 0.36 (hexanes/EtOAc, 4:1); HR–ESI–MS *m/z* 433.0935 $[M+H]^+$ (calc. for $C_{24}H_{17}O_8^+$, 433.0918); ^{1}H NMR (600 MHz, $CDCl_3$) δ_H 12.09 (s, 1H), 12.05 (s, 1H), 8.15 (d, *J* = 8.9 Hz, 2H), 7.87 (d, *J* = 1.6 Hz, 1H), 7.85 (dd, *J* = 7.5, 1.0 Hz, 1H), 7.70 (dd, *J* = 8.1, 7.8 Hz, 1H), 7.36 (d, *J* = 1.6 Hz, 1H), 7.32 (dd, *J* = 8.4, 1.0 Hz, 1H), 7.22 (d, *J* = 8.9 Hz, 2H), 5.44 (s, 2H), 2.33 (s, 3H); ^{13}C NMR (150 MHz, $CDCl_3$) δ_C 192.7, 181.6, 167.7, 164.3, 162.8, 162.6, 158.4, 143.5, 137.4, 134.1, 133.5, 131.5, 127.0, 124.9, 122.5, 121.9, 120.3, 118.6, 115.7, 115.3, 65.3, 21.3.

6.3.19 *(1,8-dihydroxy-9,10-dioxo-9,10-dihydroanthracen-3-yl)methyl 3,4-dimethoxybenzoate* ***(6.23):***

Yellow-orange powder, 4.7 mg, yield 54%, R_f = 0.45 (hexanes/EtOAc, 4:1); HR–ESI–MS *m/z* 435.1084 $[M+H]^+$ (calc. for $C_{24}H_{19}O_8^+$, 435.1074); ^{1}H NMR (500 MHz, $CDCl_3$) δ_H 12.10 (s,

1H), 12.06 (s, 1H), 7.89 (d, J = 1.6 Hz, 1H), 7.85 (dd, J = 7.5, 1.1 Hz, 1H), 7.78 (dd, J = 8.4, 2.0 Hz, 1H), 7.77 (dd, J = 8.2, 7.8 Hz, 1H), 7.60 (d, J = 2.0 Hz, 1H), 7.36 (d, J = 1.6 Hz, 1H), 7.32 (dd, J = 8.4, 1.1 Hz, 1H), 6.93 (d, J = 8.5 Hz, 1H), 5.43 (s, 2H), 3.96 (s, 6H) ^{13}C NMR (125 MHz, $CDCl_3$) δ_C 192.7, 181.6, 165.8, 162.8, 162.6, 153.4, 148.8, 146.9, 137.3, 133.91, 133.5, 124.8, 124.0, 122.4, 121.8, 120.2, 118.5, 115.8, 115.3, 112.1, 110.4, 65.0, 56.1.

6.3.20 *(1,8-dihydroxy-9,10-dioxo-9,10-dihydroanthracen-3-yl)methyl 3,4,5-trimethoxybenzoate* ***(6.24):***

Yellow-orange powder, 5.1 mg, yield 55%, R_f = 0.52 (hexanes/EtOAc, 4:1); HR–ESI–MS *m/z* 465.1187 $[M+H]^+$ (calc. for $C_{25}H_{21}O_9^+$, 465.1180); ^{1}H NMR (500 MHz, $CDCl_3$) δ_H 12.09 (s, 1H), 12.05 (s, 1H), 7.89 (d, J = 1.6 Hz, 1H), 7.85 (dd, J = 7.5, 1.1 Hz, 1H), 7.70 (dd, J = 8.2, 7.7 Hz, 1H), 7.35 (s, 2H), 7.33 (d, J = 1.6 Hz, 1H), 7.32 (dd, J = 8.4, 1.1 Hz, 1H), 5.44 (s, 2H), 3.93 (s, 9H); ^{13}C NMR (125 MHz, $CDCl_3$) δ_C 192.7, 181.5, 165.7, 162.8, 162.6, 159.8, 153.1, 146.6, 137.4, 134.0, 133.5, 124.8, 124.3, 122.5, 120.2, 118.5, 115.8, 115.4, 107.1, 65.2, 61.0, 56.3.

6.3.21 *(E)–(1,8-dihydroxy-9,10-dioxo-9,10-dihydroanthracen-3-yl)methyl-3-(3,4-dimethoxy phenyl) acrylate* ***(6.25):***

Yellow-orange powder, 4.2 mg, yield 46%, R_f = 0.40 (hexanes/EtOAc, 4:1); HR–ESI–MS *m/z* 461.1245 $[M+H]^+$ (calc. for $C_{26}H_{21}O_8^+$, 461.1231); ^{1}H NMR (500 MHz, $CDCl_3$) δ_H 12.02 (s, 1H), 11.99 (s, 1H), 7.78 (d, J = 1.6 Hz, 1H), 7.78 (dd, J = 7.6, 1.1 Hz, 1H), 7.66 (d, J = 15.9 Hz, 1H), 7.63 (dd, J = 8.3, 7.6 Hz, 1H), 7.27 (d, J = 1.6 Hz, 1H), 7.25 (dd, J = 8.4, 1.1 Hz, 1H), 7.07 (dd, J = 8.3, 1.9 Hz, 1H), 7.02 (d, J = 1.9 Hz, 1H), 6.82 (d, J = 8.3 Hz, 1H), 6.35 (d, J = 15.9 Hz, 1H), 5.26 (s, 2H), 3.87 (s, 3H), 3.86 (s, 3H). ^{13}C NMR (125 MHz, $CDCl_3$) δ_C 192.7, 181.7, 166.7, 162.8,

162.7, 151.4, 149.3, 146.9, 146.1, 137.3, 133.9, 133.6, 127.1, 124.8, 123.0, 122.4, 120.2, 118.5, 115.8, 115.3, 114.6, 111.0, 109.6, 64.6, 56.0, 55.9.

6.3.22 ***(****E)–(1,8-dihydroxy-9,10-dioxo-9,10-dihydroanthracen-3-yl)methyl 3-(3,4,5-trimethoxy phenyl) acrylate* ***(6.26):***

Yellow-orange powder, 4.5 mg, yield 46%, R_f = 0.46 (hexanes/EtOAc, 4:1); HR–ESI–MS *m/z* 491.1352 $[M+H]^+$ (calc. for $C_{27}H_{23}O_9^+$, 491.1337);. ^{1}H NMR (500 MHz, $CDCl_3$) δ_H 12.04 (s, 1H), 11.99 (s, 1H), 7.80 (d, *J* = 1.6 Hz, 1H), 7.79 (dd, *J* = 7.6, 1.1 Hz, 1H), 7.64 (dd, *J* = 8.3, 7.6 Hz, 1H), 7.63 (d, *J* = 15.9 Hz, 1H), 7.28 (d, *J* = 1.6 Hz, 1H), 7.26 (dd, *J* = 8.4, 1.1 Hz, 1H), 6.73 (s, 2H), 6.39 (d, *J* = 15.9 Hz, 1H), 5.27 (s, 2H), 3.84 (s, 6H), 3.83 (s, 3H); ^{13}C NMR (125 MHz, $CDCl_3$) δ_C 192.7, 181.6, 166.3, 162.8, 162.6, 153.5, 146.7, 146.1, 140.4, 137.3, 133.9, 133.5, 129.6, 124.8, 122.4, 120.2, 118.5, 116.2, 115.8, 115.3, 105.4, 64.7, 61.0, 56.2.

6.3.23 *(E)–(1,8-dihydroxy-9,10-dioxo-9,10-dihydroanthracen-3-yl)methyl 3-(3,5-dimethoxy phenyl) acrylate* ***(6.27):***

Yellow-orange powder, 3.5 mg, yield 38%, R_f = 0.40 (hexanes/EtOAc, 4:1); HR–ESI–MS *m/z* 461.1224 $[M+H]^+$ (calc. for $C_{26}H_{21}O_8^+$, 461.1231); ^{1}H NMR (600 MHz, $CDCl_3$) δ_H 12.09 (s, 1H), 12.06 (s, 1H), 7.86 (dd, *J* = 7.6, 1.1 Hz, 1H), 7.85 (d, *J* = 1.6 Hz, 1H), 7.70 (dd, *J* = 8.3, 7.6 Hz, 1H), 7.70 (d, *J* = 15.9 Hz, 1H), 7.33 (d, *J* = 1.6 Hz, 1H), 7.32(dd, *J* = 8.4, 1.1 Hz, 1H), 6.70 (d, *J* = 2.2 Hz, 2H), 6.52 (t, *J* = 2.3 Hz, 1H), 6.51(d, *J* = 15.9 Hz, 1H), 5.33 (s, 2H), 3.83 (s, 6H); ^{13}C NMR (150 MHz, $CDCl_3$) δ_C 192.8, 181.7, 166.4, 162.7, 161.2, 146.8, 146.3, 137.5, 136.1, 134.1, 133.7, 124.9, 122.6, 120.3, 118.7, 117.7, 116.0, 115.5, 106.2, 103.2, 77.2, 64.9, 55.5.

6.3.24 *(E)–(1,8-dihydroxy-9,10-dioxo-9,10-dihydroanthracen-3-yl)methyl 3-(2,4-dimethoxy phenyl) acrylate* ***(6.28):***

Yellow-orange powder, 4.3 mg, yield 47%, R_f = 0.40 (hexanes/EtOAc, 4:1); HR–ESI–MS *m/z* 461.1212 $[M+H]^+$ (calc. for $C_{26}H_{21}O_8^+$, 461.1231); ^{1}H NMR (600 MHz, $CDCl_3$) δ_H 12.08 (s, 1H), 12.07 (s, 1H), 8.01 (d, *J* = 16.1 Hz, 1H), 7.85 (dd, *J* = 7.7, 1.1 Hz, 1H), 7.85 (d, *J* = 1.6 Hz, 1H), 7.70 (dd, *J* = 8.2, 7.7 Hz, 1H), 7.47 (d, *J* = 8.6 Hz, 1H), 7.34 (d, *J* = 2.3 Hz, 1H), 7.32 (dd, *J* = 8.4, 1.1 Hz, 1H), 6.54 (d, *J* = 16.1 Hz, 1H), 6.53, 6.53, 6.52 (dd, *J* = 8.6, 2.3 Hz, 1H), 6.47 (d, *J* = 2.3 Hz, 1H), 5.32 (s, 2H), 3.89 (s, 3H), 3.85 (s, 3H); ^{13}C NMR (150 MHz, $CDCl_3$) δ_C 192.7, 181.6, 167.3, 163.0, 162.6, 160.1, 147.2, 146.8, 141.6, 137.2, 133.8, 133.6, 130.9, 124.7, 122.4, 120.1, 118.6, 118.3, 116.4, 115.9, 114.8, 105.3, 98.5, 64.4, 55.5.

6.3.25 *(E)–(1,8-dihydroxy-9,10-dioxo-9,10-dihydroanthracen-3-yl)methyl 3-(2,3-dimethoxy phenyl) acrylate* ***(6.29):***

Yellow-orange powder, 4.1 mg, yield 45%, R_f = 0.40 (hexanes/EtOAc, 4:1); HR–ESI–MS *m/z* 461.1242 $[M+H]^+$ (calc. for $C_{26}H_{21}O_8^+$, 461.1231);. ^{1}H NMR (600 MHz, $CDCl_3$) δ_H 12.08 (s, 1H), 12.06 (s, 1H), 8.12 (d, *J* = 16.2 Hz, 1H), 7.86 (d, *J* = 1.6 Hz, 1H), 7.85 (dd, *J* = 7.4, 1.1 Hz, 1H), 7.70 (dd, *J* = 8.3, 7.6 Hz, 1H), 7.34 (d, *J* = 1.6 Hz, 1H), 7.32 (dd, *J* = 8.4, 1.1 Hz, 1H), 7.20 (dd, *J* = 7.9, 1.2 Hz, 1H), 7.08 (t, *J* = 8.0 Hz, 1H), 6.97 (dd, *J* = 8.1, 1.3 Hz, 1H), 6.59 (d, *J* = 16.2 Hz, 1H), 5.34 (s, 2H), 3.89 (s, 6H); ^{13}C NMR (150 MHz, $CDCl_3$) δ_C 192.7, 181.5, 166.6, 162.8, 162.6, 153.2, 148.7, 146.8, 141.0, 137.3, 133.9, 133.6, 128.3, 124.7, 124.2, 122.4, 120.2, 119.4, 118.5, 118.3, 115.8, 115.3, 114.3, 64.7, 61.4.

6.3.26 *(E)–(1,8-dihydroxy-9,10-dioxo-9,10-dihydroanthracen-3-yl)methyl 3-(2,5-dimethoxy phenyl) acrylate* ***(6.30):***

Yellow-orange powder, 3.4 mg, yield 37%, R_f = 0.36 (hexanes/EtOAc, 4:1); HR–ESI–MS *m/z* 461.1211 $[M+H]^+$ (calc. for $C_{26}H_{21}O_8^+$, 461.1231); ^{1}H NMR (600 MHz, $CDCl_3$) δ 12.07 (s, 1H), 12.06 (s, 1H), 8.07 (d, *J* = 16.1 Hz, 1H), 7.86 (d, *J* = 1.6 Hz, 1H), 7.85 (dd, *J* = 7.4, 1.1 Hz, 1H), 7.70 (dd, *J* = 8.3, 7.6 Hz, 1H), 7.34 (d, *J* = 1.6 Hz, 1H), 7.32 (dd, *J* = 8.4, 1.1 Hz, 1H), 7.07 (d, *J* = 3.0 Hz, 1H), 6.93 (dd, *J* = 9.0, 3.0 Hz, 1H), 6.87 (d, *J* = 9.0 Hz, 1H), 6.62 (d, *J* = 16.1 Hz, 1H), 5.33 (s, 2H), 3.86 (s, 3H), 3.81 (s, 3H); ^{13}C NMR (150 MHz, $CDCl_3$) δ_C 192.8, 181.7, 166.9, 163.0, 162.7, 153.7, 153.2, 147.1, 141.6, 137.4, 134.1, 133.7, 124.9, 123.8, 122.6, 120.3, 118.7, 117.8, 116.0, 115.4, 113.5, 112.7, 77.2, 64.8, 56.2.

6.3.27 *(E)–(1,8-dihydroxy-9,10-dioxo-9,10-dihydroanthracen-3-yl)methy 3-(3,4-methylene dioxyphenyl) acrylate* ***(6.31):***

Yellow-orange powder, 4.0 mg, yield 53%, R_f = 0.32 (hexanes/EtOAc, 4:1); HR–ESI–MS *m/z* 445.0912 $[M+H]^+$ (calc. for $C_{25}H_{17}O_8^+$, 445.0918); H NMR (500 MHz, $CDCl_3$) H NMR (500 MHz, $CDCl_3$) δ_H 12.09 (s, 1H), 12.07 (s, 1H), 7.86 (d, *J* = 1.6 Hz, 1H), 7.85 (dd, *J* = 7.4, 1.1 Hz, 1H), 7.70 (dd, *J* = 8.3, 7.6 Hz, 1H), 7.69 (d, *J* = 15.9 Hz, 1H), 7.33 (d, *J* = 1.6 Hz, 1H), 7.32 (dd, *J* = 8.4, 1.1 Hz, 1H), 7.07 (d, *J* = 1.7 Hz, 1H), 7.04 (dd, *J* = 8.0, 1.7 Hz, 1H), 6.83 (d, *J* = 8.0 Hz, 1H), 6.37 (d, *J* = 15.9 Hz, 1H), 6.02 (s, 2H), 5.32 (s, 2H); ^{13}C NMR (125 MHz, $CDCl_3$) δ_C 192.8, 181.7, 166.7, 163.0, 162.8, 150.1, 148.6, 147.0, 141.6, 137.5, 134.0, 133.7, 128.7, 125.0, 124.9, 122.6, 120.3, 118.7, 116.0, 115.4, 115.1, 108.8, 106.8, 101.8, 64.8.

6.4 References and Notes

1. Dai,Y.; Harinantenaina, L.; Bowman, J.; Brodie, P. J.; Goetz, M.; Cassera, M. B.; Kingston, D. G. I. Isolation of antiplasmodial anthraquinones from *Kniphofia ensifolia* and synthesis and structure–activity relationships of related compounds. (Submitted for Publication) *Bioorg. Med. Chem.* 2013.

2. Jarvis, L. Marketing mother nature's molecules. *Chem. Eng. News* **2012,** *90*, 30.

3. Dai, Y.; Harinantenaina, L.; Brodie, P. J.; Goetz, M.; Shen, Y.; TenDyke, K.; Kingston, D. G. I. Antiproliferative homoisoflavonoids and bufatrienolides from *Urginea depressa*. *J. Nat. Prod.* **2013**, *76*, 865–872.

4. Clark, V. R.; Barker, N. P.; Mucina, L. The Sneeuberg: A new centre of floristic endemism on the Great Escarpment, South Africa. *S. Afr. J. Bot.* **2009,** *75*, 196–238.

5. Chase, M. W.; De Bruijn, A. Y.; Cox, A. V.; Reeves, G.; Rudall, P. J.; Johnson, M. A. T.; Eguiarte, L. E. Phylogenetics of Asphodelaceae (Asparagales): An analysis of plastid rbcL and trnL-F DNA sequences. *Ann. Bot. (Oxford, U. K.)* **2000,** *86*, 935–951.

6. Habtemariam, S. Knipholone anthrone from *Kniphofia foliosa* induces a rapid onset of necrotic cell death in cancer cells. *Fitoterapia* **2010,** *81*, 1013–1019.

7. Wube, A. A.; Bucar, F.; Asres, K.; Gibbons, S.; Rattray, L.; Croft, S. L. Antimalarial compounds from *Kniphofia foliosa* roots. *Phytother. Res.* **2005,** *19*, 472–476.

8. Blitzke, T.; Porzel, A.; Masaoud, M.; Schmidt, J. A chlorinated amide and piperidine alkaloids from *Aloe sabaea*. *Phytochemistry* **2000,** *55*, 979–982.

9. García-Sosa, K.; Villarreal-Alvarez, N.; Lübben, P.; Peña-Rodríguez, L. M. Chrysophanol, an

antimicrobial anthraquinone from the root extract of *Colubrina greggii*. *J. Mex. Chem. Soc.* **2006,** *50*, 76–78.

10. Danielsen, K.; Aksnes, D. W.; Francis, G. W. NMR study of some anthraquinones from rhubarb. *Magn. Reson. Chem.* **1992,** *30*, 359–360.

11. Dagne, E.; Steglich, W. Knipholone: a unique anthraquinone derivative from *Kniphofia foliosa*. *Phytochemistry* **1984,** *23*, 1729–1731.

12. Dagne, E.; Berhanu, E.; Steglich, W. New bianthraquinone pigments from *Kniphofia species*. *Bull. Chem. Soc. Ethiop.* **1987**, *1*, 32–35.

13. Van Wyk, B. E.; Yenesew, A.; Dagne, E. The chemotaxonomic significance of root anthraquinones and pre-anthraquinones in the genus *Lomatophyllum* (Asphodelaceae). *Biochem. Syst. Ecol.* **1995,** *23*, 805–808.

14. Fujitake, N.; Suzuki, T.; Fukumoto, M.; Oji, Y. Predomination of dimers over naturally occurring anthraquinones in Soil. *J. Nat. Prod.* **1998,** *61*, 189–192.

15. Conner, J. M.; Gray, A. I.; Reynolds, T.; Waterman, P. G. Anthracene and chromone derivatives in the exudate of *Aloe rabaiensis*. *Phytochemistry* **1989,** *28*, 3551–3553.

16. Chang, C. L.; Zhang, L. J.; Chen, R. Y.; Kuo, L. M. Y.; Huang, J. P.; Huang, H. C.; Lee, K. H.; Wu, Y. C.; Kuo, Y. H. Antioxidant and anti-inflammatory phenylpropanoid derivatives from *Calamus quiquesetinervius*. *J. Nat. Prod.* **2010,** *73*, 1482–1488.

17. Hosny, M.; Rosazza, J. P. N. Novel isoflavone, cinnamic Acid, and triterpenoid glycosides in soybean molasses. *J. Nat. Prod.* **1999,** *62*, 853–858.

18. Pecere, T.; Gazzola, M. V.; Mucignat, C.; Parolin, C.; Vecchia, F. D.; Cavaggioni, A.; Basso,

G.; Diaspro, A.; Salvato, B.; Carli, M.; Palù, G. Aloe-emodin is a new type of anticancer agent with selective activity against neuroectodermal tumors. *Cancer Res.* **2000,** *60*, 2800–2804.

19. Srinivas, G.; Babykutty, S.; Sathiadevan, P. P.; Srinivas, P. Molecular mechanism of emodin action: transition from laxative ingredient to an antitumor agent. *Med. Res. Rev.* **2007,** *27*, 591–608.

20. Dai, Y.; Harinantenaina, L.; Brodie, P. J.; Callmander, M. W.; Randrianasolo, S.; Rakotobe, E.; Rasamison, V. E.; Kingston, D. G. I. Isolation and synthesis of two antiproliferative calamenene-type sesquiterpenoids from *Sterculia tavia* from the Madagascar rain forest. *Bioorg. Med. Chem.* **2012,** *20*, 6940–6944.

21. Bennett, T. N.; Paguio, M.; Gligorijevic, B.; Seudieu, C.; Kosar, A. D.; Davidson, E.; Roepe, P. D. Novel, rapid, and inexpensive cell-based quantification of antimalarial drug efficacy. *Antimicrob. Agents Chemother.* **2004,** *48*, 1807–1810.

22. Smilkstein, M.; Sriwilaijaroen, N.; Kelly, J. X.; Wilairat, P.; Riscoe, M. Simple and inexpensive fluorescence-based technique for high-throughput antimalarial drug screening. *Antimicrob. Agents Chemother.* **2004,** *48*, 1803–1806.

23. Harinantenaina, L.; Bowman, J. D.; Brodie, P. J.; Slebodnick, C.; Callmander, M. W.; Rakotobe, E.; Randrianaivo, R.; Rasamison, V. E.; Gorka, A.; Roepe, P. D.; Cassera, M. B.; Kingston, D. G. I. Antiproliferative and antiplasmodial dimeric phloroglucinols from *Mallotus oppositifolius* from the Madagascar dry forest. *J. Nat. Prod.* **2013,** *76*, 388–393.

24. Rivero-Cruz, B.; Rivero-Cruz, I.; Rodríguez-Sotres, R.; Mata, R. Effect of natural and synthetic benzyl benzoates on calmodulin. *Phytochemistry* **2007,** *68*, 1147–1155.

Chapter 7: Miscellaneous Natural Products Studied

7.1 Introduction

During the search for novel anticancer and antimalarial agents, some extracts yielded only known compounds. These known compounds isolated from various species are reported in this chapter, in order to provide a complete record of the work that has been done, and also to document the botanical sources of the isolated compounds.

7.2 Extract Studied

7.2.1 *Octolepis ibityensis* Stem (Thymelaeaceae)

The crude extract of stems of *Octolepis ibityensis* had an IC_{50} value 13 μg/mL against the A2780 cell line. Liquid–liquid partition from 2100 mg crude afforded 298 mg in the CH_2Cl_2 fraction with an IC_{50} value of 2.4 μg/mL. An LH-20 size exclusion open column (CH_2Cl_2/MeOH, 1:1) was then applied for further separation, to yield four fractions, among which fraction 2 (117 mg) was the most active one, with an IC_{50} value of 0.43 μg/mL. A normal phase silica gel column (hexanes/EtOAc, 3:2) yielded fourteen fractions. Four sub-fractions (I to IV) displayed IC_{50} values lower than 1.0 μg/mL, and Fractions II, III, and IV were subjected to HPLC on a C_{18} column to yield four known and active compounds, 4'-methylapigenin (**7.1**)[1], syringaresinol (**7.2**)[2], cucurbitacin B (**7.3**)[3] and cucurbitacin D (**7.4**)[4], with the IC_{50} values of 0.32, 2.4, 0.59 and 0.28 μg/mL, respectively.

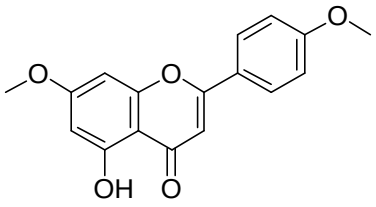

7.1

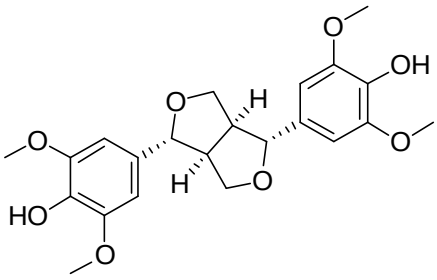

7.2

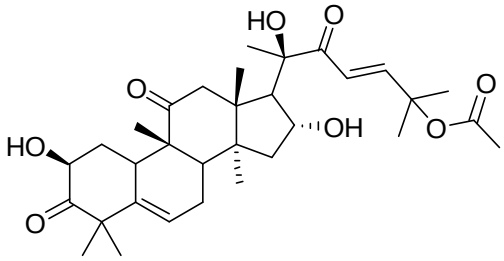

7.3

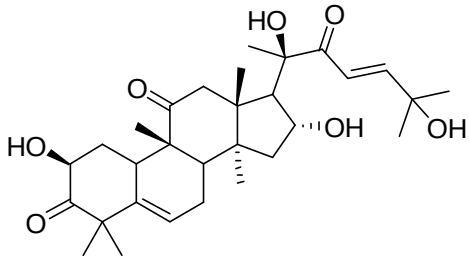

7.4

7.2.2 *Polyscias floccosa* Leaf (Araliaceae)

The crude extract of *Polyscias floccosa* leaf had an IC_{50} value 11 μg/mL against A2780 cell line. Liquid–liquid partition from 100 mg crude afforded 14.7 mg in the CH_2Cl_2 fraction with an IC_{50} value of 2.4 μg/mL. LH-20 size exclusion open column was then applied for further separation, obtaining three fractions, among which fraction 3 (14.8 mg) was the most active one, with the IC_{50} values of 3.0 μg/mL. A normal phase silica gel column was used to obtain eleven fractions, among which fraction 5 and fraction 9 are identified as the known and pure triterpene saponins, cauloside A (**7.5**)[5] and hederagenin-3-*O*-*α*-*β*-arabinopyranosyl-(1→2)-*α*-L-rhamnopyranoside (**7.6**)[6], with IC_{50} values of 2.8 and 2.2 μg/mL, respectively.

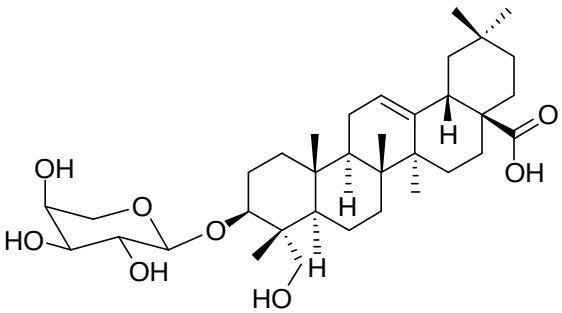

7.5

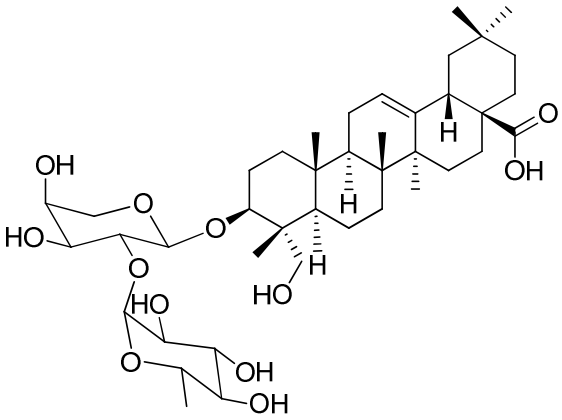

7.6

7.2.3 *Sterculia capuronii* Arènes Leaf (Sterculiaceae)

The crude extract of *Sterculia capuronii* Arènes leaf had an IC_{50} value 16 μg/mL against the A2780 cell line. Liquid–liquid partition of 900 mg crude extract afforded 297 mg in the dichromethane fraction with an IC_{50} value of 8.9 μg/mL. LH-20 size exclusion open column was then applied for further separation, obtaining two active fractions (F1: 63.5 mg, F2: 133.2 mg) with the IC_{50} values of 8.7 and 8.8 μg/mL, respectively. A normal phase silica gel column was used to get 23 fractions from F2. Two sub-fractions (F2-17 and F2-21) displayed IC_{50} values of 8.9 and 5.0, respectively. F2-21 was subjected to another silica gel column to yield two known triterpenes, erythrodiol (**7.7**)[7] and uvaol (**7.8**)[8], which had IC_{50} values of 9.3 and 11 μg/mL, respectively.

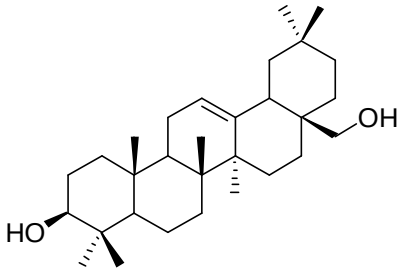

7.7

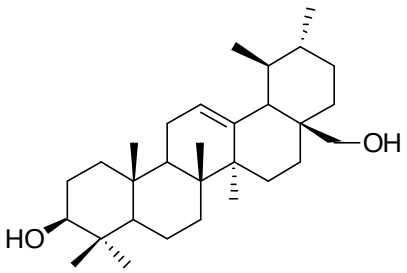

7.8

7.2.4 *Antiaris toxicaria* Fruit (Moraceae)

The crude extract of *Antiaris toxicaria* fruit had an IC_{50} value of 9 μg/mL against the A2780 cell line. Liquid–liquid partition of 100 mg crude extract gave a 63.3 mg hexanes fraction with an IC_{50} value of 3 μg/mL. A normal phase silica gel column (hexanes/EtOAc, 4:1) yielded seven fractions. Two sub-fractions (F4 and F5) were pure alkyl phenols (**7.9** and **7.10**),[9, 10] which displayed IC_{50} values of 7.1 and 8.6 μg/mL, respectively.

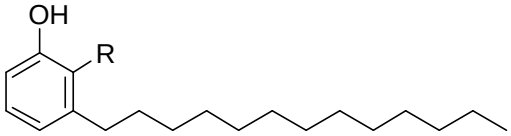

7.9 R= H;
7.10 R= OH

7.2.5 *Xerophyta retinervis* (Velloziaceae)

The crude extract of *Xerophyta retinervis* had an IC_{50} value more than 20 μg/mL against the A2780 cell line. Liquid–liquid partition of 100 mg of the crude extract gave 20.4 mg of hexanes soluble fraction (IC_{50} 14 μg/mL), 10.9 mg of the CH_2Cl_2 fraction and 65.5 mg of the aqueous MeOH fraction with IC_{50} values both more than 20 μg/mL. LH-20 size exclusion column chromatography of the hexanes fraction afforded six fractions, of which the most active fraction (3.4 mg) had an IC_{50} of 9.2 μg/mL. This fraction was then applied to a silica gel column and eluted with hexanes/EtOAc, 9:1 to yield a known pure stilbenoid **7.11**[11] (2.9 mg), whose IC_{50} is 2.9 μg/mL.

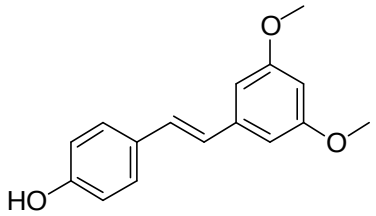

7.11

7.2.6 *Viridiflorum sims* Balk (Pittosporum)

The crude extract of *Viridiflorum sims* Balk had an IC_{50} value 8.4 μg/mL against the A2780 cell line. Liquid–liquid partition of 1 g crude afforded 711 mg in the *n*-BuOH fraction with an IC_{50} value of 8.1 μg/mL. Separation on an HP-20 Diaion open column (MeOH and H_2O gradient) give 333 mg of an active fraction with an IC_{50} value of 9.7 μg/mL. A normal phase silica gel column ($CHCl_3$/MeOH/H_2O, 5:7:1) yielded 26 fractions, the second of which showed an IC_{50} value of 0.77 μg/mL, while 11 fractions in the middle appeared to be crystalline. These crystals are believed to belong to members of triterpene-saponin family of compounds. The separation was discontinued due to the difficulties of further purification.

7.3 References and Notes

1. Greenham, J.; Harborne, J. B.; Williams, C. A. Identification of lipophilic flavones and flavonols by comparative HPLC, TLC and UV spectral analysis. *Phytochem. Analysis.* **2003,** *14*, 100–118.

2. Monthong, S. P., Nuntasaen, N.; Pompimon, W. (+)-Syringaresinol lignan from new species *Magnolia thailandic. Am. J. Appli.Sci.* **2011,** *8*, 1268–1271.

3. Jacobs, H.; Singh, T.; Reynolds, W. F.; McLean, S. Isolation and ^{13}C-NMR assignments of cucurbitacins from *Cayaponia angustiloba*, *Cayaponia racemosa*, and *Gurania subumbellata*. *J. Nat. Prod.* **1990,** *53*, 1600–1605.

4. Seger, C.; Sturm, S.; Haslinger, E.; Stuppner, H. NMR signal assignment of 22-deoxocucurbitacin D and cucurbitacin D from *Ecballium elaterium* L. (Cucurbitaceae). *Monatshefte für Chemie / Chemical Monthly* **2005,** *136*, 1645–1649.

5. Mshvildadze, V.; Elias, R.; Faure, R.; Debrauwer, L.; Dekanosidze, G.; Kemertelidze, E.; Balansard, G. Triterpenoid saponins from berries of *Hedera colchica*. *Chem. Pharm. Bull.* **2001,** *49*, 752–754.

6. Kizu, H. T. Studies on the constituents of Clematis species. V. On the saponins of the root of *Clematis chinensis* Osbeck. *Chem. Pharm. Bull.* **1982,** *30*, 3340–3346.

7. Duquesnoy, E.; Castola, V.; Casanova, J. Triterpenes in the hexanes extract of leaves of *Olea europaea* L.: analysis using ^{13}C-NMR spectroscopy. *Phytochem. Anal.* **2007,** *18*, 347–353.

8. Siddiqui, S.; Hafeez, F.; Begum, S.; Siddiqui, B. S. Kaneric acid, a new triterpene from the leaves of *Nerium oleander. J. Nat. Prod.* **1986,** *49*, 1086–1090.

9. Saitta, M.; Giuffrida, D.; La Torre, G. L.; Potortì, A. G.; Dugo, G. Characterisation of alkylphenols in pistachio (*Pistacia vera* L.) kernels. *Food Chem.* **2009,** *117*, 451–455.

10. Itokawa, H.; Totsuka, N.; Nakahara, K.; Maezuru, M.; Takeya, K.; Kondo, M.; Inamatsu, M.; Morita, H. A quantitative structure–activity relationship for antitumor activity of long-chain phenols from *Ginkgo biloba* L. *Chem. Pharm. Bull.* **1989,** *37*, 1619–1621.

11. Jo, G.; Hyun, J.; Hwang, D.; Lee, Y. H.; Koh, D.; Lim, Y. Complete NMR data of methoxylated *cis*- and *trans*-stilbenes as well as 1,2-diphenylethanes. *Magn. Reson. Chem.* **2011,** *49*, 374–377.

Chapter 8: Conclusions

8.1 Isolation of Bioactive Natural Products

In our continuing search for biologically active natural products from tropical dry and rainforests as part of our engagement in an International Cooperative Biodiversity Group (ICBG) program and a collaborative research project established between Virginia Tech and the Institute for Hepatitis and Virus Research (IHVR), more than fifteen plants were selected for initial inspection. Nine of them were fractionated to yield fourteen new and seventeen known compounds, guided by antiproliferative activity against the A2780 human ovarian cancer cell line. One antimalarial extract was selected for fractionation to yield two new and seven known compounds, guided by antiplasmodial activity against the Dd2 strain of *Plasmodium falciparum*.

8.1.1 *Anticancer Extracts*

Investigation of an endemic Madagascan plant of the *Uvaria* genus for antiproliferative activity against the A2780 ovarian cancer cell line led to the isolation of two new acetogenins, uvaricin A and uvaricin B, with modest antiproliferative activity against A2780 ovarian cancer cells, with IC_{50} values of 6.4 $\pm$ 0.8 μM and 8.8 $\pm$ 1.4 μM, respectively.

Investigation of the endemic Madagascan plant *Sterculia tavia* (Malvaceae) for antiproliferative activity against the A2780 ovarian cancer cell line led to the isolation of two new bioactive calamenene-type sesquiterpenoids, named tavinin A and *epi*-tavinin A, together with the known sesquiterpenoid mansonone G. The structures of the two new compounds were confirmed by *de novo* synthesis. The three isolated sesquiterpenoids had modest antiproliferative activities

against the A2780 ovarian cancer cell line, with IC_{50} values of 10 ± 0.9, 5.5 ± 0.9, and 6.7 ± 0.3 μM, respectively.

Investigation of the endemic Madagascan plant *Nematostylis anthophylla* (Rubiaceae) for antiproliferative activity against the A2780 ovarian cancer cell line led to the isolation of the known triterpene saponin randianin and the two new bioactive triterpene saponins 2"-*O*-acetylrandianin and 6"-*O*-acetylrandianin. The three isolated triterpene saponins displayed moderate antiproliferative activity, with IC_{50} values of 2.2 ± 0.2, 1.2 ± 0.1 and 1.7 ± 0.3 μM, respectively, against the A2780 ovarian cancer.

Investigation of the South African plant *Urginea depressa* Baker (Asparagaceae Juss.) for antiproliferative activity against the A2780 ovarian cancer cell line led to the isolation of the six new homoisoflavonoids urgineanins A–F, two known bufatrienolides, and two new bufatrienolides urginins B and C. Five homoisoflavonoids urgineanins A–E showed strong antiproliferative activities against the A2780 ovarian cancer cell line with IC_{50} values of 0.32 ± 0.05, 3.4 ± 0.2, 1.35 ± 0.1, 0.35 ± 0.06 and 1.44 ± 0.08 μM, respectively, while the less oxygenated analog urgineanin F had a much lower activity, with an IC_{50} value of 23 ± 1.2 μM. In addition, the four bufatrienolides had strong antiproliferative activities against the same cell line, with IC_{50} values of 24 ± 6, 11 ± 2, 111 ± 8 and 41 ± 3 nM, respectively.

8.1.2 *Antimalarial Extracts*

Bioassay guided separation of the South African plant *Kniphofia ensifolia* for antiplasmodial activity led to the isolation of two new anthraquinones, named kniphofiones A and B, together with

three known bioactive anthraquinone monomers, and four known bisanthraquinones. Two of the dimeric compounds displayed the strongest antiplasmodial activity among all the isolated compounds, with IC_{50} values of 0.4 ± 0.1 and 0.2 ± 0.1 μM, respectively. The two new compounds displayed modest activities, with IC_{50} values of 26 ± 4 and 9 ± 1 μM, respectively. Due to the synthetic accessibility of the new compounds, a structure–activity relationship study was conducted. As a result, one analog of kniphofione B, the 3,4-dimethoxycaffeic acid derivative of aloe-emodin, was found to have the highest activity among all the aloe-emodin derivatives, with an IC_{50} value of 1.3 ± 0.2 μM.

Appendix (1D, 2D NMR and CD Spectra)

^{1}H NMR spectrum of **2.2** in $CDCl_3$ (500 Hz)

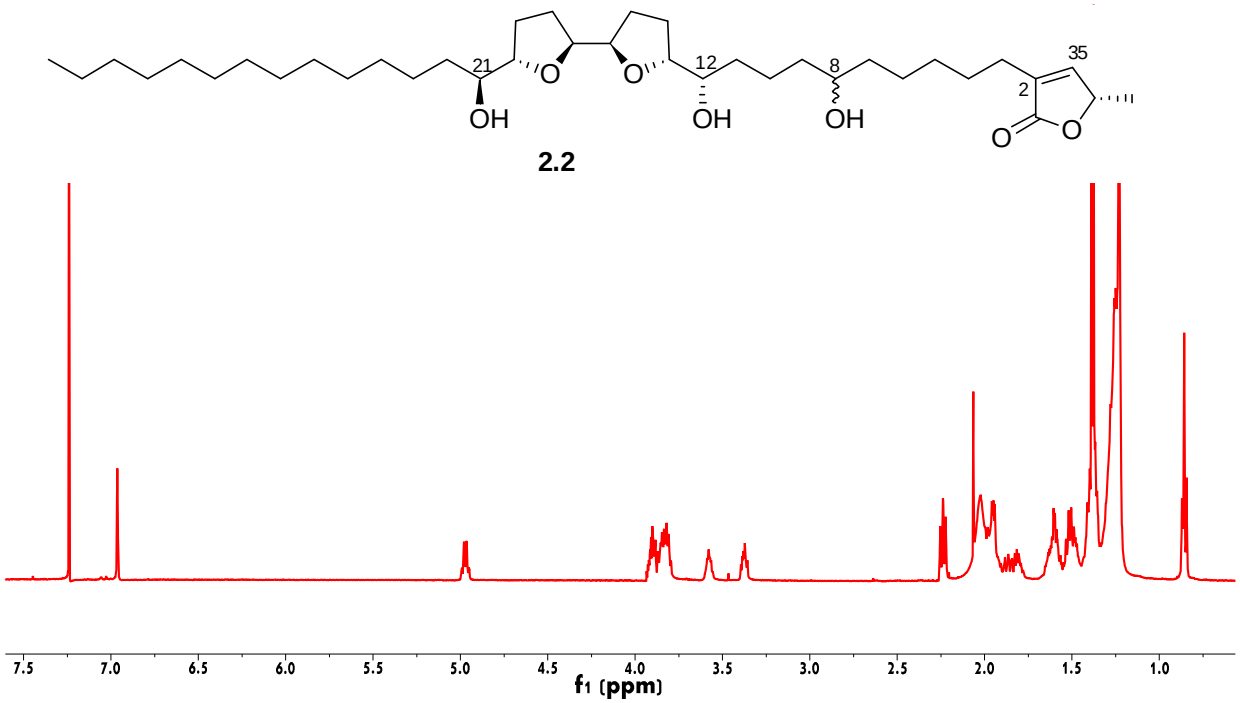

^{13}C NMR spectrum of **2.2** in $CDCl_3$ (125 Hz)

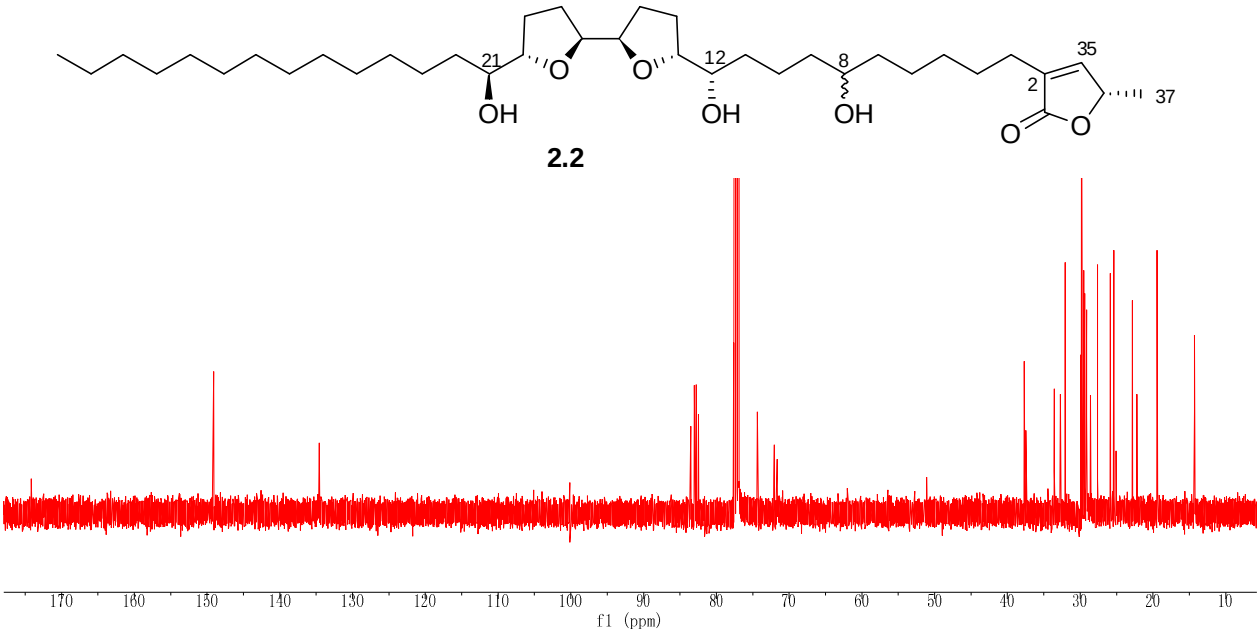

^{1}H NMR spectrum of **2.3** in $CDCl_3$ (500 Hz)

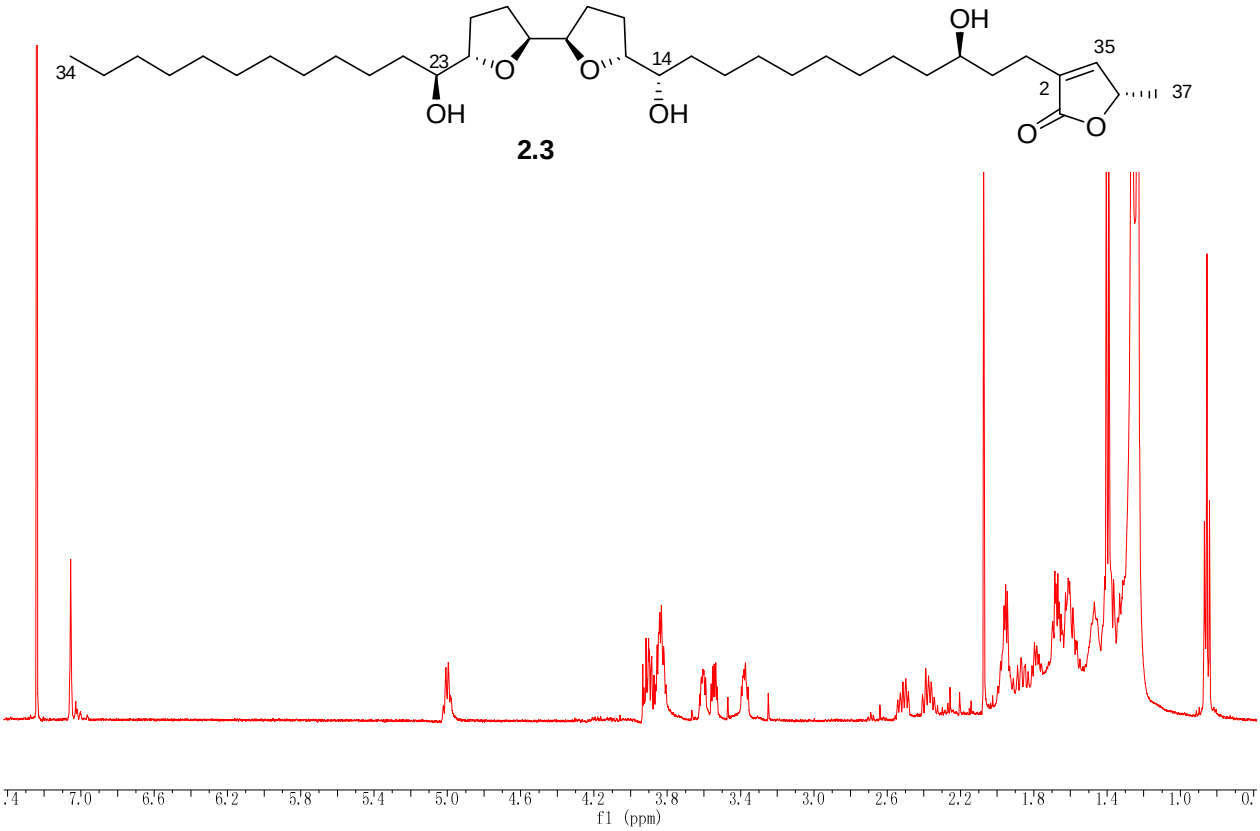

^{13}C NMR spectrum of **2.3** in $CDCl_3$ (125 Hz)

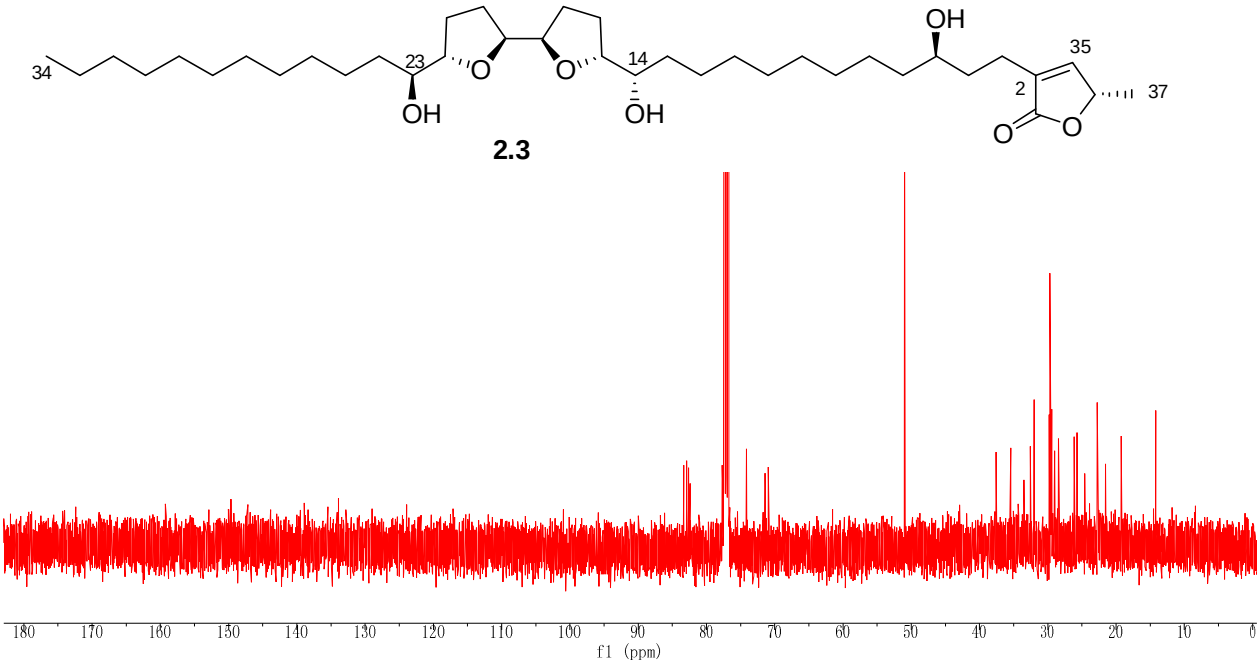

^{1}H NMR spectrum of **3.4** in acetone-d_6 (600 Hz)

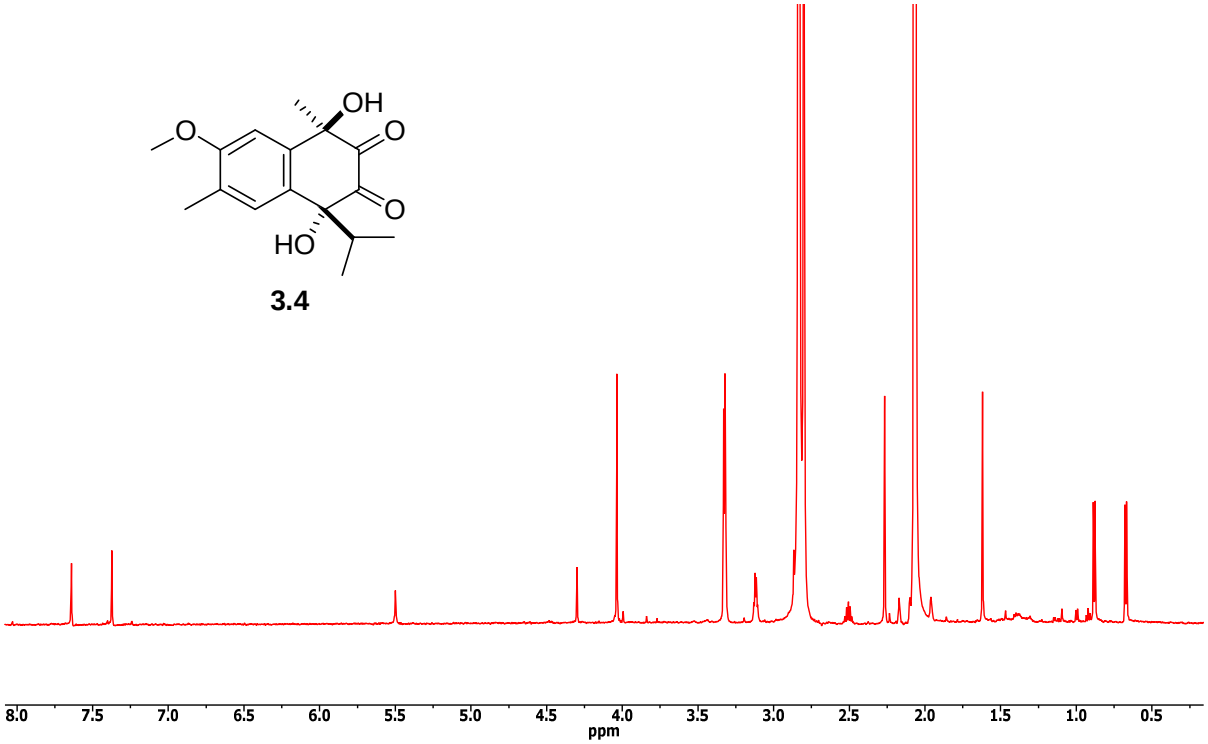

gHMBC spectrum of **3.4** in acetone-d_6

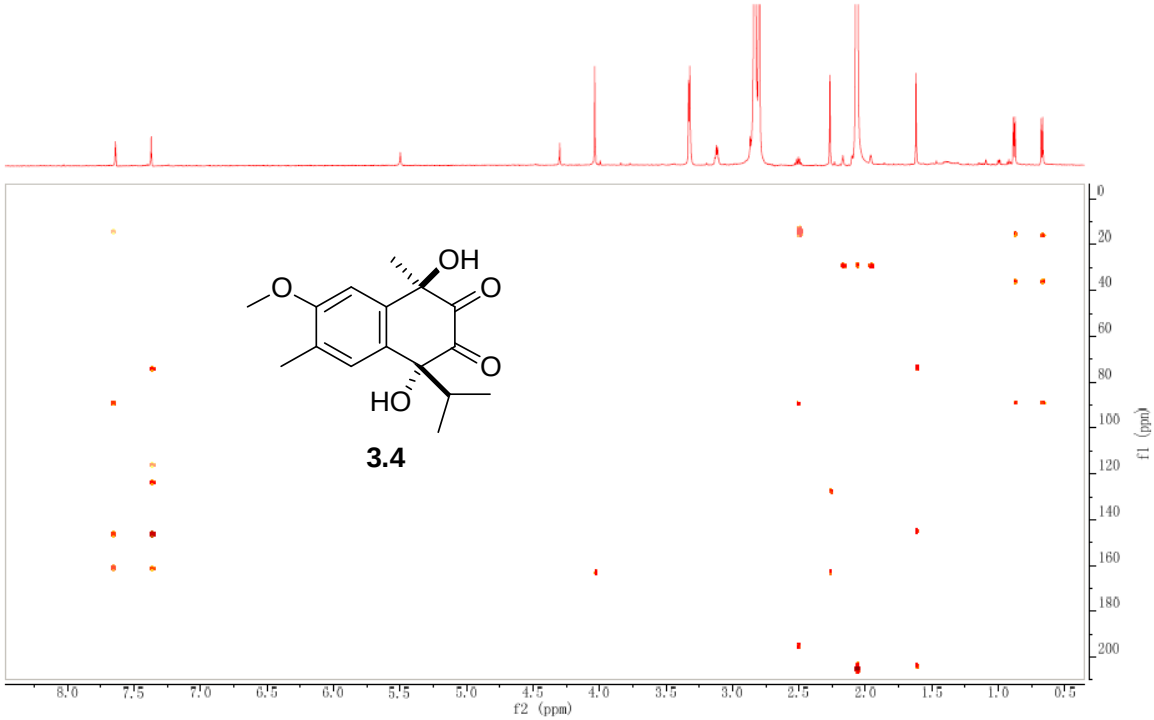

gHSQC spectrum of **3.4** in acetone-d_6

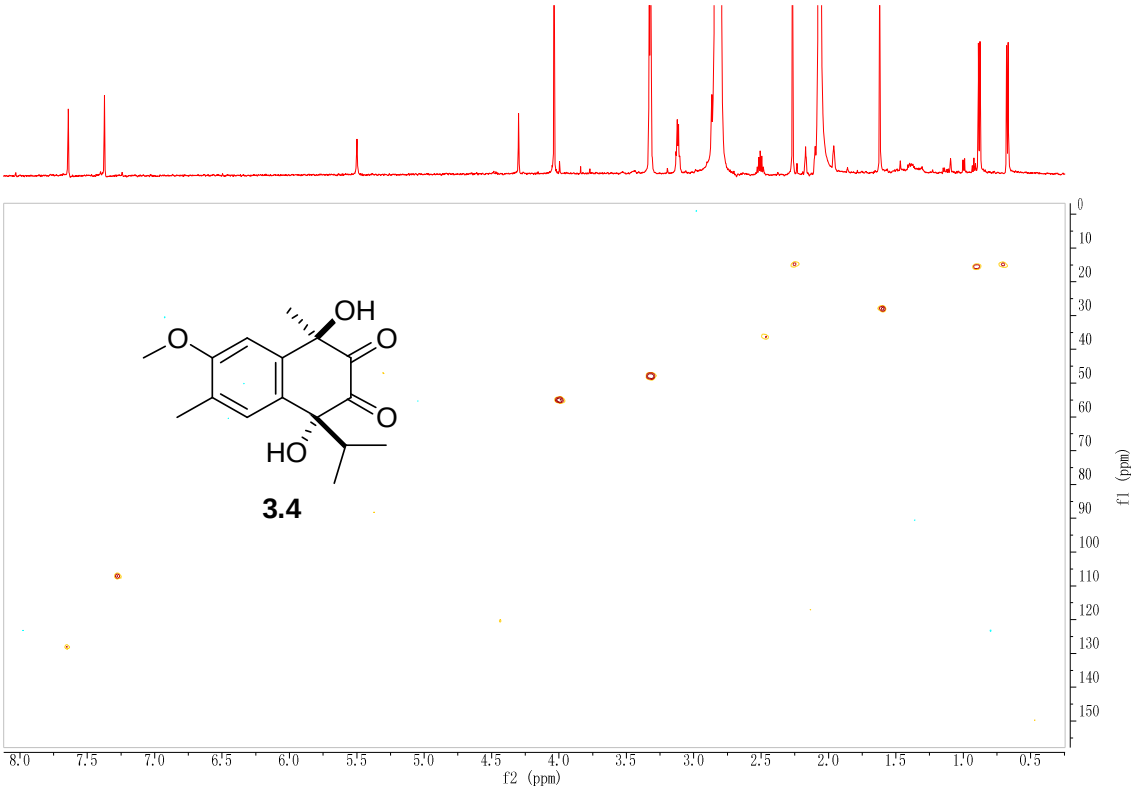

gCOSY spectrum of **3.4** in acetone-d_6

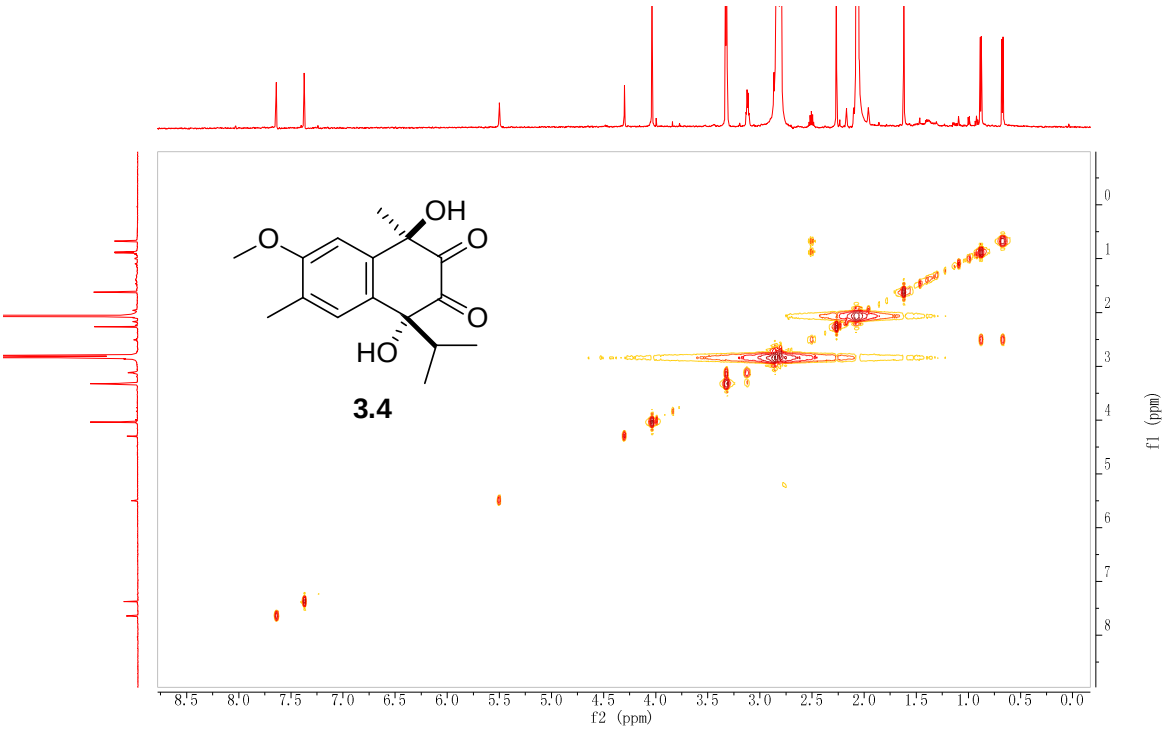

^{1}H NMR spectrum of **3.5** in acetone-d_6 (600 Hz)

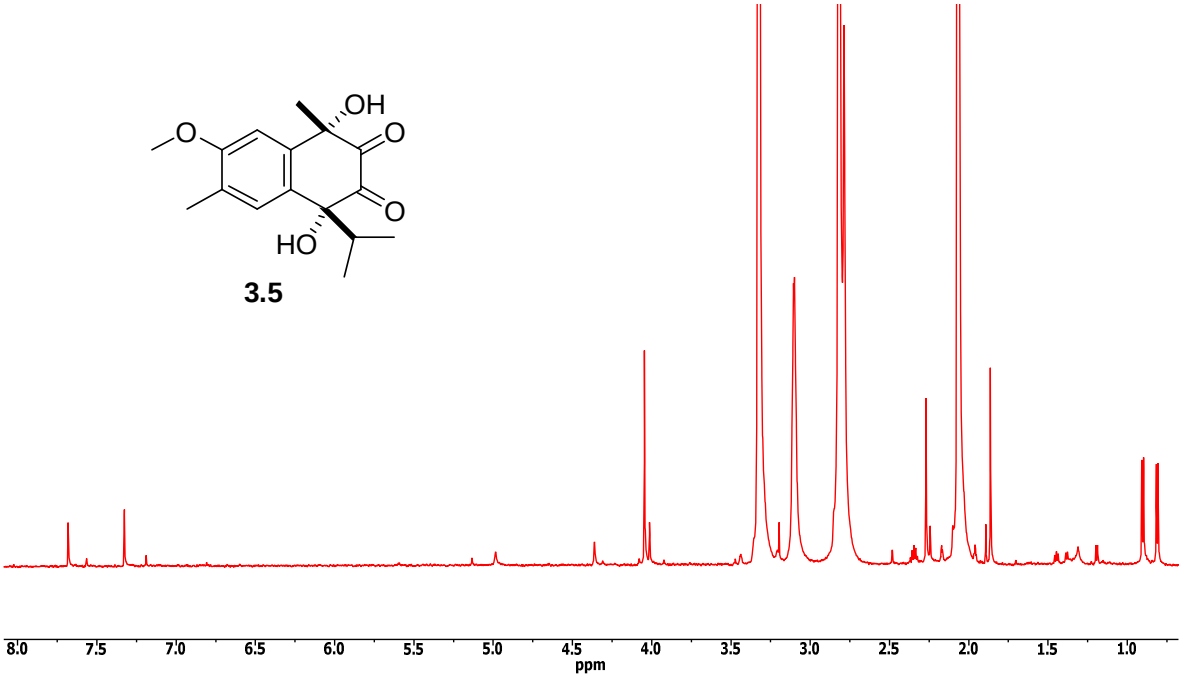

gHMBC spectrum of **3.5** in acetone-d_6

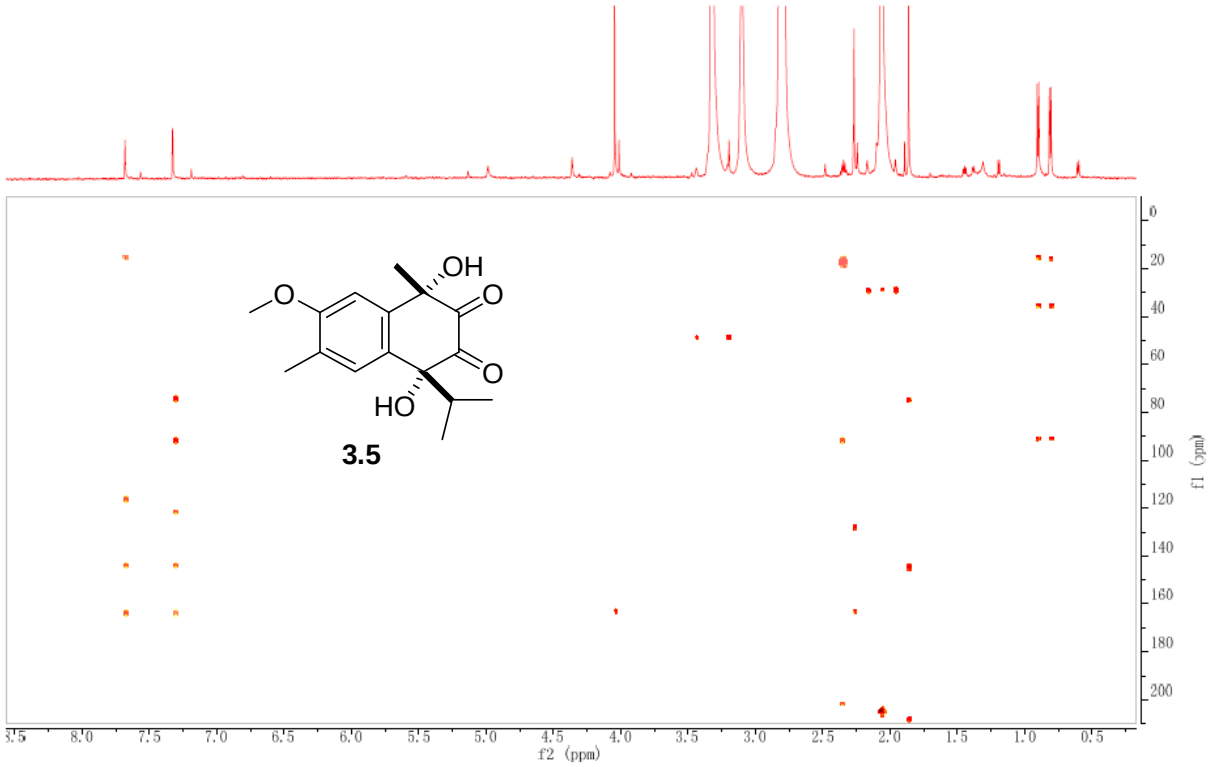

gHSQC spectrum of **3.5** in acetone-d_6

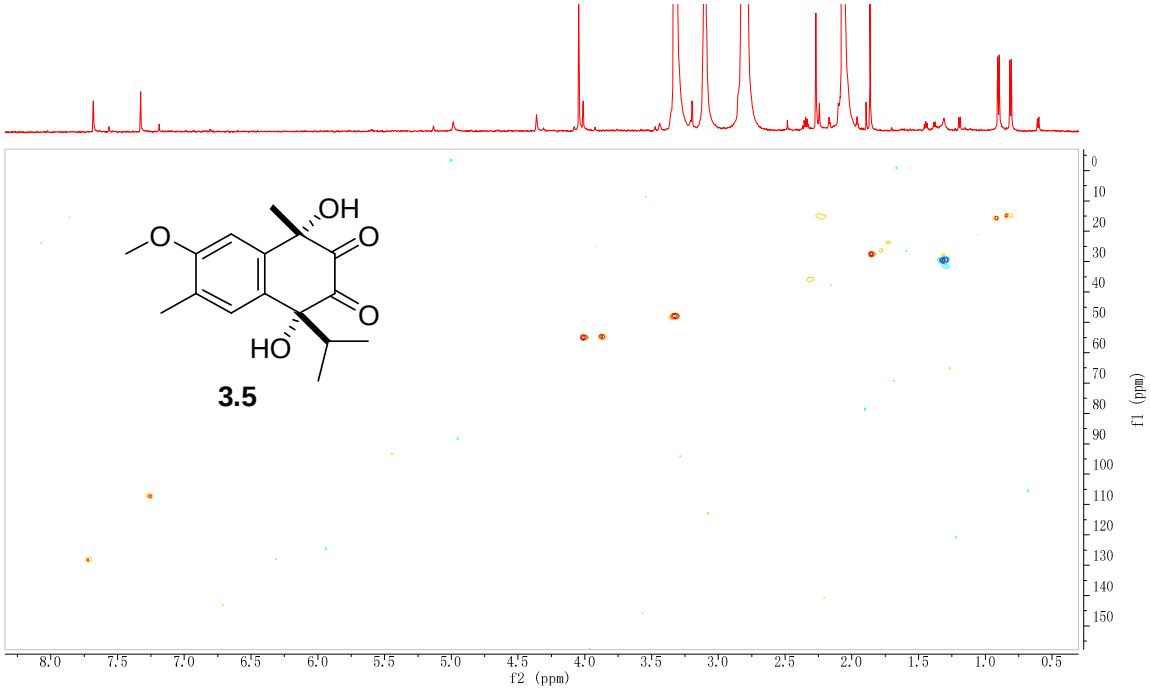

gCOSY spectrum of **3.5** in acetone-d_6

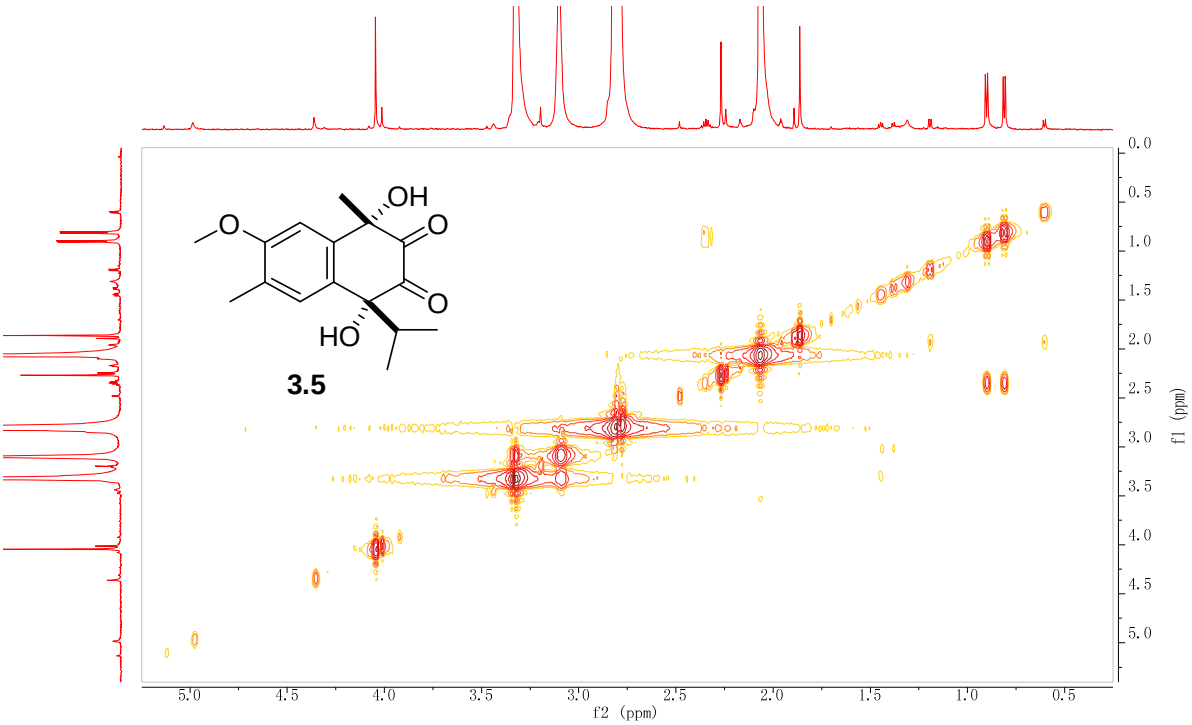

^{1}H NMR spectrum of **3.13** in $CDCl_3$ (500 Hz)

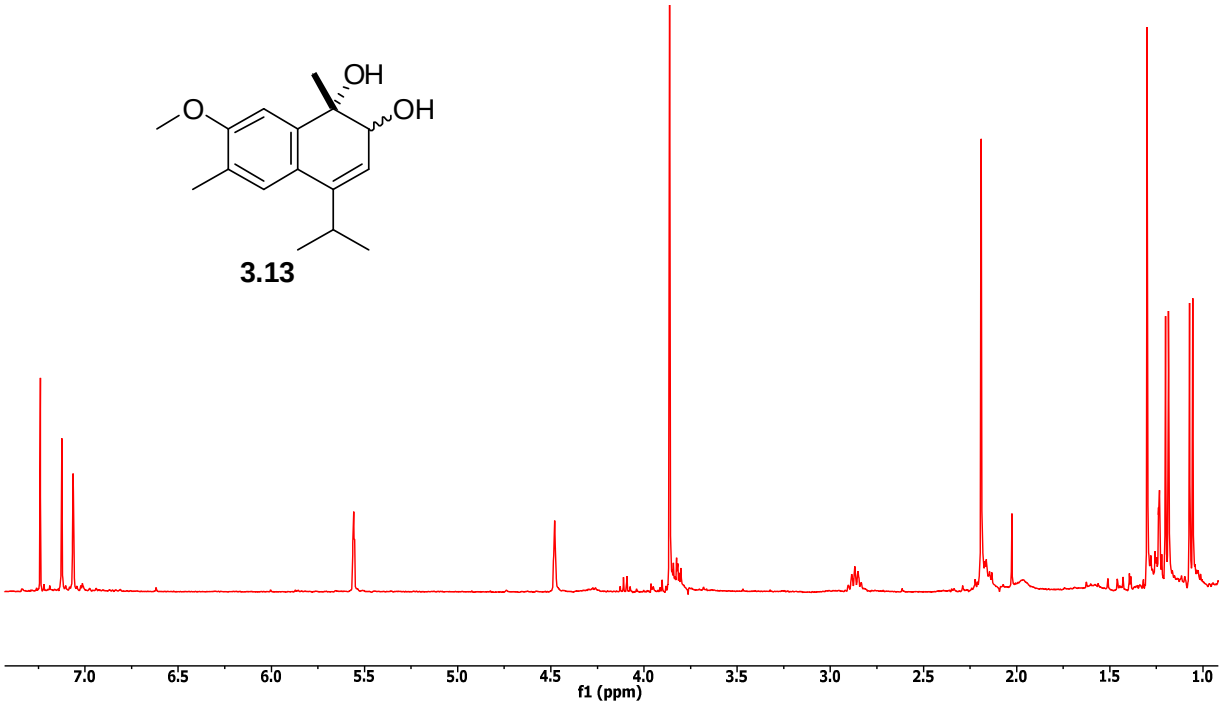

^{13}C NMR spectrum of **3.13** in $CDCl_3$ (125 Hz)

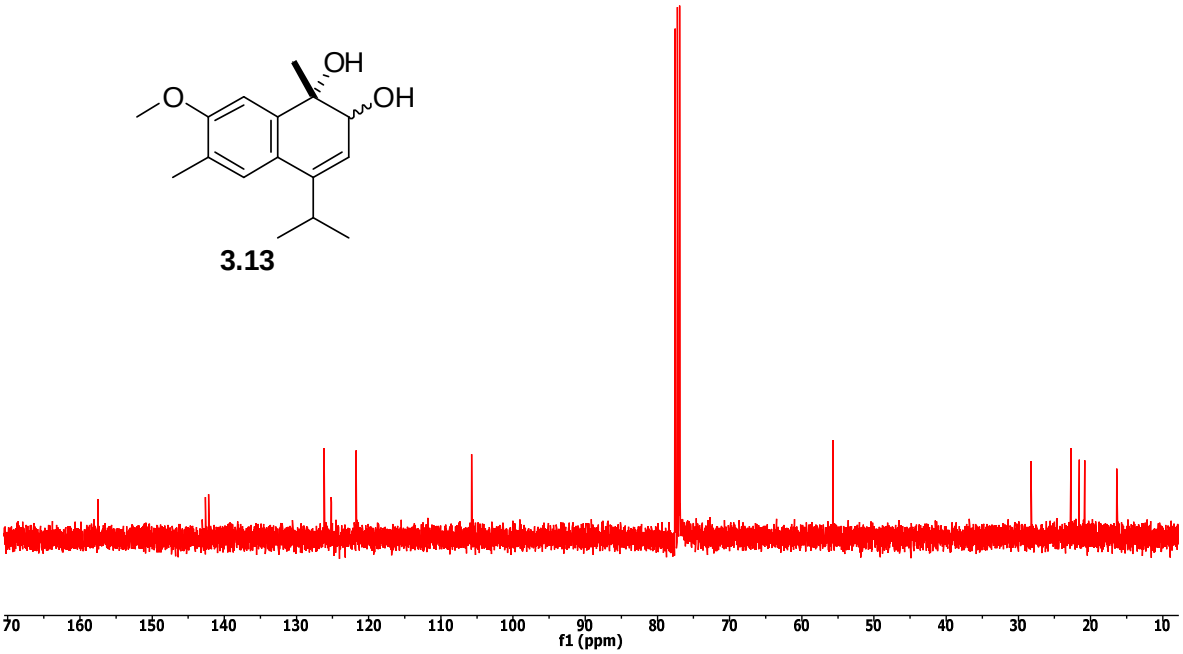

^{1}H NMR spectrum of **4.5** in acetone-d_5 (500 Hz)

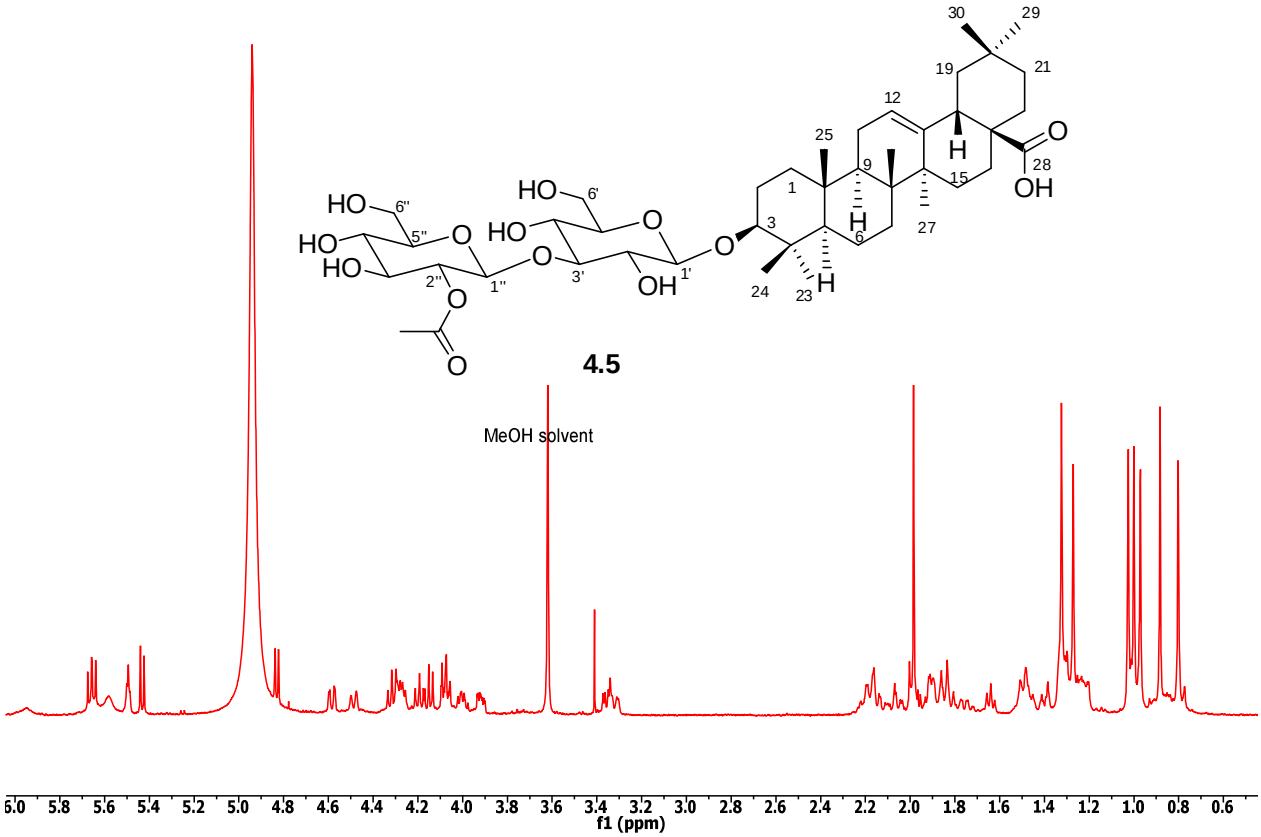

^{13}C NMR spectrum of **4.5** in acetone-d_5 (125 Hz)

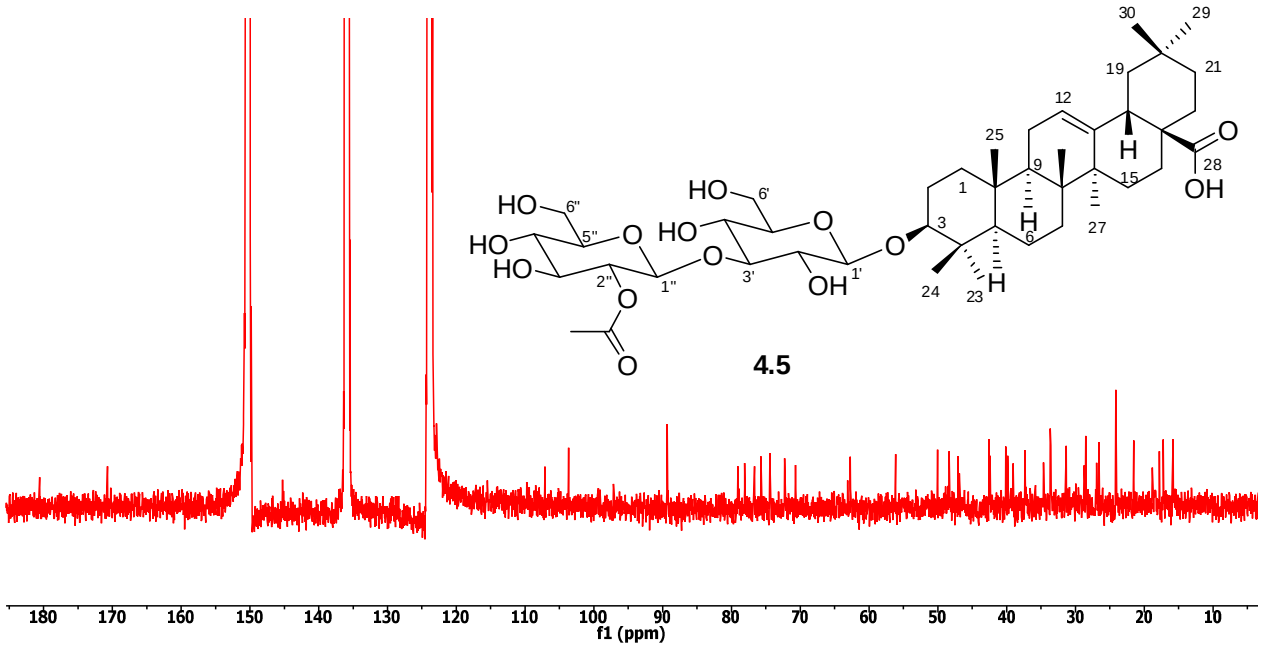

^{1}H NMR spectrum of **4.6** in acetone-d_5 (500 Hz)

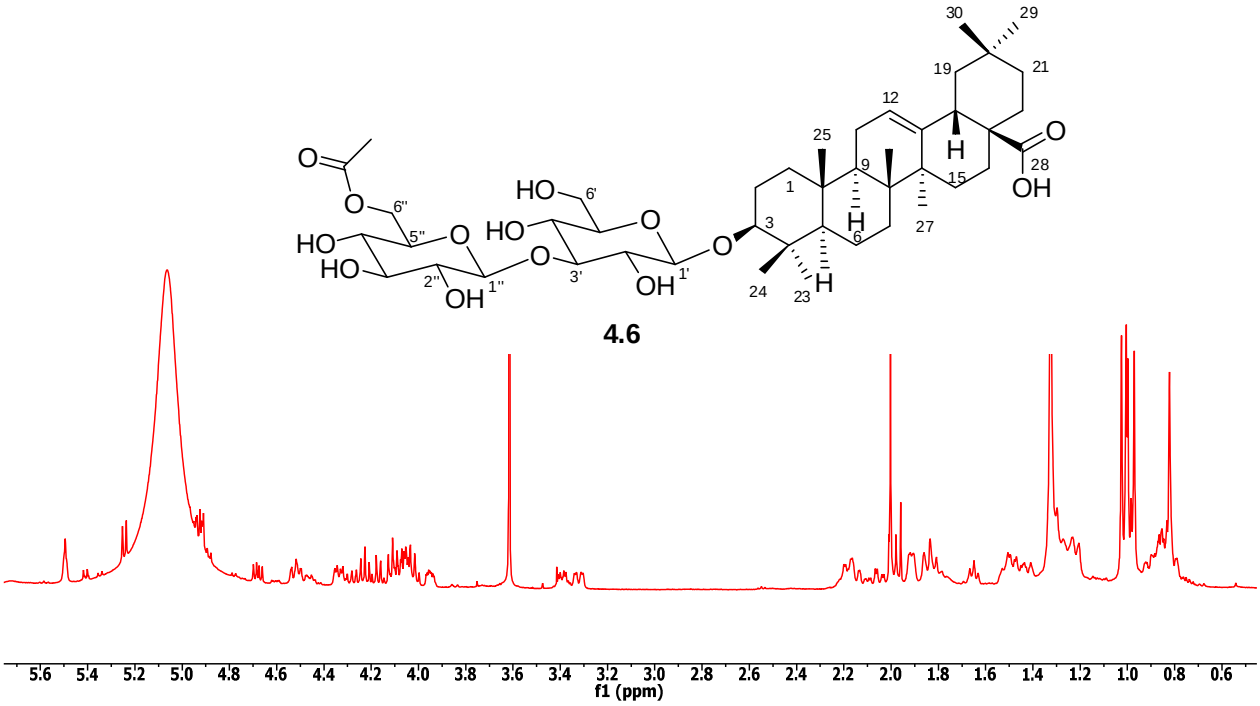

^{13}C NMR spectrum of **4.6** in acetone-d_5 (125 Hz)

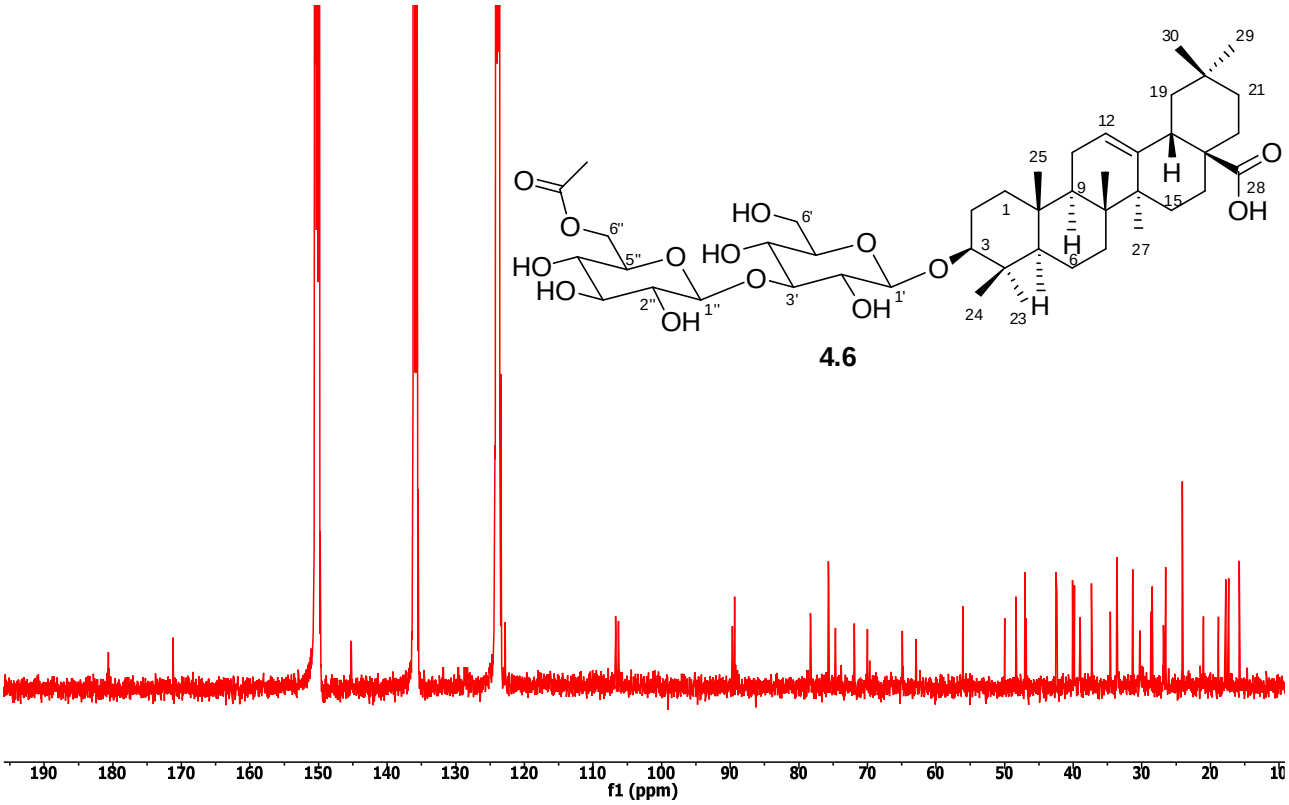

^{1}H NMR spectrum of **5.4** in DMSO-d_6 (600 Hz)

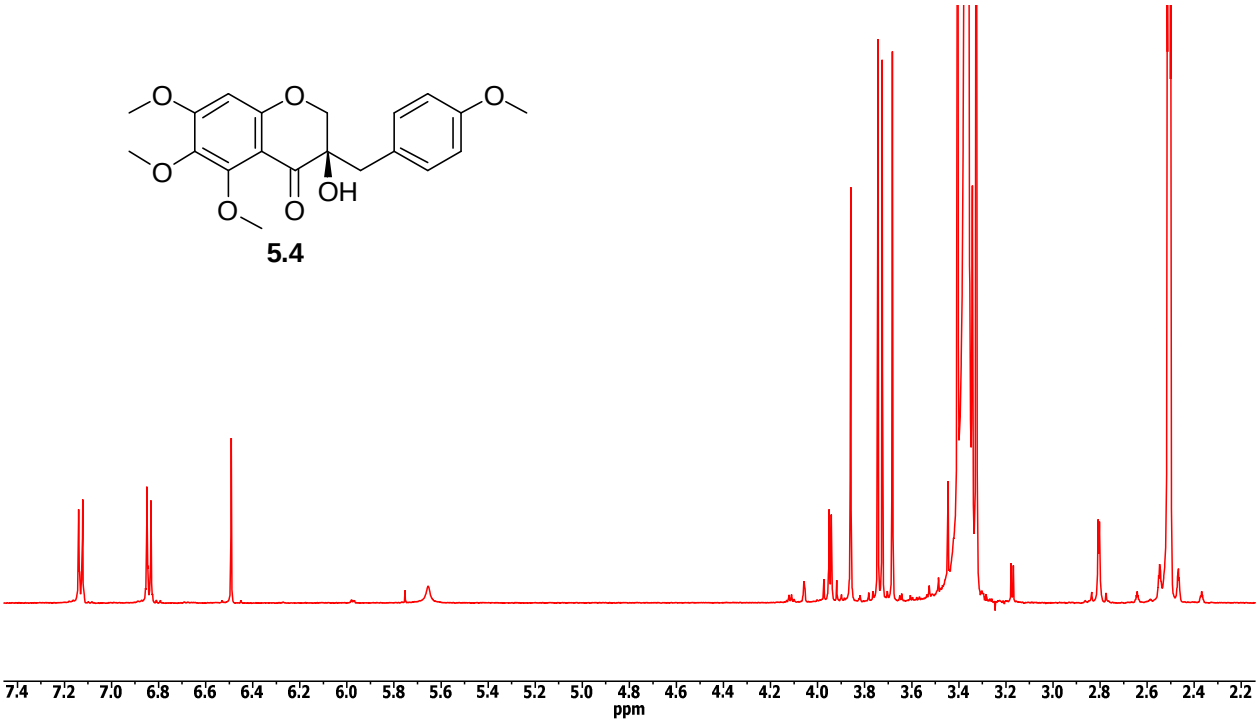

^{13}C NMR spectrum of **5.4** in DMSO-d_6 (150 Hz)

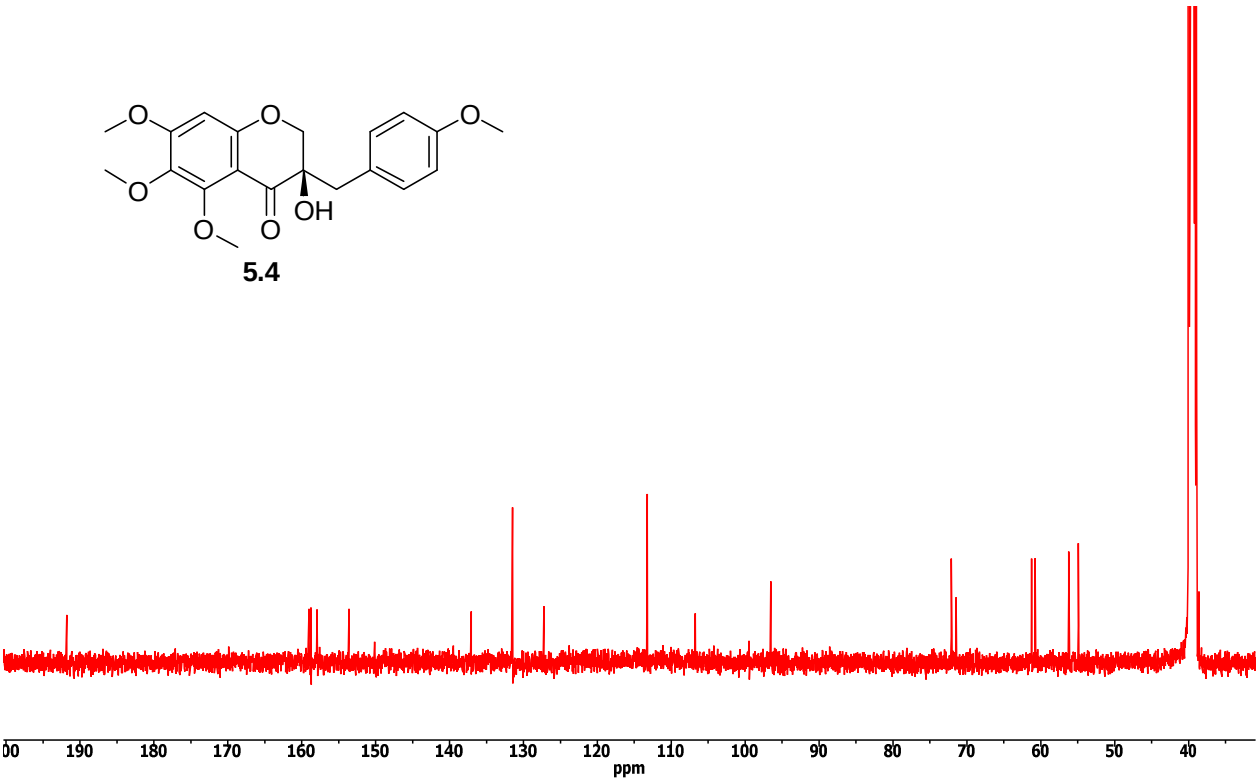

^{1}H NMR spectrum of **5.5** in DMSO-d_6 (600 Hz)

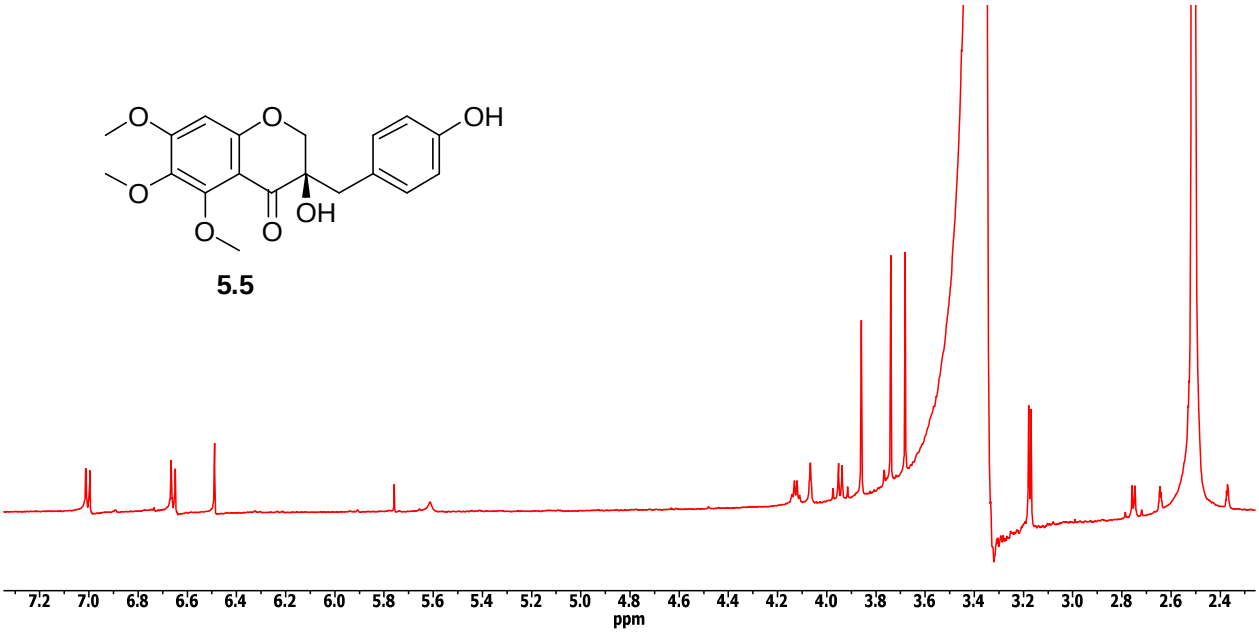

gHMBC spectrum of **5.5** in DMSO-d_6

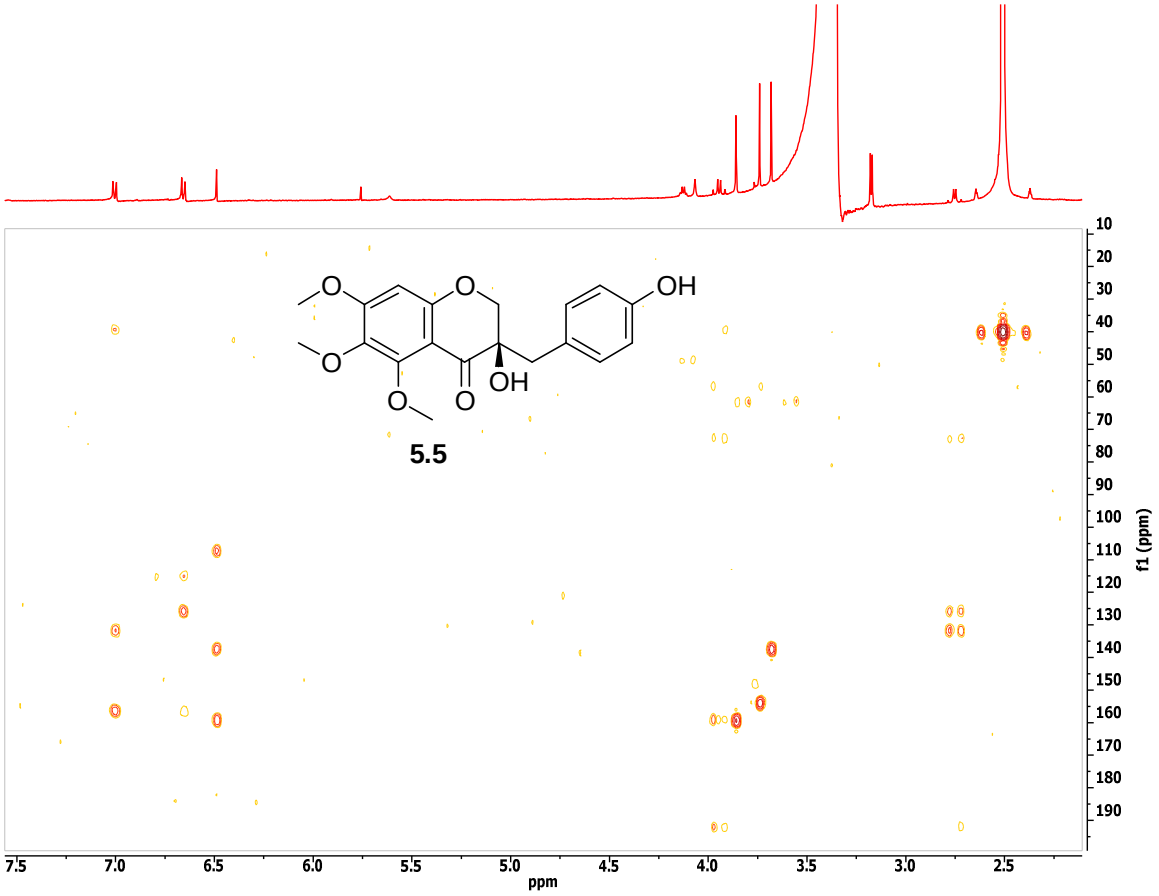

gHMQC spectrum of **5.5** in DMSO-d_6

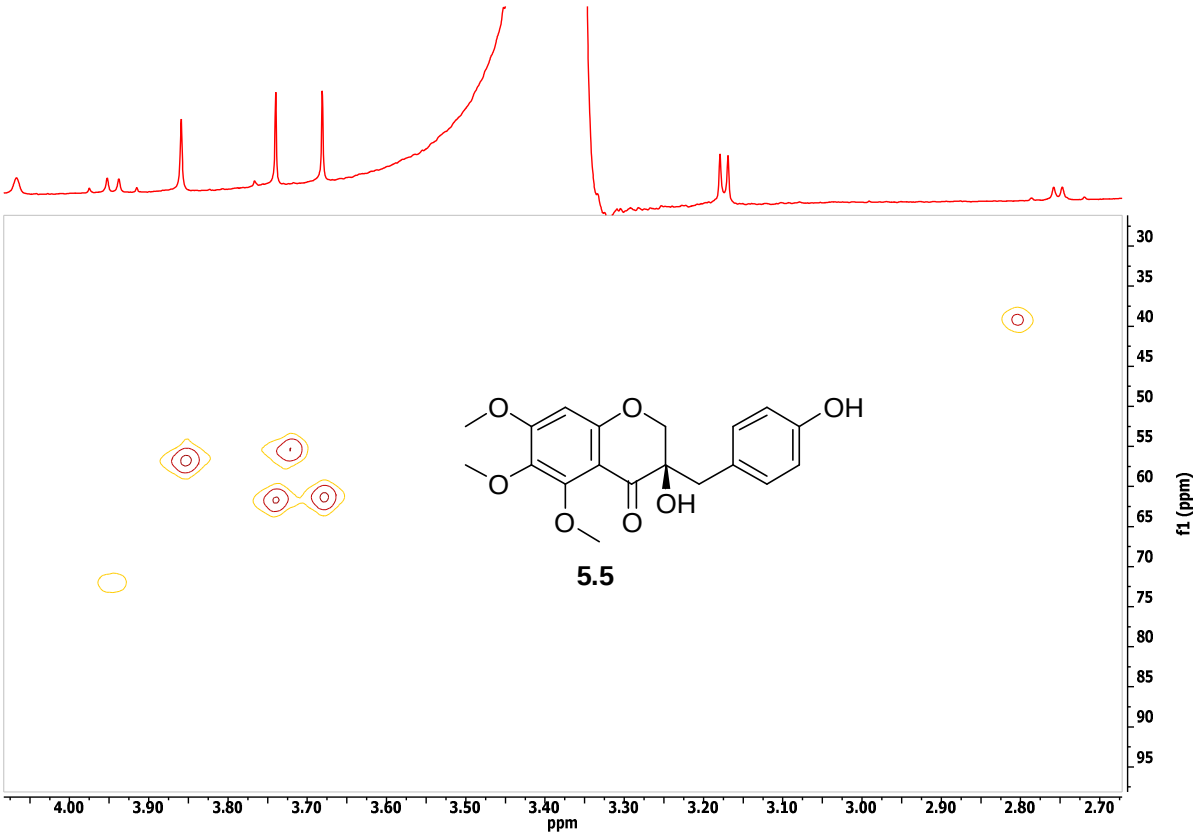

Circular Dichroism Spectrum for compound **5.5**

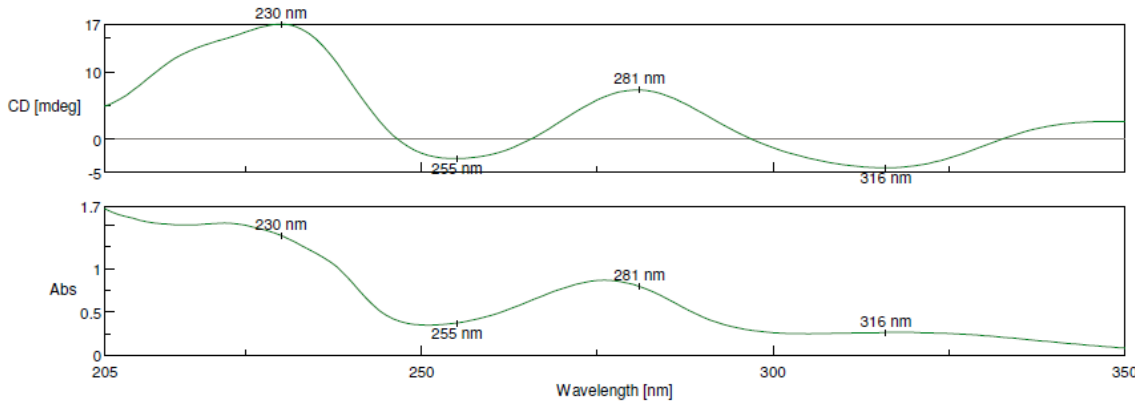

^{1}H NMR spectrum of **5.7** in DMSO-d_6 (600 Hz)

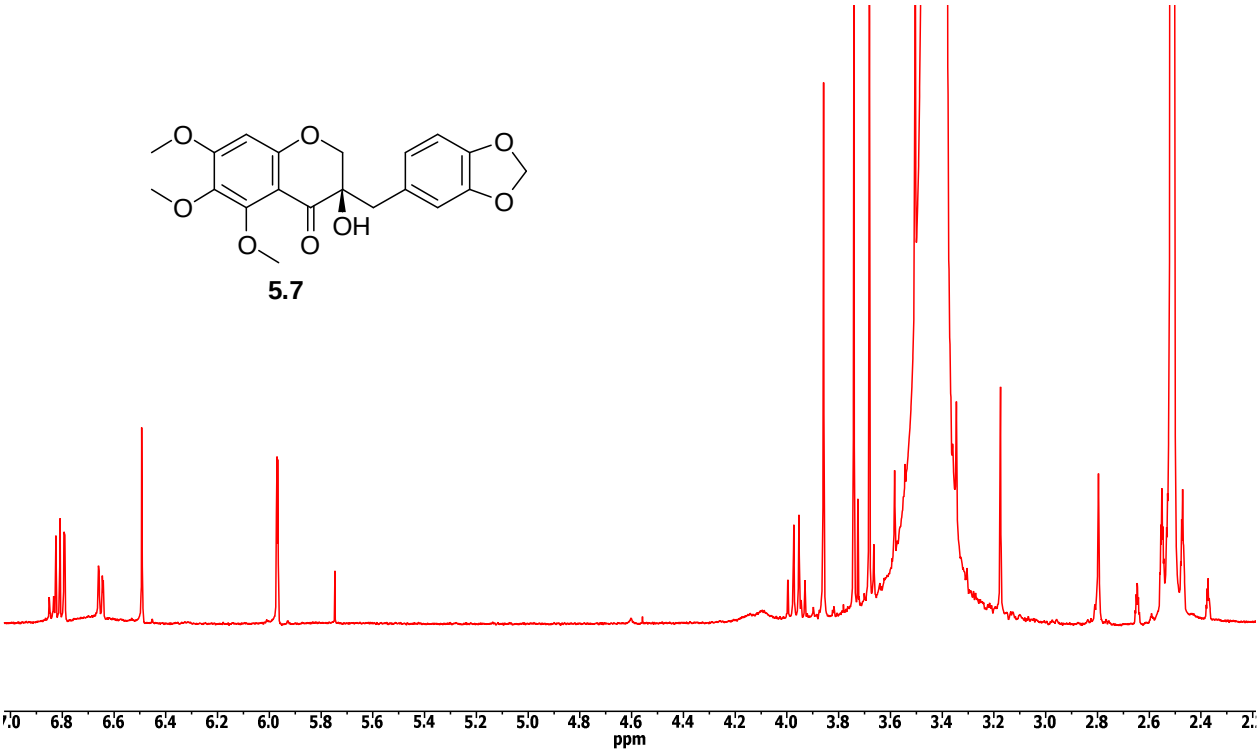

^{13}C NMR spectrum of **5.7** in DMSO-d_6 (150 Hz)

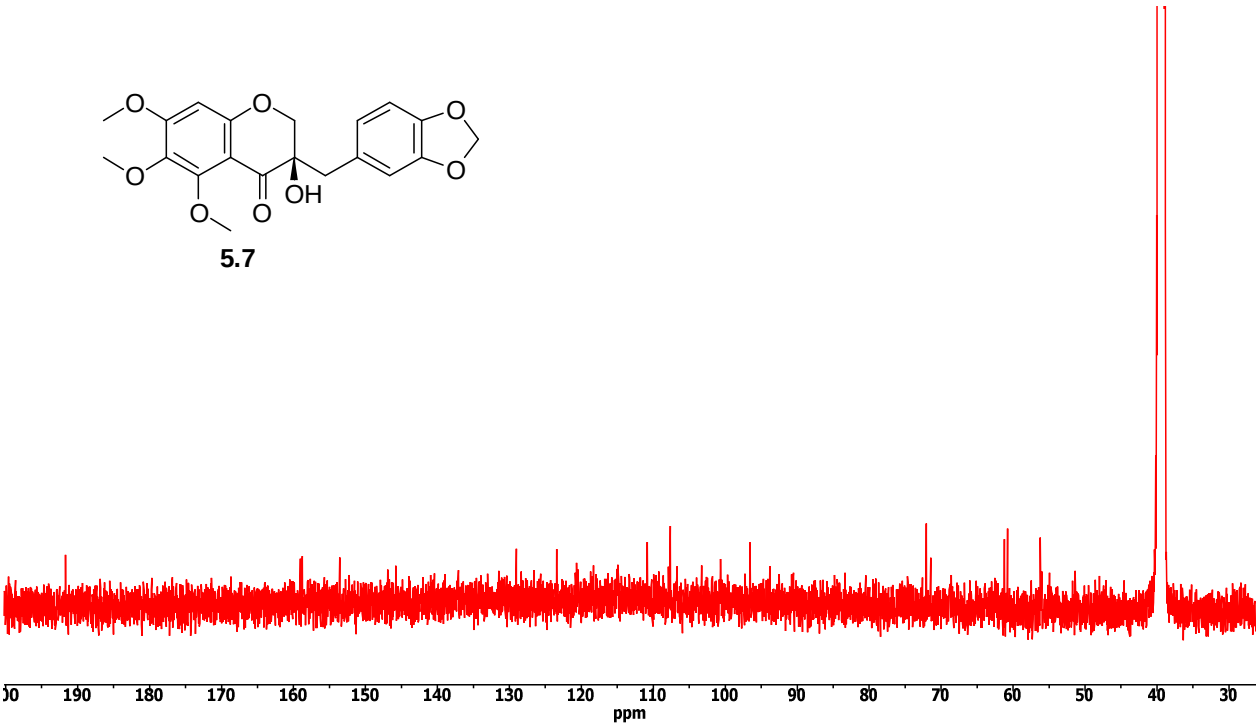

gHMBC spectrum of **5.7** in DMSO-d_6

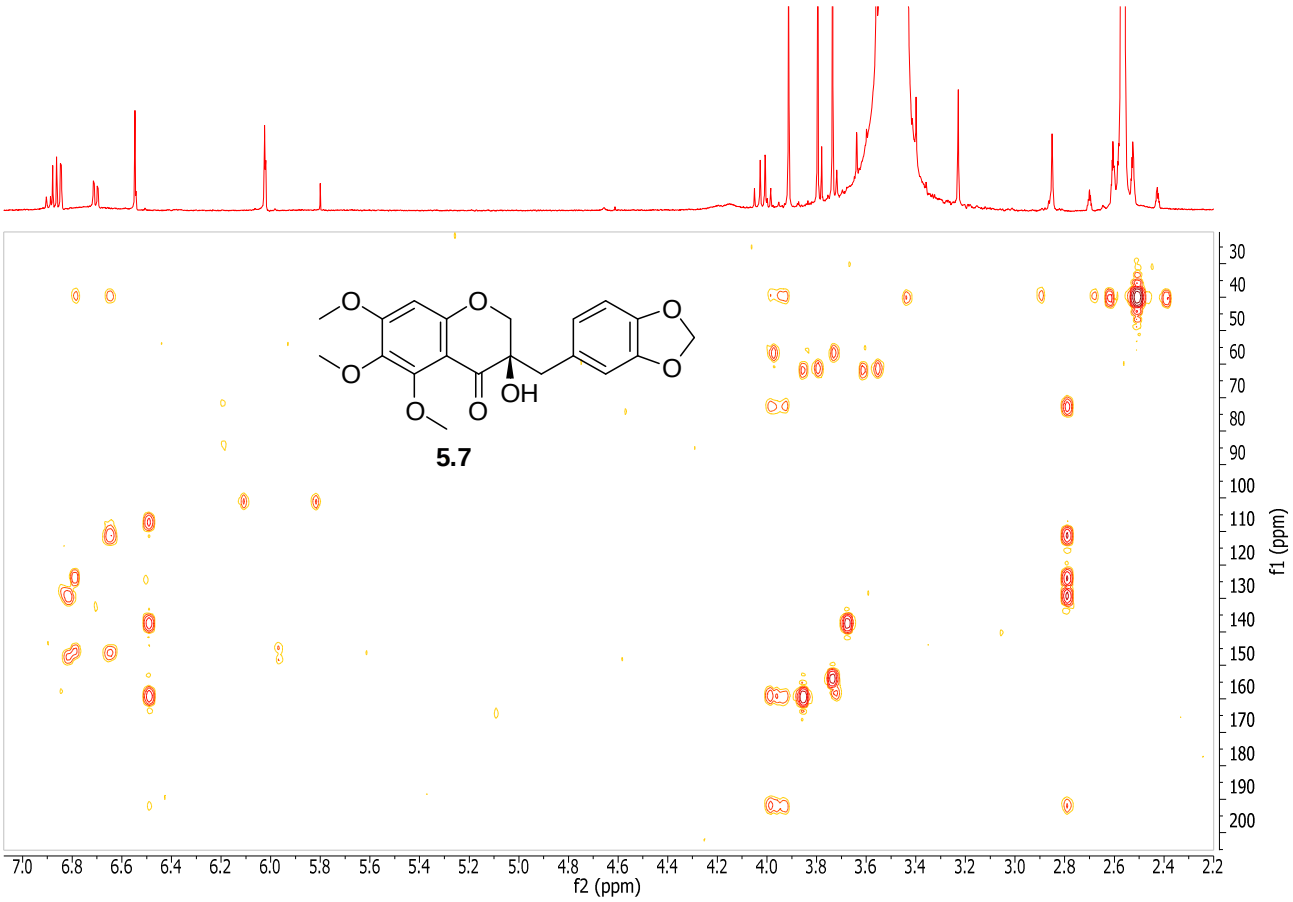

Circular Dichroism Spectrum for compound **5.7**

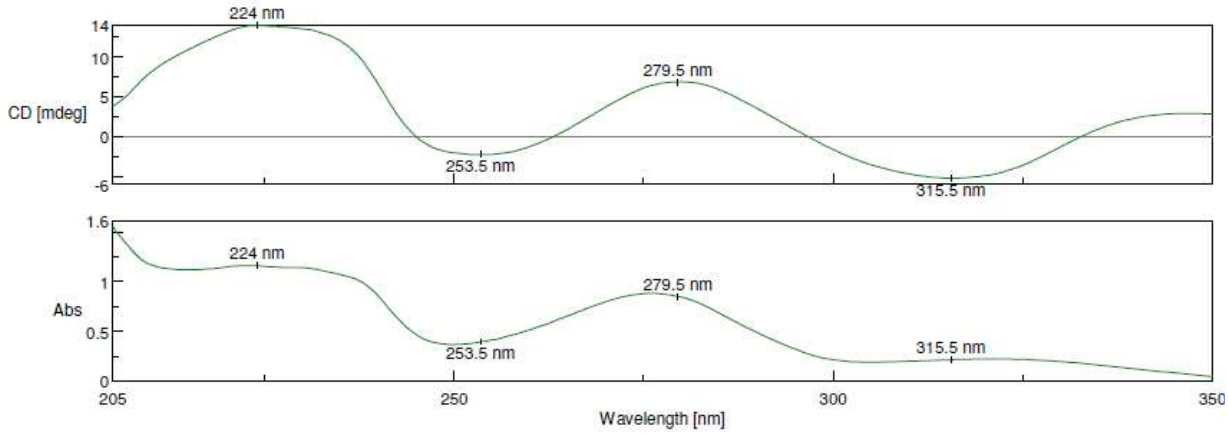

^{1}H NMR spectrum of **5.8** in DMSO-d_6 (600 Hz)

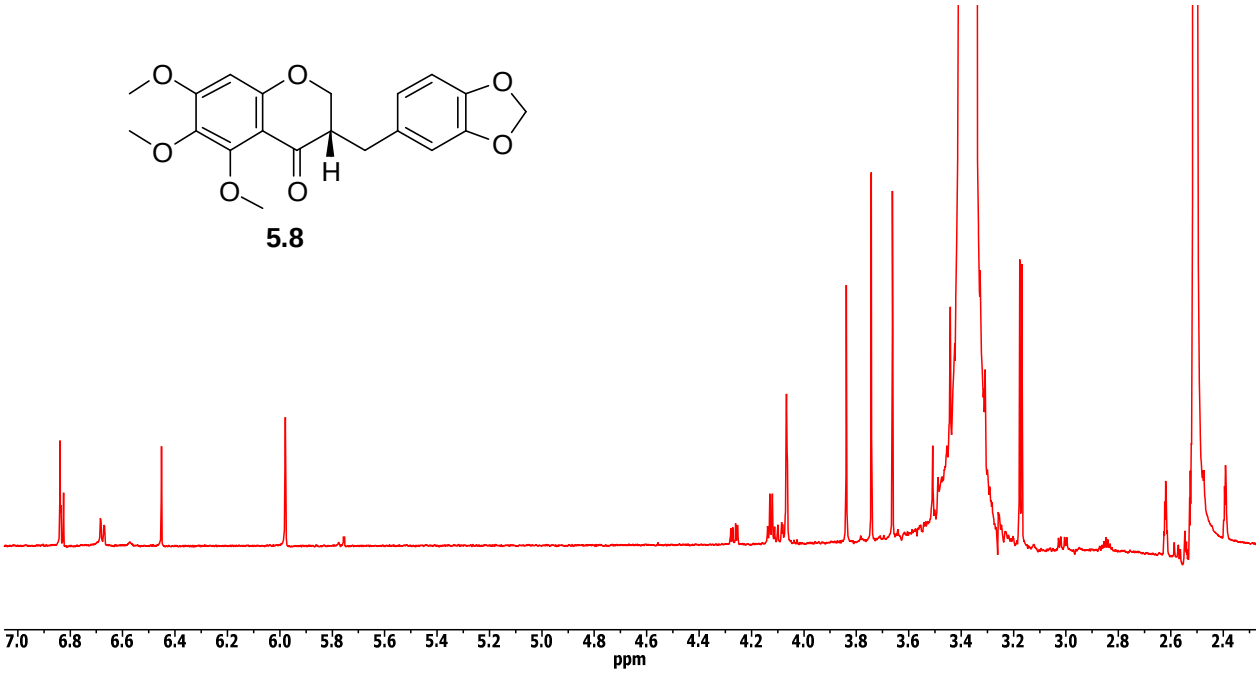

gHMBC spectrum of **5.8** in DMSO-d_6

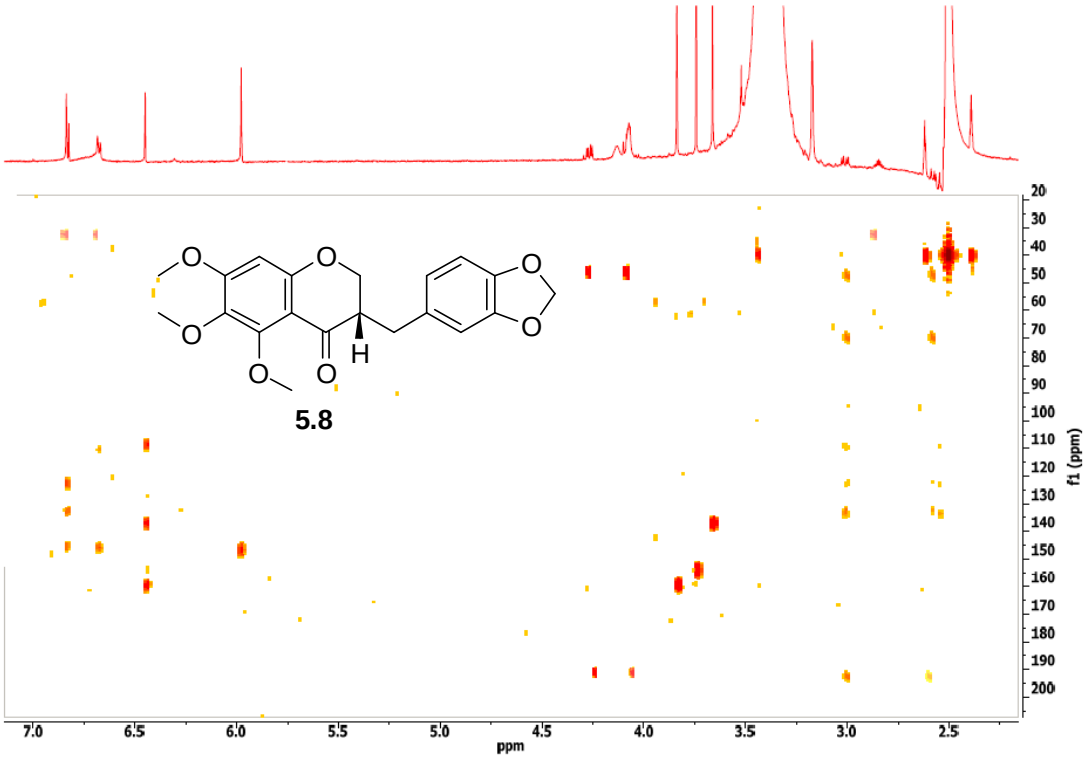

gHSQC spectrum of **5.8** in DMSO-d_6

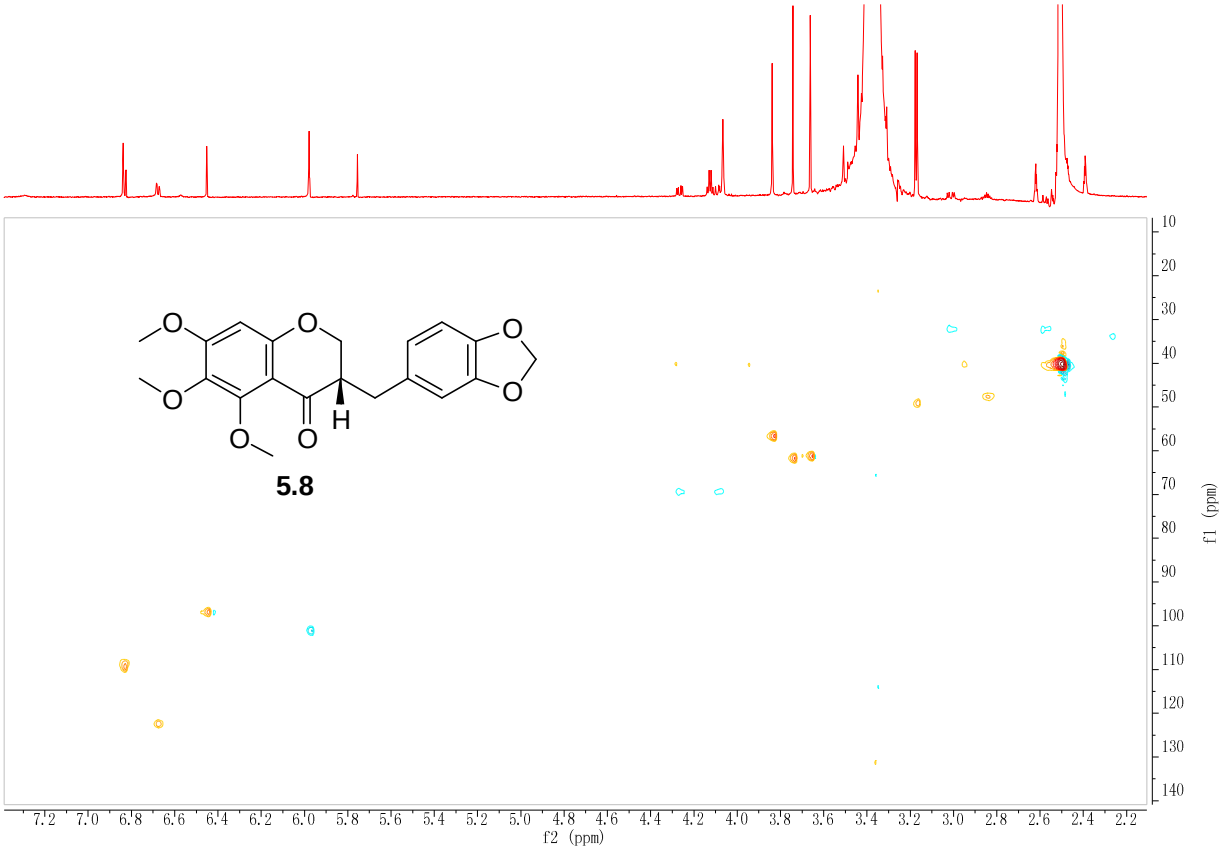

Circular Dichroism Spectrum for compound **5.8**

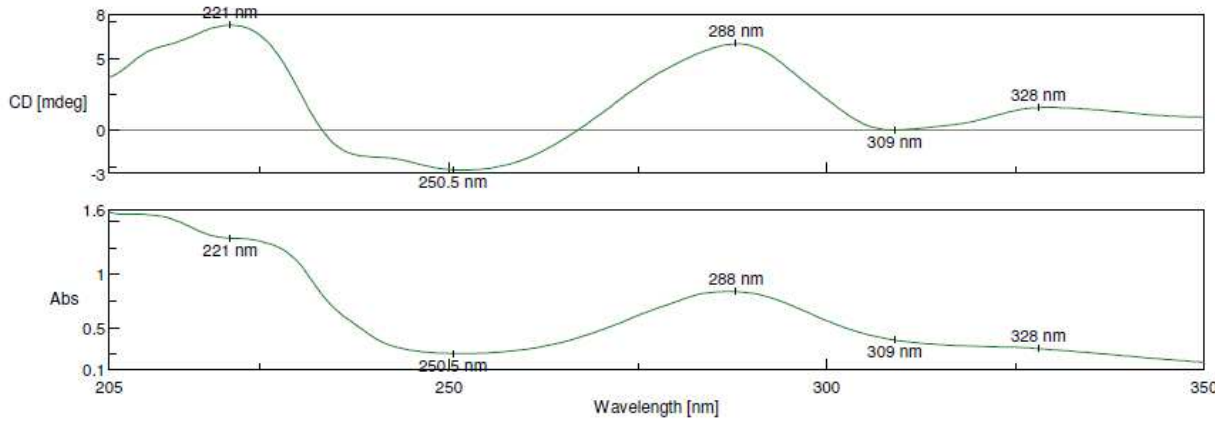

^{1}H NMR spectrum of **5.10** in CD_3OD (600 Hz)

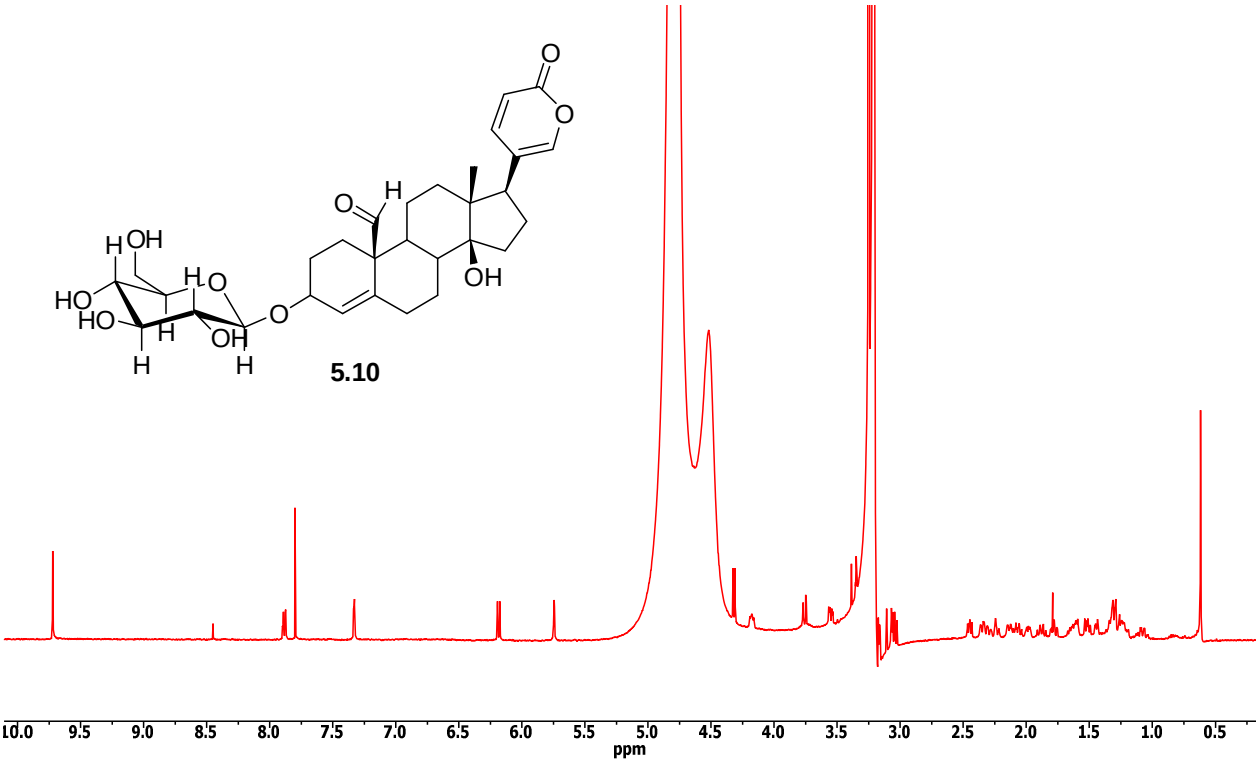

gHMBC spectrum of **5.10** in CD_3OD

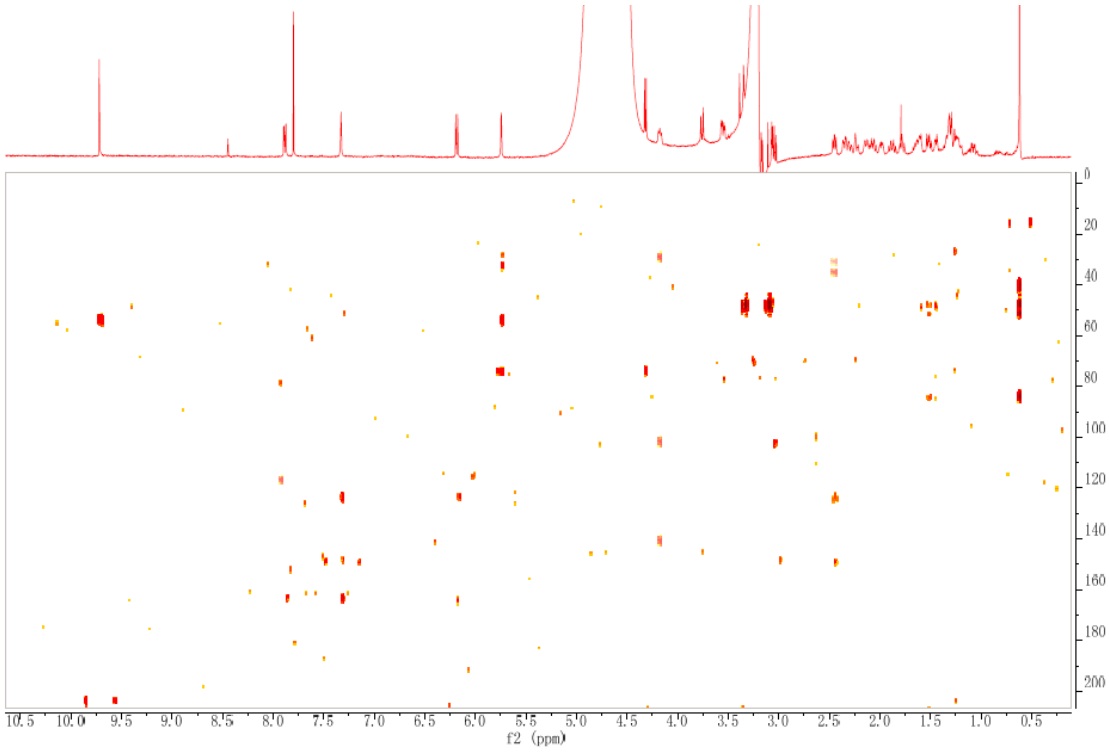

gHSQC spectrum of **5.10** in CD_3OD

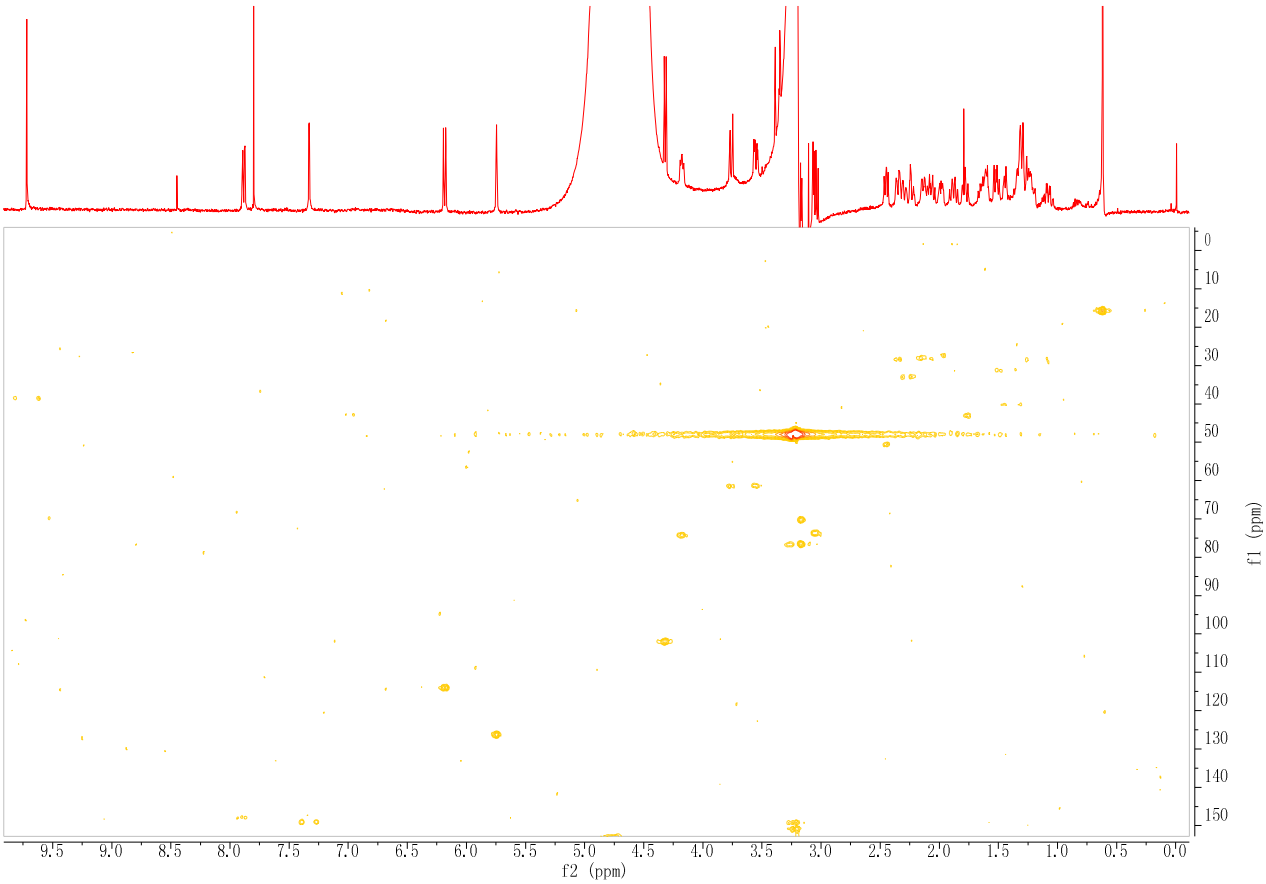

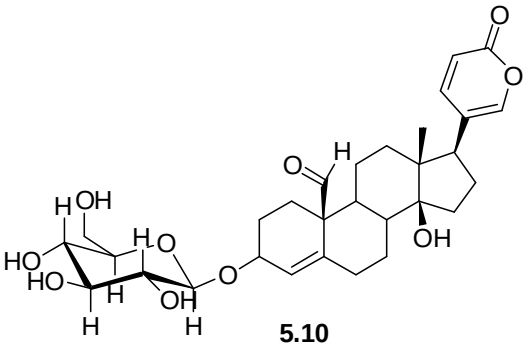

^{1}H NMR spectrum of **5.11** in CD_3OD (600 Hz)

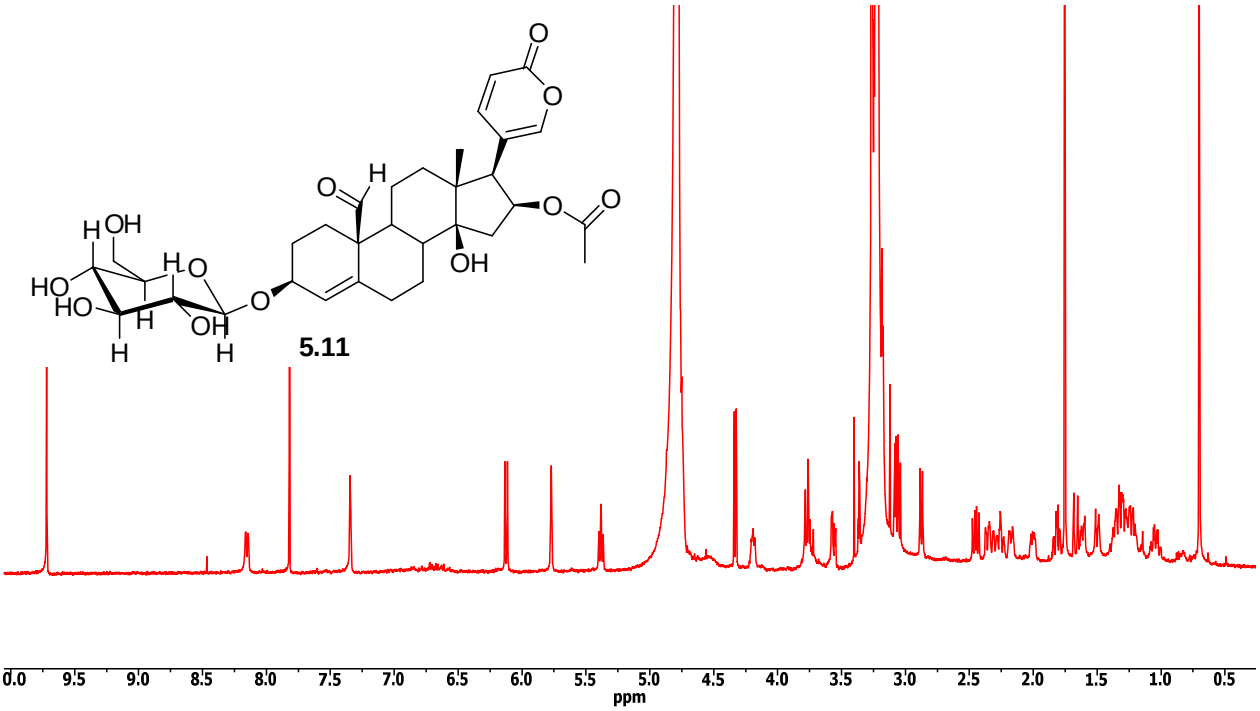

^{13}C NMR spectrum of **5.11** in CD_3OD (150 Hz)

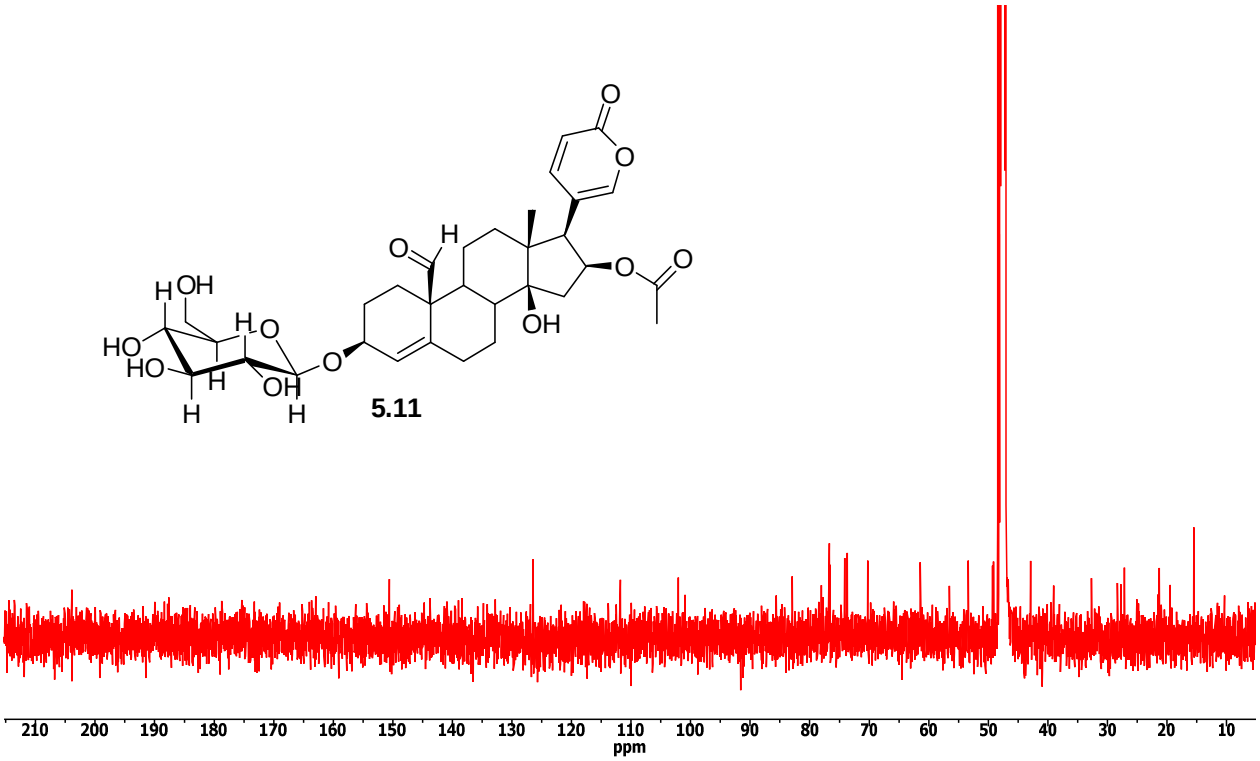

gHMBC spectrum of **5.11** in CD_3OD

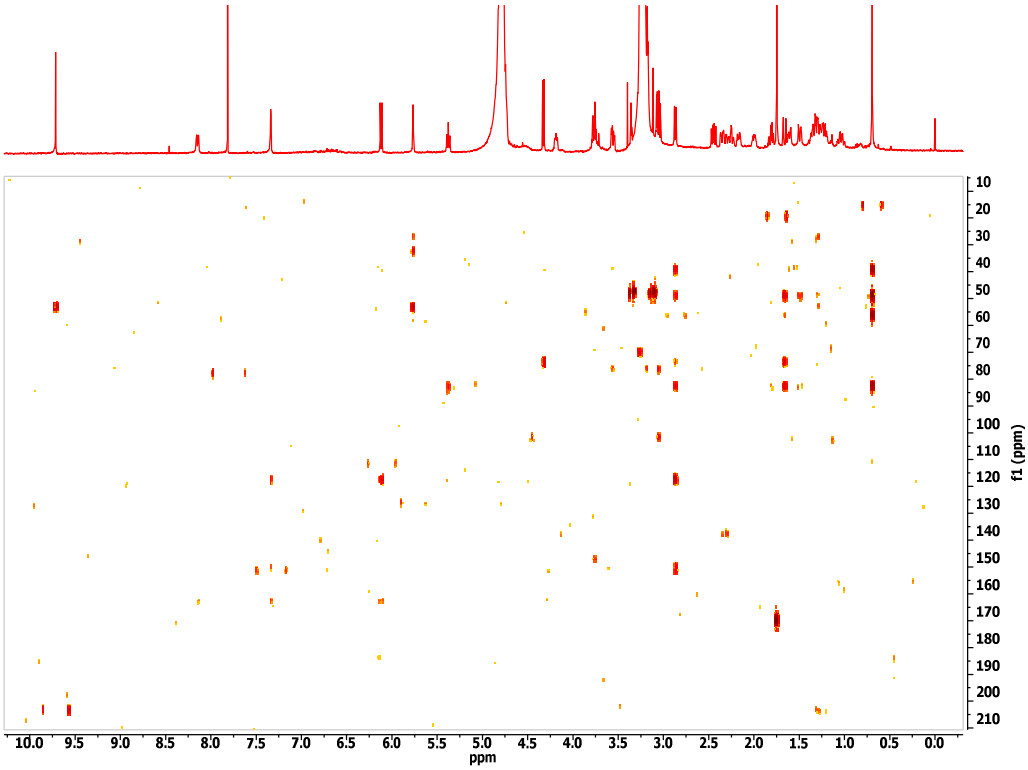

gHSQC spectrum of **5.11** in CD_3OD

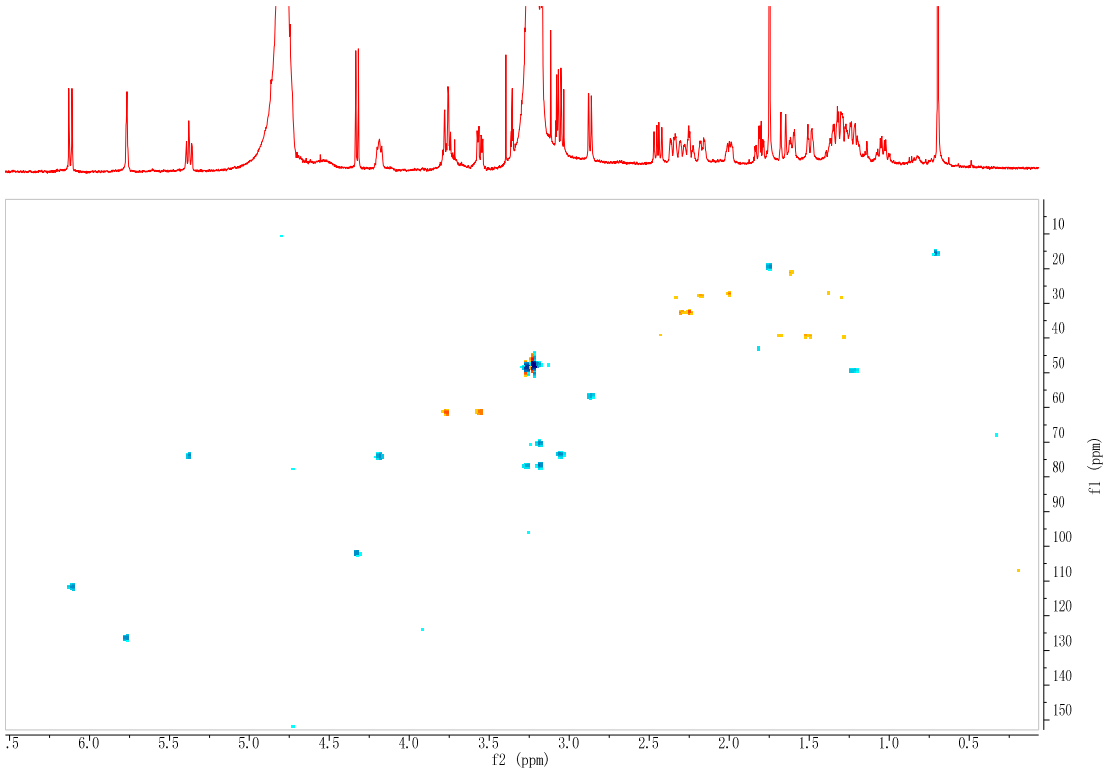

^{1}H NMR spectrum of **5.13** in CD_3OD (600 Hz)

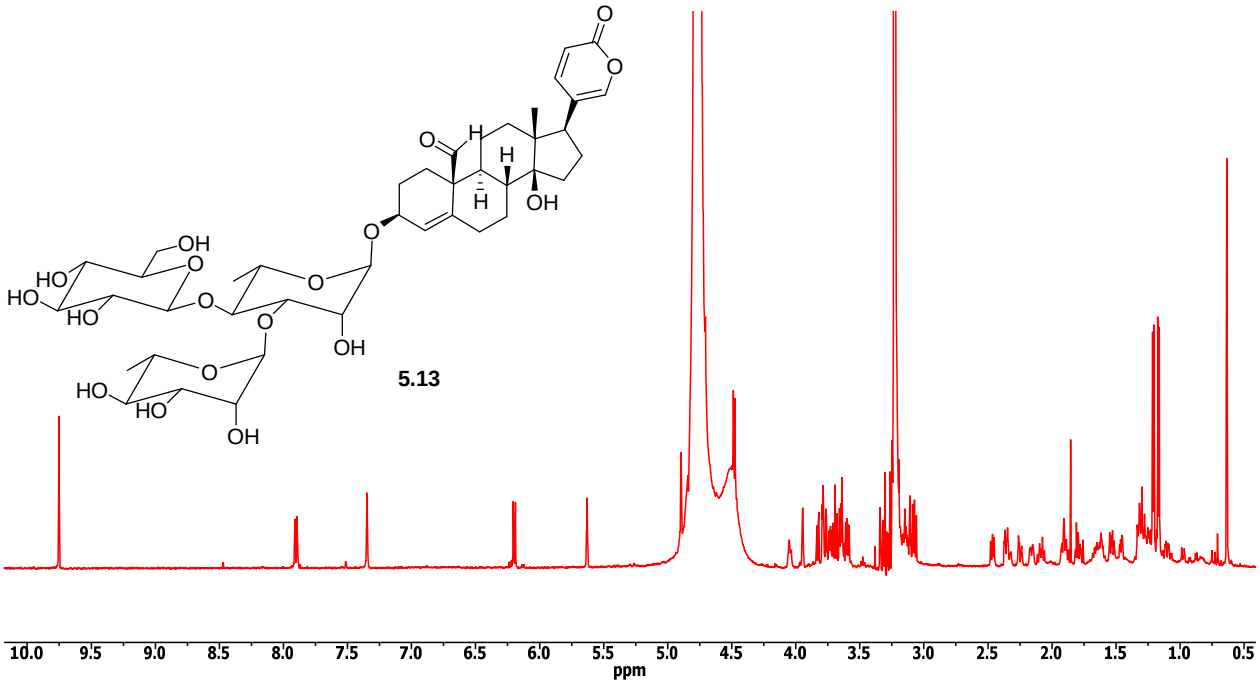

^{13}C NMR spectrum of **5.13** in CD_3OD (150 Hz)

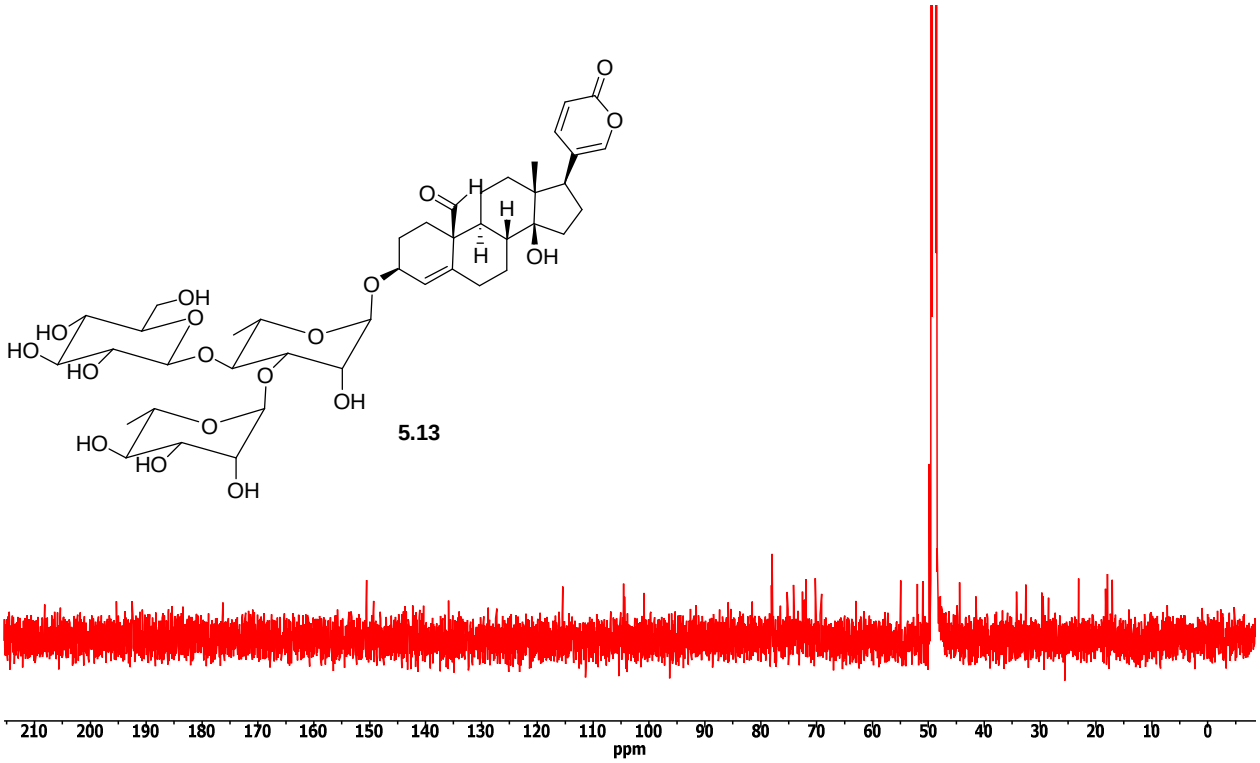

gHMBC spectrum of **5.13** in CD_3OD

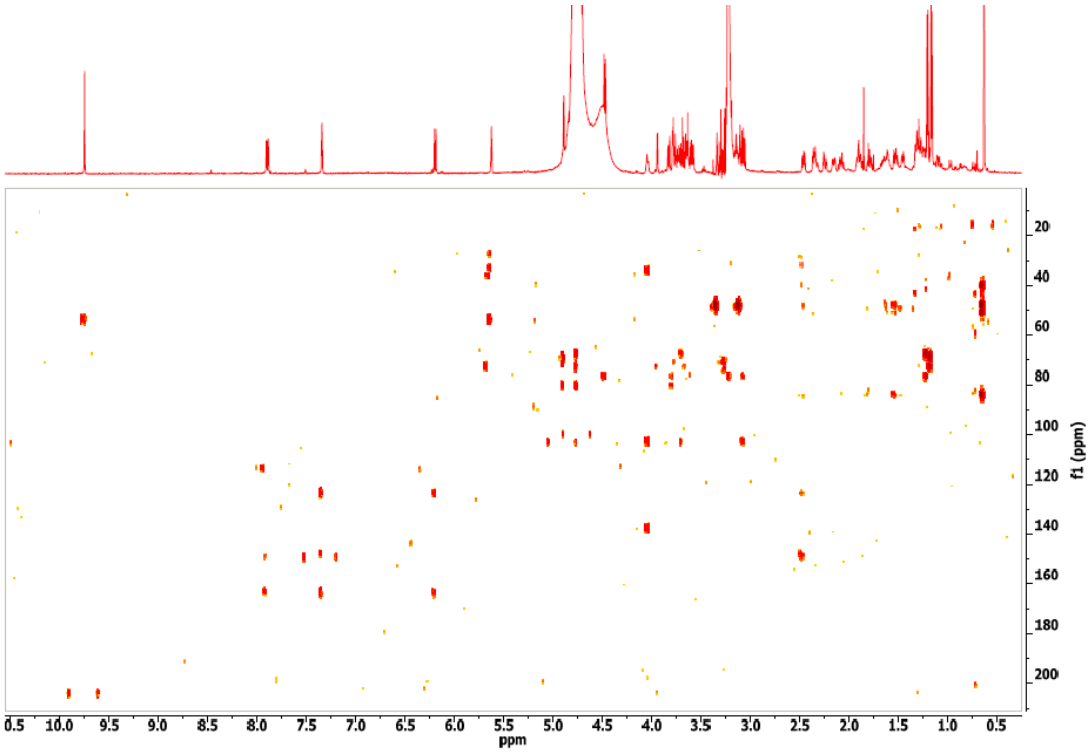

gHSQC spectrum of **5.13** in CD_3OD

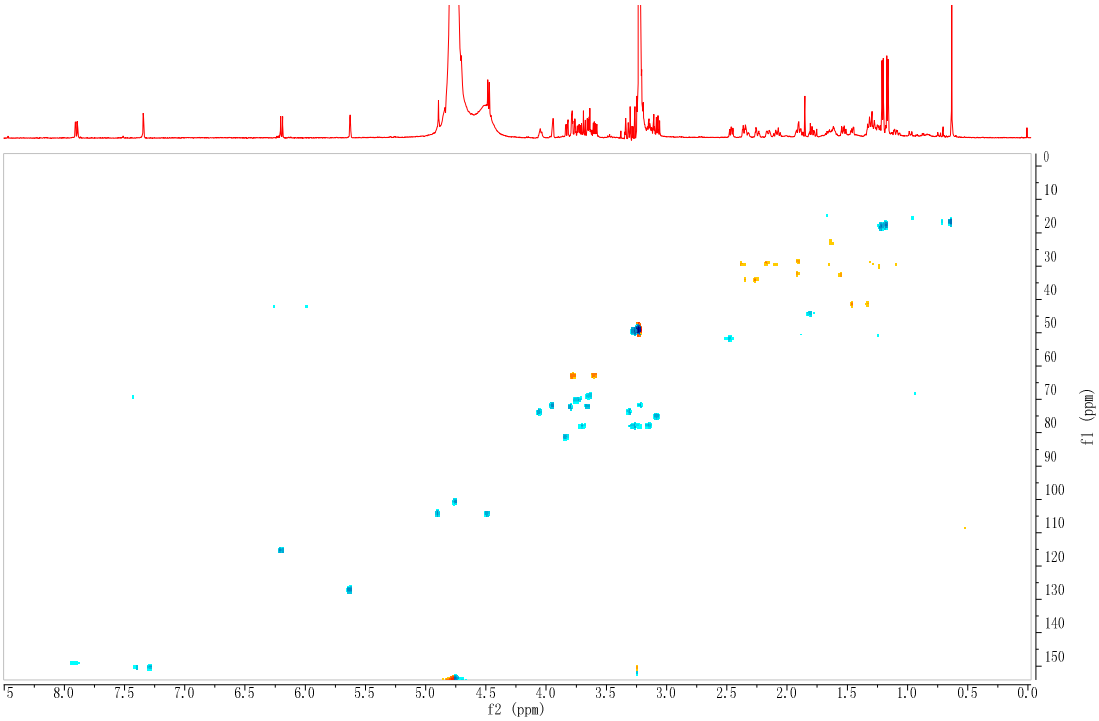

^{1}H NMR spectrum of **6.6** in $CDCl_3$ (600 Hz)

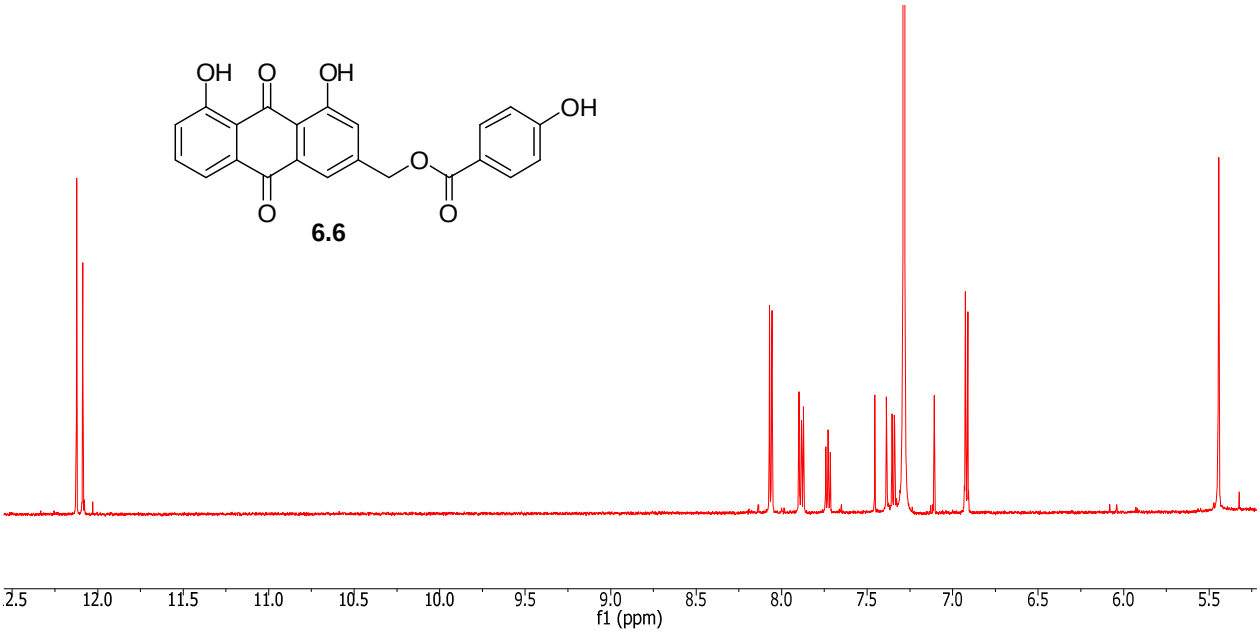

^{13}C NMR spectrum of **6.6** in $CDCl_3$ (150 Hz)

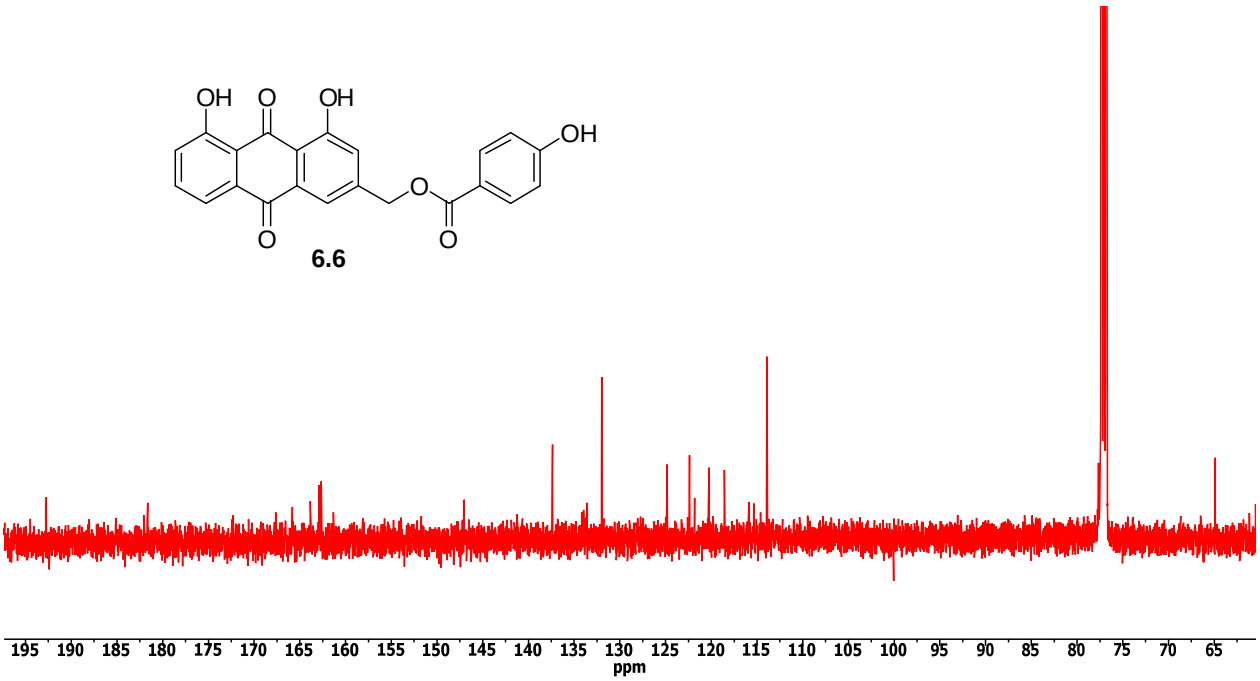

gHSQC spectrum of **6.6** in $CDCl_3$

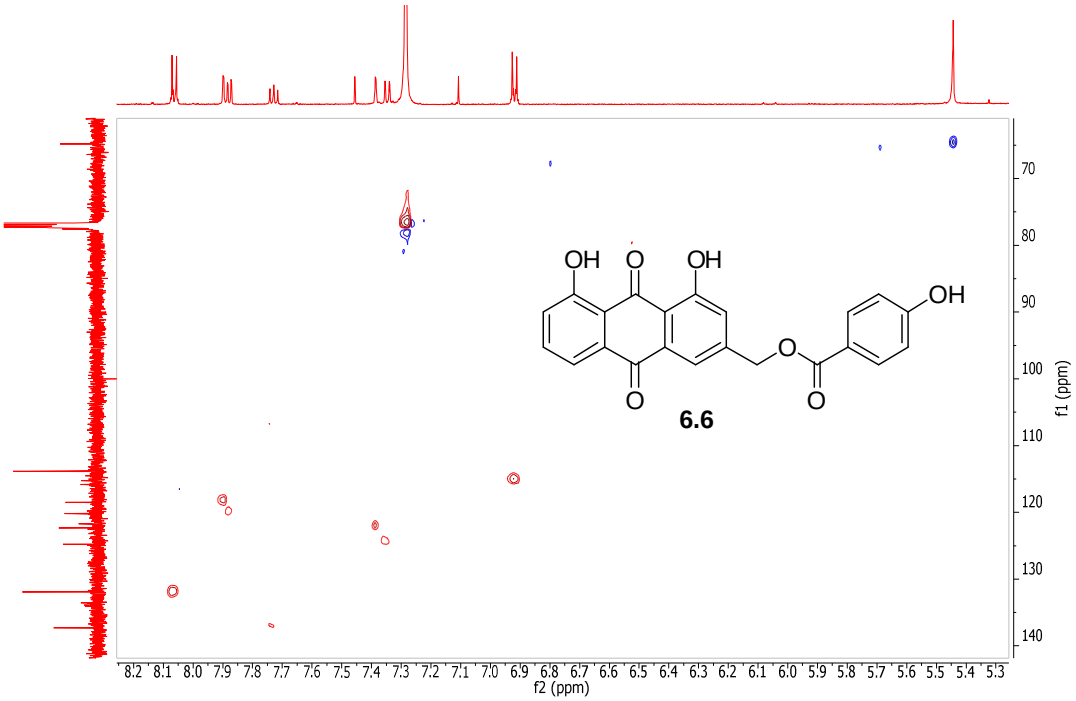

gHMBC spectrum of **6.6** in $CDCl_3$

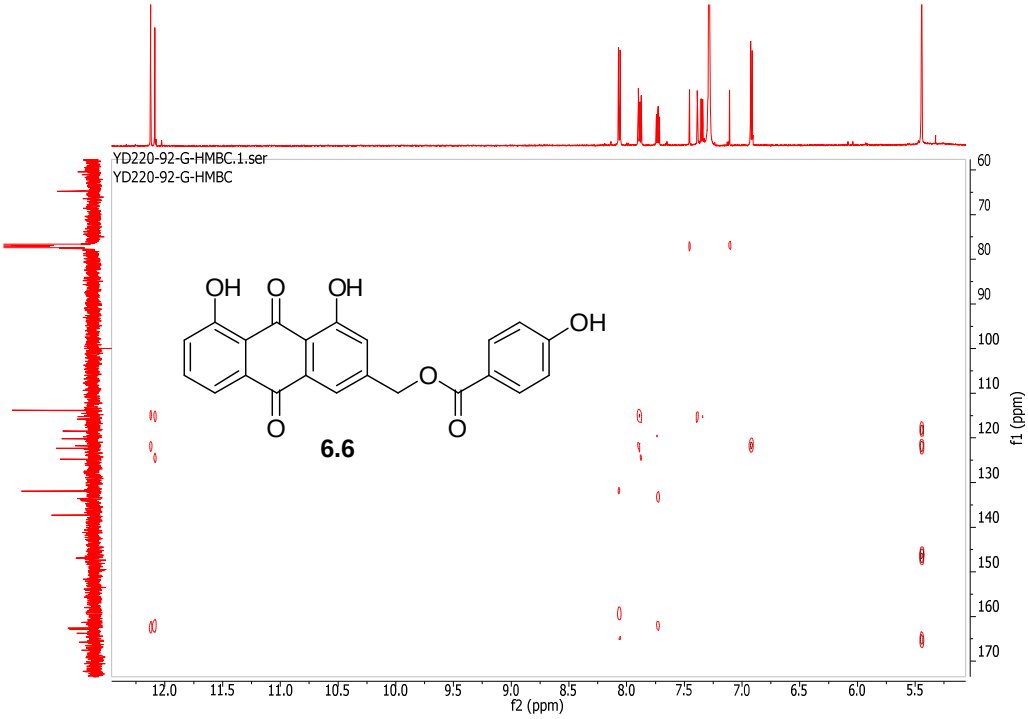

^{1}H NMR spectrum of **6.7** in $CDCl_3$ (600 Hz)

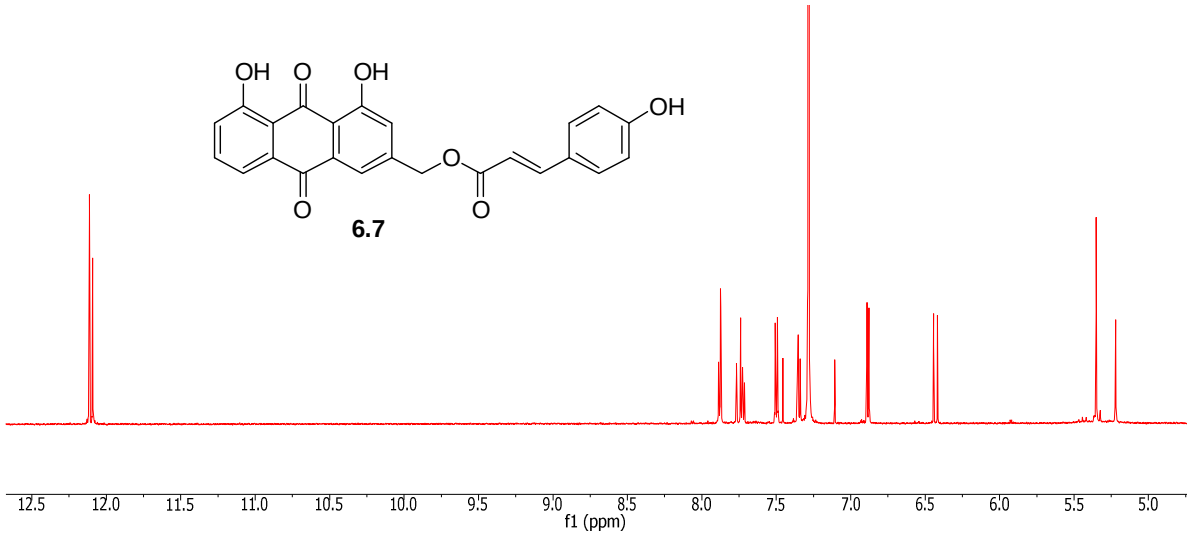

^{13}C NMR spectrum of **6.7** in $CDCl_3$ (150 Hz)

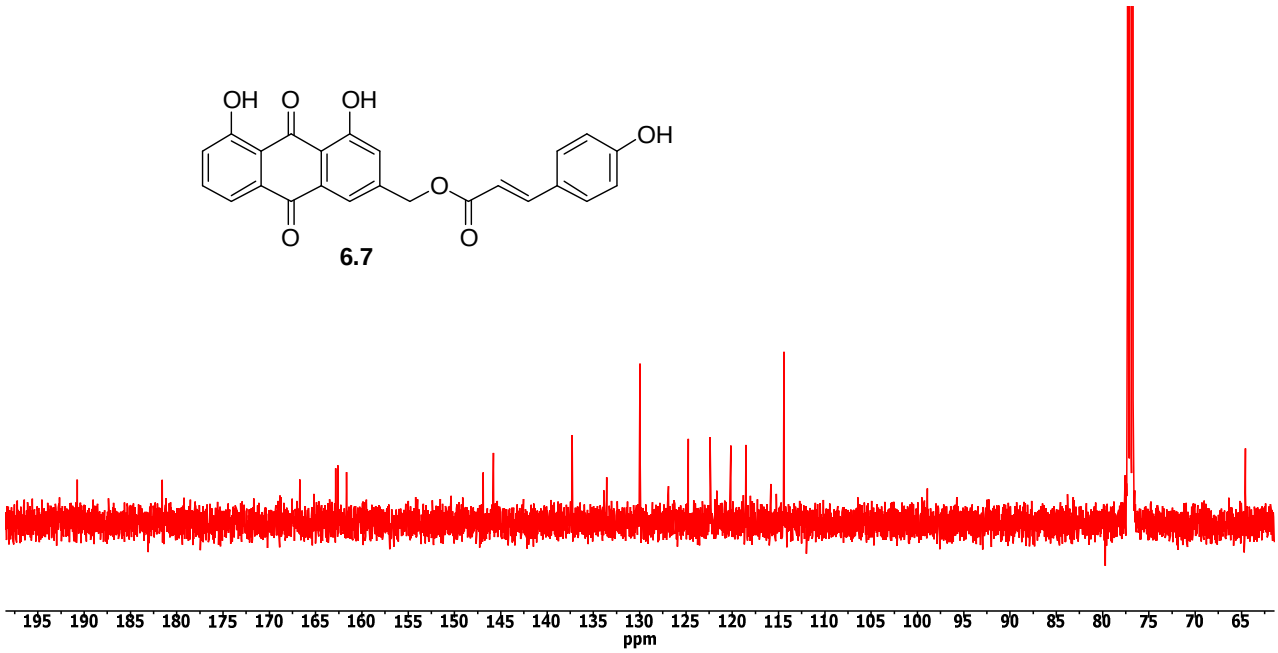

gHSQC spectrum of **6.7** in $CDCl_3$

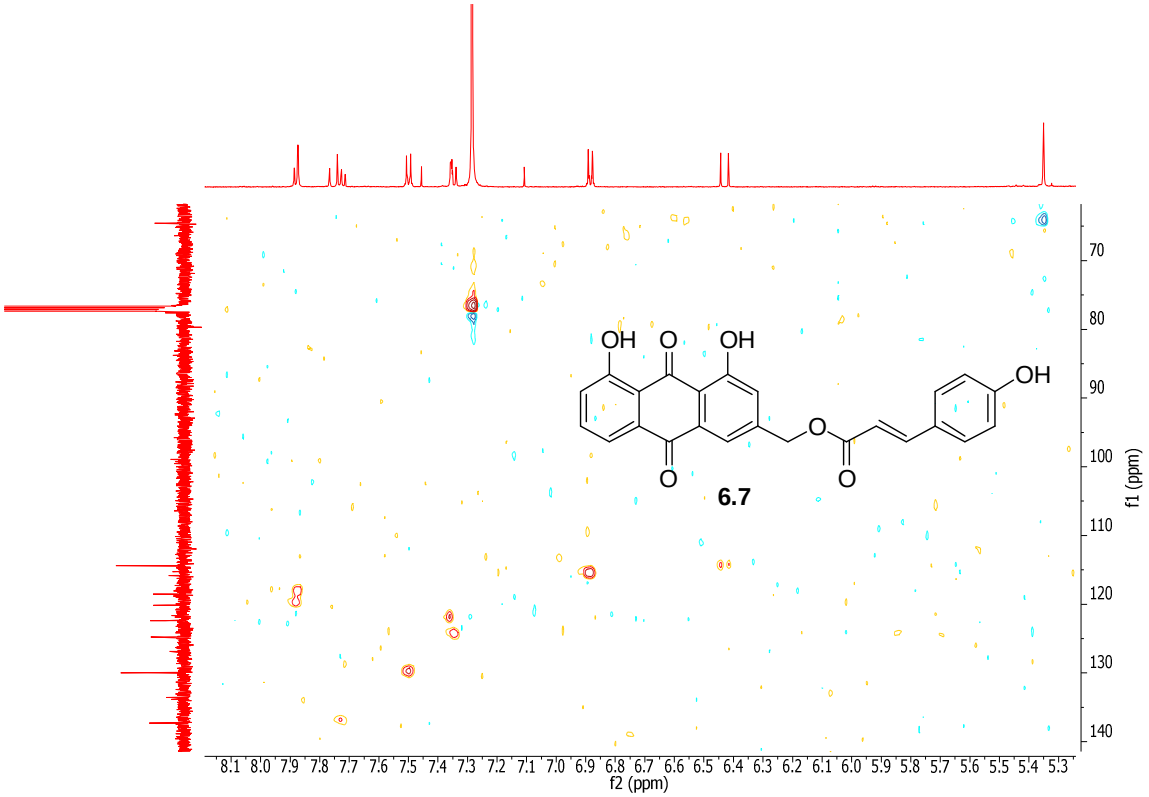

gHMBC spectrum of **6.7** in $CDCl_3$

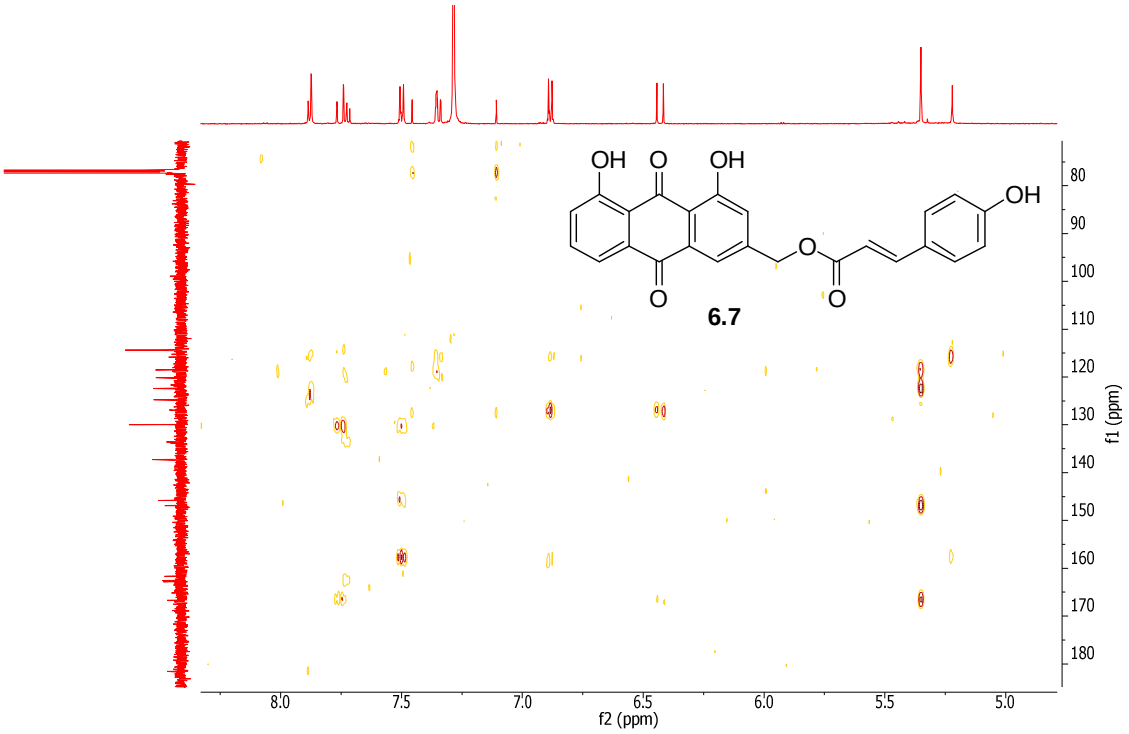

^{1}H NMR spectrum of **6.13** in $CDCl_3$ (500 Hz)

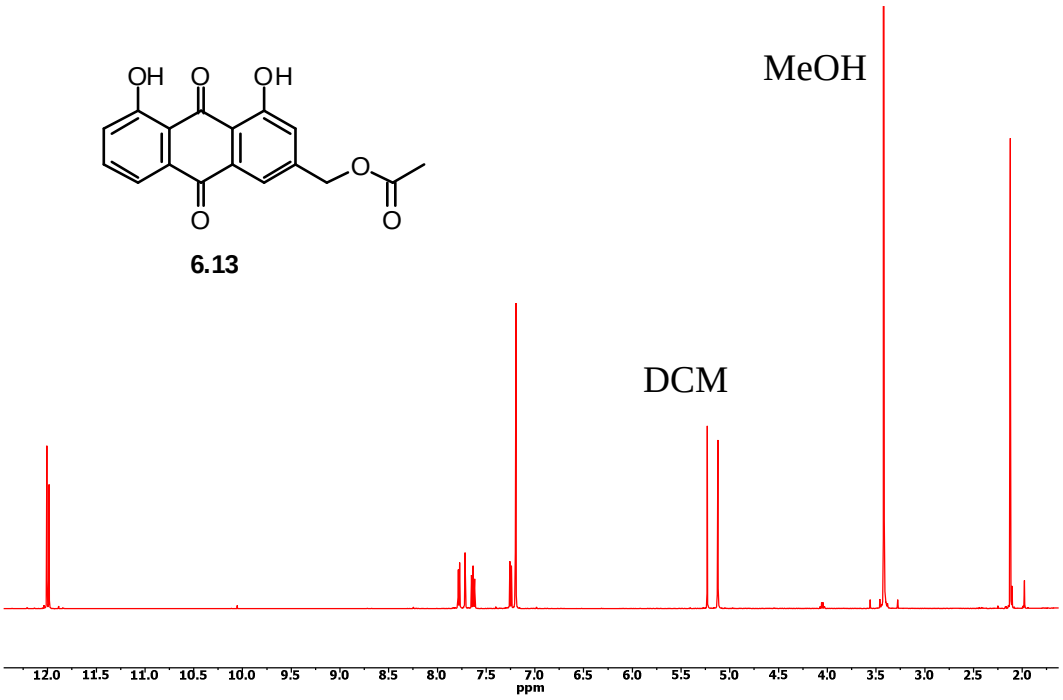

^{13}C NMR spectrum of **6.13** in $CDCl_3$ (125 Hz)

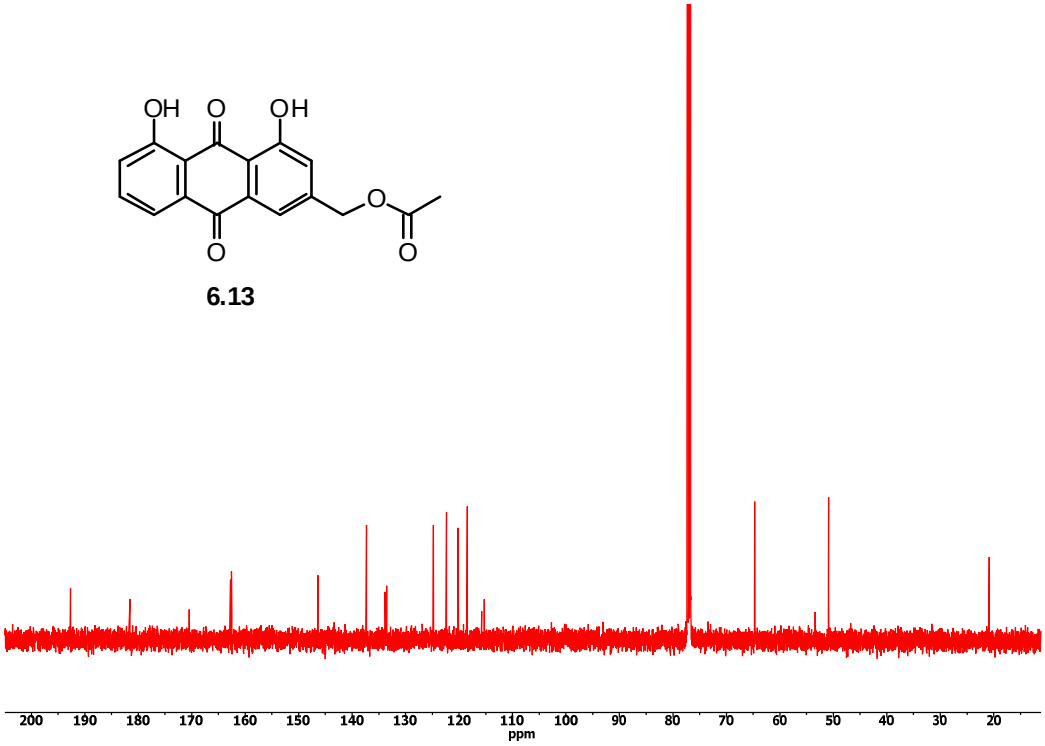

^{1}H NMR spectrum of **6.14** in $CDCl_3$ (500 Hz)

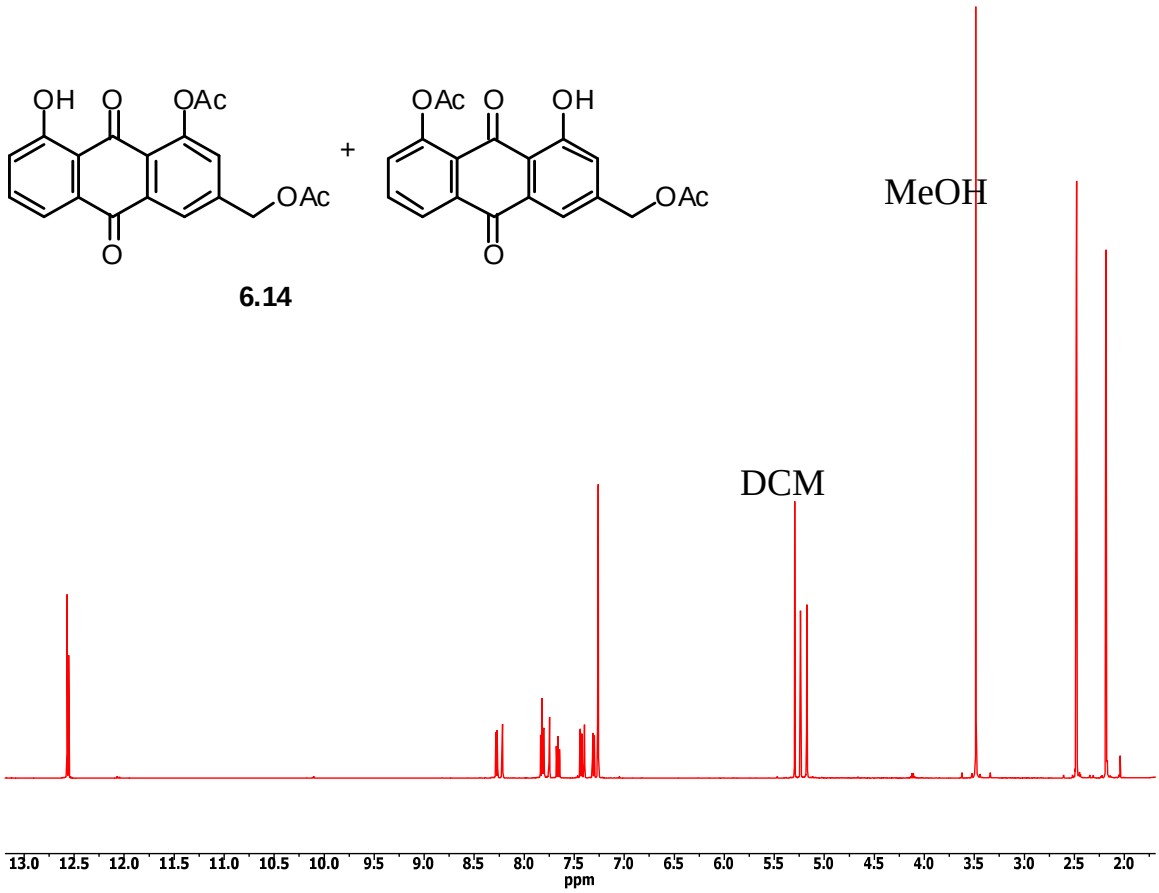

^{1}H NMR spectrum of **6.15** in $CDCl_3$ (500 Hz)

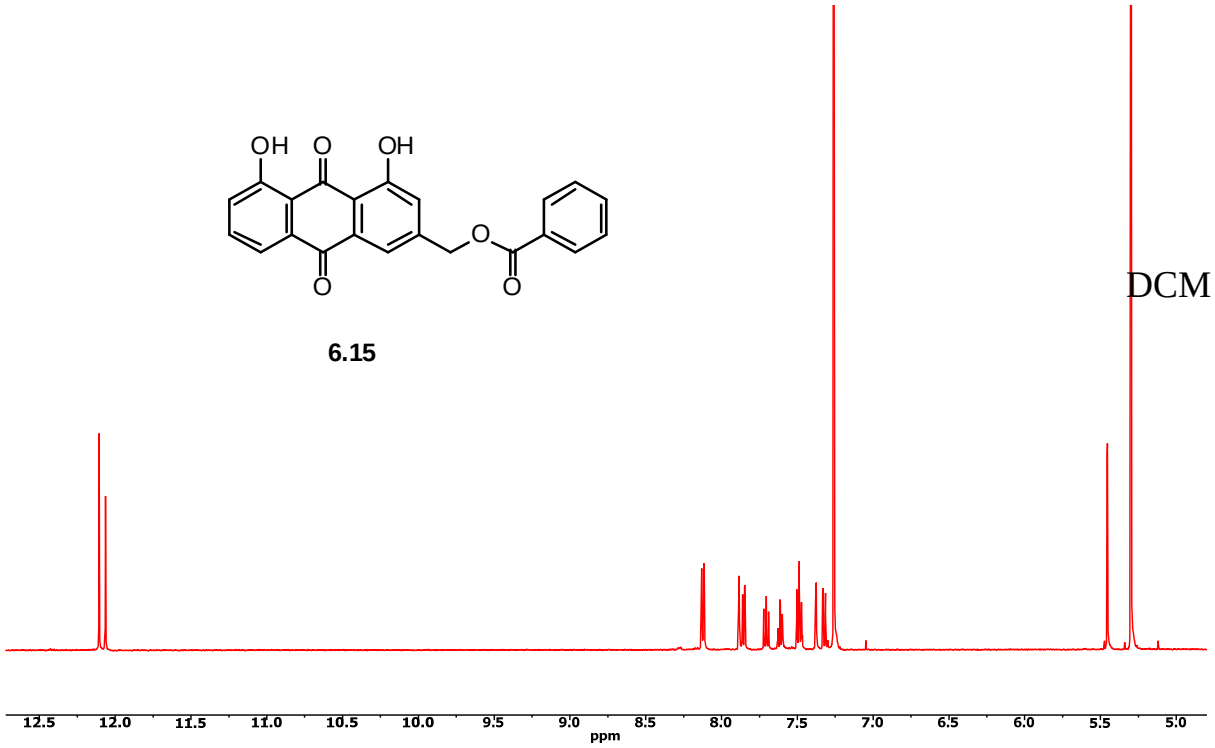

^{13}C NMR spectrum of **6.15** in $CDCl_3$ (125 Hz)

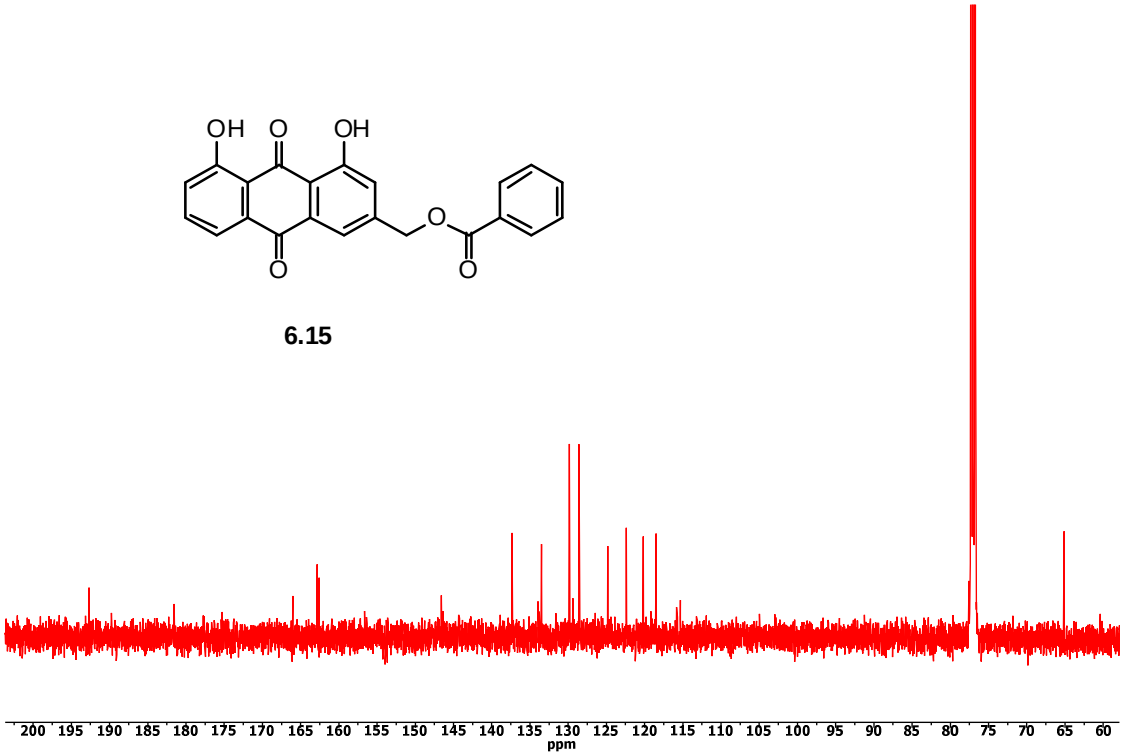

^{1}H NMR spectrum of **6.16** in $CDCl_3$ (500 Hz)

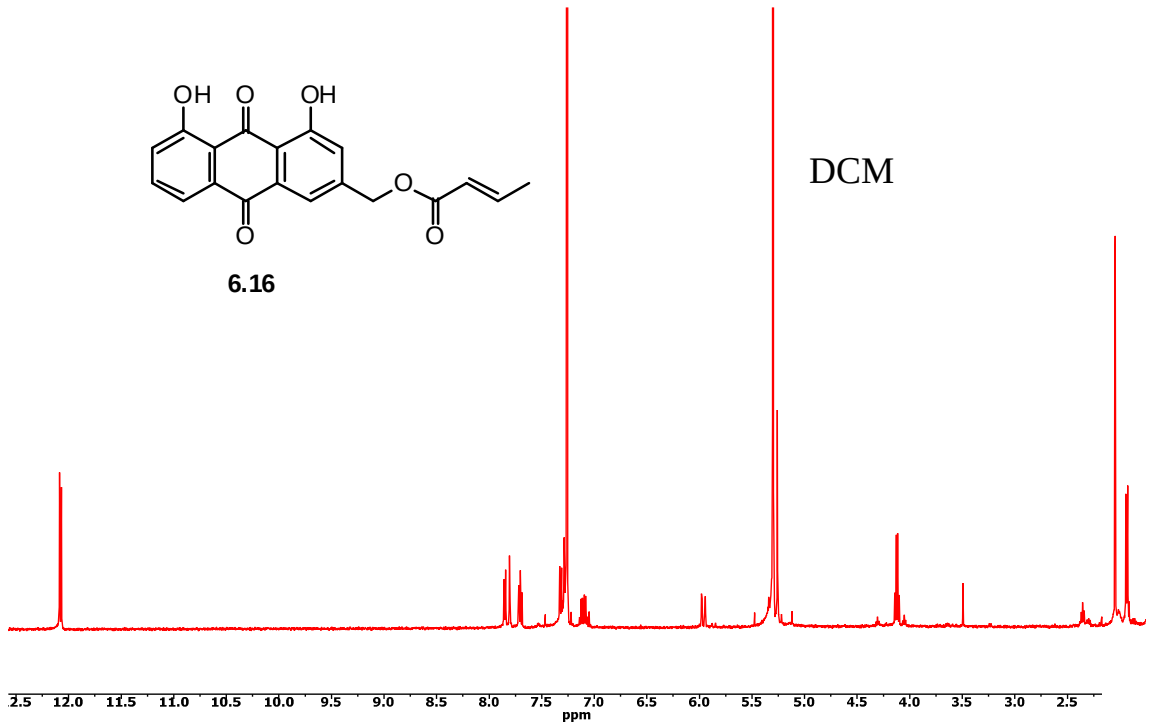

^{13}C NMR spectrum of **6.16** in $CDCl_3$ (125 Hz)

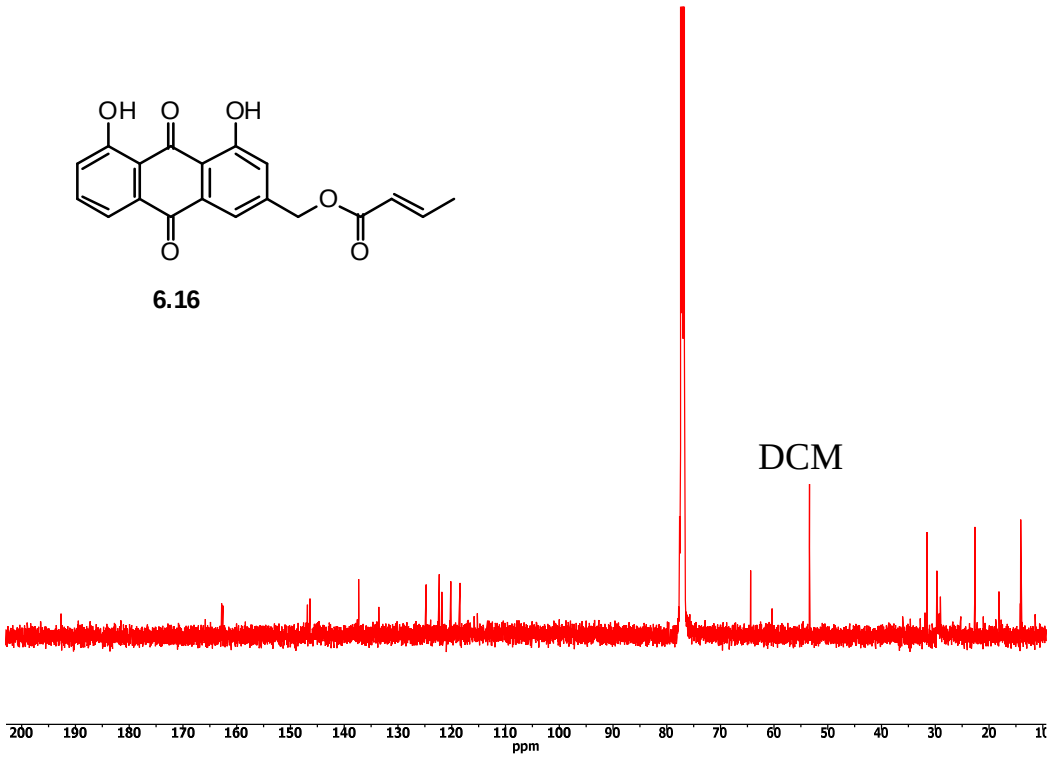

^{1}H NMR spectrum of **6.17** in $CDCl_3$ (500 Hz)

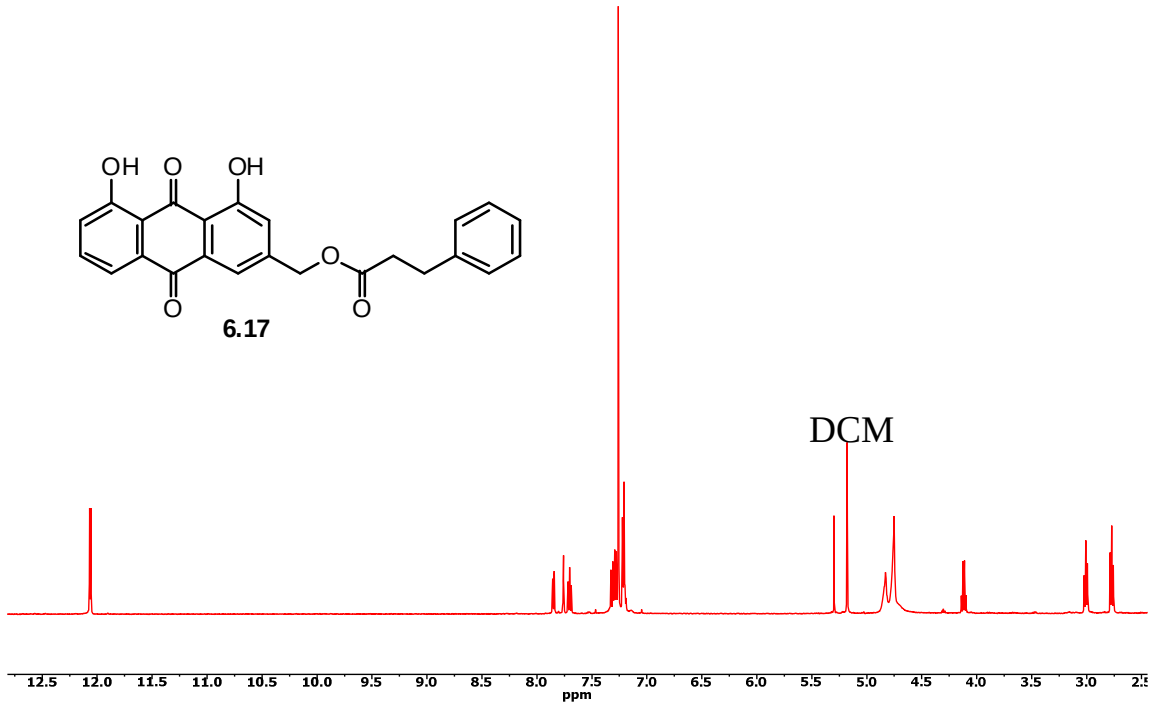

^{13}C NMR spectrum of **6.17** in $CDCl_3$ (125 Hz)

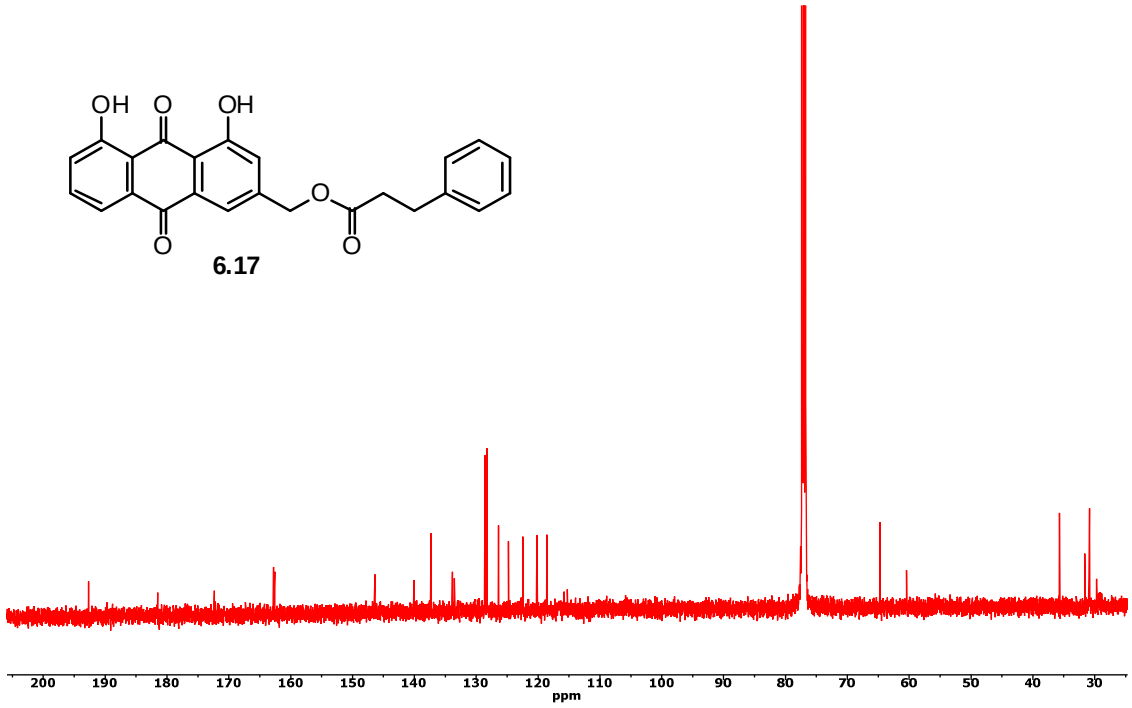

^{1}H NMR spectrum of **6.18** in $CDCl_3$ (500 Hz)

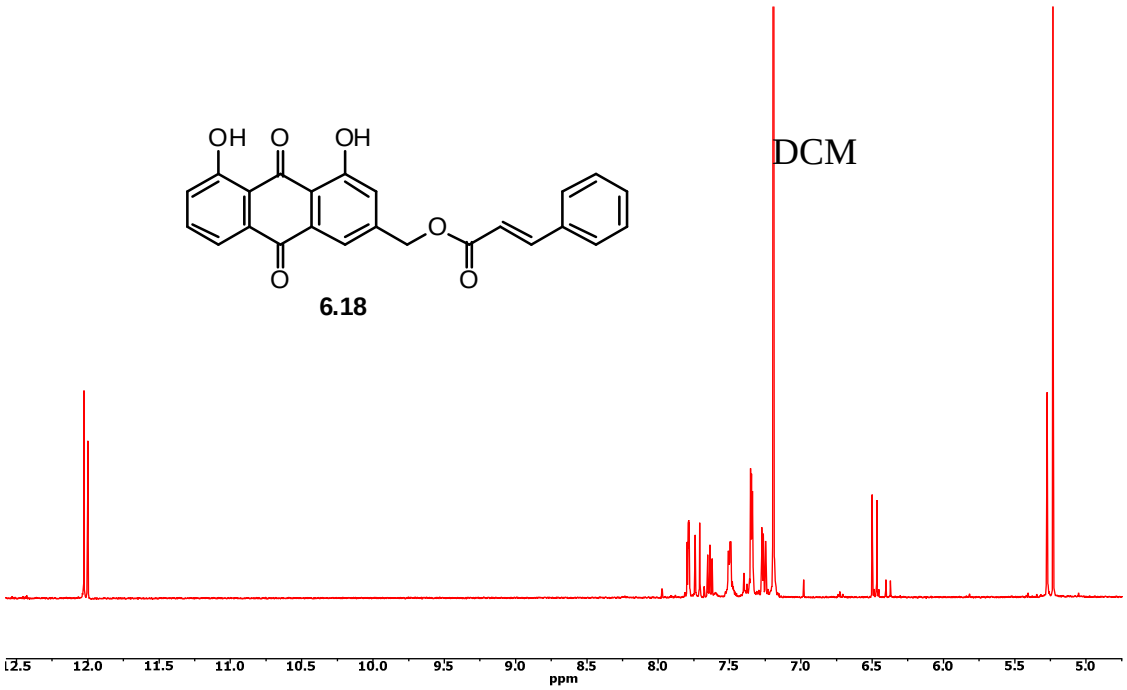

^{13}C NMR spectrum of **6.18** in $CDCl_3$ (125 Hz)

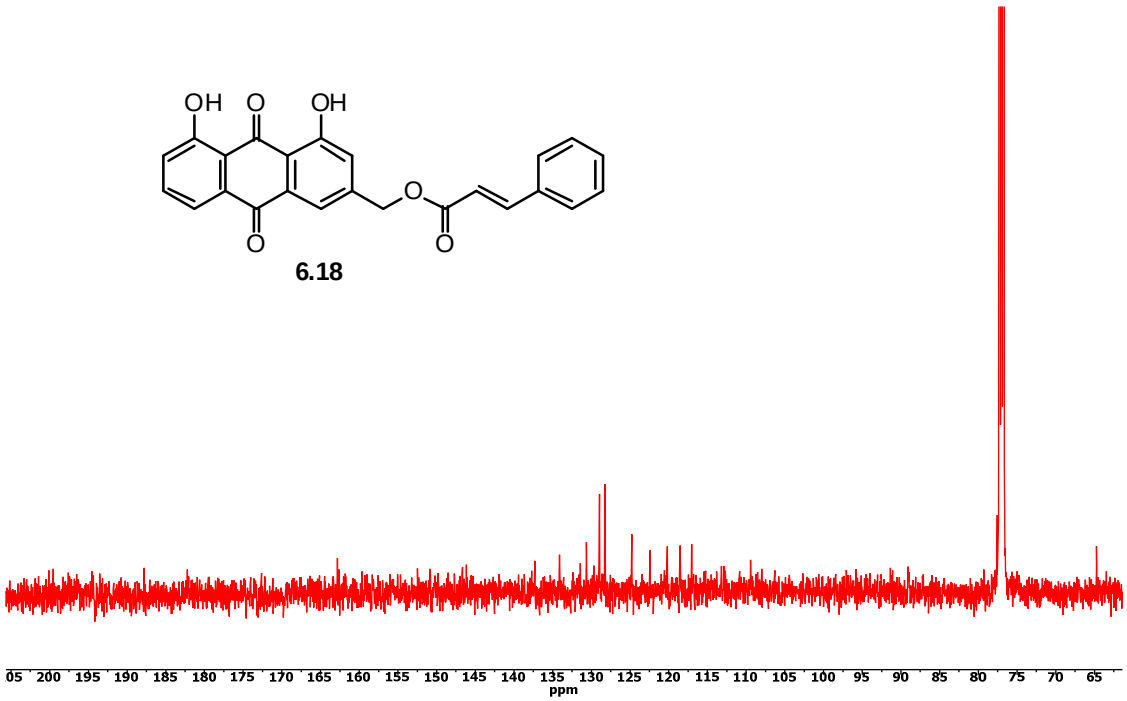

^{1}H NMR spectrum of **6.19** in $CDCl_3$ (500 Hz)

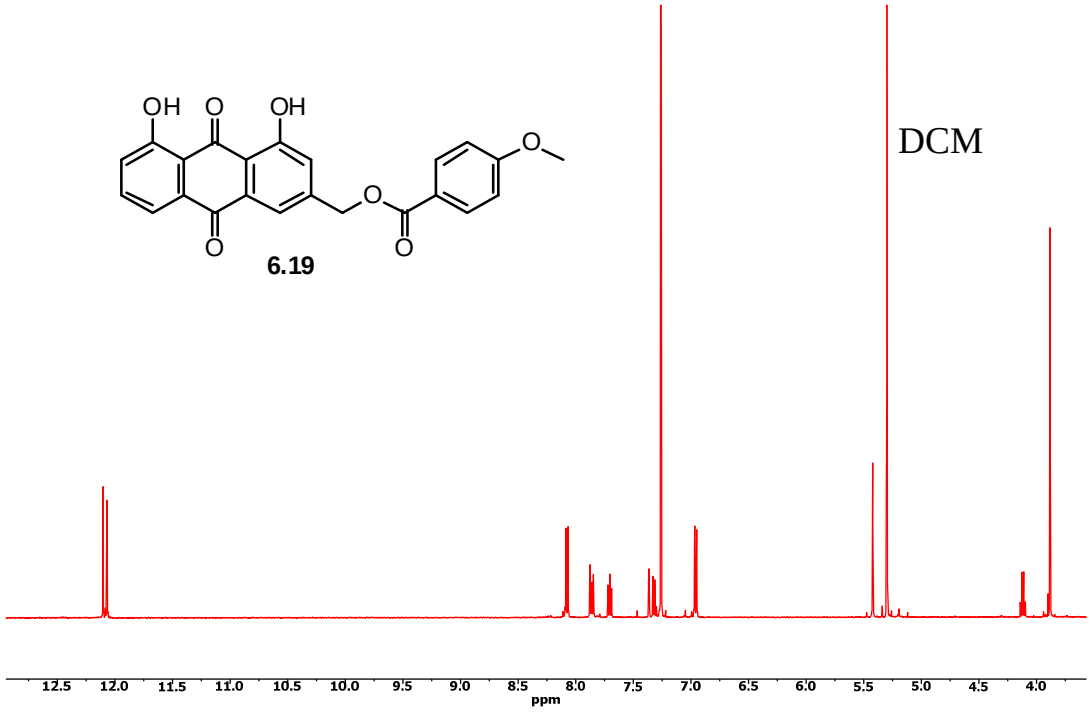

^{13}C NMR spectrum of **6.19** in $CDCl_3$ (125 Hz)

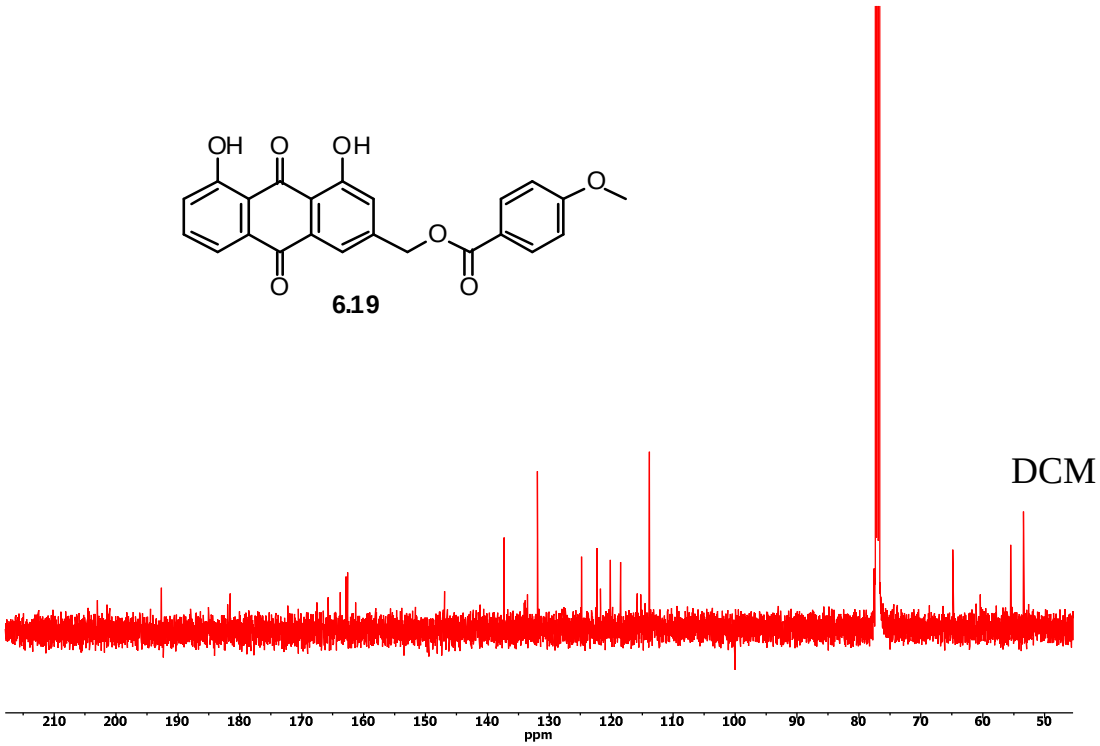

^{1}H NMR spectrum of **6.20** in $CDCl_3$ (500 Hz)

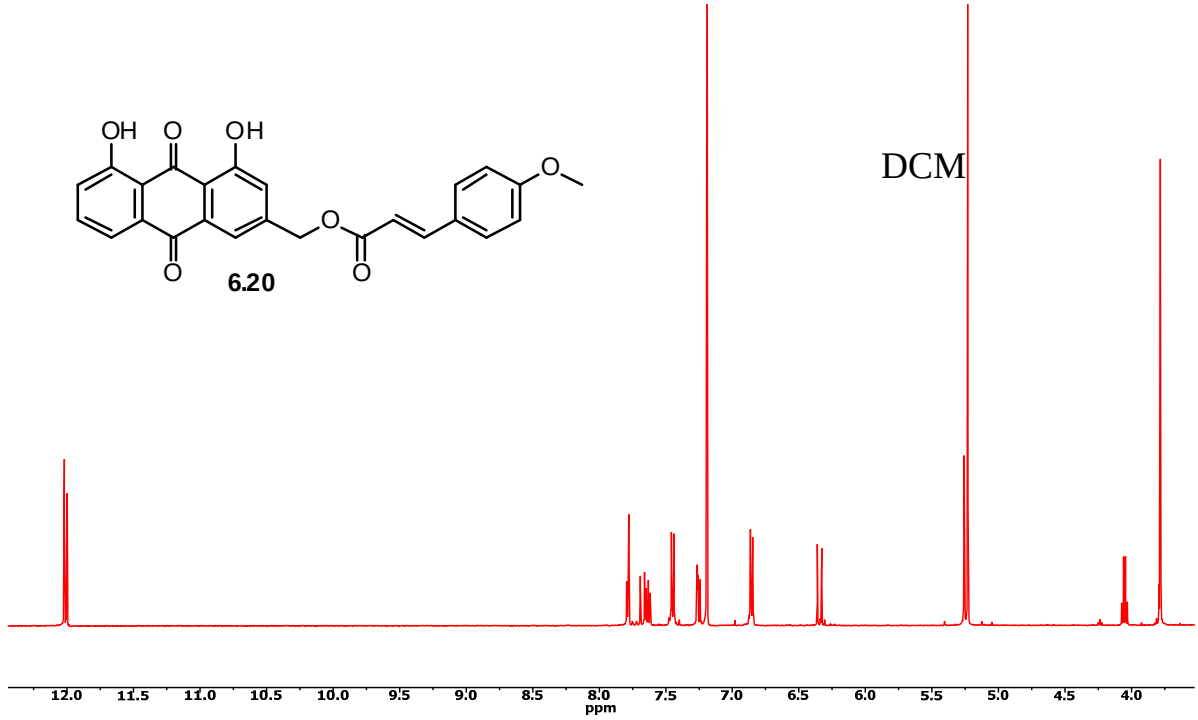

^{13}C NMR spectrum of **6.20** in $CDCl_3$ (125 Hz)

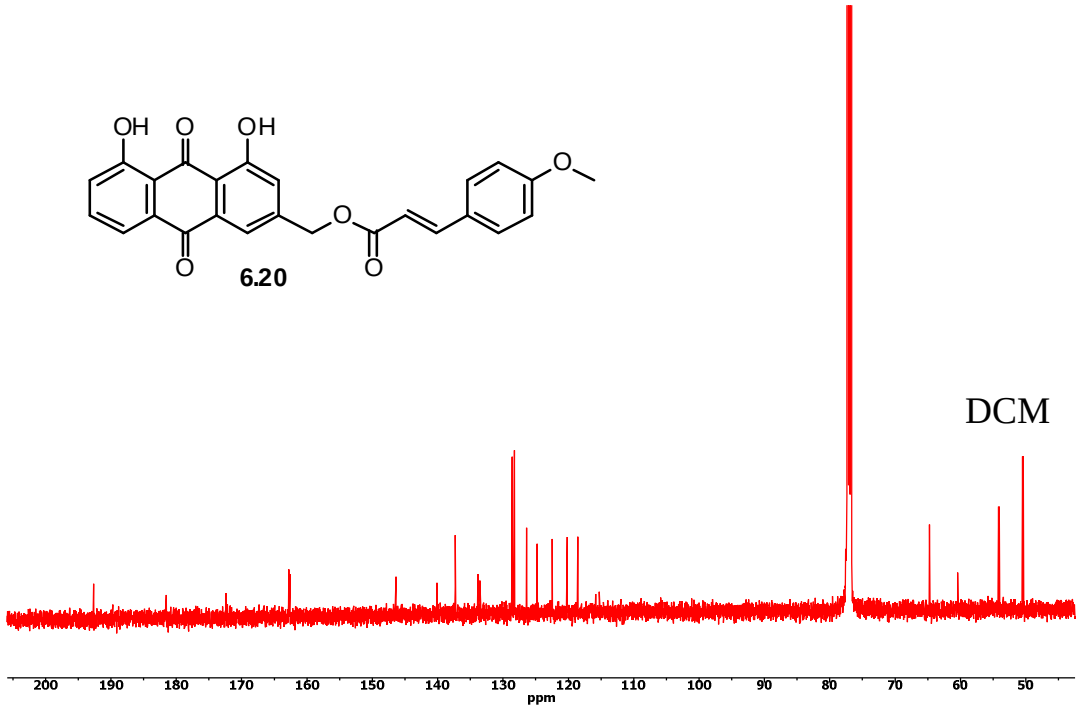

^{1}H NMR spectrum of **6.21** in $CDCl_3$ (600 Hz)

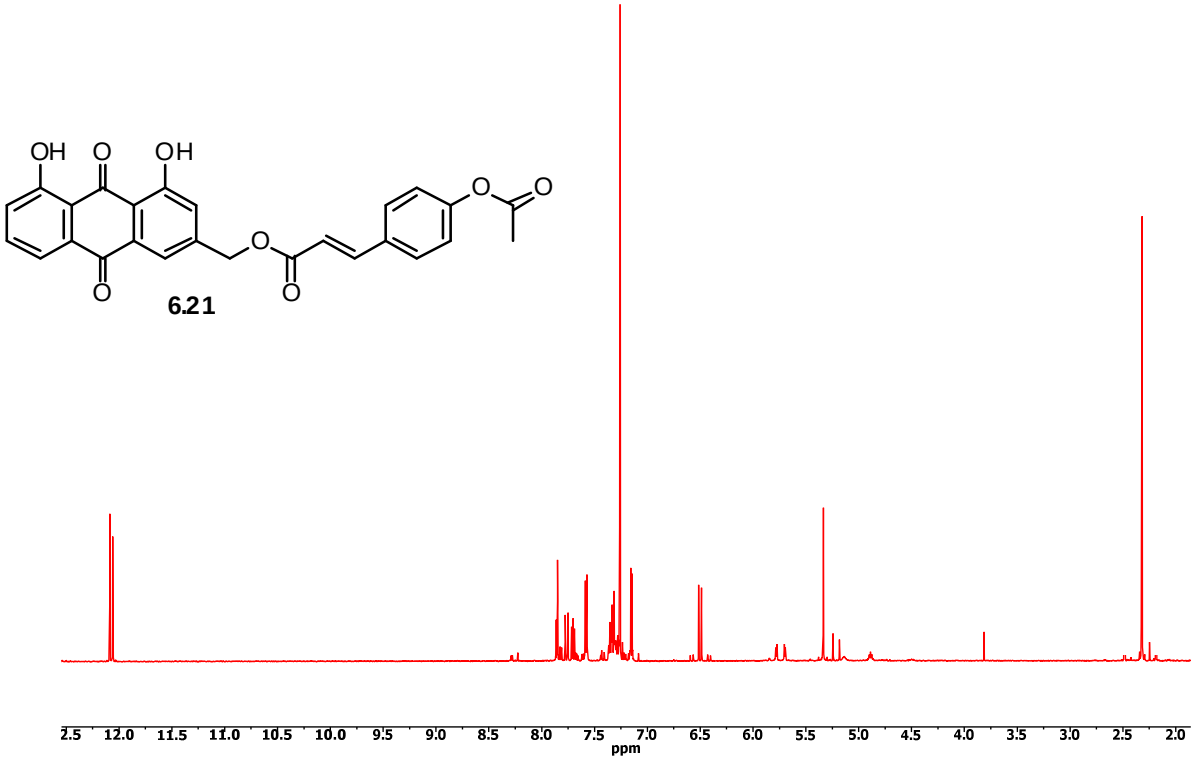

^{13}C NMR spectrum of **6.21** in $CDCl_3$ (150 Hz)

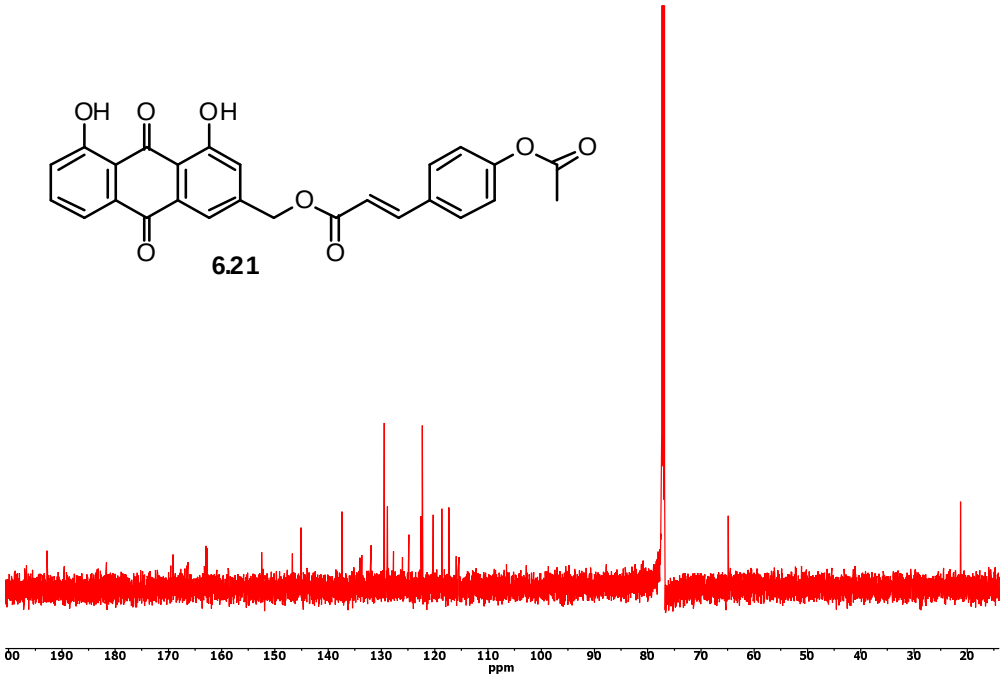

^{1}H NMR spectrum of **6.22** in $CDCl_3$ (600 Hz)

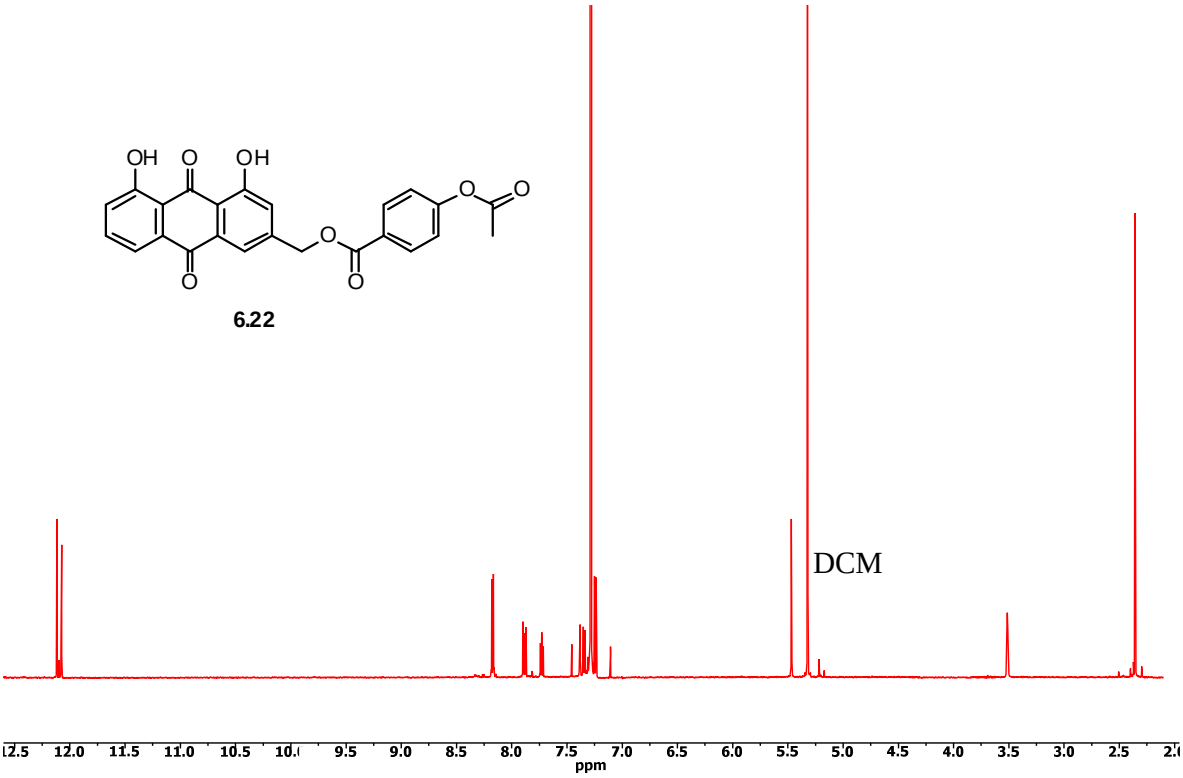

^{13}C NMR spectrum of **6.22** in $CDCl_3$ (150 Hz)

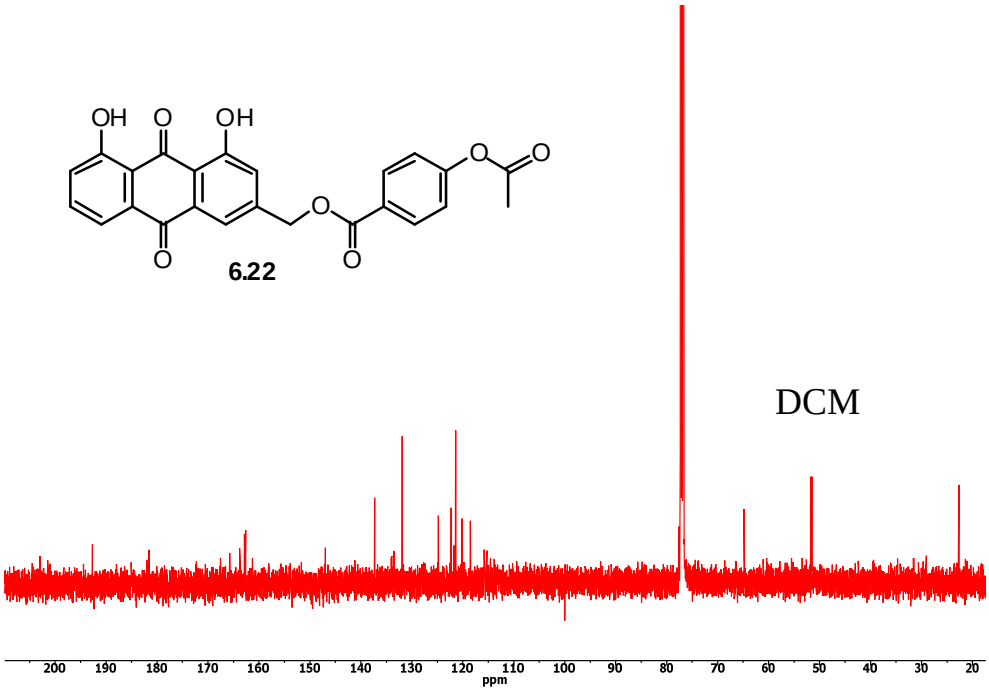

^{1}H NMR spectrum of **6.23** in $CDCl_3$ (500 Hz)

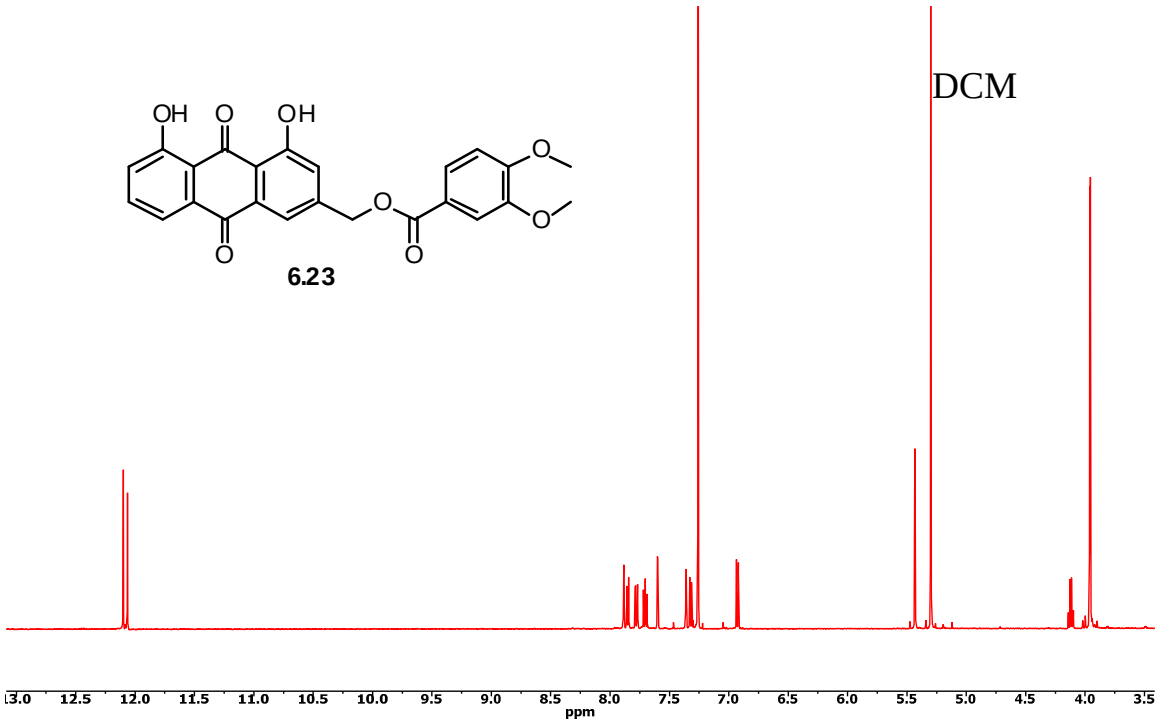

^{13}C NMR spectrum of **6.23** in $CDCl_3$ (125 Hz)

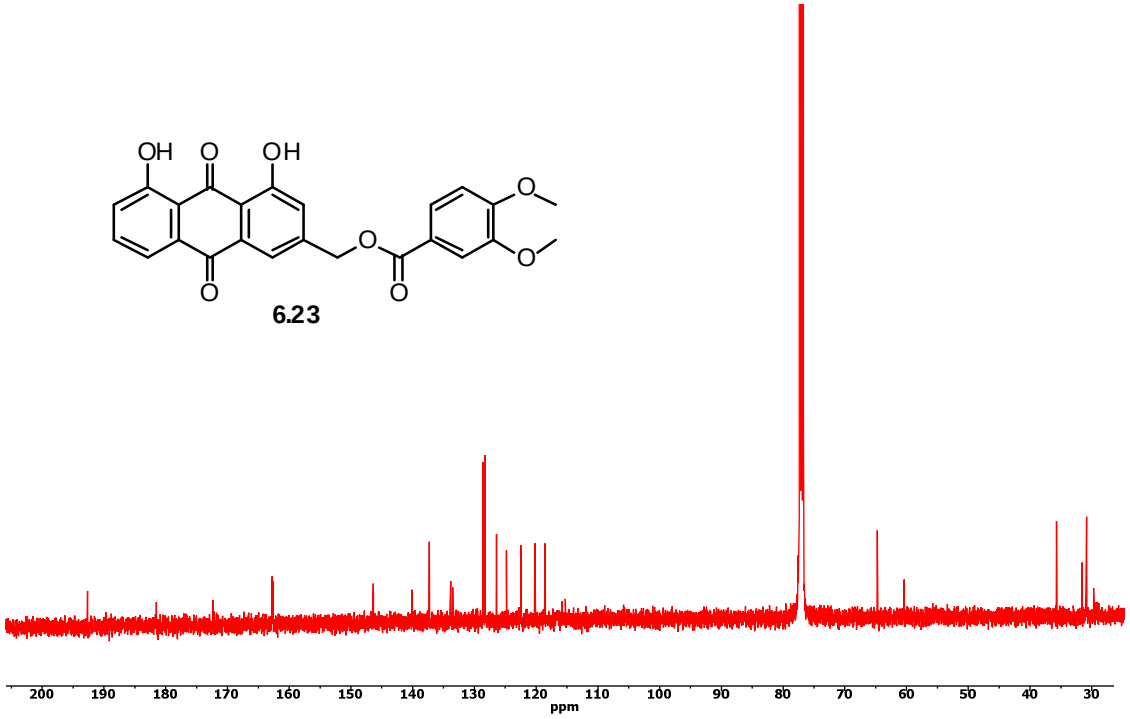

^{1}H NMR spectrum of **6.24** in $CDCl_3$ (500 Hz)

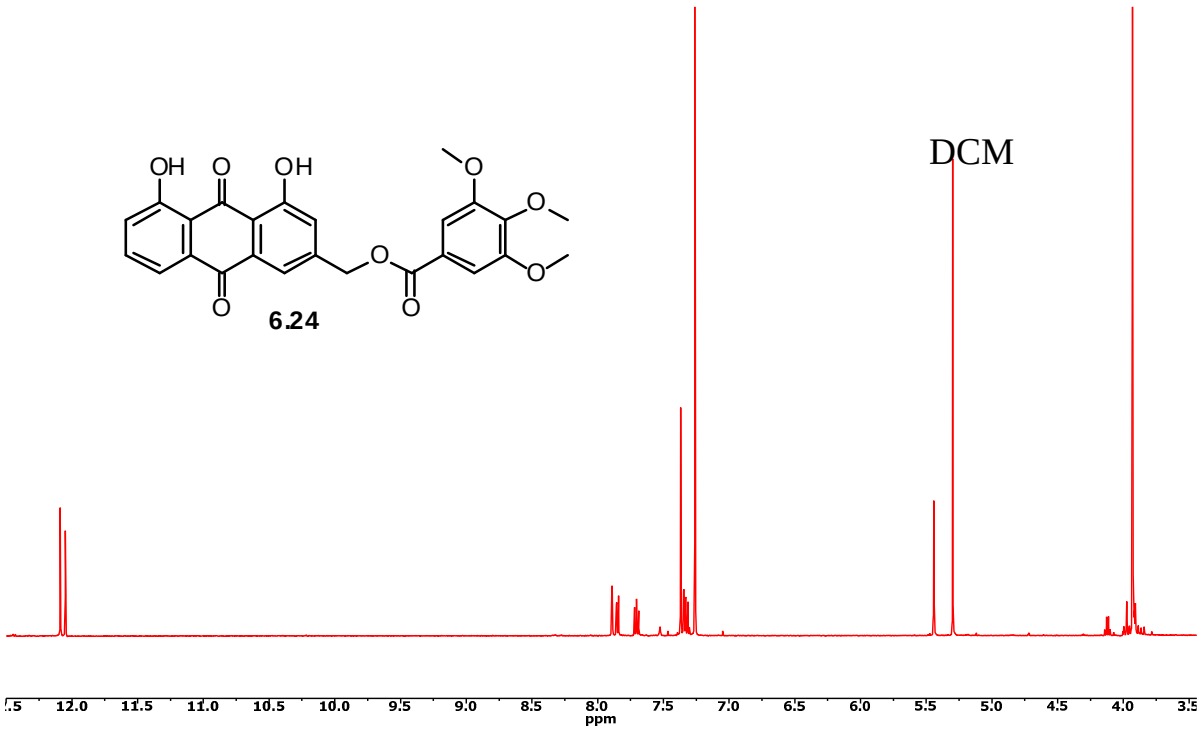

^{13}C NMR spectrum of **6.24** in $CDCl_3$ (125 Hz)

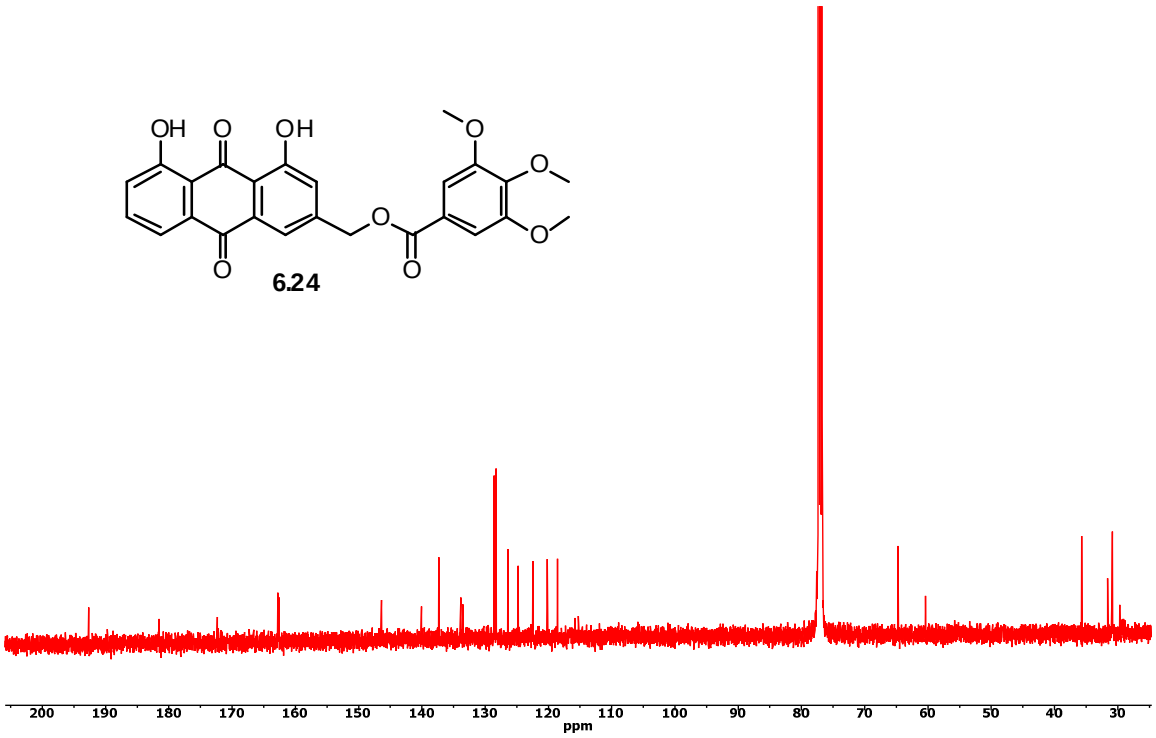

^{1}H NMR spectrum of **6.25** in $CDCl_3$ (500 Hz)

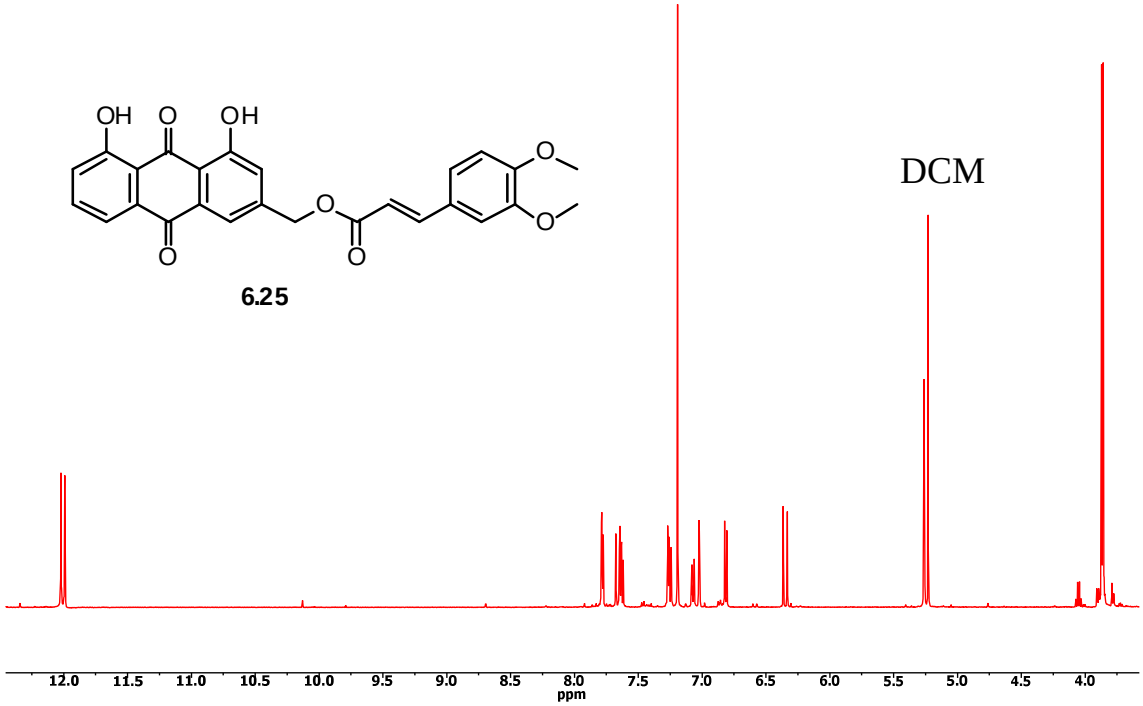

^{13}C NMR spectrum of **6.25** in $CDCl_3$ (125 Hz)

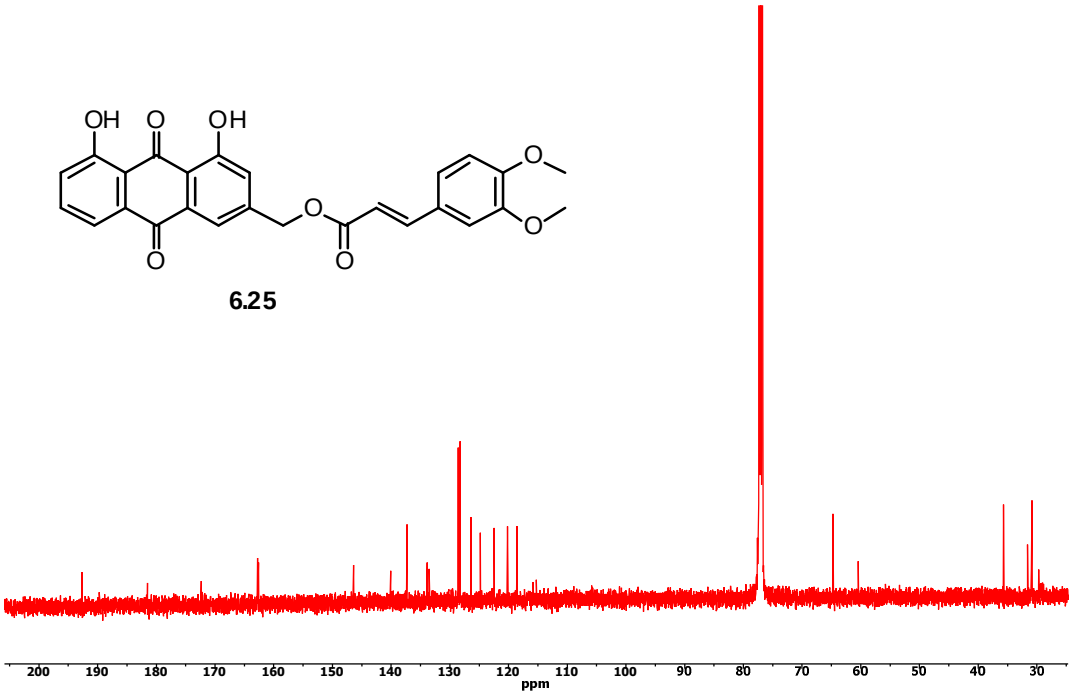

^{1}H NMR spectrum of **6.26** in $CDCl_3$ (500 Hz)

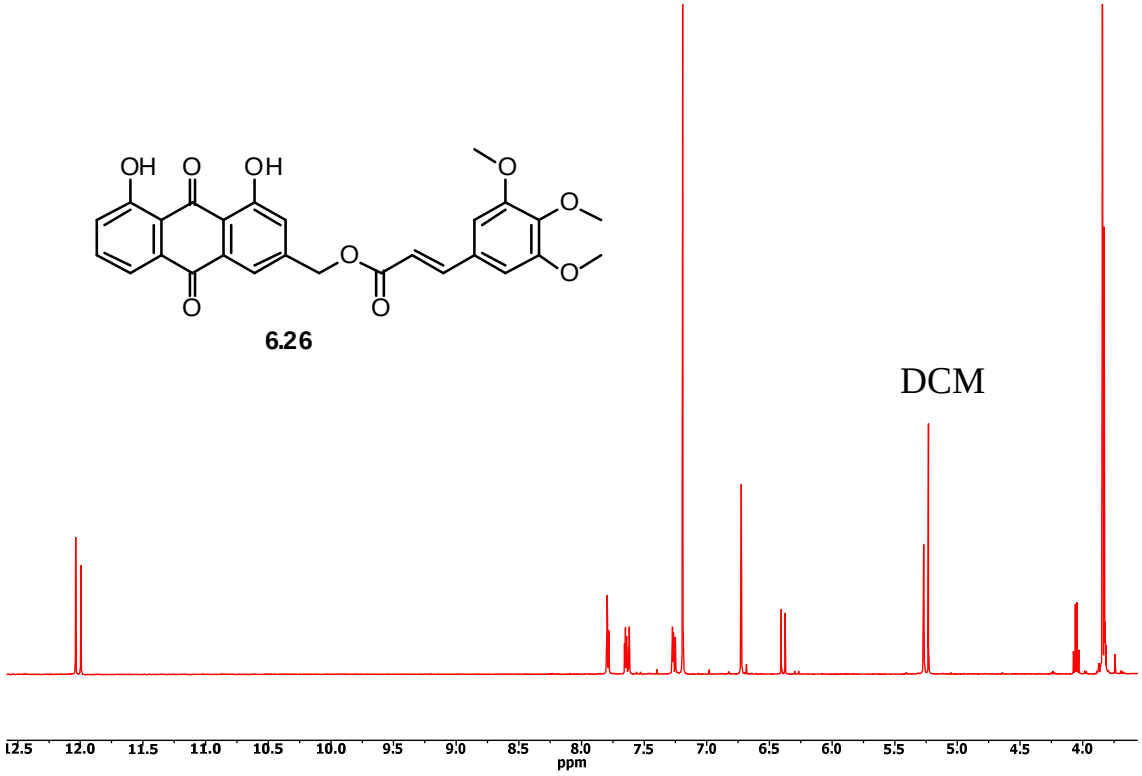

^{13}C NMR spectrum of **6.26** in $CDCl_3$ (125 Hz)

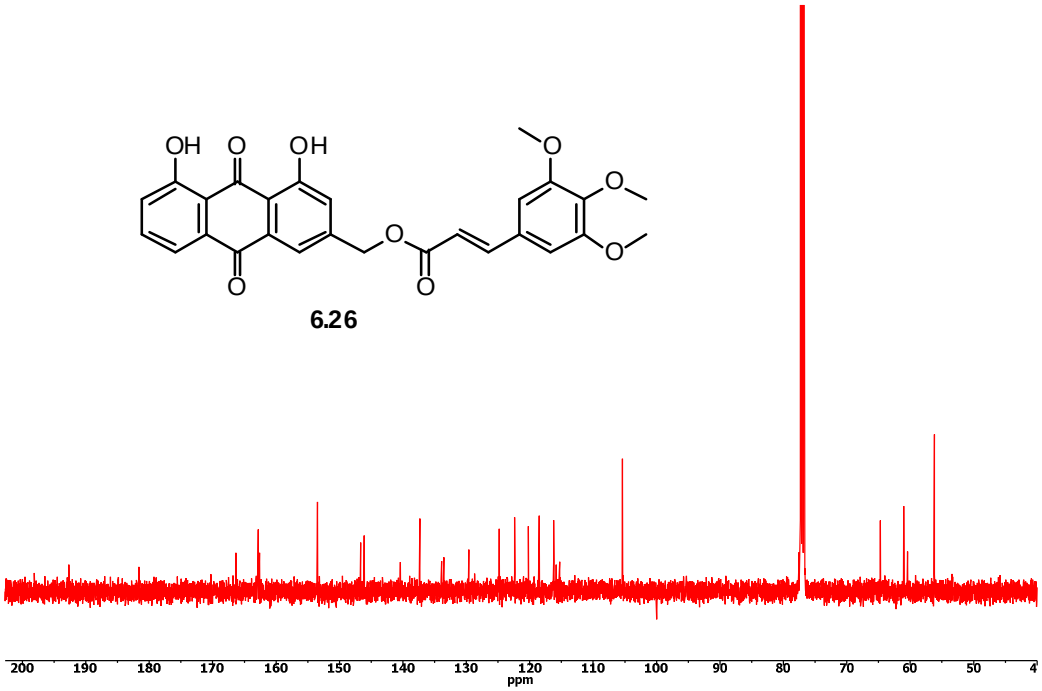

^{1}H NMR spectrum of **6.27** in $CDCl_3$ (500 Hz)

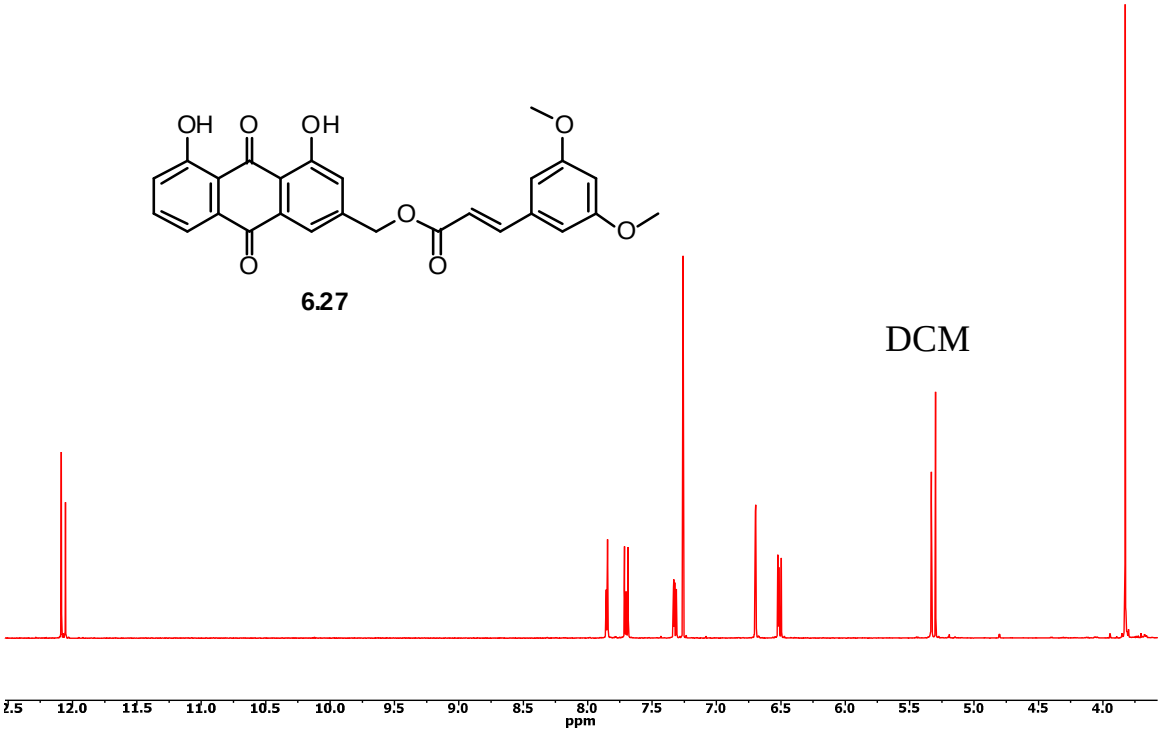

^{13}C NMR spectrum of **6.27** in $CDCl_3$ (125 Hz)

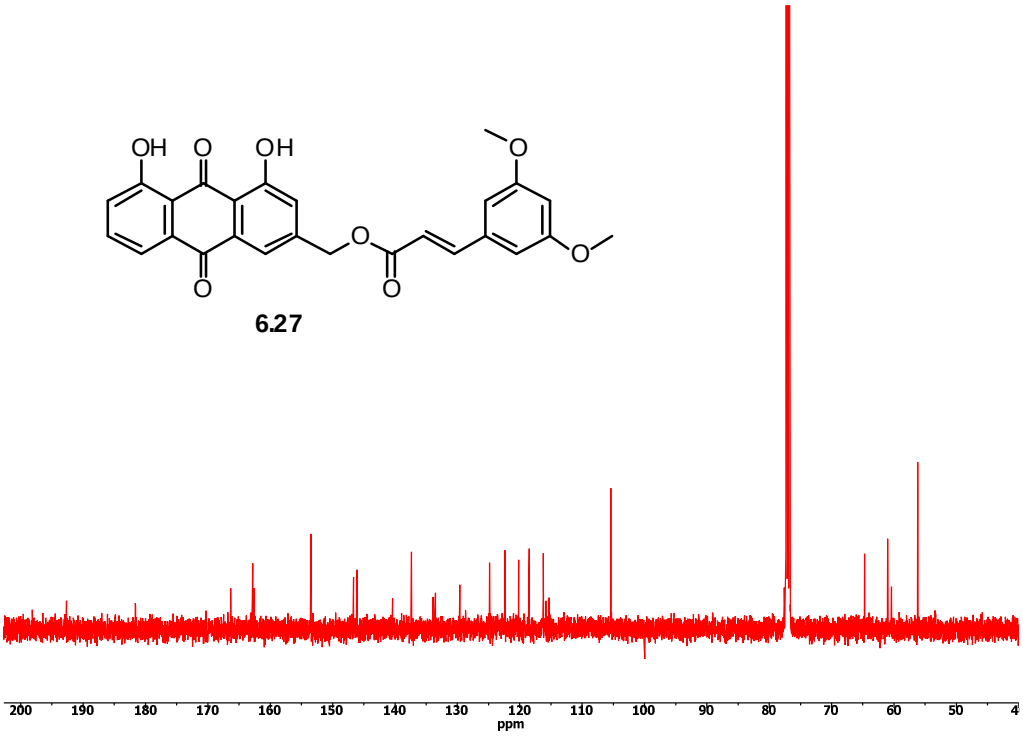

^{1}H NMR spectrum of **6.28** in $CDCl_3$ (600 Hz)

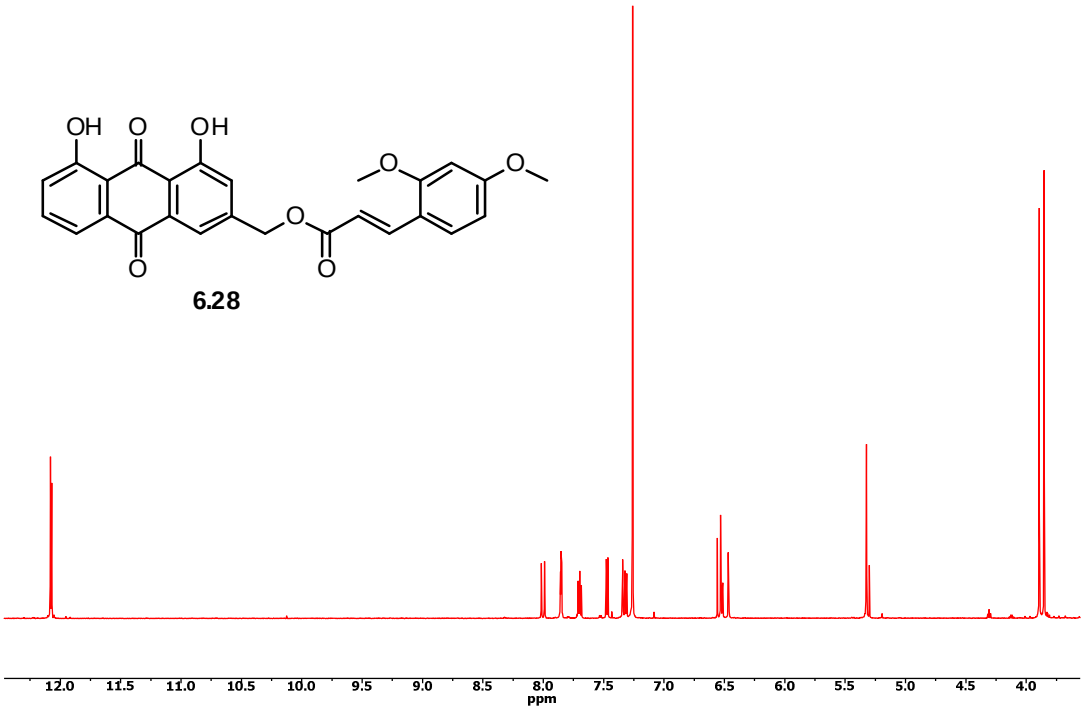

^{13}C NMR spectrum of **6.28** in $CDCl_3$ (150 Hz)

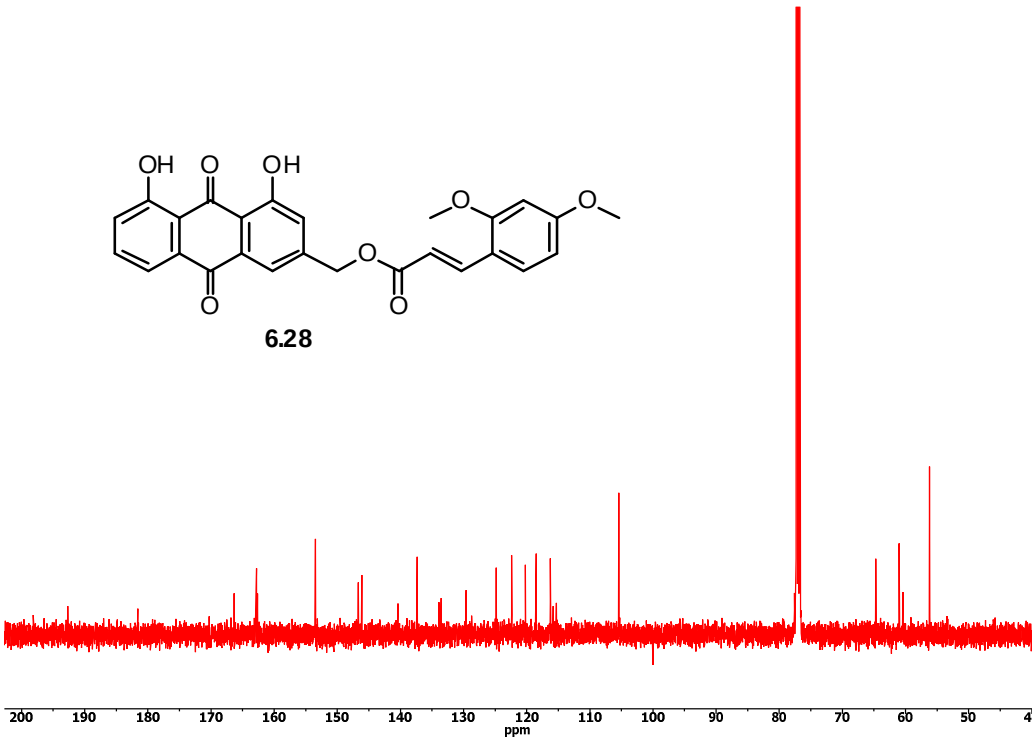

^{1}H NMR spectrum of **6.29** in $CDCl_3$ (600 Hz)

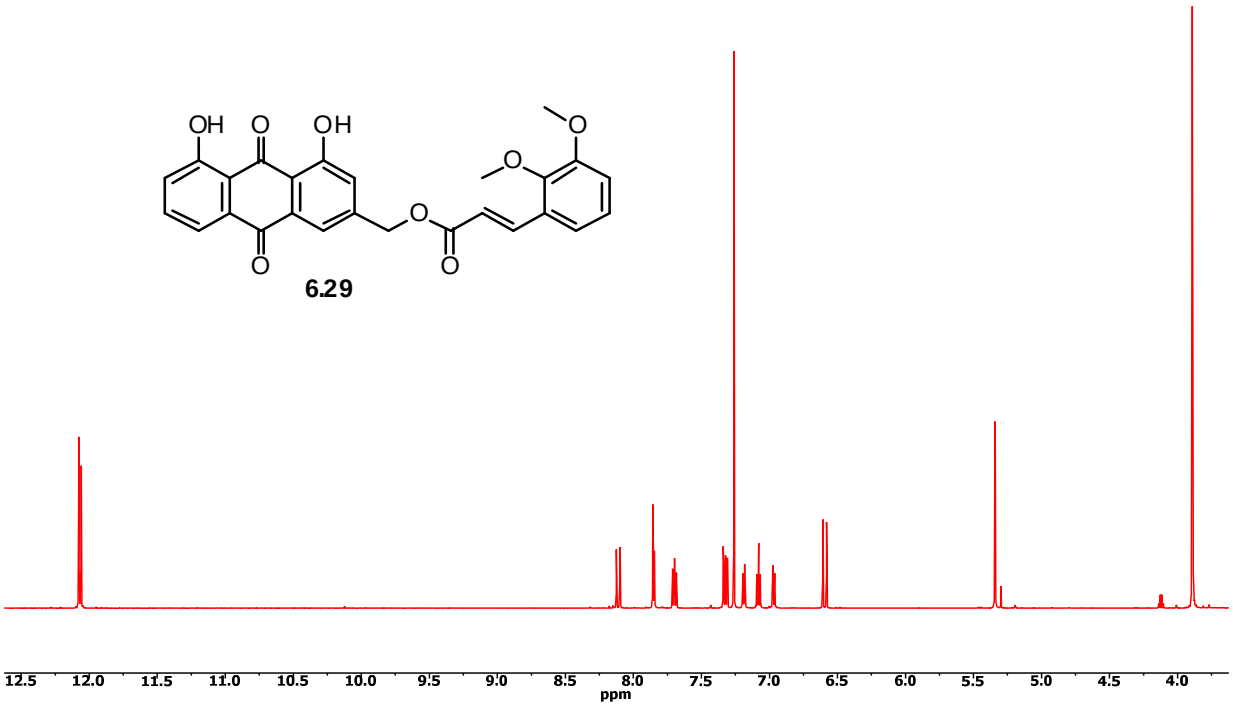

^{13}C NMR spectrum of **6.29** in $CDCl_3$ (150 Hz)

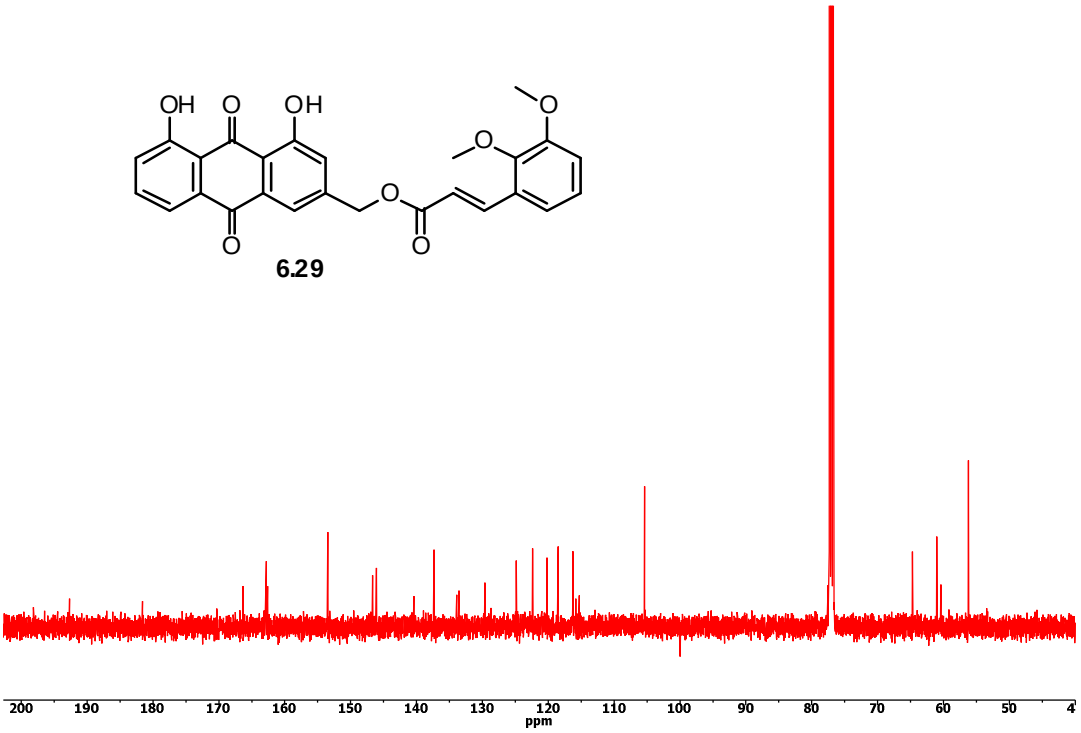

^{1}H NMR spectrum of **6.30** in $CDCl_3$ (600 Hz)

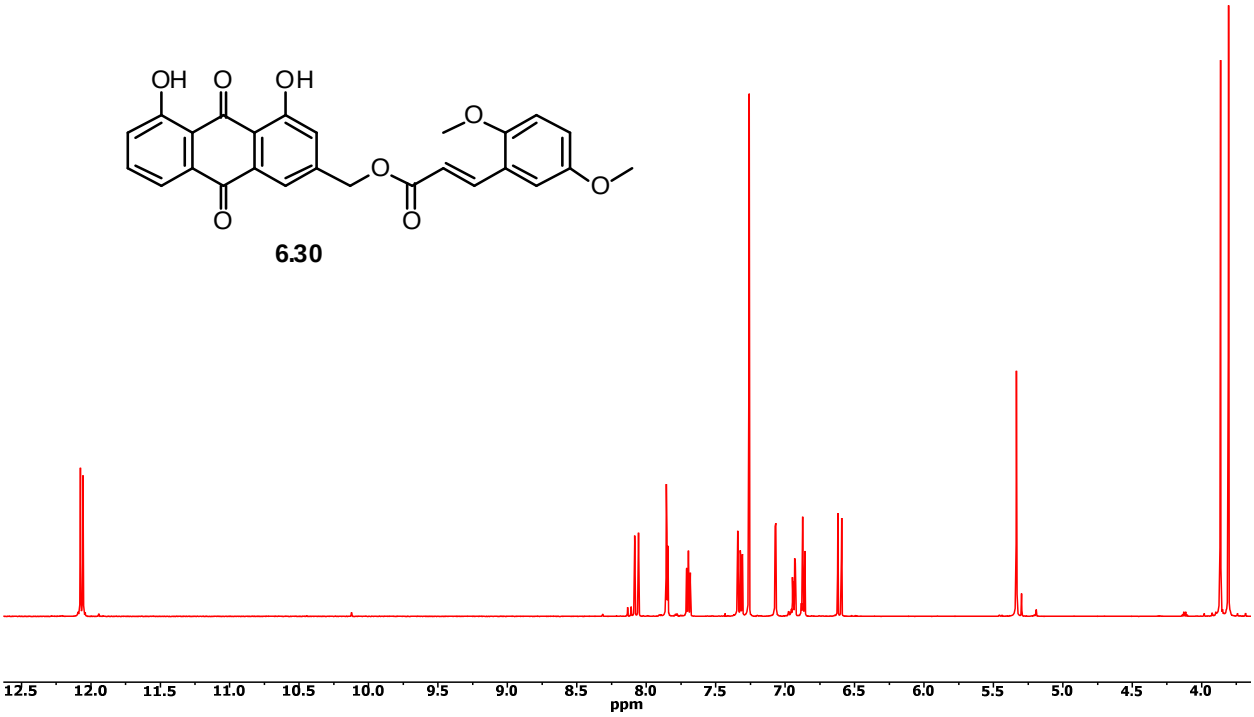

^{13}C NMR spectrum of **6.30** in $CDCl_3$ (150 Hz)

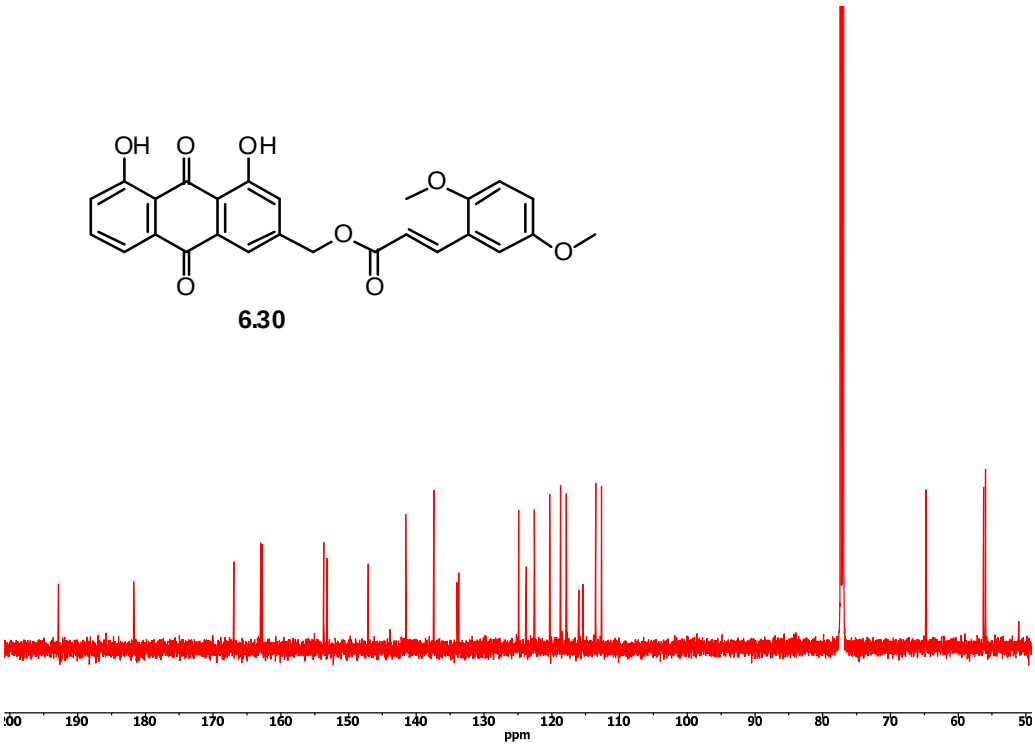

^{1}H NMR spectrum of **6.31** in $CDCl_3$ (500 Hz)

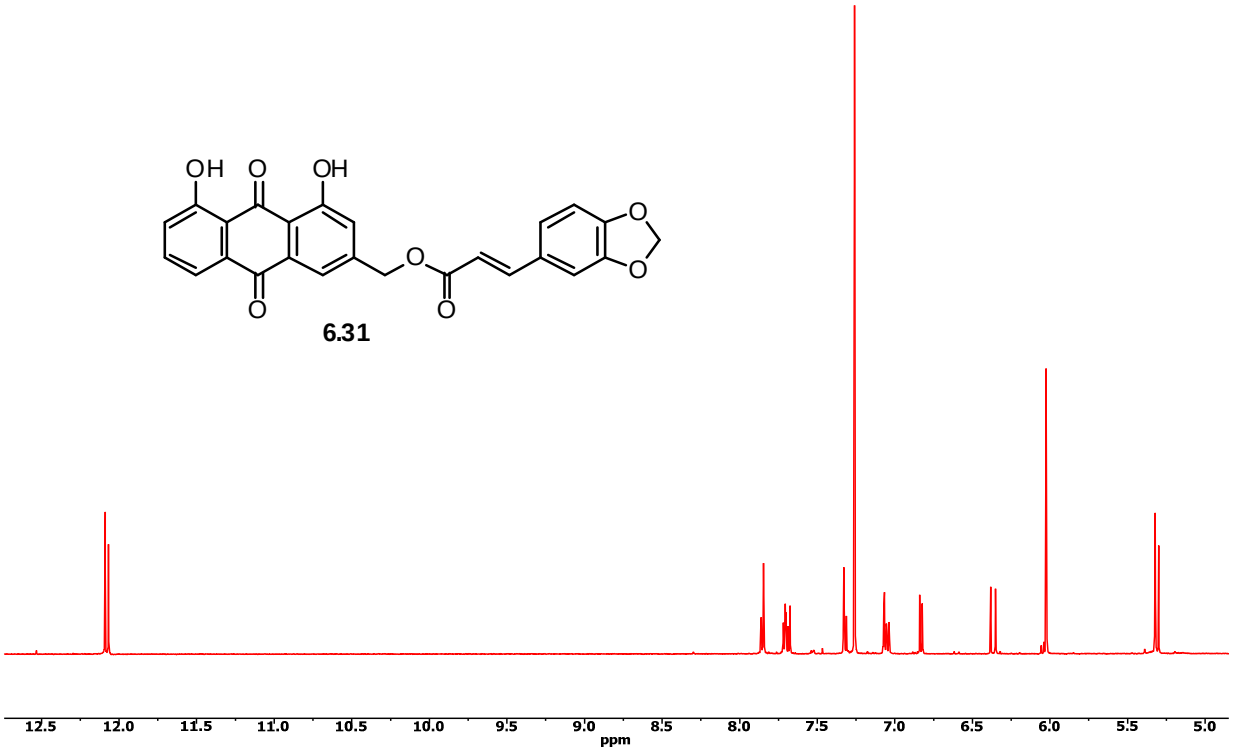

^{13}C NMR spectrum of **6.31** in $CDCl_3$ (125 Hz)